Optimum Design of Composite Structures using Lamination Parameters

Thesis submitted in fulfilment of the requirement for the degree of

Doctor of Philosophy

By

Xiaoyang Liu

September 2019

School of Engineering, Cardiff University

Abstract

The optimised design of composite structures has attracted great interest from researchers, in the pursuit of developing more effective and efficient optimisation methods. In this thesis, two-stage layup optimisation methods based on the use of lamination parameters are developed for both single laminates and large-scale composite laminates with ply drop-offs.

For the optimisation of a single laminate, the highly efficient exact strip software VICONOPT is employed in the first stage to minimise the weight of the structure with lamination parameters and laminate thicknesses as design variables. In the second stage, a new method which incorporates the branch and bound method with a layerwise technique is combined with a checking strategy to logically search the stacking sequences satisfying the layup design constraints to match the optimised lamination parameters using four ply angles (i.e. 0°, 90°, +45° and −45°). In addition, the 10% constraint in terms of the feasible regions of the lamination parameters for the four predefined ply angles is studied and imposed in the first stage optimisation. The superior performance of this method is demonstrated by comparison with a stochastic-based genetic algorithm.

For more complex blended composite laminates, the multilevel optimisation software VICONOPT MLO is improved to include lamination parameters and laminate thicknesses as design variables and used in the first stage optimisation to minimise the weight of the structure. During this iterative multilevel optimisation, the finite element software ABAQUS is used to conduct the static analysis of the whole structure to obtain load distributions at the start of each design cycle, based on which the exact strip software VICONOPT is then employed to optimise each of the component panels. In the second stage optimisation, whilst ply drop-off between adjacent panels causes ply discontinuity and needs to be avoided, ensuring ply continuity across adjacent panels significantly complicates the process of optimising the stacking sequences. Accordingly, a novel Dummy Layerwise Branch and Bound method (DLBB) which incorporates the dummy layerwise technique with the branch and bound method is developed to logically search the blended stacking sequences for the whole structure to match the optimised lamination parameters. This two-stage method is applied to a benchmark wing box to demonstrate its effectiveness.

To improve the efficiency of the second stage optimisation for these blended composite laminates, a novel parallel computation method DLBB-GAGA is developed. Firstly, a Guide-based Adaptive Genetic Algorithm (GAGA) which stochastically searches the stacking sequences to match the target lamination parameters is developed. After this, GAGA is implemented in a parallel process with the DLBB method in the parallel DLBB-GAGA method, combing the advantages of both the logic and stochastic-based searches. Comparisons are made between the three methods, results demonstrate that benefit is gained from the combination of the two different methods.

Acknowledgements

First of all, I would like to express my deepest gratitude to my supervisors, Prof. David Kennedy and Prof. Carol Featherston, for their continuous guidance and kind support throughout my PhD study. It was their excellent supervision and consistent encouragement that made the completion of this thesis possible. I am also really grateful to Dr Shuang Qu who directed me to be a PhD student and introduced me to Prof. David Kennedy and Prof. Carol Featherston.

I would like to thank Cardiff University and China Scholarship Council for providing the funding to complete my doctoral study. I am also grateful to my colleagues and friends at Cardiff University for their company, friendship and direct or indirect help. Special thanks must go to Ning Han, for her love and warm support during my study.

I would like to sincerely thank my beloved family especially my parents, for their unconditional support and great confidence in me. Finally, I would like to dedicate this thesis to my grandmother for her great love.

Contents

Abstract ..... **i**

Acknowledgements ..... **iii**

Contents ..... **v**

List of figures ..... **ix**

List of tables ..... **xv**

Nomenclature ..... **xix**

Chapter 1 General Introduction **1**

1.1 General background 1

1.2 Thesis objectives 5

1.3 Thesis structure 6

1.4 Publication list 8

Chapter 2 Literature Review **9**

2.1 Continuous optimisation for composite structures 9

2.2 Discrete optimisation for composite structures 11

2.3 Multilevel optimisation 15

2.4 Lamination parameters 16

2.4.1 Feasible regions of lamination parameters 16

2.4.2 Optimisation methods based on lamination parameters 18

2.5 Blending optimisation 21

2.6 Layup optimisation based on parallel computation 25

Chapter 3 Theoretical Background **27**

3.1 Mechanics of composite laminates 27

3.1.1 Stress-strain relations of composite lamina 27
3.1.2 Constitutive equations of composite laminates..... 29
3.1.3 Lamination parameters..... 31
3.2 Method of feasible directions 32
3.3 Genetic algorithms..... 35
3.4 Branch and bound method..... 37
3.5 Parallel computation..... 38

Chapter 4 VICONOPT 41

4.1 Introduction..... 41
4.2 Theoretical background 41
4.2.1 The exact strip method..... 41
4.2.2 The Wittrick-Williams algorithm 42
4.3 Analysis features of VICONOPT 43
4.3.1 VIPASA analysis 43
4.3.2 VICON analysis..... 46
4.4 Optimisation features of VICONOPT 48
4.4.1 Structural optimisation in VICONOPT 49
4.4.2 Lamination parameter optimisation in VICONOPT..... 52
4.4.3 VICONOPT MLO 54

Chapter 5 Two-stage Layup Optimisation of Single Composite Laminates..... 57

5.1 Introduction..... 57
5.2 Methodology..... 58
5.2.1 First stage optimisation..... 58
5.2.2 Second stage optimisation 61
5.2.2.1 Layerwise branch and bound method..... 62
5.2.2.2 Addition of constraints..... 67
5.2.2.3 Genetic algorithm..... 72

5.3 Results and discussion 73
5.3.1 Layup optimisation of a simply supported rectangular laminate 73
5.3.2 Layup optimisation of stiffened panels 82
5.4 Conclusions 86

Chapter 6 Two-stage Layup Optimisation of Blended Composite Laminates ... 87
6.1 Introduction 87
6.2 Methodology 88
6.2.1 First stage optimisation 88
6.2.2 Second stage optimisation 91
6.3 Results and discussion 98
6.3.1 First stage optimisation results 101
6.3.2 Second stage optimisation results 104
6.3.2.1 Layup design without blending constraint 105
6.3.2.2 Layup design with blending constraint 108
6.4 Conclusions 113

Chapter 7 Parallel Computation Method for Optimisation of Composite Laminates 115
7.1 Introduction 115
7.2 Methodology 116
7.2.1 Guide-based adaptive genetic algorithm 116
7.2.2 Parallel DLBB-GAGA method 121
7.3 Results and discussion 124
7.3.1 Symmetric case 124
7.3.2 Constrained case 129
7.4 Conclusions 137

Chapter 8 Conclusions and Suggestions for Future Work 139

8.1 Conclusions 139

8.2 Suggestions for future work..... 141

References 143

Appendix A Lamination Parameters of the Layups Obtained in Chapter 7.... 167

Appendix B Buckling Modes of the Wing Box Structures Obtained in Chapter 7 171

List of figures

Figure 1.1 The composition of an example composite laminate..... 1

Figure 1.2 The three successive stages for designing an aircraft. 3

Figure 3.1 An orthotropic lamina whose principal material directions are rotated by θ with respect to the reference coordinate directions, and its deformation is based on the Kirchhoff-Love hypothesis (AB=$A'B'$). 27

Figure 3.2 A laminate consisting of n layers. 30

Figure 3.3 Usable and feasible direction along which the objective function is decreased without violating any constraint (based on (Vanderplaats and Moses 1973)). 34

Figure 3.4 GAs operators (a) crossover, (b) mutation, and (c) permutation. 36

Figure 3.5 A decision tree of the branch and bound method. 38

Figure 4.1 Typical prismatic plate assemblies (Wittrick and Williams 1974). 44

Figure 4.2 In-plane loadings of a typical component plate. 44

Figure 4.3 Nodal lines in (a) are straight and perpendicular to the longitudinal direction, which is consistent with simply supported end conditions. Nodal lines in (b) are skewed due to anisotropy or shear loads, approximating the simply supported end condition. 46

Figure 4.4 An infinitely long plate assembly in VICON with crosses denoting point supports, (a) plan view, (b) isometric view (Williams *et al*. 1991)..... 47

Figure 4.5 Flow chart of VICONOPT optimisation..... 50

Figure 4.6 An example of the penalization process on the feasible region of $\xi_{1,2}^{D}$.... 53

Figure 4.7 Flowchart of the multilevel optimisation process of VICONOPT MLO. 55

Figure 5.1 Restricted feasible regions of lamination parameters $\xi^{A}_{1,2,3,}$ when considering the minimum percentage constraint $p_{\min} = 0.1$. 61

Figure 5.2 Restricted feasible regions of lamination parameters $\xi^{D}_{1,2,3,}$ for symmetric laminates, when considering the minimum percentage constraint $p_{\min} = 0.1$. 61

Figure 5.3 An illustrative branch and bound decision tree for optimising two plies. 62

Figure 5.4 Application of the global layerwise technique to optimisation of an 8 ply laminate. (The layers in the current case loop are bold, and the other ones are not allowed to change.) 64

Figure 5.5 Flow chart of the improved LBB method. 66

Figure 5.6 Checking strategy for balance constraint. (a) θ_4 cannot be +45°. (b) θ_4 must be +45°. 67

Figure 5.7 Checking strategy for contiguity constraint for the laminate with even number of plies. 69

Figure 5.8 Checking strategy for contiguity constraint for the laminate with odd number of plies. 70

Figure 5.9 The contribution of each lamination parameter to the difference between target and actual lamination parameters for the 18 cases considered. 77

Figure 5.10 Plot of actual lamination parameters against target lamination parameters in lamination parameter space. 78

Figure 5.11 Comparison between GAs and the improved LBB method. (a) Example 2: Symmetric. (b) Example 1: Basic 81

Figure 6.1 Flow chart of the proposed first stage multilevel optimisation using lamination parameters. 89

Figure 6.2 Flow chart of the dummy layerwise branch and bound (DLBB) method. 92

Figure 6.3 The dummy layerwise technique: starting layout of the dummy layerwise table. 93

Figure 6.4 Decision trees with a possible determined layup: (a) in the first case of the first pass of the first cycle; (b) in the second case of the first pass of the first cycle..... 95

Figure 6.5 Layout changes after the first pass of the first cycle..... 96

Figure 6.6 A possible starting layup for the second cycle. 96

Figure 6.7 (a) Geometry of the wing box and the load case. (b) Bottom panels, ribs and spars. 99

Figure 6.8 Geometry of the component panels (in mm). 100

Figure 6.9 (a) Total mass comparison of the top panels. (b) Mass comparisons of each individual panel. 103

Figure 6.10 Buckling modes obtained using the optimised lamination parameters and rounded thicknesses. (a) First buckling mode with buckling load factor = 1.15. (b) Second buckling mode with buckling load factor = 1.17. 105

Figure 6.11 Buckling modes obtained using the stacking sequences without considering blending constraint. (a) First buckling mode with buckling load factor = 1.09. (b) Second buckling mode with buckling load factor = 1.15. 107

Figure 6.12 Buckling modes obtained using the blended stacking sequences. (a) First buckling mode with buckling load factor = 1.08. (b) Second buckling mode with buckling load factor = 1.14. 112

Figure 7.1 An example illustrating the blending process in GAGA. 117

Figure 7.2 Flow chart illustrating the guide-based adaptive genetic algorithm (GAGA). 118

Figure 7.3 Optimisation process for the parallel DLBB-GAGA method in MATLAB. (The left column represents the simplified DLBB process and the right GAGA, and the message passing functions described in text are shown in bold.)... 122

Figure 7.4 Comparisons between the DLBB method, GAGA and the parallel method for blended skins. (a) The results of GAGA and the parallel method are averaged values of 10 runs. (b) Examples of a GAGA run and a parallel method run are shown in comparison. 125

Figure 7.5 Comparisons between the DLBB method, GAGA and the parallel method for (a) blended right hand side flanges and (b) blended left hand side flanges. 126

Figure 7.6 Comparison between the DLBB method, GAGA and the parallel method for (a) blended right hand side webs and (b) blended left hand side webs. 127

Figure 7.7 Comparison between the DLBB method, GAGA and the parallel method for blended skins under symmetry, balance, and four layup design constraints. 129

Figure 7.8 Comparison between the DLBB method, GAGA and the parallel method for (a) blended right hand side flanges and (b) blended left hand side flanges, under symmetry, balance, and four layup design constraints. 131

Figure 7.9 Comparisons between the DLBB method, GAGA and the parallel method for (a) blended right hand side webs and (b) blended left hand side webs, under symmetry, balance, and four layup design constraints. 132

Figure B.1 First buckling mode with buckling load factor = 1.06 (DLBB method). 171

Figure B.2 Second buckling mode with buckling load factor = 1.11 (DLBB method). 171

Figure B.3 Third buckling mode with buckling load factor = 1.15 (DLBB method). 172

Figure B.4 First buckling mode with buckling load factor = 1.03 (GAGA). 172

Figure B.5 Second buckling mode with buckling load factor = 1.13 (GAGA). 173

Figure B.6 Third buckling mode with buckling load factor = 1.15 (GAGA). 173

Figure B.7 First buckling mode with buckling load factor = 1.08 (parallel method). 174

Figure B.8 Second buckling mode with buckling load factor = 1.14 (parallel method). 174

Figure B.9 Third buckling mode with buckling load factor = 1.15 (parallel method). 175

List of tables

Table 5.1 Contribution of each ply orientation to the in-plane lamination parameters. 60

Table 5.2 Properties and dimensions of the example laminate. 73

Table 5.3 Stage 1 optimisation results..... 75

Table 5.4 Stage 2 optimisation results obtained from the improved LBB method. .. 75

Table 5.5 Comparison between GAs and the improved LBB method for four symmetric examples from Table 5.4. 80

Table 5.6 Comparison between GAs and the improved LBB method for two non-symmetric examples from Table 5.4. 80

Table 5.7 Optimum lamination parameters and Γ for the two methods..... 84

Table 5.8 Optimum stacking sequences for the two methods. 85

Table 6.1 Material properties. 100

Table 6.2 Starting layup and ply thicknesses (mm) (optimised results from Fischer *et al.* (2012)). 101

Table 6.3 Re-distributions of axial load and bending moment after the multilevel optimisation. 102

Table 6.4 Optimisation results of the first stage. 104

Table 6.5 Stacking sequences of top panels without blending constraint. 106

Table 6.6 Lamination parameters of the optimised stacking sequences without blending constraint..... 108

Table 6.7 Stacking sequences of skins with blending constraint. 109

Table 6.8 Stacking sequences of left and right hand side flanges with blending constraint. 109

Table 6.9 Stacking sequences of left and right hand side webs with blending constraint. 109

Table 6.10 Lamination parameters of the stacking sequences of skins. 110

Table 6.11 Lamination parameters of the stacking sequences of left and right hand side flanges. 110

Table 6.12 Lamination parameters of the stacking sequences of left and right hand side webs. 110

Table 7.1 Stacking sequences of skins obtained using DLBB method. 133

Table 7.2 Stacking sequences of left and right hand side flanges obtained using DLBB method. 134

Table 7.3 Stacking sequences of left and right hand side webs obtained using DLBB method. 134

Table 7.4 Stacking sequences of skins obtained using GAGA. 134

Table 7.5 Stacking sequences of left and right hand side flanges obtained using GAGA. 135

Table 7.6 Stacking sequences of left and right hand side webs obtained using GAGA. 135

Table 7.7 Stacking sequences of skins obtained using parallel method. 135

Table 7.8 Stacking sequences of left and right hand side flanges obtained using parallel method. 136

Table 7.9 Stacking sequences of left and right hand side webs obtained using parallel method. 136

Table A.1 Lamination parameters of the layups of skins obtained using DLBB. ... 167

Table A.2 Lamination parameters of the layups of left and right hand side flanges obtained using DLBB. 167

Table A.3 Lamination parameters of the layups of left and right hand side webs obtained using DLBB. 167

Table A.4 Lamination parameters of the layups of skins obtained using GAGA. .. 168

Table A.5 Lamination parameters of the layups of left and right hand side flanges obtained using GAGA. 168

Table A.6 Lamination parameters of the layups of left and right hand side webs obtained using GAGA. 168

Table A.7 Lamination parameters of the layups of skins obtained using parallel method. 169

Table A.8 Lamination parameters of the layups of left and right hand side flanges obtained using parallel method. 169

Table A.9 Lamination parameters of the layups of left and right hand side webs obtained using parallel method. 169

Nomenclature

$\mathbf{A}, \mathbf{B}, \mathbf{D}$	extensional, coupling and bending stiffness matrices
$\mathbf{D}$	nodal displacements vector
d	difference between P_{cp}s for adjacent genes
E_{11}, E_{22}	Longitudinal and transverse moduli
$\mathbf{E}_i$	constraint matrix for $\lambda = \lambda_i$
f	fitness value in genetic algorithm
f'	larger fitness value of the two individuals to be crossed
f_{ave}	average fitness value in the population
f_{max}	maximum fitness value in the population
f_m	mutation factor giving different layers different P_m
f_{ei}	eigenvalue of the unperturbed design
f'_{eij}	eigenvalue of the perturbed design
f_{xi}, f_{yi}, f_{xyi}	longitudinal, transverse and shear force per unit length for each element
$f_{xyplate}$	shear force per unit length for each of the component plates in the panel
f_{yplate}	transverse force per unit length for each of the component plates in the panel
F_{xpanel}	longitudinal axial load of the panel
F_{st}	stabilisation factor
G_{12}	shear modulus
h	laminate thickness

h_p	ply thickness
J	number of eigenvalues which are less than a trial value
J_0	value of J if all the nodal freedoms of the structure were restrained
J_{0i}	J_0 calculated for $\lambda = \lambda_i$
J_m	value of J for a constituent member of a structure when its ends are fixed
$\mathbf{K}$	global stiffness matrix
$s\{\mathbf{K}\}$	sign count of $\mathbf{K}$
$\mathbf{K}^{\Delta}$	upper triangular matrix
$\mathbf{K_m}$	member stiffness matrices
l	panel length
L	interval between which buckling mode repeats in VICON analyses
L_b, U_b	lower and upper bound of branch and bound method
M_x, M_y, M_{xy}	moment resultants
M_{xpanel}	longitudinal bending moment of the panel
N_e	number of elements in the panel
N_l	number of elements along the length of the panel
N_{pl}	number of elements in the component plates
N_{panel}	number of panels in the blended structure
N_x, N_y, N_{xy}	stress resultants
n	total number of layers in the laminate
n_a	number of active constraints
n_{av}	number of active and violated constraints

n_b	number of buckling modes considered
n_{ca}, n_{cy}	case loop number and cycle loop number
n_{cont}	maximum number of successive plies with the same orientation
n_d	number of design variables
n_e	number of genes in the chromosome
n_g	number of inequality constraints
n_h	number of equality constraints
n_{left}	number of layers left to choose in the current case loop
n_θ	number of plies with orientation θ
P	perturbation loads vector
P_c	probability of crossover
P_{cp}	probability of the gene being selected as cross point
P_{cmax}, P_{mmax}, P_{pmax}	maximum values of P_c, P_m and P_p
P_{cmin}, P_{mmin}, P_{pmin}	minimum values of P_c, P_m and P_p
P_i	probability of individual being selected
$P_{i.j}$	position of the layer in the dummy layerwise table
P_m	probability of mutation
P_p	probability of permutation
p_c	actual buckling load of a structure
p_d	required buckling load of a structure
p_{mi}	penalty terms in genetic algorithm
$p_{\min}$	minimum proportion of each fibre orientation

Q_{ij}	items in reduced stiffnesses
$\bar{Q}_{ij}$	items in transformed reduced stiffnesses
$\mathbf{R}$	matrix defined in equation (4.8)
r	number of constraints
S	search space in branch and bound
S_i	subsets of the search space
$\boldsymbol{S}^q$	move direction vector
s	population size
u, v, w	displacements in the *x*, *y*, and *z* direction
U_i	material stiffness invariants
w_{ei}	width of element
w_j	weighting factors
$\mathbf{x}$	a set of design variables
$\mathbf{x}_L, \mathbf{x}_U$	lower and upper bounds of design variables
z	distance between the lamina and the mid-plane
$z_k,$	distance from the mid-plane to the bottom of the layer
Z_u, Z_l	upper and lower limits of f_m
α	scalar move distance
α_e	empirical factor
α_{ij}	perturbation size parameter
β	scalar used to determine the move direction vector

Γ	difference between the target and actual lamination parameters
$\varepsilon_1, \varepsilon_2, \gamma_{12}$	strains in the principal material directions
ε_x^0, ε_y^0, γ_{xy}^0	strains of the mid-plane of the laminate
θ	ply angle
θ_{diff}	difference between the orientations of two adjacent plies
θ_i	factor used to move the design away from the current active constraints
κ_x , κ_y, κ_{xy}	curvatures of the mid-plane of the laminate
λ	longitudinal half-wavelength
λ_i	a set of longitudinal half-wavelengths
υ_{12}	major poisson's ratio
ξ	parameter for VICON analyses
$\xi^A_{1,2,3,4}, \xi^B_{1,2,3,4}, \xi^D_{1,2,3,4}$	in-plane, coupling, and out-of-plane lamination parameters
σ_1, σ_2	stresses in the principal material directions
τ_{12}	shear stress in the principal material direction
φ	penalty term in VICONOPT optimisation
Φ	weighting factor
Ψ	rotation amplitude

Chapter 1
General Introduction

1.1 General background

Composite materials are increasingly being adopted in the aerospace, marine, automotive and civil industries because of their outstanding mechanical performance including high strength-to-weight and stiffness-to-weight ratios, strong resistance to corrosion, fatigue and impact, as well as low thermal expansion (Jones 1999). Composite materials, as the name implies, are made up at least two different types of material, providing advantages in performance over that of the individual constituent materials (Gürdal *et al.* 1999). As one of the most common composite materials, composite laminates are stacked with a set of layers each of which is composed of matrix material and fibres which can be placed with different orientations for different layers as shown in Figure 1.1. The most significant benefit derived from the use of composite laminates over conventional materials is that they can be designed to meet different requirements by tailoring their lay-up to achieve different stiffnesses and strengths.

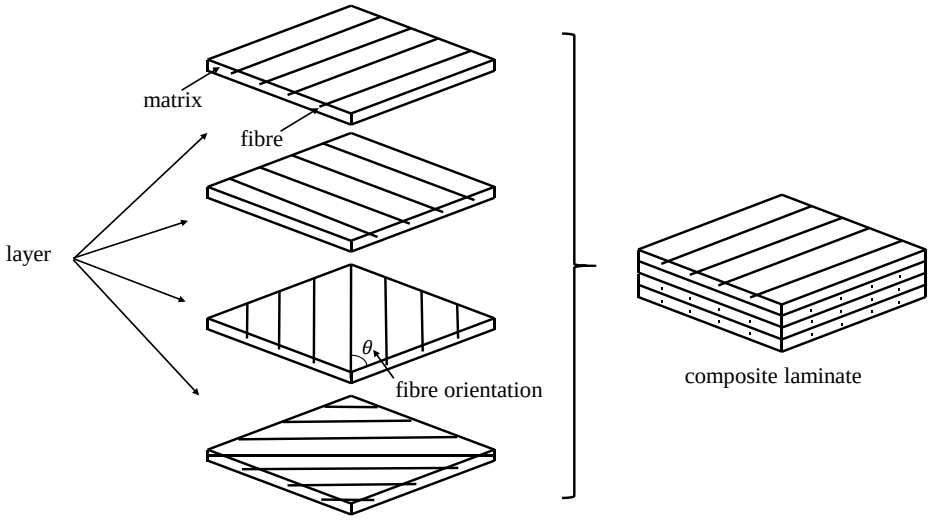

Figure 1.1 The composition of an example composite laminate.

Minimising the weight of vehicles is always a vital problem, which relates to the reduction of CO_2 emissions and the cost of material and fuel. Over a lifetime of 20 years, a reduction of 1 tonne of weight in an aircraft can achieve a reduction of 120 tonnes in CO_2 emissions and roughly 2.7 million pounds worth of fuel (Jenny 2014). According to a report from the International Civil Aviation Organization (ICAO 2013), the global fuel consumption of aircraft will be between 216 and 239 Mt in 2020, causing CO_2 emissions of between 682 and 755 Mt. Besides this, the CO_2 emissions are predicted to be three times higher in 2050 than nowadays. In order to alleviate this problem, targets of fuel efficiency for different periods are set by ICAO, for example the fuel efficiency is expected to improve by an average rate of 1.76 percent per annum for the period between 2020 and 2030. In 2016, ICAO (ICAO 2016) adopted a Carbon Offsetting and Reduction Scheme for International Aviation (CORSIA) to urge its member states to make more contribution to the fight against the growth of fuel consumption and CO_2 emissions in aviation.

In order to meet the growing demand of developing eco-friendly and economical aircraft, the application of lightweight materials to replace conventional metallic materials has been explored over the last few decades. As the best alternative material, composite laminates have been extensively used in aircraft. For example, in the Airbus A350 XWB, composite laminates made of carbon fibre reinforced polymer (CFRP) account for 53 percent of its airframe (Hellard 2008), achieving a 25 percent reduction in fuel burn compared with the conventional aluminium airframe (Poulton 2018). As a star product of Boeing, the Boeing 787 Dreamliner comprises 50 percent CFRP laminate in its airframe even including doors and interiors (Hawk 2005). With related technologies (e.g. maintenance and repair) becoming mature, larger amounts of laminated composite materials will be incorporated into aircraft structures in the future (Morimoto *et al.* 2017).

When designing an aircraft, there are three successive stages as shown in Figure 1.2: conceptual design, preliminary design, and detailed design. First, many different design concepts are proposed in the conceptual design stage during which the basic structural concepts and loading information as well as the chosen materials are defined for the aircraft. In the following preliminary design stage, a great number of candidate

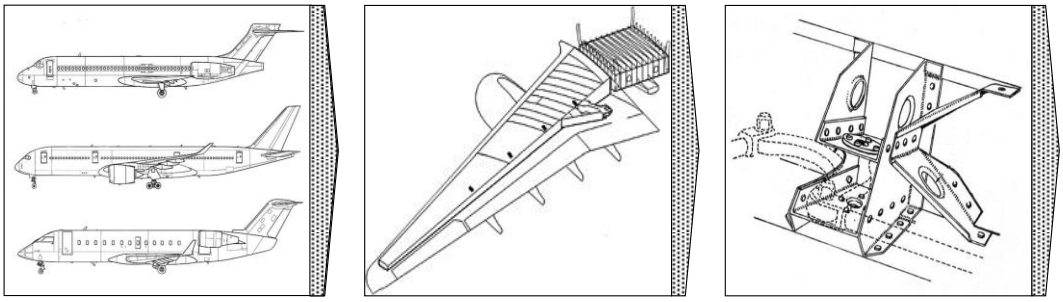

Conceptual design Preliminary design Detailed design

Figure 1.2 The three successive stages for designing an aircraft.

designs are analysed and optimised subject to multidisciplinary requirements in order to obtain the most appropriate design. Large numbers of loading cases are considered in different types of analyses at this stage to model various possible situations. Finally, the complete design information, which includes every single detail of the selected structural components and can be used directly to guide production, is obtained in the detailed design stage. It is necessary to use the most powerful analysis and design methods such as nonlinear Finite Element Analysis (FEA) in the detailed design stage. Compared with the detailed design stage, the preliminary design stage needs less detailed analyses but has to deal with larger numbers of design cases. Therefore, reliable and more efficient design methods need to be employed in the preliminary design stage.

As laminated composite structures are increasingly used in the airframe, the optimised design of them becomes very significant, and can achieve further weight reductions in the aircraft. However, layup optimisation design is still a challenging task, especially the development of highly efficient design tools. To reduce weight or improve structural performance, the ability to vary the stiffness of laminated composite structures can be used to expand the design space by changing the number and fibre orientations of the built-up plies. Consideration of design cost and manufacturing

limitations means that the fibre orientations in laminated composite structures are usually restricted to 0°, 90°, +45° and −45° and the ply thicknesses are always fixed. In addition to this, in order to prolong the service life of these laminated composite structures and avoid structural damage such as delamination and cracking, a number of layup design constraints which provide rules and limitations on choosing the layup for single laminates should be considered in the optimisation (Niu 1992). For example, there is a limitation on the maximum number of successive plies with the same fibre orientation in the laminate to minimise edge splitting. Moreover, for large scale laminated composite structures such as the wings and fuselage, the presence of ply drop-offs further complicates this optimisation as the continuity of plies across adjacent laminates needs to be taken into account. Otherwise, the stacking sequence mismatches of adjacent laminates cause stress concentrations and also increase the level of difficulty in the manufacturing process. Implementing a continuity constraint between adjacent laminates was firstly termed 'blending' by Kristinsdottir *et al.* (2001). Consideration of these layup design requirements narrows the design space; however, the discrete nature and strict rules for stacking sequences inevitably cause more difficulties in the optimisation process.

Genetic algorithms (GAs) have become the most popular method for optimising stacking sequences because of their effective performance in discrete processes. However, as a stochastic search method, GA incur high computational costs and cannot prove that the optimised stacking sequences are globally optimal. Furthermore, with the development of computational technology, parallel computation in which several executions of processes are able to operate simultaneously provides a good way to improve the efficiency of the optimisation design. Research on developing parallel computation methods for layup optimisation focuses on parallel GAs in which the optimisation task is divided into several parts which are then distributed to GAs running on parallel processors. Although parallel GAs can achieve improvements in efficiency, their inherent shortcomings in the stochastic searching process cannot be overcome.

The large number of layers in a laminate results in a large number of design variables in layup optimisation, making the process time consuming. To reduce the number of design variables in the optimisation, lamination parameters which are independent of

the number of layers can be employed instead of the individual ply angles (Tsai *et al.* 1968). When using lamination parameters as design variables, the optimisation is usually divided into two stages where the continuous optimisation of the lamination parameters and laminate thicknesses is implemented in the first stage. The optimised lamination parameters are then used as targets for the discrete optimisation of the stacking sequences in the second stage, the aim of which is to find stacking sequences to match the lamination parameters determined in the first stage as closely as possible.

In contrast to finite element software which requires a large computational resource, the highly efficient panel analysis and optimum design software VICONOPT (Williams *et al.* 1991) provides a potential alternative for layup optimisation and has been extended to include the use of lamination parameters as design variables (Kennedy *et al.* 2010). Earlier limitations in terms of the ability of the code to model three dimensional large scale structures have been addressed through the development of VICONOPT MLO (Fischer 2002) which combines FE analysis of a whole structure, such as an aircraft wing, with VICONOPT optimum design of each of the constituent prismatic stiffened panels, thus avoiding the drawbacks of both techniques. However, lamination parameters have not been used as design variables in VICONOPT MLO. Besides, the stacking sequence is fixed in VICONOPT MLO optimisation and the thickness of each layer is optimised continuously, so no allowance has been made for practical laminate design rules.

1.2 Thesis objectives

From the above, the aim of this thesis is to develop more efficient and reliable two-stage layup optimisation design methods for laminated composite structures to obtain more practical designs based on the use of lamination parameters.

For a single laminate, instead of using the stochastic search method in the second stage, a more effective and efficient layup optimisation method which performs logic search will be developed, with consideration of the layup design constraints. Correspondingly, where possible in the first stage optimisation in VICONOPT, the relationships between lamination parameters and layup design constraints will be explored.

For large scale composite laminates with ply drop-offs, the objective of the first stage optimisation is to introduce lamination parameters as design variables into VICONOPT MLO to expand its design space. Then in the second stage, as the blending constraint significantly complicates the process of searching the layups, the layup optimisation method will be extended for optimising these more complex blended layups.

Moreover, in order to further improve the efficiency of the second stage blending optimisation, a parallel computation method which is able to combine the advantages of both logic and stochastic-based search methods is proposed. To do this, a guide-based blending method incorporating an improved adaptive genetic algorithm will be developed and implemented in the parallel process with the extended layup optimisation method in order to achieve better optimisation results.

1.3 Thesis structure

This thesis has been divided into eight chapters. Following the general introductions in this chapter, Chapter 2 provides a literature review of the optimisation of laminated composite structures.

In Chapter 3, a background to the theories of optimisation is presented, including the mechanics of composite laminates, the use of lamination parameters to express stiffness matrices, and the feasible direction method (Vanderplaats and Moses 1973) which is the embedded continuous optimisation method used in VICONOPT. The principles of two discrete optimisation methods, GAs and the branch and bound (BB) method are also described. Finally, the mechanism of parallel computation is introduced at the end of the chapter.

Chapter 4 gives a description of the main features of VICONOPT. The fundamental theories of VICONOPT are described first. Then, as the two basic analyses available in VICONOPT, VIPASA and VICON are introduced and the differences between them are presented. After that, the basic optimisation features of VICONOPT are described, followed by an introduction to employing lamination parameters as design

variables in VICONOPT. Finally, the optimisation features of VICONOPT MLO are presented.

Chapter 5 presents a two-stage layup optimisation method for a single laminate. VICONOPT is employed to optimise the lamination parameters and laminate thicknesses in the first stage optimisation. After that, in order to ensure the optimised layup obtained in the second stage can be used in practice, several layup design constraints are added into the Layerwise Branch and Bound method (LBB) combining the branch and bound method with a global layerwise technieque. In addition, the feasible region for the lamination parameters with a layup design constraint which requires a minimum percentage of each of four possible ply orientations is studied. Good performance of this method is illustrated by comparison with a GA for a range of problems with different combinations of the layup design constraints, as well as comparisons with the results of other researchers' work (Herencia *et al.* 2007).

In Chapter 6, the two-stage method is extended for optimising large scale blended laminates. The optimisation capability of VICONOPT MLO is improved to use lamination parameters and laminate thicknesses as design variables instead of the real layup and this software rather than VICONOPT is used in the first stage of the optimisation. Then to determine the complex blended layups in the second stage, a new Dummy Layerwise Branch and Bound method (DLBB) is presented. This two-stage method is applied to a wing box benchmark problem (Fischer *et al.* 2012) to demonstrate its efficacy and potential.

Chapter 7 describes a parallel computation method developed for the second stage optimisation for blended laminates. Firstly, a Guide-based Adaptive Genetic Algorithm (GAGA) is developed for searching the layups to match the target lamination parameters obtained from the first stage optimisation. After that, this stochastic-based search method GAGA is employed in a parallel computation method to run in parallel with the logic-based search method DLBB developed in Chapter 6 to optimise the layups of blended laminates, combining the advantages of both types of searches. Results compare the three methods, which are presented after the descriptions of the methods.

Chapter 8 offers conclusions for this work along with recommendations for the development of the proposed methods in future work.

1.4 Publication list

Journal papers:

Liu, X., Featherston, C.A. and Kennedy, D. (2019). Two-level layup optimization of composite laminate using lamination parameters. *Composite Structures* **211**: 337-350. doi: https://doi.org/10.1016/j.compstruct.2018.12.054.

Liu, X., Featherston, C.A. and Kennedy, D. Optimization of blended composite structures using lamination parameters. Submitted to Thin-Walled Structures (2019).

Liu, X., Featherston, C.A. and Kennedy, D. Optimization of blended composite structures using parallel computation method. To be submitted to Computers and Structures (2019).

Conference papers:

Liu, X., Patel, H., Featherston, C.A. and Kennedy, D. (2016). Two level layup optimization of composite plate using lamination parameters. *Proceeding of the 24th UK Conference of the Association for Computational Mechanics in Engineering*. pp. 205-208.

Liu, X., Featherston, C.A. and Kennedy, D. (2018). Two-stage layup optimization of blended composite structures using lamination parameters. *21th International Conference on Composite Structures*. pp. 27-28.

Chapter 2
Literature Review

As composite structures can be specified for particular applications by tailoring their layups, the optimisation of composite structures has attracted a large amount of research and many optimisation methods have been developed. In this chapter, a review of the literature on the research related to this thesis is presented.

2.1 Continuous optimisation for composite structures

In contrast to the optimisation of isotropic panels which mainly focuses on the structural geometry and cross sectional dimensions, the optimisation of composite structures pays more attention to their layups which dominate their structural performance. Layup optimisation is always a complex and challenging task because of its non-convex, non-linear, multi-dimensional nature in the space of the ply angles and the large number of design variables which can be both continuous and discrete. In some research, especially earlier research, layup optimisation is treated as a continuous optimisation problem by allowing the ply thicknesses or ply angles to have continuous values, for which mathematical programming methods (MP) are generally required. Schmit and Rarshi (1977) minimised the weight of symmetric and balanced laminates by the continuous optimisation of the ply thicknesses for some preselected layups by using a linear programming (LP) method. The non-linear strength and buckling constraints needed to be linearised for the linear programming method in the optimisation. Hu (1991) employed a sequential linear programming (SLP) method together with a move-limit procedure to conduct a layup optimisation for buckling load maximisation with the ply angles treated as continuous design variables. The finite element method (FEM) was employed for the buckling analysis in the optimisation process. As layup optimisations are always non-linear optimisation problems, non-linear mathematical programming methods are more widely used. Kicher and Chao (1971) conducted a continuous optimisation of ply angles and structural dimensions for the weight minimisation of composite cylinders using a quasi-Newton (QN)

method (Fletcher and Powell 1963). Hirano (1979) maximised the buckling load of composite laminates by optimising the ply angles, which have continuous values, using Powell's conjugate direction method (Powell 1964). Powell's method was also used by Sun and Hansen (1988) and Sun (1989) for the buckling load maximisation of laminated cylindrical shells with continuous ply angles as design variables. As Powell's conjugate direction method doesn't require the derivative of the objective function, fast convergence can be achieved. Bruyneel and Fleury (2002) employed a sequential convex programming method (SCP) based on the method of moving asymptotes (MMA) for the continuous optimisation of composite structures in which the design variables could be the structure's geometry, ply thickness or ply angles. As the most commonly used gradient-based optimisation method, sequential quadratic programming (SQP) was also employed for the continuous layup optimisation problem in the works of Mahadevan and Liu (1998); Liu (2001) and Blasques and Stolpe (2011) to minimise the weight of composite structures with continuous ply thicknesses and ply angles as design variables.

The method of feasible directions (MFD) (Vanderplaats and Moses 1973) was also found to be an effective continuous optimisation method for composite structures (Vanderplaats and Weisshaar 1989). It then played an important role in further research. Fukunaga and Vanderplaats (1991) optimised ply thicknesses and ply angles with continuous values to minimise the weight of composite laminates subject to strength constraints using MFD. Kumar and Tauchert (1991) utilised MFD to optimise continuous ply thicknesses and ply angles for the maximisation of buckling capacity, the buckling solutions being obtained by the Rayleigh-Ritz method. Spallino *et al.* (1999) optimised the continuous ply thicknesses of some preassigned layups to minimise weight using MFD. Topal and Uzman (2007; 2009) conducted layup optimisations to achieve buckling load maximisation by changing the continuous ply angles under different boundary conditions. MFD was employed for the optimisation processes along with the FEM for the buckling analysis. In Butler and Williams (1992), MFD was employed as the underlying method in VICONOPT for the continuous optimisation of composite laminates, and the exact strip method was employed for the buckling analysis in the optimisation process. As a common drawback of the gradient-based optimisation methods, the continuous layup optimisations may trapped in a local optimum, however, this can be compensated for using different starting points.

Continuous layup optimisation can also be implemented with lamination parameters and polar parameters as design variables. A review of using lamination parameters for layup optimisation is given in Section 2.4, but the utilization of polar parameters is not reviewed in this thesis. A comprehensive review can be found in Albazzan *et al.* (2019).

2.2 Discrete optimisation for composite structures

Because of the manufacturing requirements for composite structures, ply angles are usually restricted to specific values and the thickness of an individual ply is fixed in practice. Discrete layup optimisation is therefore more meaningful for practical design and so has attracted more interest from researchers. Due to the presence of discrete design variables, the continuous optimisation methods mentioned above are not appropriate for such optimisations, and discrete optimisation methods should be explored. Park (1982) optimised two ply angles with opposite values to maximise the strength of composite laminates, all the values of the ply angle being investigated by using a enumeration method. Graesser *et al.* (1991) employed a random search method to optimise the ply angles to obtain laminates with the least number of plies which could satisfy specified strength constraints. Haftka and Walsh (1992) and Nagendra *et al.* (1992) used the integer programming method for the buckling optimisation of symmetric and balanced composite laminates. When searching the stacking sequence during the optimisation process, the continuity layup design constraint, limiting the maximum number of successive plies with the same fibre orientation to be four, was expressed mathematically by four binary variables coded for the four permitted ply orientations. Kim and Hwang (2005) optimised stacking sequences to minimise strain energy using the branch and bound method based on an ideal layer procedure. The ideal layers, initially assigned with unachievable stiffnesses, were replaced by real layers in the sequence. Hence the lower bounds of branches inevitably increase, and if any exceeds the upper bound the branch can be discarded directly without further exploration. In contrast to the enumeration method, the bounding process in the branch and bound method prunes the poor branches in the decision tree which have been proved unable to improve on the objective function, so improving the efficiency.

Over the past decades, genetic algorithms (GAs) based on a heuristic search have become the most popular method for layup optimisation problems. Callahan and Weeks (1992) conducted layup optimisation to minimise the weight of composite laminates under strength and stiffness constraints using GAs. Le Riche and Haftka (1993) optimised the stacking sequences of composite laminates for buckling load maximisation subject to strain and continuity constraints using GAs. A permutation operator which shuffles the order of plies was firstly developed for stacking sequence optimisation, achieving reductions in the cost of the genetic search. Nagendra *et al.* (1996) applied GAs for the minimum weight design of stiffened composite laminates subjected to buckling and strain constraints. Todoroki and Sasai (1999) maximised the buckling load of balanced composite cylinders subject to continuity and another disorientation layup design constraint which requires the angle difference between two adjacent plies to be no greater than 45° using GAs. The constraints were implemented with a repair procedure instead of using the conventional penalty method. In Soremekun *et al.*'s work (2001), an elitism procedure which can propagate the best results to the next generation in a GA was improved to enhance its searching capability. The improved GAs were applied to a layup optimisation for the buckling load maximisation of a simply supported laminate, and results suggested that the genetic search had a better performance. Park *et al.* (2008) used GAs with a memory technique and an improved permutation operator to improve the efficiency of minimum weight optimisation of composite laminates. In Walker and Smith (2003); Deka *et al.* (2005); Almeida and Awruch (2009), multi-objective layup optimisation methods for composite laminates were explored, in which GAs were utilised in combination with FEM. Although FEM has been a common analysis method for layup optimisation, it incurs a high computational cost. As GAs require a huge number of fitness function evaluations during the iterative search process, employing FEM for structural analysis makes the searching process time-consuming. In Abouhamze and Shakeri (2007), GAs were associated with an artificial neural network (ANN) which was trained by several FEAs and used for fitness function evaluation to improve the efficiency of the optimisation for maximising the natural frequency and buckling load of cylindrical laminates. In Liu *et al.*'s work (2008), the highly efficient exact strip software VICONOPT was employed for the fitness function evaluation of GAs in a two-stage layup optimisation subject to strength, buckling and layup design constraints. In the first stage, the laminate was treated as an equivalent orthotropic panel for which

continuous optimisation was conducted on the cross sectional dimensions using the design option of VICONOPT. Then, in order to substitute the orthotropic panel with a laminate, GAs were used to select discrete stacking sequences in the second stage during which the structural performance of the laminate was evaluated by the analysis option of VICONOPT. Irisarri *et al.* (2011) employed GAs for the optimisation of stiffened composite laminates, the fitness functions being obtained based on approximated structural performances. Sadr and Bargh (2012) conducted layup optimisation for maximising the natural frequency of symmetric laminates using GAs along with the finite strip method for structural analysis. Le Manh and Lee (2014) used GAs combined with isogeometric analysis in layup optimisation for maximising the strength of composite laminates. In order to improve the efficiency of layup optimisation with GAs, some efforts have been made to develop adaptive GAs (AGAs). As the performance of GAs is mainly dependent on the parameters chosen, an AGA which provides variable probabilities for crossover and mutation according to the performance of each chromosome was firstly introduced in Srinivas and Patnaik (1994). Hwang *et al.* (2014) applied AGAs for stacking sequence optimisation for maximising the natural frequencies of composite laminates. An *et al.* (2015) utilised AGAs for the minimum weight design of composite laminates under strength and buckling constraints.

Apart from GAs, some other heuristic search methods for layup optimisation have also been studied. Aiming at obtaining the maximum buckling capacity of composite laminates, Erdal and Sonmez (2005) conducted stacking sequence optimisation by using the simulated annealing (SA) algorithm. In Akbulut and Sonmez (2011), SA was applied for the minimum weight design of composite laminates subject to in-plane and out-of-plane loadings with the number of plies and ply angles as design variables. In the early stage of the SA optimisation process, poor results are also acceptable with a probability, to prevent the premature convergence. Suresh (2007) and Kathiravan and Ganguli (2007) employed the particle swarm optimisation (PSO) algorithm for the optimal design of a composite box-beam structure with the ply angles as design variables. Chang *et al.* (2010) conducted stacking sequence optimisation for maximising the buckling loads of composite laminates under a continuity constraint using PSO. A memory procedure was applied to prevent evaluating repeated layups to reduce solution time. Bargh and Sadr (2012) maximised the natural frequency of

composite laminates by optimising their ply angles using PSO. The ant colony algorithm (ACA) was utilised in Aymerich and Serra (2008); Wang *et al.* (2010) and Sebaey *et al.* (2011) for layup optimisation in maximising the buckling load capacity of composite laminates. Fakhrabadi *et al.* (2013) employed the discrete shuffled frog leaping (DSFL) algorithm for minimising the weight and cost of composite laminates simultaneously with ply thickness, ply angles and number of plies as design variables. The PSO, ACO and DSFL methods are all population-based methods based on mimicking the behaviours of animals in nature. Pai *et al.* (2003) employed the tabu search (TS) method to optimise the stacking sequence of symmetric and balanced composite laminates for maximisation of buckling and strength capacity under continuity constraint. The advantage of the TS method is that the previously searched results are not allowed to recur in the following steps. Rao and Arvind (2005) investigated the application of the scatter search (SS) method to the layup optimisation of composite laminates for both maximisation of the buckling capacity for a certain thickness and minimisation of the weight subject to the required constraints. Hemmatian *et al.* (2014) used the gravitational search algorithm (GSA) to conduct layup optimisation to achieve minimum weight and cost for composite laminates. Jing *et al.* (2015b) proposed a permutation search algorithm for the buckling load maximisation of composite laminates. In the work of Almeida (2016), the harmony search algorithm (HSA) was utilised for stacking sequence optimisation for maximising the buckling performance. A new solution is generated according to all the solutions in the current group. In addition, hybrid methods which combine the merits of some of the above methods have also been explored. The SA was combined with TS in Rao and Arvind (2007) to maximise the buckling load of composite laminates under strain and continuity constraints, so once a result is evaluated in SA process it will not be revaluated again, reducing the computational cost. To improve the efficiency of layup optimisation, hybrid GA-PSO methods have been developed for weight minimisation (Barroso *et al.* 2017) as well as buckling load maximisation (Vosoughi *et al.* 2017), the mutation operator of GA is implemented into the PSO optimisation process to provide more diversity to the solutions. Moreover, instead of using a heuristic optimisation method, Bruyneel *et al.* (2012) optimised the discrete ply angles of composite laminates based on a topology optimisation technique which defined the stiffness of each ply as a weighted sum of the candidate stiffness properties

related to different ply angles, converting the discrete ply angle optimisation into a continuous optimisation of weighting factors.

2.3 Multilevel optimisation

When designing large scale composite structures such as an aircraft wing or fuselage which includes complex geometry and a large number of design variables, multilevel optimisation based on the idea of divide and conquer provides a good solution. Multilevel optimisation consists of design iterative loops between the global level process which implements optimisation or analysis for the entire structure and the local level process which separately optimises the structural components in detail, decomposing a large optimisation problem into several small ones. Multilevel optimisation was proposed in the 1970s, and was employed for the minimum weight design of an aircraft wing (Giles 1971) and fuselage (Sobieszczanski and Leondorf 1972). Schmit and Mehrinfar (1982) developed a multilevel optimisation method for minimising the weight of an aircraft wing made of stiffened composite laminates. In Watkins and Morris (1987); Kam and Lai (1989) and Antonio *et al*. (1995), multilevel optimisation was employed to optimise ply thicknesses and angles which were taken as continuous design variables for achieving minimum weight design of large composite structures. In order to improve the efficiency of the multilevel optimisation, a response surface method was used to replace the time consuming buckling analysis techniques in the optimisation process in Balabanov *et al*. (1996); Ragon *et al*. (1997) and Liu *et al*. (2000). In Liu *et al*.'s work (2000), a two level optimisation method based on the response surface method was developed, with continuous optimisation for ply thicknesses carried out to minimise the weight of the whole wing structures at the global level, and then stacking sequences with maximum buckling capacity obtained by discrete optimisation using a permutation GA during a local level optimisation. Gasbarri (2009) employed multilevel optimisation to determine the stacking sequences which achieved maximum flutter speed for an aircraft wing.

In the 1990s, the Group for Aeronautical Research and Technology in Europe (GARTEUR) reviewed and investigated multilevel optimisation for the design of composite aircraft wings in collaboration with industry and academia. The GARTEUR

Action Group published their research in a three volume report (GARTEUR 1997a,b,c), and multilevel optimisation employing existing analysis and optimisation software for the overall system level and more detailed panel level was recommended. In response to this, the multilevel optimisation software VICONOPT MLO (Fischer 2002) was developed at Cardiff University. The finite element software MSC/NASTRAN (MSC Software Corporation 1999a) was employed to implement the static analysis of the whole structure at system level, and the highly efficient finite strip software VICONOPT was used for the optimum design of each of the structure's components based on the results of this static analysis at panel level. The multilevel optimisation was based on the interactions of the design variables and loading conditions between these two levels during the iterative process. In its later version, VICONOPT MLOP (Qu *et al*. 2011), the multilevel optimisation was extended to include postbuckling effects.

2.4 Lamination parameters

In order to reduce the large number of design variables in composite layup optimisation, lamination parameters which are independent of the number of plies were first introduced in Tsai *et al.* (1968). The stiffness matrix can then be expressed as a linear function of these lamination parameters instead of the conventional set of equations with a large number of ply orientations. Grenestedt and Gudmundson (1993) demonstrated that the optimisation problem is convex if the lamination parameters are employed as design variables.

2.4.1 Feasible regions of lamination parameters

The feasible regions of lamination parameters should be treated as constraints when employing lamination parameters as design variables. At the very beginning of the work on lamination parameters, the feasible regions of two in-plane parameters (Miki 1982) and two out-of-plane parameters (Miki 1985) were defined for symmetric laminates which excluded extension-bending coupling. Then the feasible regions of four in-plane or four out-of-plane lamination parameters of symmetric laminates were determined in Fukunaga and Sekine's works (1992; 1994). For specially orthotropic laminates which exclude shear-extension, extension-bending, and bending-twisting

couplings, the feasible regions of the two membrane and two bending lamination parameters and the relations between the membrane and bending lamination parameters were studied in Fukunaga and Vanderplaats (1991). Later, in Grenestedt and Gudmundson (1993), more accurate relationships between the lamination parameters were presented. Up to now, the most accurate feasible regions of lamination parameters for specially orthotropic laminates were obtained by Wu *et al.* (2013). In later work (Raju *et al.* 2014), the shear-extension and bending-twisting coupling effects were considered, and the explicit feasible regions of the four membrane and four bending lamination parameters were determined.

In Diaconu *et al.* (2002), the feasible regions in the general design space of the total twelve lamination parameters were first presented. Setoodeh *et al.* (2006) obtained approximated feasible regions of lamination parameters which were expressed as linear inequality constraints. Liu *et al.* (2004) obtained a hexagonal feasible region for the out-of-plane lamination parameters for given amounts of 0°, 90°, +45° and −45° plies. After that, explicit expressions between the membrane, coupling and bending lamination parameters when the ply angles were restricted to 0°, 90°, +45° and −45° were determined in Diaconu and Sekine (2004). Bloomfield *et al.* (2009) investigated the feasible regions of lamination parameters for any predetermined set of ply angles, and as an example, the feasible regions of lamination parameters for ply angles restricted to 0°, ±30°, ±45°, ±60° and 90° were presented.

One shortcoming of using lamination parameters as design variables is that it is hard to implement the strength and layup design constraints into the feasible regions, because these constraints are usually ply-dependent problems. Ijsselmuiden *et al.* (2008) studied the feasible regions of lamination parameters when implementing the Tsai-Wu strength criteria to the optimisation problem, although the obtained domains in the feasible regions were conservative. In Abdalla *et al.*'s work (2009), the feasible regions of lamination parameters with consideration of the layup design constraint requiring each ply angle (without restricting the values to 0°, 90°, +45° and −45°) to comprise a proportion of at least 10% of the total layup for balanced laminates were obtained. Both the feasible regions obtained for strength and those based on layup

design constraint in these two pieces of research were obtained regardless of restrictions on ply angles.

2.4.2 Optimisation methods based on lamination parameters

Miki and Sugiyama (1993) maximised the stiffness and strength of symmetric and orthotropic laminates using a graphical design approach based on the feasible regions of two flexural lamination parameters. In Kogiso *et al.*'s stacking sequence optimisation (1994), an approximation method based on two flexural lamination parameters was employed to reduce the cost of buckling evaluations in GAs. Fukunaga *et al.* (1995) obtained the maximum buckling performance of symmetric laminates by optimising four flexural lamination parameters using MFD. The stacking sequences corresponding to the optimised lamination parameters were then obtained by investigating the geometrical characteristics of the feasible regions of the lamination parameters. Foldager *et al.* (1998) minimised the compliance of laminates with ply angles as design variables. The lamination parameters of the optimised layups were obtained and used to calculate the sensitivity information needed to determine a new starting layup for the optimisation, which utilised the convexity of the design space of lamination parameter to avoid local optimum results.

Most common optimisation methods based on lamination parameters are developed by dividing the optimisation into two stages where the continuous optimisation of the lamination parameters is followed by discrete optimisation of the stacking sequences. Yamazaki (1996) first proposed this two-stage method. In his first stage optimisation, the in-plane and out-of-plane lamination parameters and structural dimensions were optimised to achieve maximum buckling performance using a LP method, then in the second stage GAs were employed to search for the layup which has lamination parameters closest to the optimised lamination parameters obtained in the first stage. After that, a lot of explorations were made for developing more appropriate methods for the two-stage optimisation. Todoroki and Haftka (1998) improved the second stage optimisation by adding a repair strategy to the GA for implementing layup design constraints. With the purpose of finding layups having a better match to the target lamination parameters, Autio (2000) investigated the performances of GAs with different coding schemes for the second stage optimisation. The ply thicknesses were

also considered as design variables in the GAs with a fitness function added with penalty terms for implementing layup design constraints. In Todoroki and Sasai (2002) and Todoroki and Ishikawa (2004), continuous optimisation was employed first to obtain the optimal lamination parameters based on a global response surface approximation and then a more accurate approximation was constructed around this optimum using a zooming response surface method. Secondly, a GA was used to optimise the stacking sequence around the optimal lamination parameters and the buckling performance of each individual layup was evaluated by the obtained approximations. Herencia *et al.* (2007; 2008) developed a two-stage method for minimising the weight of long anisotropic laminates with T-shaped stiffeners. Firstly, the three membrane and three flexural lamination parameters and laminate thicknesses were optimised by mathematical programming under buckling, strength and lamination parameters constraints, and secondly the obtained lamination parameters were used as targets in a GA to find the actual layup subjected to layup design constraints. In their later work (Herencia *et al.* 2008), a first order linear Taylor series was used to approximate the design constraints and to form the fitness function of the GA in order to improve the second stage optimisation. Irisarri *et al.* (2012) optimised the lamination parameters for buckling load maximisation in a first stage based on a successive approximation technique, and then the stacking sequence was optimised in a second stage where a GA based on multipoint structural approximation was performed starting from the optimum results of the first stage. The approximation methods are used to reduce the computational cost of the constraint evaluations. Liu and Toropov (2013) optimised the number of plies of each ply angle (0°, 90°, +45° and $-45°$) and the flexural lamination parameters to minimise the weight of laminates during the first stage of their optimisation, followed by a permutation GA used to shuffle the ply orders to match the optimised flexural lamination parameters at the second stage. Wu *et al.* (2014) conducted a two-stage layup optimisation for orthotropic laminates considering postbuckling behaviour. Moreover, the two-stage layup optimisation method was also employed in Kameyama and Fukunaga (2007); Dillinger *et al.* (2013); Bach *et al.* (2017) and Othman *et al.* (2018) for aeroelastic tailoring problems, with the consideration of flutter and divergence speed etc.

Although the second stage of these two level optimisations is a pure mathematical problem without time-consuming structural analysis, the high computational cost of

GAs should not be neglected especially for laminates with large numbers of plies. Many alternative methods have been explored to improve the effectiveness and efficiency of the second stage optimisation. Bloomfield *et al.* (2009) employed a PSO to search for optimum stacking sequences in the second stage optimisation. In their later work (2010), the selection of ply angles by GAs, PSO and ACA was investigated and the methods compared, concluding the ACA to be the best for discrete layup optimisation. Whilst good results could be obtained using ACA and PSO, as heuristic algorithms they still required high computational resources. Todoroki and Terada (2004) and Todoroki and Sekishiro (2008) proposed a fractal branch and bound method combined with a response surface approximation for determining optimal stacking sequences. Benefiting from the fractal pattern of branches, all the neighbouring layups near the optimal lamination parameters were efficiently searched. Besides, in order to avoid defining the feasible regions of the lamination parameters, Dutra and Almeida (2015) created a laminate database which stores the lamination parameters for all possible laminates. Hence stacking sequences can be obtained directly once the optimal lamination parameters are determined.

In Narita (2003) and Narita and Turvey (2004), a layerwise optimisation (LO) method, based on the fact that the outer layers have greater influence on the bending effect than the inner layers, was proposed for the layup optimisation of symmetric composite laminates in order to maximise fundamental natural frequencies and buckling performance. Instead of optimising the layers simultaneously, they were optimised sequentially from the outermost layers, the layers that had not been optimised being initially assumed to have zero stiffness. This process solves multi-dimensional optimisation problems using a one-dimensional search, improving the efficiency of the optimisation. The LO method was also employed for the optimisation of laminated sandwich structures (Honda *et al.* 2013; Akoussan *et al.* 2017). Honda *et al.* (2009) proposed a two-stage optimisation method to maximise the natural frequencies of a composite laminate. The four out-of-plane lamination parameters were optimised in the first stage, then in the second stage a LO method was utilised to search the corresponding stacking sequences. However, the LO methods described above has the drawback of getting trapped in local optimum solutions. A LBB method combining an improved layerwise technique with the branch and bound method was explored in a two-stage optimisation by Kennedy *et al.* (2010), in which the exact strip software

VICONOPT was extended by introducing lamination parameters as design variables in the first stage. The optimised lamination parameters were treated as targets in the second stage and the optimal stacking sequence, which has lamination parameters closest to the targets was obtained efficiently using the LBB method.

2.5 Blending optimisation

In real applications, stiffness variation for different parts of laminated composite structures is often required, which can be achieved by changing either the fibre orientation over the plane of each ply or the thicknesses of different laminates in different parts of the structure. Detailed reviews regarding the optimisation of variable angle tow laminates can be found in Nikbakt *et al.* (2018) and Albazzan *et al.* (2019). This section concentrates on variable stiffness laminates with ply drop-off. In large scale built-up composite structures, drop-off results in changes in thickness and layup between adjacent panels, potentially leading to stacking sequence mismatches, causing stress concentrations as well as increasing the level of difficulty in the manufacturing process. Therefore, ensuring ply continuity between adjacent panels, which is commonly referred to as a blending problem (Kristinsdottir *et al.* 2001), is essential. Consequently as well as layup design constraints, blending constraints should also be considered when designing multi-panel composite laminated structures in practice.

Liu and Haftka (2001) optimised a wing box structure for weight minimisation with the consideration of a blending constraint which was implemented by measuring the continuities of material composition and stacking sequences between adjacent panels with mathematical expressions. These measurements can be treated as general design constraints and are easily implemented on the design variables in the optimisation process. However, if the number of design variables is large, implementing the blending constraints in such a way could result in highly constrained problems. Therefore, several optimisation methods which are able to output blended stacking sequences without adding extra constraints have been developed. In the minimum weight optimisation performed by Kristinsdottir *et al.* (2001), the greater-than-or-equal-to method which consistently drops plies from the thickest region to the periphery was proposed and combined with a random search method to optimise

blended layups. However, once a ply is dropped when designing a thinner laminate, then it is not allowed to be added back for a thicker laminate. Soremekun *et al.* (2002) developed a GA-based method incorporating the concepts of sub-laminate and design variable zones for the optimisation of a 3×3 array of sandwich panels and an 18-panel horse-shoe shaped structure in which the load for each panel was fixed. First of all, each design variable zone (i.e. panel) was optimised individually to obtain the minimum weight. According to the optimised layup, sub-laminates composed of the same continuous layers in adjacent design variable zones were determined and used for the blending optimisation. If the blended laminates could not satisfy the constraints, layers needed to be added to the sub-laminates and then each design zone was individually optimised again. This process was repeated until the convergence requirements were met. Following this further concepts and methods based on GAs were developed to obtain blended structures. Adam *et al.* (2004) proposed the guide-based blending method, a template stacking sequence, which was used as a guide and, together with the number of plies for the component panels, was optimised using GAs. The blended structures were then obtained by inwardly or outwardly dropping plies from the guide. The guide-based method was then utilised in Adam *et al.* (2007) for the multilevel layup optimisation of a wing box structure where the load in each panel was not fixed. Then in Seresta *et al.*'s work (2007), the optimisation was improved by limiting the number of plies that are added or deleted for each panel at local level, preventing large changes after the local level optimisation, and so reducing the number of global analyses. Although the blending problem can be easily solved using the guide-based method, the flexibility of the design is seriously restricted.

Liu and Butler (2007) implemented ply drop-off by a tabular method which repeats a pre-defined sub-laminate in a stacking sequences table to produce layups for component panels. Liu and Krog (2008) developed a method based on the use of ply layout cards to impose blending constraints. The ply layout cards in terms of different layer orientations were produced based on the optimised laminate thicknesses and ply percentages. The number of cards equals the number of layers of the thickest panel and the card contains the existence information of a ply angle for the whole structure. Blended layups can be obtained by optimising the sequence of the ply layout cards using a permutation GA. The shared-layer blending (SLB) method, which also requires the number of plies in each panel to be optimised in advance, was firstly proposed in

the work of Liu *et al.* (2011). Firstly, the panels were ranked in terms of the number of plies, then the layers which exist in all panels were taken into the first set, and similarly the rest of the sets which consisted of the remaining identical layers between adjacent panels in sub-regions of the whole structure were subsequently obtained. After that, a permutation GA was employed to shuffle the layers in each set to optimise the stacking sequence. In the work of Irisarri *et al.* (2014), a stacking sequence table (SST) method which includes the stacking sequences of each panel and thickness distribution over the whole structure was developed and combined with an evolutionary algorithm for optimising the blended structure. To ensure the continuity of the structure, plies were added one by one from the thinner panel to the thicker one in the SST. Jing *et al.* (2015a; 2016) developed a global sheared layer blending method based on the SLB. When creating a new set of layers, the SLB was improved by combining with a panel-continuity technique to determine accurate shared-layer distributions over the structure. The SST was then used to obtain the stacking sequences based on the shared layers of GSLB. More reasonable distribution of shared layers can be obtained when the structures are divided into several separate sub-regions. Fan *et al.* (2016) introduced a GA with ply-composition and ply-ranking chromosomes for each individual, the use of these two chromosomes ensures the obtained layup of each individual panel automatically satisfies the blending constraint. Yang *et al.* (2016) proposed a ply drop sequence method (PDS) which is an extension of the guide-based method. Instead of dropping plies inwardly or outwardly, any plies in the thicker panel could be dropped to obtain a thinner one, and hence, compared with the conventional guide-based method, the PDS method provides more design flexibilities. Due to the good performance and ease of implementation of PDS, similar concepts were later applied to the optimisation of tapered wind turbine blades (Albanesi *et al.* 2018) and tapered aircraft wing panels (Shrivastava *et al.* 2019). In contrast to the blending optimisation methods based on stochastic search, an enumeration method was employed in Zein *et al.* (2014; 2016) to search the blended layups with predefined numbers of layers for each ply orientation. The stacking sequences violating the layup design constraints were pruned away during the backtracking process to improve the efficiency. Sørensen *et al.* (2014) proposed a Discrete Material and Thickness Optimisation (DMTO) which is a topology inspired method for blending problems. The discrete optimisation problem can thus be solved using a continuous optimisation method, but this method only allows external ply drop-offs. Recently, Sjølund *et al.*

(2018) improved the DMTO method by allowing internal ply drop-offs during the blending optimisation process. In Zeng *et al.*'s work (2019), a multiple SST was combined with a SA to optimise stacking sequences for composite structures with ply drop-offs. Rather than employing one template in the SST blending optimisation, different templates were used for separate sub-regions.

When introducing lamination parameters as design variables for the optimisation of blended composite structures, a number of two-stage optimisation methods have been developed. Ijsselmuiden *et al.* (2009) proposed a two-stage method for optimising blended stacking sequences. The out-of-plane lamination parameters and thickness of each panel were optimised under a local buckling constraint to minimise the weight during the first stage using a successive approximation scheme, following which a guide-based GA based on single-point structural approximation was utilised to optimise the blended stacking sequences starting from the optimum results obtained in the first stage. In Liu *et al.*'s work (2015), the SQP method was employed together with FEA in the first stage to conduct a weight optimisation where the out-of-plane lamination parameters and the number of plies of each angle were used as design variables. After that, in order to match the optimised lamination parameters with the given number of plies, the SLB method combined with permutation GAs was employed to search the blended stacking sequences of the whole structure subject to a number of layup design constraints and criteria in the second stage. There are no time consuming constraint evaluations in the second stage optimisation, which is more important to these large-scale blended structures. In order to decrease the discrepancy between the continuous and discrete optimisations caused by the blending constraint, Macquart *et al.* (2016) studied the blending constraints in lamination parameter space. The derived blending constraint was applied to aeroelastic optimisation of an aircraft wing (Macquart *et al.* 2017), but it made the optimisation non-convex if the lamination parameters and the laminate thicknesses were both employed as design variables. By utilising multipoint structural approximation in a two-stage optimisation, Meddaikar *et al.* (2017) minimised the weight of a large-scale composite structure based on lamination parameters and laminate thicknesses in the first stage, with the blended stacking sequences obtained using SST combined with GAs in the second stage.

2.6 Layup optimisation based on parallel computation

In order to improve the efficiency of layup optimisation, some efforts have been made to use parallel computation methods. Punch *et al.* (1994) employed a coarse-grain parallel GA for the optimisation of a composite beam. The population of GAs was divided into several subpopulations which were distributed to different processors with a migration operator for exchanging information between them. The optimisation was speeded up by solving small problems separately based on the subpopulations, and the individual exchanges between subpopulations decreased the probability of premature convergence. Henderson (1994) conducted layup optimisation of composite laminates using parallel GAs. The GA operations (i.e. selection, crossover, mutation) were implemented in a main processor for the whole population, with only the time-consuming fitness evaluations parallelized. This parallel GA process is commonly referred to as a master-slave parallel GA. In the work of Omkar *et al.* (2012), a parallel PSO was developed for the weight and cost optimisation of composite structures, two swarms being optimised in parallel with different objectives. The search directions of each swarm were influenced by the exchanged particles coming from the other swarm, making the optimisation converge to results achieving both objectives. Rocha *et al.* (2014) proposed a hybrid parallel GA for the optimisation of composite structures. A coarse-grain parallel GA was employed to partition the population into several subpopulations which were assigned with different genetic parameters to mimic an evolution environment. Meanwhile, the fitness evaluations of each subpopulation were parallelized by a master-slave parallel GA to reduce the solution time.

For optimising large scale composite structures, the use of parallel computation methods becomes more necessary. Adam *et al.* (2003) optimised blended composite structures based on the parallelization of a GA where each component panel was simultaneously optimised on a different processor. The good individuals were sent to the adjacent populations in which the local individuals which were measured close to the migrants were rewarded by giving them higher fitness values, increasing the similarities between adjacent panels. This method cannot however ensure fully blended stacking sequences. In their later work (2004), the guide-based method was proposed for implementing blending constraints. Instead of conducting concurrent panel optimisations, parallelization was utilised to improve the efficiency of the

optimisation by distributing the fitness evaluations to different processors. In cases where fitness evaluations are obtained based on FEA, alleviating the computational workload becomes more necessary. In the works of Adams *et al.* (2007), Seresta *et al.* (2007) and Jin *et al.* (2011; 2016), master-slave parallel GAs were employed in the blending optimisations to reduce the large amount of computational time required by the global FEA for the whole structure during the fitness evaluation process. The works reviewed here have focused on the parallelism of GA dividing one big problem into several small ones. However, the inherent shortcoming of GAs in stochastic searching cannot be overcome.

To take the optimisation for composite structures forward, new highly efficient two-stage optimisation methods based on the use of lamination parameters for both single and blended composite laminates are developed and presented in this thesis. For the first stage optimisation, the exact strip software VICONOPT is used for single laminates and the multilevel optimisation code VICONOPT MLO is improved and used for blended laminates. In the second stage, layup optimisation methods which perform logic-based search are developed for optimising layups for single and blended laminates, and a parallel computation method combining a logic-based search with a stochastic-based search is also developed for optimising blended layups.

Chapter 3
Theoretical Background

3.1 Mechanics of composite laminates

Classical Lamination Theory (CLT) is effective for the analysis and design of thin laminates subject to small deflections (Jones 1999; Gürdal *et al.* 1999). Several assumptions are made in CLT, such as the assumption of a perfect bond between layers and the pure bending assumptions of the Kirchhoff-Love hypothesis. Correspondingly, as shown in Figure 3.1, a line originally straight and perpendicular to the mid-plane remains straight and perpendicular to it during the deformation analysis of laminates with CLT. The out-of-plane displacements are assumed to be constant through the thickness. The stresses and strains in the out-of-plane direction are neglected and the through-the-thickness shear deformations are ignored.

3.1.1 Stress-strain relations of composite lamina

A layer in a laminate is also known as a lamina which is the basic component of a laminate. A unidirectional fibre-reinforced lamina is orthotropic with three orthogonal planes of material symmetry each of which defines a principal material direction as shown in Figure 3.1.

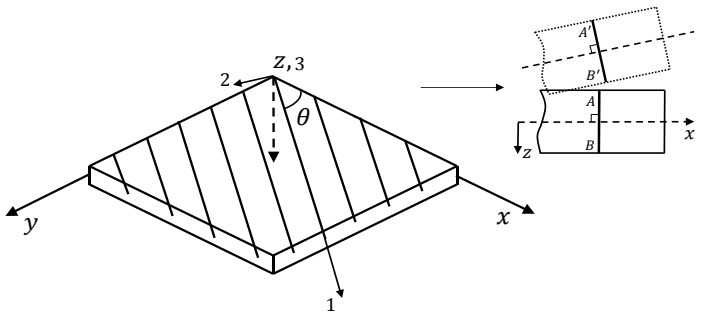

Figure 3.1 An orthotropic lamina whose principal material directions are rotated by θ with respect to the reference coordinate directions, and its deformation is based on the Kirchhoff-Love hypothesis (AB=$A'B'$).

Based on CLT, for a lamina subjected to in-plane loading and bending, the stress-strain relations are

$$\begin{bmatrix}\sigma_1\\ \sigma_2\\ \tau_{12}\end{bmatrix}=\begin{bmatrix}Q_{11} & Q_{12} & 0\\ Q_{12} & Q_{22} & 0\\ 0 & 0 & Q_{66}\end{bmatrix}\begin{bmatrix}\varepsilon_1\\ \varepsilon_2\\ \gamma_{12}\end{bmatrix} \tag{3.1}$$

where σ_1, σ_2 and τ_{12}, and ε_1, ε_2 and γ_{12} are respectively the stresses and strains in the principal material directions. Q_{ij} are the reduced stiffnesses which are defined in terms of four independent engineering material constants in principal material directions 1 and 2 as

$$\begin{cases}Q_{11}=E_{11}{}^2/(E_{11}-E_{22}\upsilon_{12}{}^2)\\ Q_{22}=E_{11}E_{22}/(E_{11}-E_{22}\upsilon_{12}{}^2)\\ Q_{12}=\upsilon_{12}Q_{22}\\ Q_{66}=G_{12}\end{cases} \tag{3.2}$$

where E_{11}, E_{22} and G_{12} are respectively the longitudinal and transverse Young's moduli and the shear modulus and υ_{12} is the major Poisson's ratio.

For the case where the principal material directions do not coincide with the reference coordinate directions as shown in Figure 3.1, the coordinate transformations should be taken into account (Jones 1999). The stress-strain relations in the reference *x*-*y*-*z* coordinates can be expressed as

$$\begin{bmatrix}\sigma_x\\ \sigma_y\\ \tau_{xy}\end{bmatrix}=\begin{bmatrix}\bar{Q}_{11} & \bar{Q}_{12} & \bar{Q}_{16}\\ \bar{Q}_{12} & \bar{Q}_{22} & \bar{Q}_{26}\\ \bar{Q}_{16} & \bar{Q}_{26} & \bar{Q}_{66}\end{bmatrix}\begin{bmatrix}\varepsilon_x\\ \varepsilon_y\\ \gamma_{xy}\end{bmatrix} \tag{3.3}$$

where $\bar{Q}_{ij}$ are the transformed reduced stiffnesses. The relationships between the $\bar{Q}_{ij}$ and Q_{ij} are given as follows

$$\begin{aligned}
\bar{Q}_{11} &= Q_{11}\cos^4\theta + 2(Q_{12}+2Q_{66})\sin^2\theta\cos^2\theta + Q_{22}\sin^4\theta \\
\bar{Q}_{12} &= (Q_{11}+Q_{22}-4Q_{66})\sin^2\theta\cos^2\theta + Q_{12}(\sin^4\theta+\cos^4\theta) \\
\bar{Q}_{22} &= Q_{11}\sin^4\theta + 2(Q_{12}+2Q_{66})\sin^2\theta\cos^2\theta + Q_{22}\cos^4\theta \\
\bar{Q}_{16} &= (Q_{11}-Q_{12}-2Q_{66})\sin\theta\cos^3\theta + (Q_{12}-Q_{22}+2Q_{66})\sin^3\theta\cos\theta \\
\bar{Q}_{26} &= (Q_{11}-Q_{12}-2Q_{66})\sin^3\theta\cos\theta + (Q_{12}-Q_{22}+2Q_{66})\sin\theta\cos^3\theta \\
\bar{Q}_{66} &= (Q_{11}+Q_{22}-2Q_{12}-2Q_{66})\sin^2\theta\cos^2\theta + Q_{66}(\sin^4\theta+\cos^4\theta)
\end{aligned} \tag{3.4}$$

3.1.2 Constitutive equations of composite laminates

Based on CLT, the stresses in the k^{th} lamina in a laminates is obtained by

$$\begin{bmatrix}\sigma_x\\ \sigma_y\\ \tau_{xy}\end{bmatrix}_k = \begin{bmatrix}\bar{Q}_{11} & \bar{Q}_{12} & \bar{Q}_{16}\\ \bar{Q}_{12} & \bar{Q}_{22} & \bar{Q}_{26}\\ \bar{Q}_{16} & \bar{Q}_{26} & \bar{Q}_{66}\end{bmatrix}_k \begin{bmatrix}\varepsilon_x^0 + z\kappa_x\\ \varepsilon_y^0 + z\kappa_y\\ \gamma_{xy}^0 + z\kappa_{xy}\end{bmatrix} \tag{3.5}$$

where ε_x^0, ε_y^0 and γ_{xy}^0 and κ_x , κ_y and κ_{xy} correspond to the strains and curvatures of the mid-plane of the laminate, and z is the distance between the lamina and the mid-plane.

To obtain the stress resultants and moment resultants for the laminate, the stresses in each layer are integrated with respect to thickness as

$$\begin{bmatrix}N_x\\ N_y\\ N_{xy}\end{bmatrix} = \int_{-h/2}^{h/2}\begin{bmatrix}\sigma_x\\ \sigma_y\\ \tau_{xy}\end{bmatrix}dz = \sum_{k=1}^{n}\int_{z_{k-1}}^{z_k}\begin{bmatrix}\sigma_x\\ \sigma_y\\ \tau_{xy}\end{bmatrix}_{(k)}dz \tag{3.6}$$

$$\begin{bmatrix}M_x\\ M_y\\ M_{xy}\end{bmatrix} = \int_{-h/2}^{h/2}\begin{bmatrix}\sigma_x\\ \sigma_y\\ \tau_{xy}\end{bmatrix}zdz = \sum_{k=1}^{n}\int_{z_{k-1}}^{z_k}\begin{bmatrix}\sigma_x\\ \sigma_y\\ \tau_{xy}\end{bmatrix}_{(k)}zdz \tag{3.7}$$

where h is the laminate thickness, n is the total number of layers in the laminate, and z_k and z_{k-1} are the distances from the mid-plane to the bottom and top of the k^{th} layer, respectively, as shown in Figure 3.2.

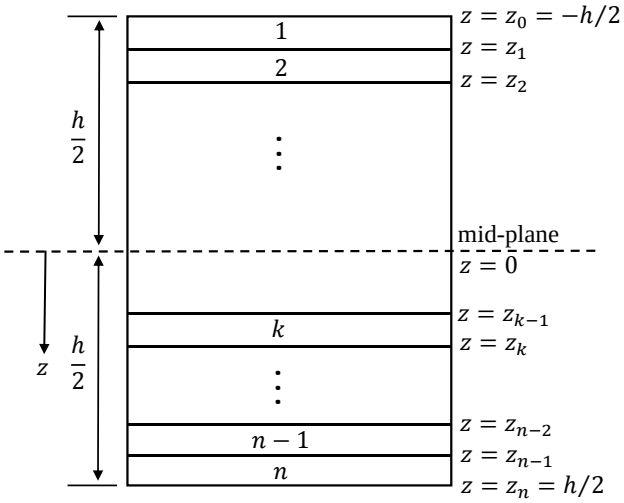

Figure 3.2 A laminate consisting of n layers.

The constitutive equations of composite laminates are then obtained by substituting equation (3.5) into equations (3.6) and (3.7) as follows

$$\begin{bmatrix} N_x \\ N_y \\ N_{xy} \\ M_x \\ M_y \\ M_{xy} \end{bmatrix} = \begin{bmatrix} A_{11} & A_{12} & A_{16} & B_{11} & B_{12} & B_{16} \\ A_{12} & A_{22} & A_{26} & B_{12} & B_{22} & B_{26} \\ A_{16} & A_{26} & A_{66} & B_{16} & B_{26} & B_{66} \\ B_{11} & B_{12} & B_{16} & D_{11} & D_{12} & D_{16} \\ B_{12} & B_{22} & B_{26} & D_{12} & D_{22} & D_{26} \\ B_{16} & B_{26} & B_{66} & D_{16} & D_{26} & D_{66} \end{bmatrix} \begin{bmatrix} \varepsilon_x^0 \\ \varepsilon_y^0 \\ \gamma_{xy}^0 \\ \kappa_x \\ \kappa_y \\ \kappa_{xy} \end{bmatrix} \tag{3.8}$$

where:

$$\begin{aligned} A_{ij} &= \sum_{k=1}^{n} \left(\bar{Q}_{ij}\right)_k \left(z_k - z_{k-1}\right) \\ B_{ij} &= \frac{1}{2} \sum_{k=1}^{n} \left(\bar{Q}_{ij}\right)_k \left(z_k^2 - z_{k-1}^2\right) \\ D_{ij} &= \frac{1}{3} \sum_{k=1}^{n} \left(\bar{Q}_{ij}\right)_k \left(z_k^3 - z_{k-1}^3\right) \end{aligned} \tag{3.9}$$

The **A**, **B**, and **D** matrices are the extensional, coupling and bending stiffness matrices, respectively. The **A** matrix relates the stress resultants to the strains and the **D** matrix relates the moment resultants to the curvatures. As for the **B** matrix, it causes the coupling between the in-plane and bending deformations for an unsymmetric laminate, however, it vanishes if the laminate is symmetric. Also, A_{16} and A_{26} are the extension-shear coupling terms which are avoided in a balanced layup. D_{16} and D_{26} are the bending-twisting coupling terms which almost always exist in laminates which include layers with off-axis fibre orientations.

3.1.3 Lamination parameters

As discussed above, the elements in the **A**, **B**, and **D** matrices depend on a large number of ply angles, which causes difficulties in optimisation. In order to circumvent this problem, the stiffness matrices can also be expressed linearly in terms of 12 lamination parameters and 5 material stiffness invariants (Tsai *et al.* 1968) as follows.

$$\begin{bmatrix} A_{11} \\ A_{22} \\ A_{12} \\ A_{66} \\ A_{16} \\ A_{26} \end{bmatrix} = h \begin{bmatrix} 1 & \xi_1^A & \xi_2^A & 0 & 0 \\ 1 & -\xi_1^A & \xi_2^A & 0 & 0 \\ 0 & 0 & -\xi_2^A & 1 & 0 \\ 0 & 0 & -\xi_2^A & 0 & 1 \\ 0 & \xi_3^A/2 & \xi_4^A & 0 & 0 \\ 0 & \xi_3^A/2 & -\xi_4^A & 0 & 0 \end{bmatrix} \begin{bmatrix} U_1 \\ U_2 \\ U_3 \\ U_4 \\ U_5 \end{bmatrix} \tag{3.10}$$

$$\begin{bmatrix} B_{11} \\ B_{22} \\ B_{12} \\ B_{66} \\ B_{16} \\ B_{26} \end{bmatrix} = \frac{h^2}{4} \begin{bmatrix} 0 & \xi_1^B & \xi_2^B & 0 & 0 \\ 0 & -\xi_1^B & \xi_2^B & 0 & 0 \\ 0 & 0 & -\xi_2^B & 0 & 0 \\ 0 & 0 & -\xi_2^B & 0 & 0 \\ 0 & \xi_3^B/2 & \xi_4^B & 0 & 0 \\ 0 & \xi_3^B/2 & -\xi_4^B & 0 & 0 \end{bmatrix} \begin{bmatrix} U_1 \\ U_2 \\ U_3 \\ U_4 \\ U_5 \end{bmatrix} \tag{3.11}$$

$$\begin{bmatrix} D_{11} \\ D_{22} \\ D_{12} \\ D_{66} \\ D_{16} \\ D_{26} \end{bmatrix} = \frac{h^3}{12} \begin{bmatrix} 1 & \xi_1^D & \xi_2^D & 0 & 0 \\ 1 & -\xi_1^D & \xi_2^D & 0 & 0 \\ 0 & 0 & -\xi_2^D & 1 & 0 \\ 0 & 0 & -\xi_2^D & 0 & 1 \\ 0 & \xi_3^D/2 & \xi_4^D & 0 & 0 \\ 0 & \xi_3^D/2 & -\xi_4^D & 0 & 0 \end{bmatrix} \begin{bmatrix} U_1 \\ U_2 \\ U_3 \\ U_4 \\ U_5 \end{bmatrix} \tag{3.12}$$

The material stiffness invariants are

$$\begin{bmatrix} U_1 \\ U_2 \\ U_3 \\ U_4 \\ U_5 \end{bmatrix} = \frac{1}{8} \begin{bmatrix} 3 & 3 & 2 & 4 \\ 4 & -4 & 0 & 0 \\ 1 & 1 & -2 & -4 \\ 1 & 1 & 6 & -4 \\ 1 & 1 & -2 & 4 \end{bmatrix} \begin{bmatrix} Q_{11} \\ Q_{22} \\ Q_{12} \\ Q_{66} \end{bmatrix} \tag{3.13}$$

The lamination parameters are obtained by the following integrals

$$\begin{bmatrix} \xi_1^k \\ \xi_2^k \\ \xi_3^k \\ \xi_4^k \end{bmatrix} = \int_{-h/2}^{h/2} Z^K \begin{bmatrix} \cos 2\theta \\ \cos 4\theta \\ \sin 2\theta \\ \sin 4\theta \end{bmatrix} dz, K = A, B, D, \begin{cases} Z^A = 1/h \\ Z^B = 4z/h^2 \\ Z^D = 12z^2/h^3 \end{cases} \tag{3.14}$$

where ξ_i^A, ξ_i^B and ξ_i^D $(i = 1,2,3,4)$ refer to the in-plane, coupling, and out-of-plane lamination parameters, respectively, and θ represents the ply orientation at depth z below the mid-surface. If the ply orientations are restricted to 0°, 90°, +45° and −45°, then $\xi_4^{A,B,D}$ are zero. The ξ_i^B $(i = 1,2,3,4)$ parameters are zero if the laminate is symmetric. Also, ξ_3^A is zero for a balanced laminate.

3.2 Method of feasible directions

As the embedded optimisation method in VICONOPT, the gradient-based MFD is used in the two-stage layup optimisations which are introduced in Chapters 5 and 6. The MFD is able to solve optimisation problems subject to inequality and equality constraints, and the derivatives of the objective and active constraints are required for obtaining the optimum results (Vanderplaats and Moses 1973).

The general optimisation problem in MFD can be described as

$$\text{Minimise} \quad F(\mathbf{x}) \tag{3.15}$$

$$\text{Subject to} \quad G_i(\mathbf{x}) \leq 0 \;\; i = 1,2,3,\ldots,n_g \tag{3.16}$$

$$H_j(\mathbf{x}) = 0 \;\; j = 1,2,3,\dots,n_h \tag{3.17}$$

$$\mathbf{x}_L \leq \mathbf{x} \leq \mathbf{x}_U \tag{3.18}$$

where $F(\mathbf{x})$ is the objective function, $G_i(\mathbf{x})$ and $H_j(\mathbf{x})$ are inequality and equality constraints respectively, $\mathbf{x}$ is a set of design variables, and $\mathbf{x}_L$ and $\mathbf{x}_U$ are the lower and upper bounds on the design variables.

The two basic factors in MFD are the move direction and the move distance, which should be selected properly when moving iteratively to a new result. The process is defined as follows

$$\mathbf{x}^{q+1} = \alpha \mathbf{S}^q + \mathbf{x}^q \tag{3.19}$$

where q is the step number in the search, α is a scalar move distance and $\mathbf{S}^q$ is a vector move direction. $\mathbf{S}^q$ is required to determine the search direction along which the objective function is decreased (usable direction) without the violation of any constraint (feasible direction). Then α should be chosen to obtain the new result.

The usability of $\boldsymbol{S}^q$ is defined mathematically as follows

$$\nabla F(\mathbf{x}^q) \cdot \mathbf{S}^q \leq 0 \tag{3.20}$$

where $\nabla F(\mathbf{x}^q)$ is referred to as the normalized analytic gradient of the objective function with respect to the independent design variables, and the feasibility of $\boldsymbol{S}^q$ can be expressed as

$$\nabla G_i(\boldsymbol{x}^q) \cdot \boldsymbol{S}^q \leq 0 \qquad i = 1,2,3 \dots n_a \tag{3.21}$$

where $\nabla G_i(\mathbf{x}^q)$ is the normalized analytic gradient of the ith active constraint and n_a is the number of active constraints at the current design point. The selected direction $\mathbf{S}^q$ must satisfy both of the above equations (3.20) and (3.21), as shown in Figure 3.3.

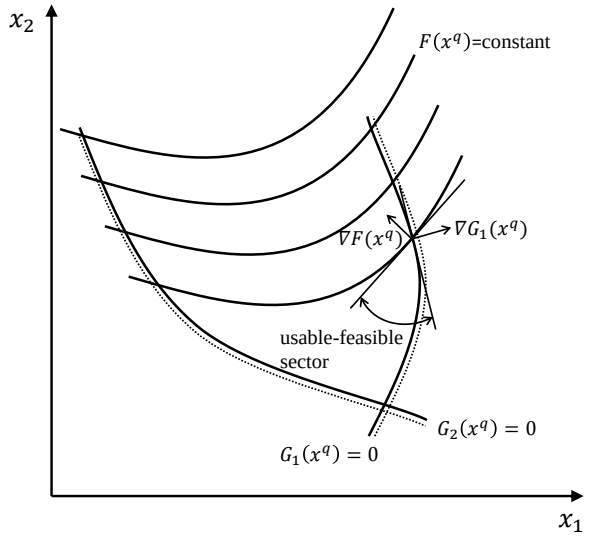

Figure 3.3 Usable and feasible direction along which the objective function is decreased without violating any constraint (based on (Vanderplaats and Moses 1973)).

As the most important part of the optimisation, the determination of $\mathbf{S}^q$ can be achieved by

$$\text{Maximise} \quad \beta \tag{3.22}$$

$$\text{Subject to} \quad \nabla F(\mathbf{x}^q) \cdot \mathbf{S}^q + \beta \leq 0 \tag{3.23}$$

$$\nabla G_i(\mathbf{x}^q) \cdot \mathbf{S}^q + \theta_i \beta \leq 0 \quad i = 1,2,3 \dots n_a \tag{3.24}$$

$$-\mathbf{1} \leq \mathbf{S}^q \leq \mathbf{1} \tag{3.25}$$

where β is a scalar and θ_i is a push-off factor. The aim of the maximisation of β is to obtain an $\mathbf{S}^q$ which leads the steepest decrease in the objective function. In order to avoid activating the same constraints at the new design point due to the curvature of the constraints, θ_i is used to move the design away from the current active constraints. To improve the efficiency of the optimisation, a larger value of θ_i is chosen for constraints with a higher degree of nonlinearity and vice versa. Compared with other gradient-based optimisation methods, MFD keeps a reasonable distance from the constraints. The maximisation problem of equations (3.22)-(3.25) can be solved using linear programming.

For the case where the obtained result violates the constraints, an $\mathbf{S}^q$ which leads the optimisation back to a feasible result while increasing the current objective function as little as possible should be determined. Correspondingly, equation (3.20) is included in the objective function, rather than taken as a constraint, as below

$$\text{Maximise} \quad \Phi\beta - \nabla F(\mathbf{x}^q) \cdot \mathbf{S}^q \tag{3.26}$$

$$\text{Subject to} \quad \nabla G_i(\mathbf{x}^q) \cdot \mathbf{S}^q + \theta_i \beta \leq 0 \quad i = 1,2,3 \ldots n_{av} \tag{3.27}$$

$$-\mathbf{1} \leq \mathbf{S}^q \leq \mathbf{1} \tag{3.28}$$

where Φ is a weighting factor and n_{av} is the number of active and violated constraints.

After the move direction $\mathbf{S}^q$ is obtained, the determination of the appropriate move distance α in the direction $\mathbf{S}^q$ can be readily performed by a one-dimensional search. A new design point is then obtained using equation (3.19).

3.3 Genetic algorithms

As a heuristic optimisation method, a GA mimics biological reproduction, natural selection and evolution based on Darwin's theory (Holland 1975). Instead of utilising the gradient information of the objective function and constraint, a stochastic search is implemented based on a population of designs. Individuals with higher fitness have more probability of being selected for the next generation. Different selection procedures can be chosen such as the roulette wheel method, tournament method, stochastic universal sampling, etc. As a typical selection method, the biased roulette wheel method operates based on the fitness of each individual design. The probability P_i of each individual being selected is obtained as

$$P_i = \frac{f_i}{\sum_{j=1}^{s} f_j} \tag{3.29}$$

where f_i is the fitness value of the current individual and s is the population size. Hence, in a biased roulette wheel consisting of s sectors, an individual with higher

fitness is assigned a proportionally larger sector, increasing the chance of being selected.

GAs are ideal for discrete optimisation problems, because the chromosomes are composed of a string of genes limited to a set of pre-determined values. For example, in layup optimisation, the ply angles are represented with genes which make up the chromosomes (i.e. stacking sequences). The optimised results are obtained by exchanging the genetic information of the chromosomes between the selected individuals using consecutive operators such as crossover, mutation and permutation, as shown in Figure 3.4.

The main operator in GAs is the crossover which processes two chromosomes to breed offspring by exchanging parts of their strings, combining the characteristics of both. Several types of crossover can be used such as one-point crossover, two-point crossover, uniform crossover and so on. An example of a two-point crossover is shown in Figure 3.4 (a). Firstly, two break points in the parents' chromosomes are randomly selected and then the genes between these points are swapped to produce new generation. Since the search capability of GAs relies on crossover, it is usually executed with high probability.

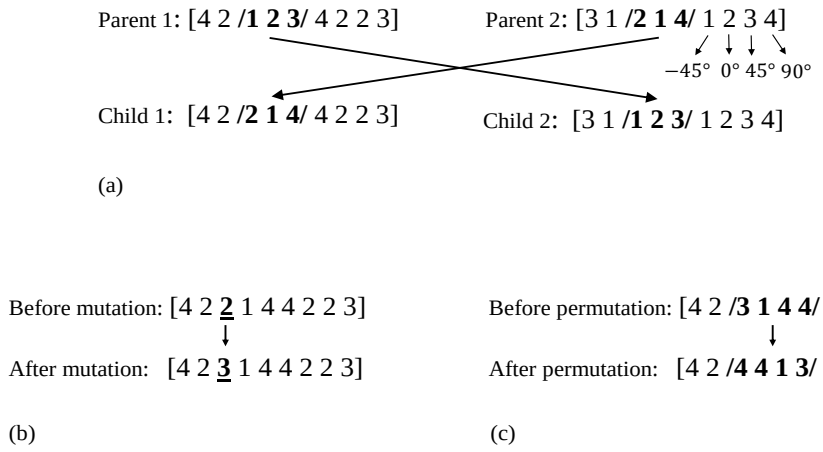

Figure 3.4 GAs operators (a) crossover, (b) mutation, and (c) permutation.

After the crossover operation is completed, the mutation operator is applied with low probability to expand the diversity of design in case of getting trapped into local optimum results. A typical mutation operator is demonstrated in Figure 3.4 (b). Genes in the chromosomes are randomly selected and changed to another permissible value. The commonly used permutation operator is also included. As shown in Figure 3.4 (c), two break points in the chromosome are randomly selected and the order of the genes between them is reversed. New populations are successively generated with the above operators until the convergence criteria are reached.

3.4 Branch and bound method

The BB method has an effective performance in discrete optimisation problems. In contrast to GAs, global optimality can theoretically be obtained as it implicitly conducts an exhaustive search. The search space is partitioned into subsets with branching and bounding operations, which constitute a rooted decision tree (Little *et al.* 1963), as shown in Figure 3.5.

With the search space S being split into smaller spaces, the branches of the tree which represent subsets of the solution set S_i are explored from the top root to the bottom branches. At the current branch e.g. branch A in Figure 3.5, the solution subset S_A is evaluated with the objective function $f(x), x \in S_A$ to determine the next branch to be explored. Unlike a complete enumeration method, BB requires less searching as a bounding process is implemented at each branch, comparing the best result in the remaining subtree with the current best solution. For a minimisation problem, if the branch A is found to be infeasible or its lower bound L_b is greater than the current upper bound U_b (i.e. current best solution), it will be pruned without further exploring its subtree S_A, improving the efficiency of the searching process. The branching and bounding processes are iteratively applied until all the branches are either searched or pruned.

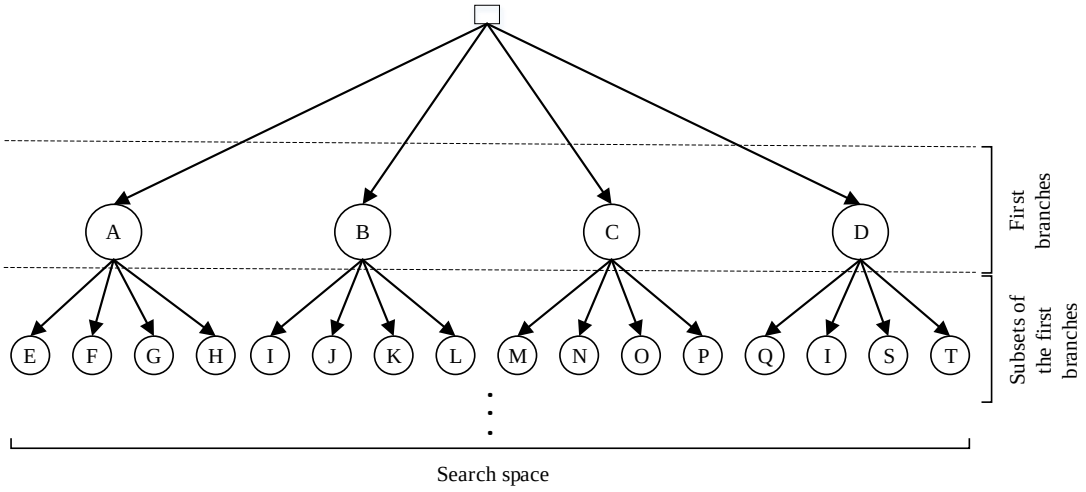

Figure 3.5 A decision tree of the branch and bound method.

The computational cost of the BB method is highly dependent on the size of the decision tree as well as its upper and lower bounds. In the case where a bounding process is unavailable, BB has to search all the possibilities in the whole search space like an enumeration method. Therefore, the decision tree should be defined properly and navigated intelligently in the optimisation to ensure its efficiency.

3.5 Parallel computation

In order to improve the computational efficiency of analysis and optimisation, parallel computation has been developed to execute several computational tasks simultaneously by utilising multiple computational resources such as a computer cluster, multi-CPUs, multi-cores, and CPU with GPU (Joubert *et al.* 2004). As multicore processors become more available in computers, parallel computation executed on different cores is becoming more accessible to researchers, providing more options for designing efficient programs.

Process decomposition and interaction are the most common problems when applying parallel computation. A massive computational work can be decomposed into several parallel works with respect to data or tasks. As a typical data-parallel model, Single Program Multiple Data (SPMD) is able to allocate different sets of data to different parallel processors (e.g. computers, CPUs, cores, etc) performing the same

calculations in order to alleviate the workload of processing huge amounts of data. As for task parallelism, the parallel program model Multiple Program Multiple Data (MPMD) can be implemented to assign different tasks to parallel processors, performing different calculations with either the same or different sets of data.

For parallel computation which requires cooperation between the parallel processors, interaction between them is required to exchange information between them. Communication between the parallel processors is commonly achieved based on shared memory or message passing. Message passing is used when the memory is not shared by the parallel processors such as under a distributed memory environment. Each parallel processor is assigned with a local memory, and the information is exchanged by sending and receiving messages between them. Correspondingly, the industry standard Message Passing Interface (MPI) has been developed, which defines library routines that can be used by several programming languages such as Fortran, C, and C++. Besides, some parallel-enabled functions and parallel structures based on MPI have also been established in Matlab (MathWorks 2017).

Chapter 4
VICONOPT

4.1 Introduction

This chapter introduces the specialist software VICONOPT, including its fundamental theory and procedures for analysis and optimisation.

The exact strip software VICONOPT (VIpasa with CONstraints and OPTimisation) was developed in 1990 at Cardiff University in collaboration with NASA Langley Research Center and British Aerospace (Williams *et al.* 1991; Kennedy and Featherston 2010), and comprises the earlier programs VIPASA (Vibration and Instability of Plate Assemblies including Shear and Anisotropy) (Wittrick and Williams 1974) and VICON (VIpasa with CONstraints) (Anderson. *et al.* 1983). VICONOPT performs buckling, postbuckling and free vibration analyses of prismatic plate assemblies of isotropic and anisotropic plates and provides a strong structural optimisation tool for preliminary aircraft design.

4.2 Theoretical background

4.2.1 The exact strip method

The exact strip method, which is an alternative to the finite element method, is employed in VICONOPT. In contrast to the finite element method, the structure is divided into strips, of which the stiffness and mass are assumed to be distributed continuously, instead of discretising stiffness and mass at specific nodes. The member stiffness matrices $\mathbf{K}_{\boldsymbol{m}}$ which are used to assemble the global stiffness matrix **K** for the structure are obtained by solving the partial differential equations which govern the in-plane and out-of-plane deformations of the component strips. The relationship between the global stiffness matrix, the nodal displacements vector **D** and perturbation loads vector **P** can be described as

$$\mathbf{KD} = \mathbf{P} \tag{4.1}$$

The calculation of critical buckling load factors or undamped natural frequencies is achieved by solving the eigenproblem

$$\mathbf{KD} = \mathbf{0} \tag{4.2}$$

Compared with the finite element method, the reduced number of nodes in the exact strip method results in a much smaller global stiffness matrix **K**. However, the elements of **K** are transcendental functions of the eigenparameter f_e and hence highly non-linear (Plank and Wittrick 1974; Cheung 1976; Dawe 1977). Therefore, the methods developed for linear eigenproblems cannot be employed to obtain the critical buckling loads and natural frequencies, which has led to the development of an iterative search procedure, the Wittrick-Williams algorithm.

4.2.2 The Wittrick-Williams algorithm

The Wittrick-Williams algorithm (Wittrick and Williams 1971; 1973) is a numerical technique which calculates J, the number of buckling load factors or natural frequencies which are less than a trial value f_e of load factor or frequency. Therefore, any difference in J between two trial values f_e is equal to the number of eigenvalues lying between them.

The general form of the Wittrick-Williams algorithm is defined as

$$J = J_0 + s\{\mathbf{K}\} \tag{4.3}$$

where $s\{\mathbf{K}\}$, the sign count of **K**, is equivalent to the number of negative leading diagonal elements of the upper triangular matrix $\mathbf{K}^{\Delta}$ which can be obtained from **K** using conventional Gauss elimination. J_0 is the number of eigenvalues that would be less than f_e if all the nodal freedoms of the structure were restrained, and can be obtained from the following equation

$$J_0 = \sum_m J_m \tag{4.4}$$

where J_m is the number of eigenvalues of each member of the structure exceeded by the trial value of f_e when the member ends are fixed and can often be obtained analytically from the governing differential equations.

After the number of eigenvalues between two trial values of f_e is found, the buckling load factors or natural frequencies in this range can be obtained easily with any required accuracy by using the simple bisection method or the more efficient multiple determinant parabolic interpolation method (Williams and Kennedy 1988; Kennedy and Williams 1991).

4.3 Analysis features of VICONOPT

4.3.1 VIPASA analysis

Typical structures that can be analysed by VICONOPT are shown in Figure 4.1, for which the critical buckling loads, undamped natural frequencies and related mode shapes can be obtained under any combination of longitudinal, transverse, shear and bending loads. The in-plane loadings for a typical component plate are shown in Figure 4.2. Note that an assembly of such prismatic plates is referred to as a panel in VICONOPT. As the first and basic part of VICONOPT, the VIPASA analysis (Wittrick and Williams 1974) is based on the exact strip method with the Wittrick-Williams algorithm as described in Section 4.2 above. As expected, VIPASA has high efficiency, and has been shown to be 1000 times faster than the finite element method (Butler and Williams 1992).

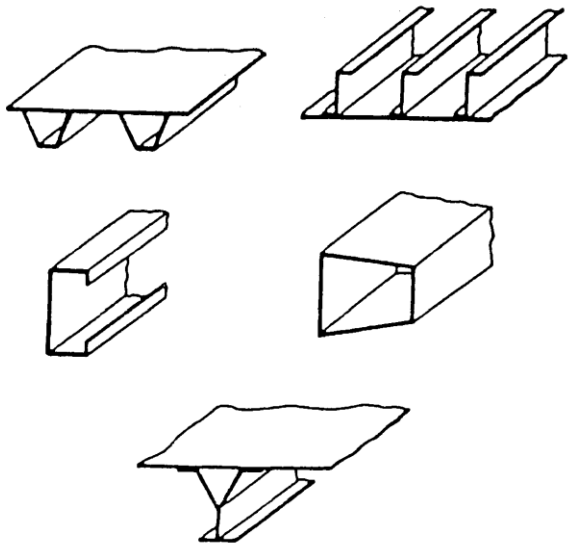

Figure 4.1 Typical prismatic plate assemblies (Wittrick and Williams 1974).

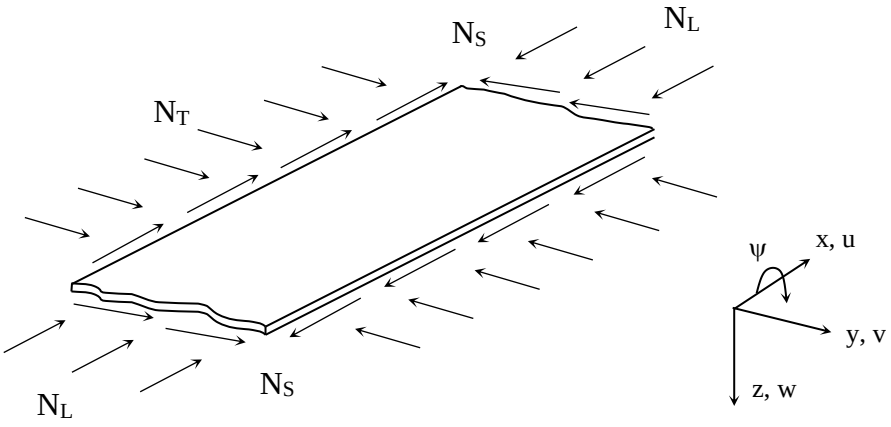

Figure 4.2 In-plane loadings of a typical component plate.

Exact membrane and bending stiffness matrices **A** and **D** can be obtained for symmetric laminates. Otherwise numerical solutions are available when the coupling stiffness matrix **B** is non-zero (Anderson and Kennedy 1993).

In VIPASA analysis, the mode of buckling and vibration is assumed to vary sinusoidally in the longitudinal direction, i.e. the displacements u, v, w and rotation Ψ shown in Figure 4.2 vary sinusoidally in the *x* direction. The buckling deflection shape is defined as

$$w = f_1(y)\sin(\frac{\pi x}{\lambda}) \tag{4.5}$$

where w is the out-of-plane displacement, λ is the half-wavelength and f_1 is a function of y only.

Any support conditions can be easily implemented at the transverse edges of a plate by adding longitudinal line supports which constrain any combinations of the four degrees of freedom (u, v, w, Ψ). However, since the plate is assumed to be infinitely long in the *x* direction, support conditions cannot be prescribed at its transverse ends. To overcome this, note that the sinusoidal assumption means that displacements are constrained at intervals of half-wavelength λ along the longitudinal axis, producing parallel nodal lines (i.e. lines of zero displacement). If the component plates are not anisotropic and are not subjected to shear loading, the nodal lines are straight and perpendicular to the longitudinal direction, which can satisfy the simply supported end conditions provided the half-wavelength λ divides exactly into the panel length l as shown in Figure 4.3(a). Exact solutions can be obtained for a range of half-wavelengths λ specified by the user by taking $\lambda = l, l/2, l/3, l/4$, etc. However, if anisotropy or shear loading exists on the plate, the nodal lines are no longer straight but skewed as shown in Figure 4.3(b), which means that the simply supported end conditions can only be satisfied approximately. Buckling and vibration results are therefore approximated and become increasingly conservative as the half-wavelength λ approaches the length of the panel l.

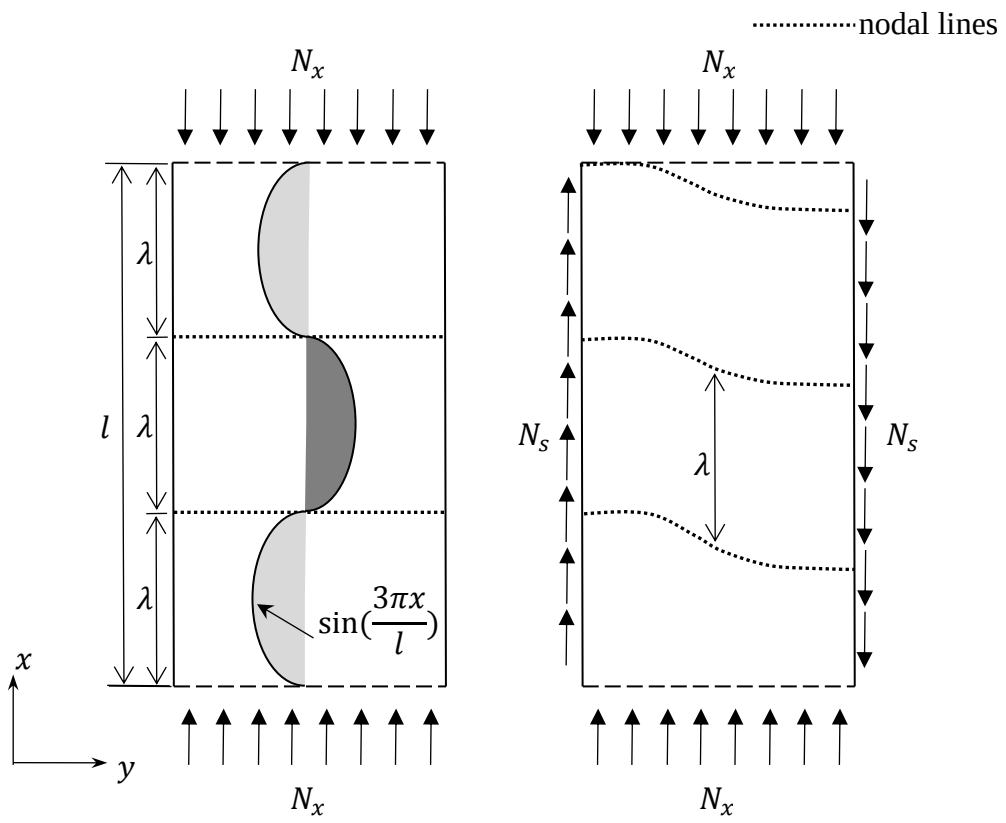

(a) Straight nodal lines (b) Skewed nodal lines

Figure 4.3 Nodal lines in (a) are straight and perpendicular to the longitudinal direction, which is consistent with simply supported end conditions. Nodal lines in (b) are skewed due to anisotropy or shear loads, approximating the simply supported end condition.

4.3.2 VICON analysis

VICON (VIpasa with CONstraints) was developed to overcome the conservative analysis of VIPASA for shear loading and anisotropy (Anderson. *et al.* 1983). Comparison of efficiency between VICON and the finite element software STAGS, shows VICON is 150 times faster (Butler and Williams 1992).

In VICON analysis, the assumptions and loading in VIPASA are retained, but the VIPASA stiffness matrices for the responses of various half-wavelengths λ are coupled using Lagrangian multipliers, marking the key difference over VIPASA analysis.

The deflections of the plate are expressed as a Fourier series involving a set of appropriate half-wavelengths λ_i. Hence the plate in VICON is assumed to be infinitely long with constraints repeating at interval l, as shown in Figure 4.4. The constraints are implemented by point supports which can restrain any chosen degree of freedom at a node of the plate at any location in the range $0 \leq x \leq l$. VICON minimises the total energy of the panel subject to any set of prescribed constraints.

The mode of buckling or vibration in VICON repeats over a length $L = Ml$, where M is an integer. Ideally, an infinite series of half-wavelengths λ_i should be considered to obtain the best results. However, to reduce the computational cost at the expense of some loss of accuracy, only a finite series of half-wavelengths λ_i is considered in the analysis. The choice of this finite series of half-wavelengths λ_i is important for obtaining the satisfactory results, and is governed by

$$\lambda_i = \frac{l}{(\xi + 2i)} \qquad (i = 0, \pm 1, \pm 2, \ldots, \pm q) \tag{4.6}$$

where $\xi = \frac{2N}{M}$, N is an integer in the range $0 \leq N \leq M/2$, hence $0 \leq \xi \leq 1$, and q is an integer. ξ and q are required to be chosen by the user, and therefore all the values of ξ that are likely to be critical should be considered to ensure the lowest buckling load can be obtained. When ξ is equal to 0 or 1, the contributions from $-q$ are the same as those from $+q$, so the negative λ_i in equation (4.6) can be ignored.

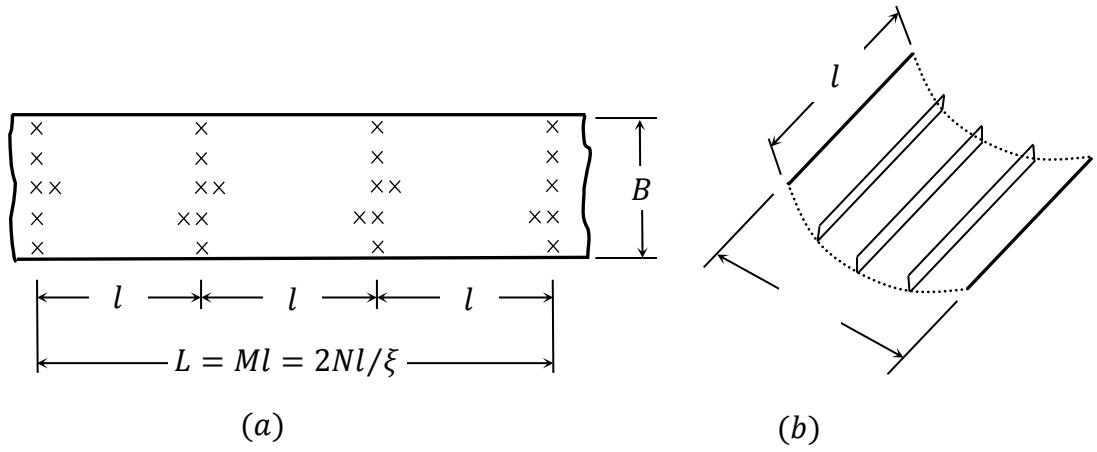

Figure 4.4 An infinitely long plate assembly in VICON with crosses denoting point supports, (a) plan view, (b) isometric view (Williams *et al*. 1991).

The way of calculating the buckling load factors and natural frequencies in VICON is similar to that using VIPASA. As the stiffness matrices in VICON are coupled with different half-wavelengths, the Wittrick-Williams algorithm has been extended accordingly to ensure the eigenvalues can be obtained with certainty (Anderson *et al.* 1983), as follows

$$J = \sum_{i=-q}^{q} (J_{0i} + s\{\mathbf{K}_i\}) + s\{\mathbf{R}\} - r \tag{4.7}$$

where

$$\mathbf{R} = -\frac{1}{L} \sum_{i=-q}^{q} \mathbf{E}_i \, \mathbf{K}_i^{-1} \mathbf{E}_i^H \tag{4.8}$$

$\mathbf{E}_i$ is the constraint matrix for $\lambda = \lambda_i$, H is Hermitian transpose, r is the order of $\mathbf{R}$ (i.e. the number of constraints), J_{0i} is J_0 calculated for $\lambda = \lambda_i$.

4.4 Optimisation features of VICONOPT

VICONOPT provides an effective and efficient structural optimisation tool for prismatic plate assemblies based on the analysis features of VIPASA and VICON. The main objective of VICONOPT optimisation is to minimise the mass of these plate assemblies subject to initial buckling, strength, stiffness and geometric constraints using continuous optimisation (Butler and Williams 1992) or discrete optimisation (Kennedy *et al.* 1999). Design variables in VICONOPT include the widths and thicknesses of the plates, the layer thicknesses and the ply orientations. To ensure geometric consistency and reduce the computational cost, the design variables can be controlled or linked to each other using embedded equality and inequality constraints. The optimisation capability of VICONOPT has been expanded by introducing lamination parameters as design variables (Kennedy *et al.* 2010). Moreover, as an extension of VICONOPT, VICONOPT MLO (Fischer 2002) has been developed for optimising complex three-dimensional structures.

4.4.1 Structural optimisation in VICONOPT

The optimisation process is illustrated in Figure 4.5. It can be seen that the optimisation is mainly based on a sequence of sizing design cycles, each including several iterative steps, and each of the optimisation procedures will be described below.

At the beginning of the optimisation, the starting configuration is examined with an initial analysis to obtain its structural performance (e.g. critical buckling load). Then, it is taken into the initial stabilisation step during which some of the design variables (e.g. the plate thicknesses) are factored uniformly to force an unstable or over-stable configuration to become just stable. The stabilisation factor F_{st} is determined by a bisection method based on the information given by the Wittrick-Williams algorithm. In the stabilisation step, the most critical buckling mode from the initial analysis is considered first, and the configuration is checked by a single iteration stability check which iterates on F_{st} to make the critical buckling load factor in equation (4.2) equal to 1. Therefore, if the value of J in equation (4.3) is greater than zero, it can be proved that the buckling constraint is violated. Correspondingly, F_{st} is required to be increased to make the configuration stable. After the most critical buckling mode is checked, the remaining modes are considered with the same stability check. Note that this stabilisation process is also employed in the subsequent sizing cycles.

After the initial analysis and stabilisation is completed, the sizing strategy starts to optimise the configuration. The first step of each sizing cycle is a constraint and sensitivity analysis during which the buckling constraints for the current configuration are calculated based on the buckling load factors which are critical, or close to critical. The sensitivities are obtained by calculating the derivatives with respect to all the design variables, each of which are perturbed in turn. Since the buckling analyses of VIPASA and VICON create transcendental eigenvalue problems, the derivatives cannot be obtained by the usual approaches developed for linear eigenvalue problems. Consequently, the derivatives are approximated by the following finite difference expression (Butler and Williams 1992).

$$\frac{\partial f_{ei}}{\partial x_j} \cong \frac{f'_{eij} - f_{ei}}{\alpha_{ij} x_j} \qquad i = 1, 2, 3, \dots, n_b, \qquad j = 1, 2, 3, \dots, n_d \tag{4.9}$$

where f_{ei} is the i[th] eigenvalue of the unperturbed design, f'_{eij} is the i[th] eigenvalue of the perturbed design of which the j[th] design variable x_j is perturbed by $\alpha_{ij}x_j$, n_b and n_d are the number of buckling modes considered and the number of design variables, respectively.

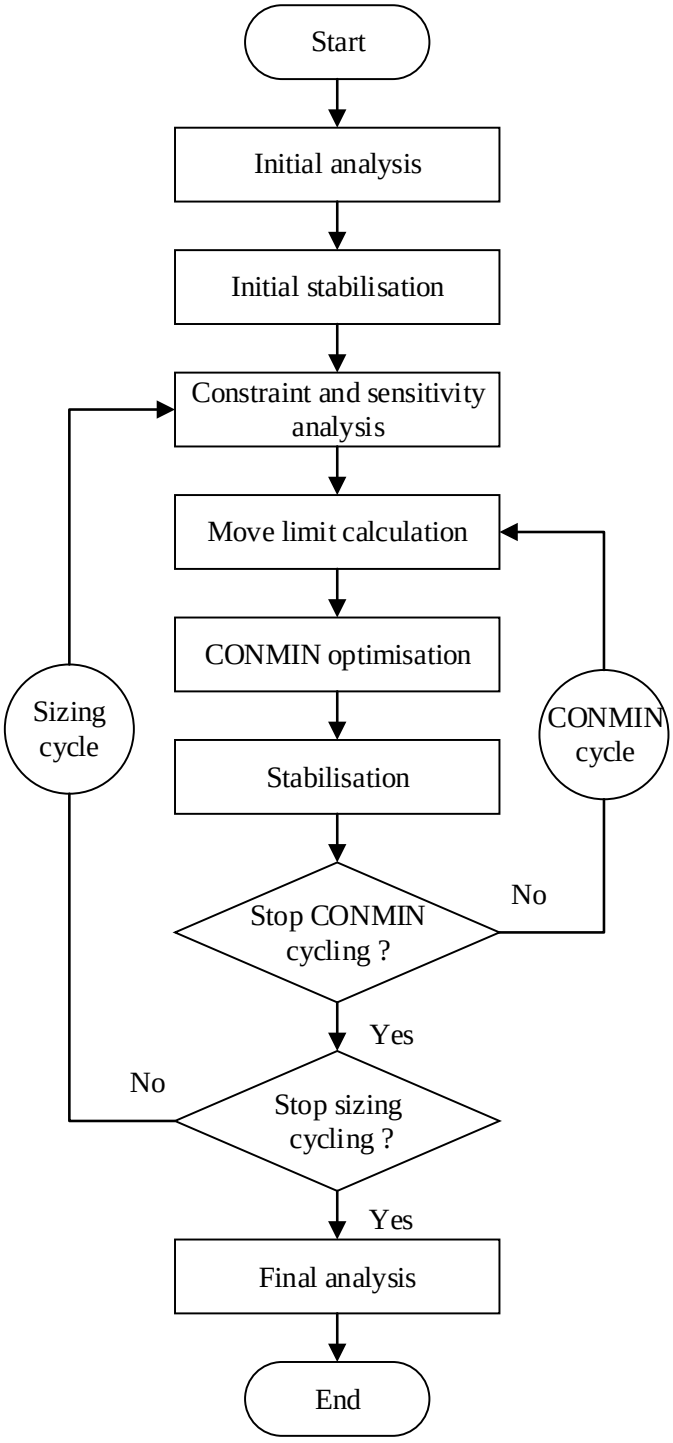

Figure 4.5 Flow chart of VICONOPT optimisation.

The perturbed eigenvalues f'_{eij} can be obtained by an efficient approximation method (Butler and Williams 1992). In case the data is unsuitable for this approximation, the method will automatically recover to a full analysis which is able to obtain f'_{eij} with certainty in all situations.

To reduce the computation time of the constraint and sensitivity analysis, a constraint deletion method (Butler and Williams 1990) is implemented, which deletes the buckling modes with buckling loads at least 15% higher than the design load by default, and any limitation on the exceeded magnitude of the design load can be specified by the user.

After the constraint and sensitivity information of the current design is obtained, the CONMIN (Vanderplaats 1983) cycle starts from a move limit calculation step which provides the upper and lower limits on each design variable for the following CONMIN optimisation step to ensure the optimum solution can be obtained properly.

In the CONMIN optimisation step, the MFD is employed to iteratively change the design variables between the upper and lower bounds given by the limit calculation step. During this gradient based optimisation, linear approximations are made to the non-linear constraints by using a first order Taylor series expansion. Note that the buckling constraints considered in the CONMIN optimisation step are only the set of critical buckling constraints retained by the constraint deletion method at the constraint and sensitivity analysis step.

A stabilisation step follows the CONMIN optimisation to make the results obtained by the CONMIN optimisation just stable in the same way as described in the initial stabilisation step. Because the non-linear constraints are approximated in the CONMIN optimisation, which may result in an infeasible design, the stabilisation step adjusts the design using the true constraints. In addition, all the buckling constraints are considered rather than only the critical set. Another benefit from the stabilisation step is that the optimisation convergence is accelerated by using these just stable results as starting points. Then in the next CONMIN cycle, the move limits are

calculated based on how much the objective function has been reduced and also on how much it had to be adjusted by stabilisation.

After the convergence criteria on the final mass are reached and the optimisation process is completed, the optimised configuration is checked in the final analysis to ensure that the design meets the user's requirements.

4.4.2 Lamination parameter optimisation in VICONOPT

VICONOPT has been extended to include the use of lamination parameters as design variables (Kennedy *et al.* 2010). The stiffness matrices **A**, **B** and **D** in VICONOPT can be obtained easily from the lamination parameters as described in Chapter 2, instead of using the usual method which integrates the transformed reduced stiffness $\overline{\mathbf{Q}}$ through the thickness of the plate. Each of the lamination parameters ξ_j^k ($j = 1,2,3,4;\ k = A,B,D$) lies between -1 and 1. For layup optimisation which requires the ply angles to be restricted to 0°, 90°, +45° and $-45°$, the following 25 lamination parameter constraints are applied, giving a restricted feasible region.

$$2\left|\xi_1^k\right| - \xi_2^k - 1 \le 0,\ \ 2\left|\xi_3^k\right| + \xi_2^k - 1 \le 0 \quad k = A,D \tag{4.10}$$

$$2|\xi_1^B| + \xi_2^B - 2 \le 0,\ \ 2|\xi_3^B| + \xi_2^B - 2 \le 0,\ \ \ |\xi_1^B| + |\xi_3^B| - 1 \le 0 \tag{4.11}$$

$$4(\xi_i^D + r)\left(\xi_i^A + r\right) \ge \left(\xi_i^A + r\right)^4 + 3(\xi_i^B)^2,\ \ i = 1,2,3,\ \ r = \pm 1 \tag{4.12}$$

$$\begin{gathered}16(2\xi_1^D + r\xi_2^D + rs)(2\xi_1^A + r\xi_2^A + rs) \ge (2\xi_1^A + r\xi_2^A + rs)^4 + \\ 12(2\xi_1^B + r\xi_2^B)^2, r = \pm 1, s = 1, -3\end{gathered} \tag{4.13}$$

$$\begin{gathered}16(2\xi_3^D + r\xi_2^D + rs)(2\xi_3^A + r\xi_2^A + rs) \ge (2\xi_3^A + r\xi_2^A + rs)^4 + \\ 12(2\xi_3^B + r\xi_2^B)^2, r = \pm 1, s = 1, -3\end{gathered} \tag{4.14}$$

$$\begin{gathered}4(\xi_1^D + r\xi_3^D + s)(\xi_1^A + r\xi_3^A + s) \ge (\xi_1^A + r\xi_3^A + s)^4 + 3(\xi_1^B + r\xi_3^B)^2, \\ r = \pm 1, s = \pm 1\end{gathered} \tag{4.15}$$

The non-linear constraints above are implemented by using an exterior penalty function method. It is noted that the feasible region is convex (Diaconu and Sekine 2004) and that the constraints of equations (4.10)-(4.15) are satisfied if all the lamination parameters ξ_j^k ($j = 1,2,3;\ k = A,B,D$) are set to zero. Thus when any of the constraints is violated, all the lamination parameters are multiplied by a scalar φ ($0 < \varphi < 1$) to move the outlying lamination parameters to the boundary of the feasible region, so that the most critical constraint is just satisfied, converting an infeasible configuration to an artificial just feasible one. For example, as can be seen from Figure 4.6, the point V violates the constraint equation (4.10) and so lies outside the triangular feasible region of the lamination parameters $\xi_{1,2}^D$. It is directed to the point S which just satisfies this constraint using the exterior penalty function method.

The exterior penalty function method employs a bisection approach to find the appropriate scalar φ ($0 < \varphi < 1$) during the penalization process. In the stiffness matrix calculations, all the lamination parameters ξ_j^k and laminate thickness h of the infeasible configurations are reduced to $\varphi\xi_j^k$ ($j = 1,2,3;\ k = A,B,D$) and φh , respectively, making them tend to violate the buckling constraints. Due to the artificially low stiffness, the infeasible configurations become unattractive during the optimisation. However, the laminate thickness h is not reduced in the mass calculations so the infeasible configuration will not have an artificially attractive objective function.

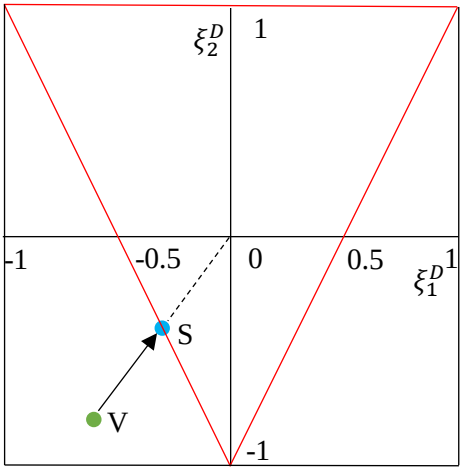

Figure 4.6 An example of the penalization process on the feasible region of $\xi_{1,2}^D$.

4.4.3 VICONOPT MLO

VICONOPT is a highly efficient expert software for the optimisation of individual panels. However, it is restricted to applications involving prismatic structures which precludes the optimisation of more complex three-dimensional structures such as an entire aircraft wing or fuselage. Following the recommendations of the Group for Aeronautical Research in Europe (GARTEUR 1997), VICONOPT MLO (Fischer 2002) was developed to address this limitation. In its later version, VICONOPT MLOP (Qu *et al.* 2011), postbuckling behaviour is also considered in the optimisation.

VICONOPT MLO is a software package which implements multilevel optimisation by combining MSC/NASTRAN FEA (MSC Software Corporation 1999a) of the whole structure at system level, with efficient VICONOPT optimum design of each of the constituent individual panels at panel level, avoiding the drawbacks of both techniques. Design variables in VICONOPT MLO include the widths and thicknesses of plates, the layer thicknesses and the ply orientations. Furthermore, VICONOPT MLO can also be used as a pre-processor for VICONOPT, which provides a Windows-based interface for the user, allowing the VICONOPT model to be created efficiently.

The multilevel optimisation process of VICONOPT MLO is illustrated in Figure 4.7. It can be seen that the finite element model is created with MSC/PATRAN (MSC Software Corporation 1999b) at the start of the optimisation and then a static analysis of the whole structure is performed by MSC/NASTRAN at system level. The quadrilateral four-node QUAD4 shell element in MSC/NASTRAN is employed for the FE static analysis, whose main aim is to obtain the stress distributions in the whole structure.

After the static analysis, VICONOPT MLO is used to automatically generate the input file (.dat) for the VICONOPT optimisation based on a set of user-defined design variables with appropriate bounds and the analysis results from MSC/NASTRAN (stress distribution, geometry, etc.) which are stored in the output file (.f06). The stresses in each element obtained from the system level analysis are used to calculate the stresses to be carried in each component panel, which are taken as applied loadings in the VICONOPT optimisation.

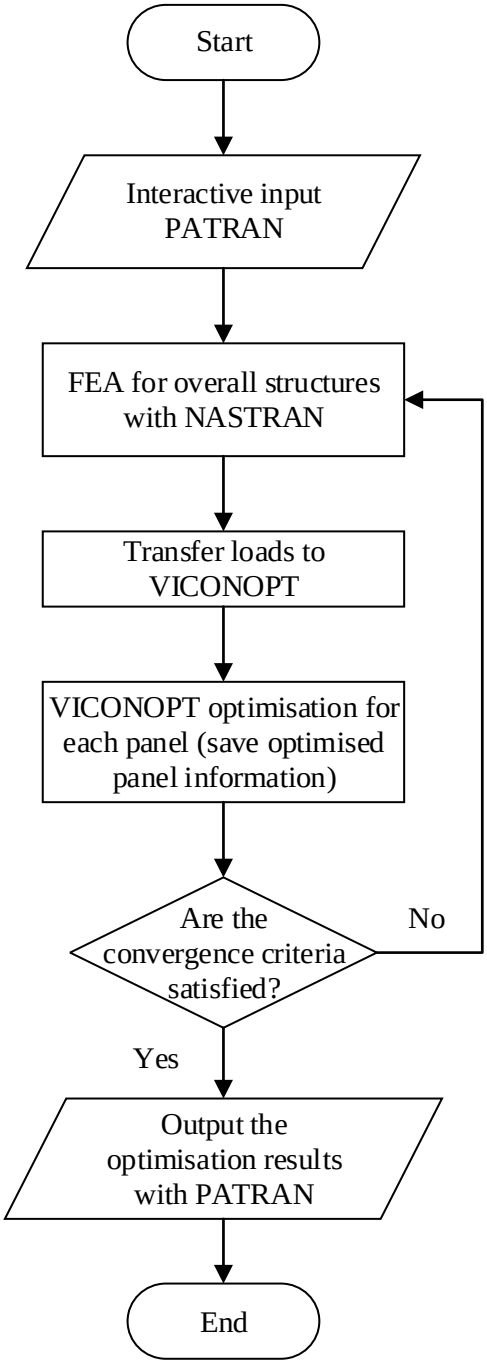

Figure 4.7 Flowchart of the multilevel optimisation process of VICONOPT MLO.

Once the preparation works are completed, VICONOPT is employed to optimise the component panels at panel level. The panel masses are minimised separately as described in Section 4.4.1, and the output files (.res) which store the optimised

geometries are transferred to VICONOPT MLO for the preparation of the next static analysis.

After all the panels are optimised by VICONOPT, VICONOPT MLO modifies the input file (.bdf) for MSC/NASTRAN based on the optimised geometries in order to incorporate the optimised designs into the system level finite element model, and a new static analysis is performed to determine the updated load distributions. These newly obtained load distributions are then used at the panel level to re-optimise the component panels. This process is repeated until convergence for total mass, individual mass and the stress distributions of each panel occurs and an optimum solution is reached in an efficient manner. VICONOPT MLO is concluded to be around 4 times faster than the optimisation purely based on FEA (Fischer *et al.* 2012).

Chapter 5
Two-stage Layup Optimisation of Single Composite Laminates

5.1 Introduction

In this chapter, an efficient method for performing layup optimisation of single composite laminates with buckling and layup design constraints is presented. This work corresponds to the first journal paper in the publication list of Section 1.4. By utilising lamination parameters, the optimisation problem is divided into two stages. During the first stage, VICONOPT is employed for buckling optimisation of the lamination parameters and laminate thickness. In the second stage, the improved LBB method combining the branch and bound method with a global layerwise technique is used to search the optimal stacking sequences to match the optimised lamination parameters obtained in the first stage.

This two-stage method is an extension of the method developed in Kennedy *et al.* (2010). In the first stage, the feasible regions for the lamination parameters with the layup design constraint requiring a specific minimum proportion of each of four possible ply orientations (i.e. 0°, 90°, +45° and −45°) are studied and added as constraints into VICONOPT. In order to ensure the optimised layup can be used in practice, the LBB method is strongly enhanced with a checking strategy which imposes any combination of symmetry, balance and up to four layup design constraints in the logic-based search process of the second stage optimisation. By comparing the improved LBB method with the use of a genetic algorithm for optimising stacking sequences under different requirements as well as comparisons with the results of other authors, the high efficiency and ability to achieve an optimal result of the improved LBB method are demonstrated.

5.2 Methodology

The aim of the optimisation is to minimise the mass of the composite laminate. The constraints are buckling, manufacturing and lamination parameter constraints. The optimisation approach is divided into two stages. The lamination parameters and total laminate thickness are used as design variables in the first stage. Ply orientations, which are restricted to 0°, 90°, +45° and −45°, are used to build the actual layup for the laminate in the second stage.

Niu (1992) listed layup design constraints for the design of composite aircraft components. In this thesis, four major layup design constraints for composite laminate design are taken into account in the two-stage optimisation process, as follows:

(1) **Contiguity constraint:** the maximum number of successive plies with the same orientation is limited to an integer n_{cont} to minimise edge splitting. $n_{\text{cont}} = 4$ in this thesis.

(2) **Disorientation constraint**: the difference between the orientations of two adjacent plies should be no greater than an angle θ_{diff}. This constraint is applied to avoid microcracking. In this thesis, θ_{diff} is set to be 45°.

(3) **Minimum percentage constraint:** each fibre orientation should comprise a proportion of at least p_{min} of the total layup to prevent the matrix from being exposed to direct loads and provide sufficient damage tolerance to the laminate. $p_{\text{min}} = 10\%$ in this thesis.

(4) **Damage tolerance constraint:** putting 0° and 90° plies on the exterior surfaces of the laminate should be avoided to provide sufficient damage tolerance after impact.

5.2.1 First stage optimisation

The exact strip software VICONOPT is used for the first stage optimisation problem which can be expressed as

$$\text{Minimise} \quad M(\mathbf{x}) \tag{5.1}$$

$$\text{Subject to} \quad G_i(\mathbf{x}) \leq 0 \quad i = 1,2,3, \ \dots, n_g \tag{5.2}$$

$$x_j^l \leq x_j \leq x_j^u \quad j = 1,2,3, \ \dots, n_d \ (n_d \leq 10) \tag{5.3}$$

where $M(\mathrm{x})$ is the laminate mass. $\mathbf{x} = (h,\ \xi_1^A, \xi_2^A, \xi_3^A, \xi_1^D, \xi_2^D, \xi_3^D, \xi_1^B, \xi_2^B, \xi_3^B)$ is the vector of design variables, $G_i(\mathbf{x})$ are inequality design constraints, including buckling and lamination parameter constraints. The implementations of these constraints in VICONOPT were described in Chapter 4.

The minimum percentage constraint, i.e. layup design constraint (3) above, is added to the lamination parameter constraints in this thesis. When giving the percentage of each ply orientation a minimum value $p_{\min}$, the feasible region of the lamination parameters is further restricted. Because the number of plies of each orientation is directly related to the in-plane lamination parameters $\xi_{1,2,3,}^A$, and the contribution of each angle is known as shown in Table 5.1, the relationship between the number of plies with each orientation and the three lamination parameters $\xi_{1,2,3}^A$ can be expressed as follows

$$n_0 + n_{45} + n_{-45} + n_{90} = n \tag{5.4}$$

$$n_0 - n_{90} = n\xi_1^A \tag{5.5}$$

$$n_0 - n_{45} - n_{-45} + n_{90} = n\xi_2^A \tag{5.6}$$

$$n_{45} - n_{-45} = n\xi_3^A \tag{5.7}$$

where the non-negative integers n and n_θ represent the total number of plies and the number of plies with orientation θ, respectively. The minimum percentage constraint can be expressed as

$$n_0/n = \xi_1^A/2 + \xi_2^A/4 + 1/4 \geq p_{\min} \tag{5.8}$$

$$n_{90}/n = -\xi_1^A/2 + \xi_2^A/4 + 1/4 \geq p_{\min} \tag{5.9}$$

$$n_{45}/n = -\xi_2^A/4 + \xi_3^A/2 + 1/4 \geq p_{\min} \tag{5.10}$$

$$n_{-45}/n = -\xi_2^A/4 - \xi_3^A/2 + 1/4 \geq p_{\min} \tag{5.11}$$

Table 5.1 Contribution of each ply orientation to the in-plane lamination parameters.

θ	ξ_1^A	ξ_2^A	ξ_3^A
0°	1	1	0
+45°	0	−1	1
−45°	0	−1	−1
90°	−1	1	0

The related lamination parameter constraints in equation (4.10) are then re-written as

$$2|\xi_1^A| - \xi_2^A + 4p_{\min} - 1 \leq 0, \;\; 2|\xi_3^A| + \xi_2^A + 4p_{\min} - 1 \leq 0 \qquad (5.12)$$

Hence, $\xi_2^A \in [4p_{\min} - 1, 1 - 4p_{\min}]$. Because of the relationship between $\xi_{1,2,3}^A$ and $\xi_{1,2,3}^D$ as illustrated in equation (4.12), $\xi_2^D \in [16{p_{min}}^3 - 1, 1 - 16{p_{min}}^3]$. Therefore, the corresponding relationships in equation (4.10) between $\xi_{1,2,3}^D$ for a symmetric laminate (i.e. $\xi_{1,2,3}^B = 0$) are changed to

$$2|\xi_1^D| - \xi_2^D + 16{p_{\min}}^3 - 1 \leq 0, \;\; 2|\xi_3^D| + \xi_2^D + 16{p_{\min}}^3 - 1 \leq 0 \qquad (5.13)$$

Feasible regions for $\xi_{1,2,3}^A$ and $\xi_{1,2,3}^D$ are shown in Figures 5.1 and 5.2 respectively. The triangular regions with the dashed lines represent the previous feasible regions given by equation (4.10). In this thesis, $p_{\min}$ is required to be 0.1 and when the minimum percentage constraint is added, these triangles are reduced to the smaller triangles surrounded by the solid lines. It is seen that the areas of the feasible regions of $\xi_{1,2,3}^A$ are reduced by 64% while those of $\xi_{1,2,3}^D$ are reduced by only about 3%.

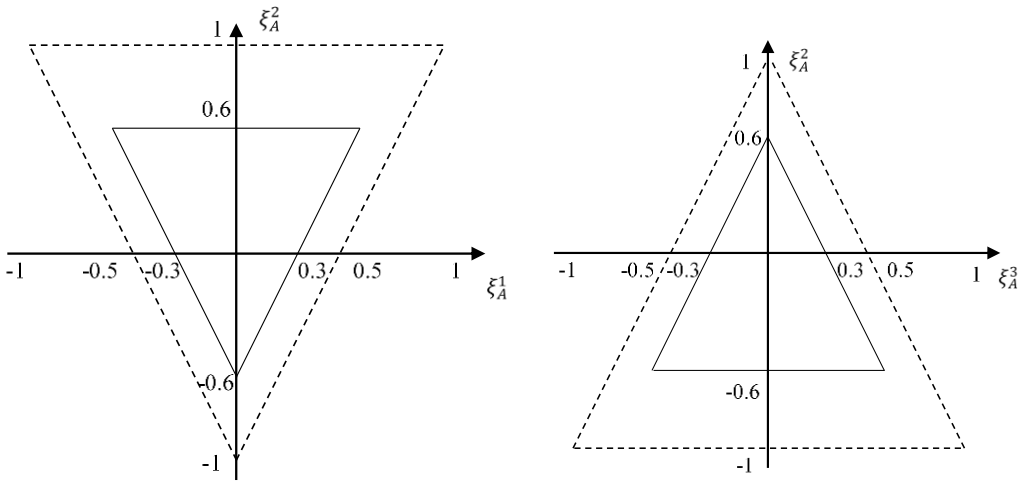

Figure 5.1 Restricted feasible regions of lamination parameters $\xi_{1,2,3,}^{A}$ when considering the minimum percentage constraint $p_{\min} = 0.1$.

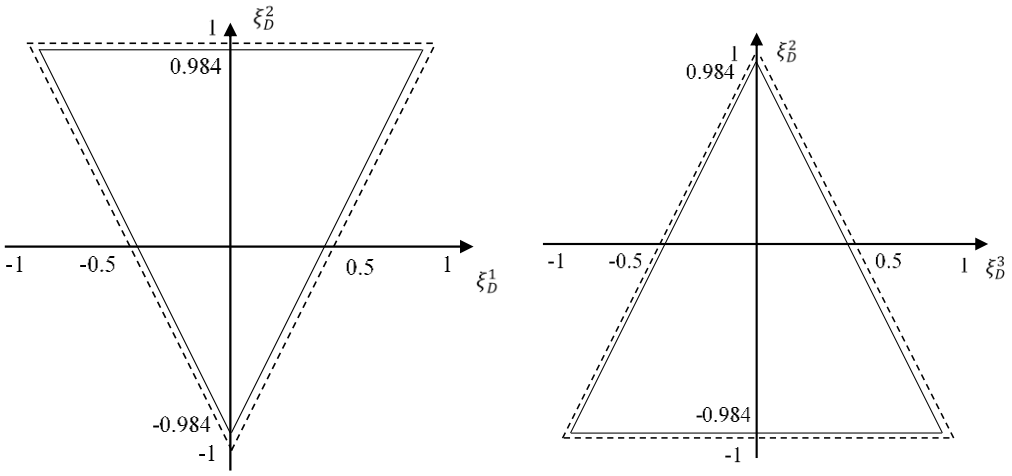

Figure 5.2 Restricted feasible regions of lamination parameters $\xi_{1,2,3,}^{D}$ for symmetric laminates, when considering the minimum percentage constraint $p_{\min} = 0.1$.

5.2.2 Second stage optimisation

After the first stage, the optimised laminate thickness h is rounded to the nearest integer multiple nh_p of the ply thickness h_p, and the optimised lamination parameters are used as target values in the second stage. The aim of this second stage is a layup to match the target values as closely as possible, with the improved LBB methods and the most popular technique GAs both having this ability to search the potential layups.

5.2.2.1 Layerwise branch and bound method

The LBB method is a combination of the branch and bound method and a global layerwise technique. In the branch and bound method, branches (i.e. choice options) constitute the decision tree of which the size (i.e. the number of levels) is dependent on the numbers of plies to be optimised. The structure of a decision tree which only considers two plies (these are denoted θ_4^4 and θ_5^4, the notation and the numbers in the boxes will be explained later) is shown in Figure 5.3.

As the problem size increases, the search time tends to grow dramatically, for example a decision tree with 16 levels potentially has $4^{16} \cong 4.3 \times 10^9$ possibilities to search. Therefore, the global layerwise technique is developed to improve the efficiency of the branch and bound process. The objective function Γ is obtained by calculating the weighted difference between the target lamination parameters given by VICONOPT and the actual lamination parameters related to the chosen ply orientations as follows

$$\Gamma = \sum_{i=1}^{3} \sum_{j=A}^{A,B,D} w_j \left| \xi^j_{i(actual)} - \xi^j_{i(target)} \right| \tag{5.14}$$

where $w_{A,B,D}$ are weighting factors, $\xi^{A,B,D}_{1,2,3(target)}$ are the target lamination parameters obtained in the first stage, and $\xi^{A,B,D}_{1,2,3(actual)}$ are the actual lamination parameters for the chosen layup.

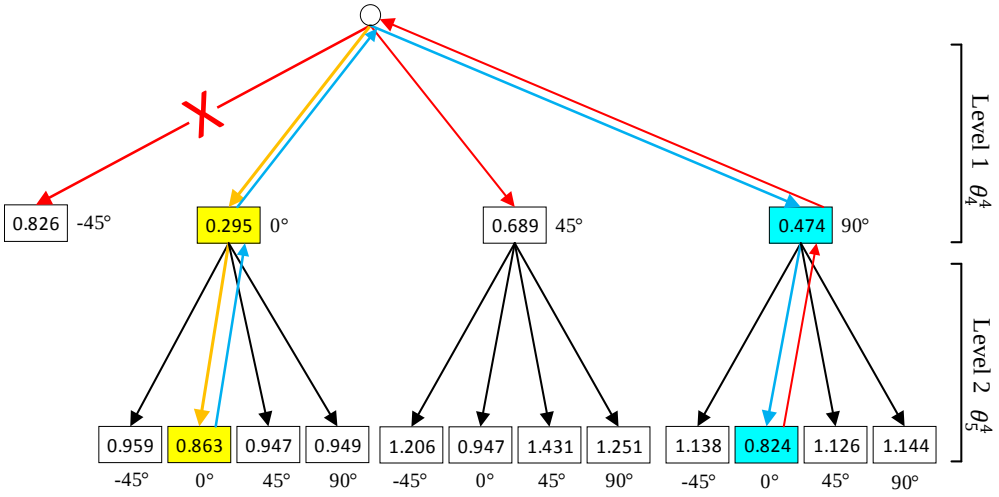

Figure 5.3 An illustrative branch and bound decision tree for optimising two plies.

The branching process can predict the route to proceed to at the next level of the decision tree by considering bounds on the achievable values of the objective function. The aim is to opt for a branch which is close to the target value of the lamination parameters. If a layup is found for which Γ is lower than that of the previous best solution, the chosen layup is saved as the incumbent solution. The bounding process is used to discard the branches which cannot improve on the objective function of the incumbent solution or which violate constraints (e.g. layup design constraints, balance constraint, symmetry constraint). Thus the process operates most efficiently on small problems or when there is a good incumbent solution.

To obtain good incumbent solutions as quickly as possible in the process, a global layerwise technique is employed to accelerate the search. This technique has three nested loops: cycle, pass and case, as shown in Figures 5.4 and 5.5. The cycle loop is the outer loop which determines how many layers are optimised at once in the decision tree. The pass loop makes the optimisation repeat from the outermost layers to ensure the result is not a local optimum with the current number of layers being optimised in the decision tree. The case loop is the inner loop in which the branch and bound optimisation is conducted on a specific subset of layers. The process is illustrated in Figure 5.4 using an example of an 8 ply laminate. For each case, the plies available for selection by the branch and bound method are shown in bold, and the optimisation starts from an arbitrary layup $(\theta_1^0, \theta_2^0, \theta_3^0, \theta_4^0, \theta_5^0, \theta_6^0, \theta_7^0, \theta_8^0)$. The ply orientations are optimised successively, working inwards from the outer plies which make the most important contributions to the out-of-plane lamination parameters $\xi_{1,2,3}^D$. In the first cycle, two plies are optimised at once. In the first case of the first pass of the first cycle the two outermost plies are optimised to become (θ_1^1, θ_8^1). The newly optimised layup is then used as the starting layup for the second case where the solution is (θ_2^1, θ_7^1), and so on. When the innermost plies (θ_4^1, θ_5^1) are obtained, the first pass of the first cycle is completed and a second pass of the first cycle is made until no further changes are made. In the second cycle, 4 plies are optimised at once, again with the process being repeated until the value of Γ cannot be reduced. The number of variable plies in the third cycle is 6 (or fewer), while all the plies are optimised in the final cycle. (For brevity in Figure 5.4, two passes are shown in cycle 2, but only one pass for the other

Cycle	0	1	1	1	1	2	2	2	2	3	3	4
Pass	0	1	1	1	1	1	1	2	2	1	1	1
Case	0	1	2	3	4	5	6	7	8	9	10	11
Var. plies	2	2	2	2	2	4	4	4	4	6	2	8
Ply1	θ_1^0	$\boldsymbol{\theta_1^1}$	θ_1^1	θ_1^1	θ_1^1	$\boldsymbol{\theta_1^5}$	θ_1^5	$\boldsymbol{\theta_1^7}$	θ_1^7	$\boldsymbol{\theta_1^9}$	θ_1^9	$\boldsymbol{\theta_1^{11}}$
Ply2	θ_2^0	θ_2^0	$\boldsymbol{\theta_2^2}$	θ_2^2	θ_2^2	$\boldsymbol{\theta_2^5}$	θ_2^5	$\boldsymbol{\theta_2^7}$	θ_2^7	$\boldsymbol{\theta_2^9}$	θ_2^9	$\boldsymbol{\theta_2^{11}}$
Ply3	θ_3^0	θ_3^0	θ_3^0	$\boldsymbol{\theta_3^3}$	θ_3^3	θ_3^3	$\boldsymbol{\theta_3^6}$	θ_3^6	$\boldsymbol{\theta_3^8}$	$\boldsymbol{\theta_3^9}$	θ_3^9	$\boldsymbol{\theta_3^{11}}$
Ply4	θ_4^0	θ_4^0	θ_4^0	θ_4^0	$\boldsymbol{\theta_4^4}$	θ_4^4	$\boldsymbol{\theta_4^6}$	θ_4^6	$\boldsymbol{\theta_4^8}$	θ_4^8	$\boldsymbol{\theta_4^{10}}$	$\boldsymbol{\theta_4^{11}}$
Ply5	θ_5^0	θ_5^0	θ_5^0	θ_5^0	$\boldsymbol{\theta_5^4}$	θ_5^4	$\boldsymbol{\theta_5^6}$	θ_5^6	$\boldsymbol{\theta_5^8}$	θ_5^8	$\boldsymbol{\theta_5^{10}}$	$\boldsymbol{\theta_5^{11}}$
Ply6	θ_6^0	θ_6^0	θ_6^0	$\boldsymbol{\theta_6^3}$	θ_6^3	θ_6^3	$\boldsymbol{\theta_6^6}$	θ_6^6	$\boldsymbol{\theta_6^8}$	$\boldsymbol{\theta_6^9}$	θ_6^9	$\boldsymbol{\theta_6^{11}}$
Ply7	θ_7^0	θ_7^0	$\boldsymbol{\theta_7^2}$	θ_7^2	θ_7^2	$\boldsymbol{\theta_7^5}$	θ_7^5	$\boldsymbol{\theta_7^7}$	θ_7^7	$\boldsymbol{\theta_7^9}$	θ_7^9	$\boldsymbol{\theta_7^{11}}$
Ply8	θ_8^0	$\boldsymbol{\theta_8^1}$	θ_8^1	θ_8^1	θ_8^1	$\boldsymbol{\theta_8^5}$	θ_8^5	$\boldsymbol{\theta_8^7}$	θ_8^7	$\boldsymbol{\theta_8^9}$	θ_8^9	$\boldsymbol{\theta_8^{11}}$

Figure 5.4 Application of the global layerwise technique to optimisation of an 8 ply laminate. (The layers in the current case loop are bold, and the other ones are not allowed to change.)

cycles.) Therefore, the branch and bound method initially optimises the layup by searching a small decision tree meaning that very low values of Γ can be obtained quickly during the first few cycles. Subsequently, when searching larger numbers of plies, the previous incumbent value of Γ is used in the bounding process, enabling many branches to be discarded without being explored. Therefore, optimised stacking sequences can be obtained efficiently.

During each case, after a new incumbent layup has been chosen or it has been shown that the currently chosen branch cannot improve on the objective function no matter which lower branches are chosen, the remaining branches in the decision tree must subsequently be explored (to seek better solutions) or discarded (if they cannot improve on the incumbent solution) in order to prove global optimality. An example is given to illustrate this backtracking process. Suppose the branch and bound process is working on the fourth case of the first pass of the first cycle as shown in Figure 5.4, of which the decision tree is shown in Figure 5.3. The required lamination parameters are $\xi_1^A = 0.27$, $\xi_2^A = 0.2$, $\xi_3^A = -0.08$, $\xi_1^D = -0.09$, $\xi_2^D = -0.12$, $\xi_3^D = -0.44$, ξ_1^B =0.1, ξ_2^B =0.8, ξ_3^B =0.1, and the incumbent layup before this case is [−45/45/−45/90/90/0/0/90] with the value of $\Gamma = 1.144$. The numbers in the boxes at the lowest level of the decision tree are the exact values of Γ for the complete layup. For those at the first level, because the layup has not yet been completed, the numbers are lower bounds for each branch, which are obtained by subtracting the maximum

achievable contribution of the remaining levels from the exact value of Γ obtained from the contributions of the preceding levels. For example, for the branch 0° at the first level in Figure 5.3, the ply angle at the second level has not been chosen and the provisional value of Γ for the uncompleted layup [−45/45/−45/0/#/0/0/90] is 0.787. The maximum achievable contribution of each of the lamination parameters of the ply at the second level can be obtained by the following equation

$$\begin{bmatrix} \xi_1^k \\ \xi_2^k \\ \xi_3^k \end{bmatrix} = \left| \int_{-h/8}^{0} Z^k \, dz \right|, k = A, B, D, \begin{cases} Z^A = 1/h \\ Z^B = 4z/h^2 \\ Z^D = 12z^2/h^3 \end{cases} \tag{5.15}$$

Hence, the maximum achievable contributions of the ply at the second level are summed to 0.492, and the lower bound for the 0° branch at the first level is obtained as $0.787 - 0.492 = 0.295$. Actually, this lower bound cannot be reached because the maximum contributions of each lamination parameter cannot be achieved simultaneously, but it can be used as a conservative limit. As can be seen from the decision tree, the branch 0° (whose lower bound 0.295 is the lowest) is chosen at the first level in the initial search (see the yellow arrows and boxes). Then at the second level the best layup 0°/0° is chosen, and the incumbent value of Γ decreases to 0.863 which is used as a new upper bound in the process. Then the backtracking process starts to check the remaining branches. The second best branch 90° at the first level is explored first (see the blue arrows and boxes), and a better layup 90°/0° is then found at the second level enabling the incumbent value of Γ to be decreased to 0.824. This is lower than the lower bound 0.826 of branch −45° at the first level, indicating that better incumbent solutions cannot be found on this branch no matter which lower branches are chosen. Hence it can be discarded directly (see the red arrows) without being explored further, thus improving the efficiency of the process. Finally the backtracking process completes searching the branch 45° and its lower branches without finding a better layup, so that the layup 90°/0° is proved to be the global optimum in the current case.

Compared with the stochastic search of GAs, the method presented herein is more reliable for finding a global optimum, because it implicitly searches all the possibilities of the stacking sequence. Often optimal results can be obtained at an early stage even

for the laminates with large numbers of plies. However, it takes a long time to prove this optimality for laminates with a large number of plies since the decision trees in later cycles are very large. Therefore, on large problems it is recommended to apply a stopping criterion such as an acceptably low value of Γ (e.g. 0.3), maximum solution time or the completion of a specific cycle (e.g. 9^{th} cycle), after which the incumbent solution will be accepted without proving optimality.

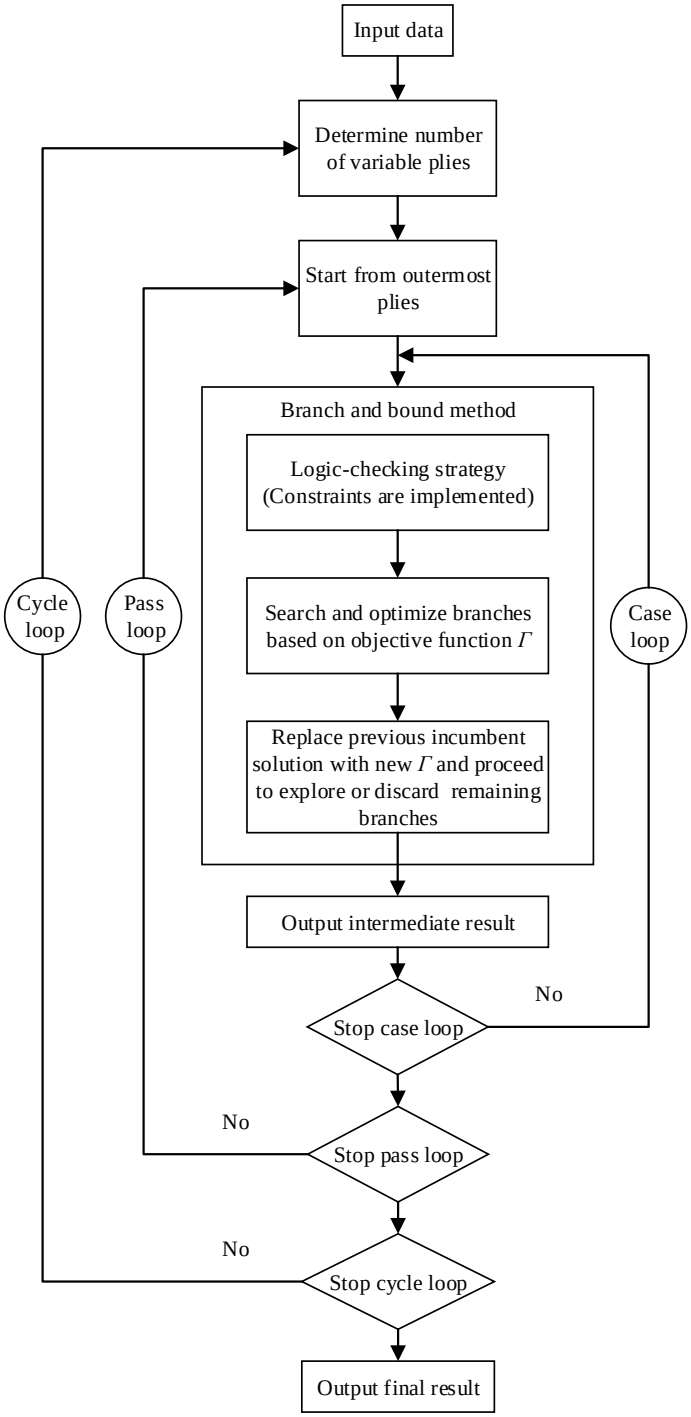

Figure 5.5 Flow chart of the improved LBB method.

5.2.2.2 Addition of constraints

A logic-based checking strategy is used for implementing constraints in the search process. When adding constraints such as the symmetry constraint, the balance constraint and the layup design constraints in the optimisation, this strategy checks and discards any branches violating constraints before every branching decision is made. Therefore, only the branches satisfying the constraints are searched at each level of the decision tree, ensuring that all the intermediate results satisfy the required constraints.

When the layup is required to be symmetric, the branching process is used to find the orientation of each ply in the top half of the laminate, and then the checking strategy will force the symmetrically located ply in the bottom half to have the same orientation, essentially halving the number of levels in the decision tree.

The balance constraint is implemented by checking the difference between the number of plies which have already been chosen with +45° (n_{45}) and those with −45° (n_{-45}) at every level of the decision tree. If the value of $n_{45} - n_{-45}$ is equal to n_{left}, the number of plies left to choose in the current case, all the remaining plies must be set to −45°. If the value $n_{45} - n_{-45} = n_{\text{left}} - 1$, the next ply cannot be set to +45°. Analogous rules apply for −45°. As shown in the examples in Figure 5.6, if there are 8 plies in a case and the first 6 plies have already been chosen, θ_4 is under selection. In Figure 5.6 (a), two +45° plies and one −45° ply have been chosen and there are only two plies left, so θ_4 is not allowed to be +45°. In Figure 5.6 (b), θ_4 must be set to

θ_1 (0°)	θ_1 (-45°)
θ_2 (45°)	θ_2 (0°)
θ_3 (90°)	θ_3 (45°)
⇒ θ_4	⇒ θ_4
θ_5	θ_5
θ_6 (-45°)	θ_6 (-45°)
θ_7 (0°)	θ_7 (-45°)
θ_8 (45°)	θ_8 (90°)

(a) (b)

Figure 5.6 Checking strategy for balance constraint. (a) θ_4 cannot be +45°. (b) θ_4 must be +45°.

+45°, owing to the fact that there are already three −45° plies but only one +45° ply with two plies left to choose. This procedure has advantages over a commonly used alternative strategy which combines a +45° ply with a −45° ply as a single design variable, which automatically violates the disorientation constraint, i.e. layup design constraint (2) above, and potentially misses the global optimal result. Furthermore, all possible balanced stacking sequences are searched using this logic-based strategy, so the global optimal layup under the balance constraint can be achieved.

Four layup design constraints are included in the logic-based search through the checking strategy. The contiguity constraint is implemented by checking plies to avoid an adjacent group with more than n_{cont} identical orientations (where n_{cont} is 4 in this thesis according to practical requirement). If such a group is formed the bounding process is forced to discard this choice. For all levels except the final two in each case, since the ply angles below the current level (towards the mid-plane) have not been chosen, only the four plies above the current level (away from the mid-plane) should be checked (hence this check starts from level 9 in Figure 5.7 at which four plies have already been chosen above it). If these plies all have the same angle, this branch at the current level is discarded. For the last two levels in the case, because the ply angles below have also been chosen previously and are not allowed to change in the current case, more possibilities for generating five successive plies with the same angle exist. For a laminate with an even number of plies, if the second last level in the case is smaller than the number of plies in the laminate minus 3, the adjacent plies that need to be checked are shown to the left of Figure 5.7, where the triangle and circles in each rectangular bar represents the ply under selection and the adjacent plies that need to be checked, respectively. As discussed above, for level 11 in this example, the leftmost bar is used to check the four plies above, and the remaining bars to check other groups of adjacent plies. As the second last level gets closer to the mid-plane, (Figure 5.7 centre and right), the last level which has not been optimised is included in some of the five successive ply groups which should not be checked in the process. Note that these groups should be checked for a symmetric laminate, because the last level is given the same ply angle as the second last level. Figure 5.8 shows the groups that need to be checked for a laminate with an odd number of plies, following a similar procedure to that described above.

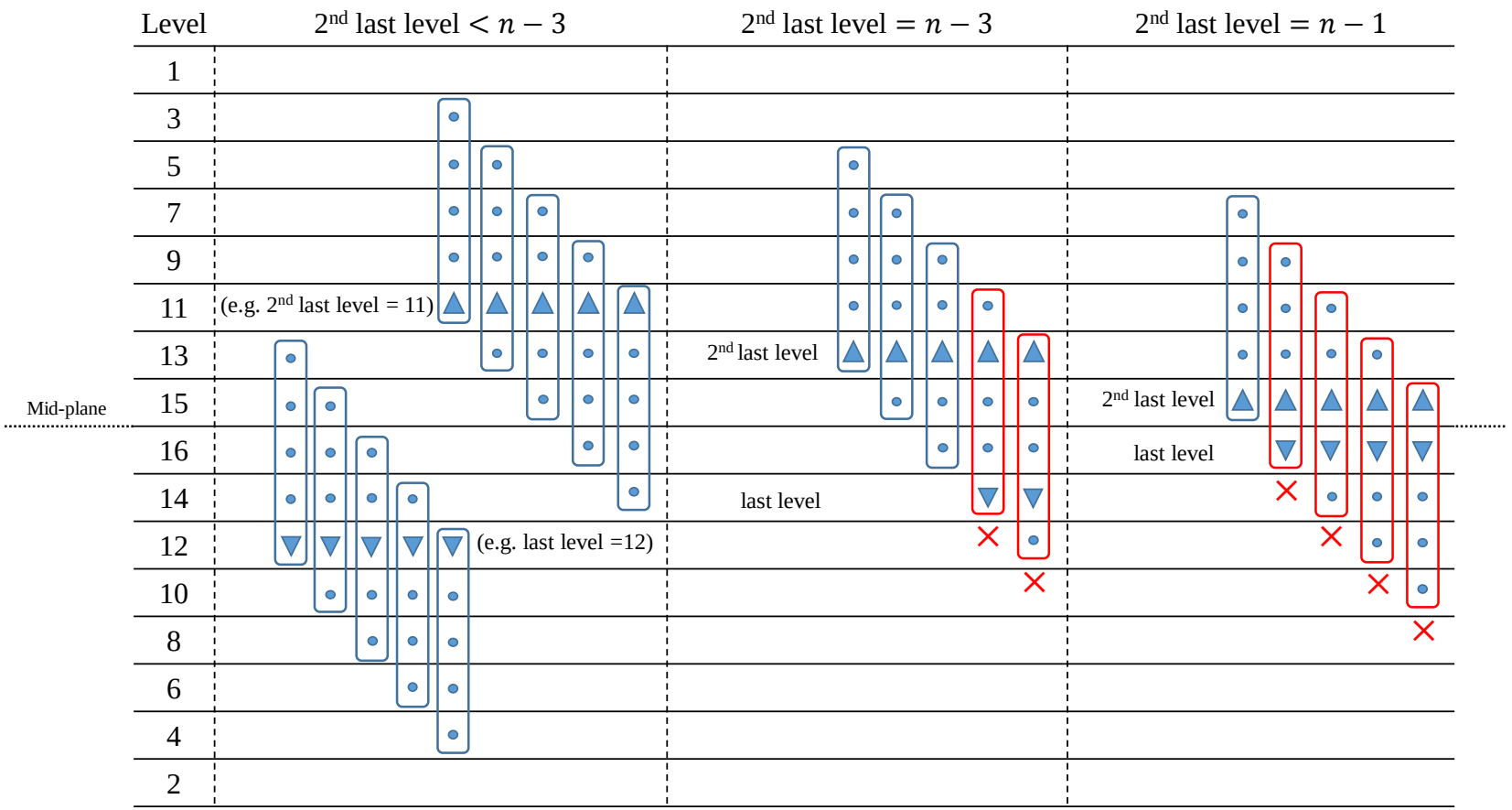

Figure 5.7 Checking strategy for contiguity constraint for the laminate with even number of plies.

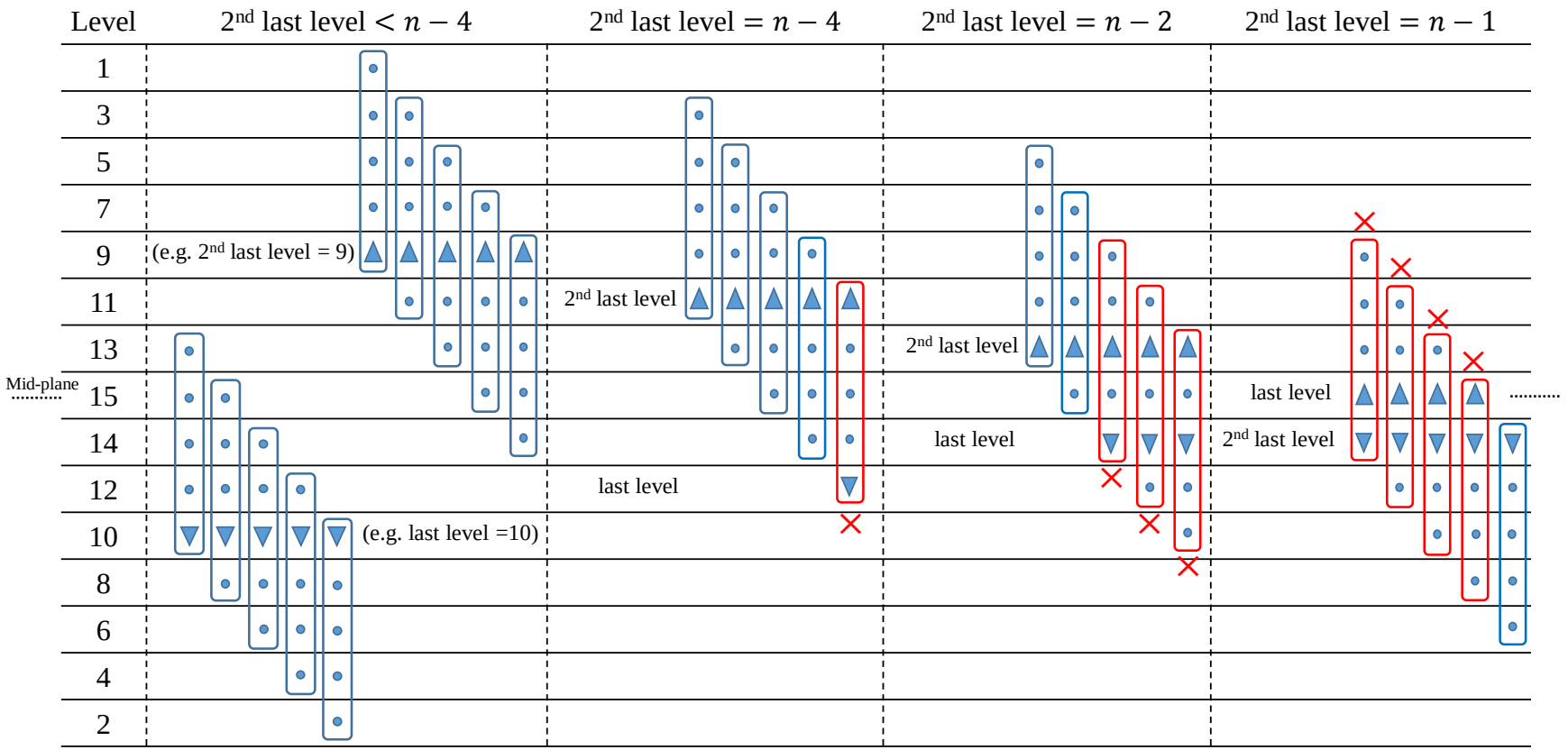

Figure 5.8 Checking strategy for contiguity constraint for the laminate with odd number of plies.

When considering the disorientation constraint, the logic-based strategy checks the already chosen plies which are adjacent to the ply under selection, and discards the choices which would makes the difference with adjacent orientations greater than θ_{diff}. For example, in the first case of the third cycle in Figure 5.4, if θ_1^9 has been chosen as +45°, ply 2 is under consideration, and ply 3 has not yet been chosen, the choices for ply 2 are compared with θ_1^9 and are restricted to 0°, +45°, 90°, i.e. the choice θ_2^9=−45° is discarded. Suppose θ_2^9 is chosen to be 0°. Then, when ply 3 is being chosen it is necessary to consider θ_2^9 and θ_4^8 simultaneously because θ_4^8 was chosen in the previous case and is fixed in this case. So if θ_4^8 is 90°, θ_3^9 can only become −45° or +45°.

As for the minimum percentage constraint, this has been included with the lamination parameter constraints in the first stage. However, to avoid a rare situation where the lamination parameters of the actual layup are located outside of the feasible region, the minimum percentage constraint is also included in the logic-based search. During the process, the percentage of each angle is calculated every time a new ply orientation is chosen, and results violating this constraint are abandoned.

The damage tolerance constraint is implemented by discarding the 0° and 90° branches when processing the two outermost plies.

The initial layup for this improved LBB method is normally chosen as a multiple of a ply group of $[-45/0/45/90]_s$, which can constitute laminates with number of plies equal to multiples of eight. For laminates with other numbers of plies, combinations of the following three groups $[-45/45]_s$, $[90 \text{ or } 0]_s$ and [0] are added at the middle of the laminate. Note that these plies should be placed next to plies with the same angle to avoid violating the disorientation constraint. Thus the logic-based search starts with a layup which satisfies all the constraints, ensuring that all the intermediate results and the final result satisfy these constraints.

5.2.2.3 Genetic algorithm

As the most popular method in layup optimisation, GAs based on a stochastic search have also been employed in the second stage as an alternative to the improved LBB method in order to make a comparison of the two techniques. The GA used herein is composed of the following procedures:

1. Generate an initial population of random layups.
2. Select individuals for reproduction based on a fitness function.
3. Create a new generation through crossover, mutation and permutation operators.
4. The balance constraint is achieved using repair operators (optional).
5. The layup design constraints are implemented by adding penalty terms to the fitness function (optional).
6. Repeat steps 2-5 until one individual satisfies the stopping criterion.

The stacking sequence of each individual is represented by a string of genes in the chromosome. The values of the genes are 1, 2, 3 and 4, corresponding to ply orientations of $-45°$, 0°, +45° and 90°, respectively. The biased roulette wheel method is employed in the selection procedure. The elitism operator is implemented to retain the best two individuals for the next generation without being changed. A two-point crossover operator with a high value of probability P_c is used, following which the gene in the chromosome is mutated with a low value of probability P_m (the commonly used values (i.e. P_c = 0.8, P_m = 0.1), and a population size of 50 are used in this chapter). After mutation, a permutation is applied to all chromosomes. The fitness function is formulated as

$$f = [\Gamma + p_{m1} + p_{m2} + p_{m3} + p_{m4}]^{-1} \tag{5.16}$$

where Γ is defined in (5.14) and p_{m1}, p_{m2}, p_{m3} and p_{m4} are penalty terms for layup design constraints (1), (2), (3) and (4), above, respectively. A new repair operator which is similar to that of Todoroki and Haftka (1998) is employed to enforce the balance constraint. This operator calculates the difference between the number of +45° plies and $-45°$ plies for each individual. If the difference is even, half of the excess plies (+45° or $-45°$) are replaced by plies ($-45°$ or +45°) from the innermost excess

plies. If the difference is odd, excess plies (+45° or − 45°) are replaced by complementary plies (−45° or +45°) until there is only one excess ply left, and this ply is then replaced by one at 0° or 90°. For the special situation when there is only one +45° or −45° ply and the number of complementary plies is 0, the innermost 0° or 90° ply is replaced by the ply required to balance the laminate.

5.3 Results and discussion

Two sets of results are presented here. In the first set, the performance of the proposed two-level layup optimisation is demonstrated with the efficiency of the improved LBB method used in the second stage illustrated by comparison with the GA. In the second set, the target lamination parameters used in the improved LBB method are taken directly from (Herencia *et al.* 2007) to further demonstrate the capability of the technique for searching stacking sequences. All the results were obtained on a 4 GHz PC.

5.3.1 Layup optimisation of a simply supported rectangular laminate

Firstly, layup optimisation results are given for a simply supported rectangular laminate loaded in longitudinal compression, the details of which are provided in Table 5.2. The required buckling load of this laminate is $p_d = 100$ kN, and the lamination parameters relating to the original layup listed at the bottom of the table are $\xi_1^A = -0.1875$, $\xi_2^A = 0.125$, $\xi_3^A = 0.0625$, $\xi_1^D = -0.5251$, $\xi_2^D = 0.2056$, $\xi_3^D = 0.1643$, $\xi_{1,2,3}^B$=0. Different combinations of constraints are imposed on this laminate.

Table 5.2 Properties and dimensions of the example laminate.

E_1 (kN/mm^2)	128
E_2 (kN/mm^2)	10.3
G_1 (kN/mm^2)	6.0
ρ (kg/mm^3)	1500
ν_{12}	0.3
Length (mm)	150
Width (mm)	100
Ply thickness (h_p) (mm)	0.125
Original total thickness (h) (mm)	4.0
Original layup	$[90_2/45/90/45/-45/90_2/45/-45/0_2/45/-45/0/90]_S$

Table 5.3 shows the optimised results from the first stage of the optimisation taken from VICONOPT. After the first stage, the buckling loads p_c of this laminate under a number of different constraints are all equal to the design load $p_d = 100$ kN, and the laminate thicknesses (h) have reduced to around 3.5 mm allowing the number of plies n_t to reduce from 32 to 28. Therefore, it is clearly seen that 12.5% mass savings are achieved for these problems during the first stage. In the basic case which is not required to be symmetric or balanced, 9 lamination parameters are allowed to vary in the optimisation, whereas in the symmetric case, $\xi^B_{1,2,3}$=0 are forced to be 0, while ξ^A_3 is forced to be 0 when the laminate is required to be balanced. The solution times of VICONOPT for these problems are all less than 1 second.

The lamination parameters listed in Table 5.3 are used as target values in the second stage optimisation where layups under different design requirements are obtained using the improved LBB method with all the weighting factors $w_{A,B,D}$ equal to 1. There are six groups of layups in Table 5.4, which correspond to the six groups of required lamination parameters in Table 5.3.

It can be seen from the penultimate column of Table 5.4 that the global optimum results for all the symmetric laminates can be obtained within a very short time, usually followed by a longer time to complete the whole search. The exception is example 15 in which the global optimum result is obtained at 6.4 seconds, but a result with a value of $\Gamma = 0.1189$ which is very close to the global optimum result is obtained at 0.38 seconds.

Table 5.3 Stage 1 optimisation results.

Constraints	ξ_1^A	ξ_2^A	ξ_3^A	ξ_1^D	ξ_2^D	ξ_3^D	ξ_1^B	ξ_2^B	ξ_3^B	n	p_c/p_d	time (s)
Basic	−0.1680	−0.0854	0.0097	0.0746	−0.7087	−0.0261	−0.0072	−0.0072	−0.0072	28	1.0	0.785
Symmetric	−0.1913	−0.0612	−0.0344	0.0259	−0.7922	−0.0303	0	0	0	28	1.0	0.559
Sym+10%	−0.0888	−0.2551	0.0856	0.0628	−0.8113	−0.0123	0	0	0	28	1.0	0.502
Balanced	−0.1542	−0.0802	0	0.0299	−0.8037	−0.0598	−0.029	−0.029	−0.029	28	1.0	0.879
Sym+bal	−0.1519	−0.0621	0	0.0437	−0.7900	−0.0233	0	0	0	28	1.0	0.395
Sym+bal+10%	−0.1196	−0.0585	0	0.0483	−0.7210	−0.0196	0	0	0	28	1.0	0.310

Table 5.4 Stage 2 optimisation results obtained from the improved LBB method.

Example	Constraints	Total plies	Layup	Γ	p_c/p_d	Time to optimum soln (s)	Total time (s)
1	Basic	28	$[-45_2/45/-45/45_2/0_2/45/90_4/45/90_5/(0/-45)_2/45/-45_2/45_2]$	0.0806	1.0	4.77	3600+
2	Symmetric	28	$[45/-45/45/-45/-45/45/-45/0_2/90_5]_S$	0.1729	1.0	0.52	7.1
3	Sym + contiguity	28	$[45/-45_2/45/-45/45/0/-45/45/90_2/0/90_2]_S$	0.1768	1.0	0.31	7.4
4	Sym + disorientation	28	$[-45_2/0/45_4/90/-45/90_3/-45/0]_S$	0.4705	0.97	0.12	0.95
5	Sym + disorientation	29	$[-45_2/0/45_4/90/-45/90_3/-45/0_2]_{MS}$	0.4254	1.06	0.9	1.4
6	Sym + 10%	28	$[45/-45_3/45_3/0_2/-45/90/45/90_2]_S$	0.0658	1.0	0.23	5.87
7	Sym + 10% + contiguity + damtol	28	$[45/-45_3/45_3/0_2/-45/90/45/90_2]_S$	0.0658	1.0	0.29	5.3
8	Sym + 10% + contiguity + damtol + disorientation	28	$[-45_2/0/45_4/90/45/90/-45/90/-45/0]_S$	0.3404	0.97	0.55	0.64
9	Sym + 10% + contiguity + damtol + disorientation	29	$[-45_2/0/45_4/90/-45/90/45/0/-45/90_2]_{MS}$	0.33	1.08	0.23	0.91
10	Balanced	28	$[-45/45/(45/-45)_2/0/-45/0/45/90_7/0_2/90/45_2/-45/45/-45_3/45]$	0.0892	1.0	3.76	3600+
11	Sym + bal	28	$[-45/45/-45/45_2/-45/0/45/-45/90/0/90_3]_S$	0.0984	1.0	0.23	5.95
12	Sym + bal + contiguity	28	$[-45/45/-45/45_2/-45/0/45/-45/90_2/0/90_2]_S$	0.1115	1.0	0.29	6.34
13	Sym + bal + disorientation	28	$[-45_2/0/45_4/90/-45/90_3/-45/0]_S$	0.3828	0.97	0.19	0.9
14	Sym + bal + disorientation	29	$[-45_2/0/45_4/90/-45/90_3/-45/0_2]_{MS}$	0.3776	1.07	0.97	1.59
15	Sym + bal + 10%	28	$[45/-45_2/45_2/-45/0/-45/0/90_4/45]_S$	0.112	1.0	6.4	9.06
16	Sym + bal + 10% + contiguity + damtol	28	$[45/-45_2/45_2/-45/0/-45/0/90_4/45]_S$	0.112	1.0	0.30	6.55
17	Sym + bal + 10% + contiguity + damtol + disorientation	28	$[-45_2/0/45_4/90/-45/90_3/-45/0]_S$	0.3307	0.97	0.49	1.01
18	Sym + bal + 10% + contiguity + damtol + disorientation	29	$[-45_2/0/45_4/90/-45/90_3/-45/0_2]_{MS}$	0.2853	1.07	0.69	1.37

As the problem size increases, the total searching time will be longer, for example, as the number of layers in the basic case is doubled, the number of layers which need to be considered for the symmetric cases, have theoretically around 4×10^{28} new possibilities added. A promising result is obtained for the basic case at 4.77 seconds but it cannot be guaranteed as the global optimum result until the whole search is completed which takes more than 1 hour. Therefore, the search is forced to stop after the 9th cycle (around 90 seconds) in this analysis, because a very low value of Γ can be obtained early in the first few cycles, and the time for completing the decision tree search starts increasing dramatically at this point, being around 9 seconds, 80 seconds and 1200 seconds in the 8th, 9th and 10th cycles, respectively. Nevertheless, for practical design, the search can be stopped as soon as an acceptable result (e.g. the value of Γ is less than 0.3) is found.

The contiguity, disorientation and damage tolerance constraints are only introduced in the second stage. Owing to the nature of the contiguity and damage tolerance constraints, they only make minimal changes to the stacking sequence, and hence have only a small impact on the buckling load.

Figure 5.9 shows the contribution of each lamination parameter in the differences between the actual lamination parameters and the target values corresponding to the 18 examples listed in Table 5.4. It is clearly seen that the differences are quite small as values of Γ are around 0.1 except when adding the disorientation constraint which causes a more significant mismatch on ξ_2^D. Figure 5.10 compares the actual lamination parameters for examples 15, 16 and 17 against the target lamination parameters in the lamination parameter space. Target lamination parameters are represented by a blue circle. As examples 15 and 16 have the same actual lamination parameters they are both represented by red crosses, while the actual lamination parameters of example 17 are represented by black crosses. It can be seen that these three examples have the same $\xi_{1,2,3}^A$, which means that despite having different layup design constraints applied these laminates have the same number of plies for each angle, hence the differences between these cases are caused only by the stacking sequences. The distances between the actual lamination parameters and the target values for the $\xi_{1,2,3}^A$ are only around 0.1 as shown in Figure 5.9. As can be seen from Figures 5.10 (c) and 5.10 (d), the

contiguity and damage tolerance constraints have no effect on the stacking sequence in example 16 and very good matches are achieved for the out-of-plane lamination parameters. However, the disorientation constraint which introduces more limitations in choosing the stacking sequences causes ξ_2^D to be far from the target in example 17.

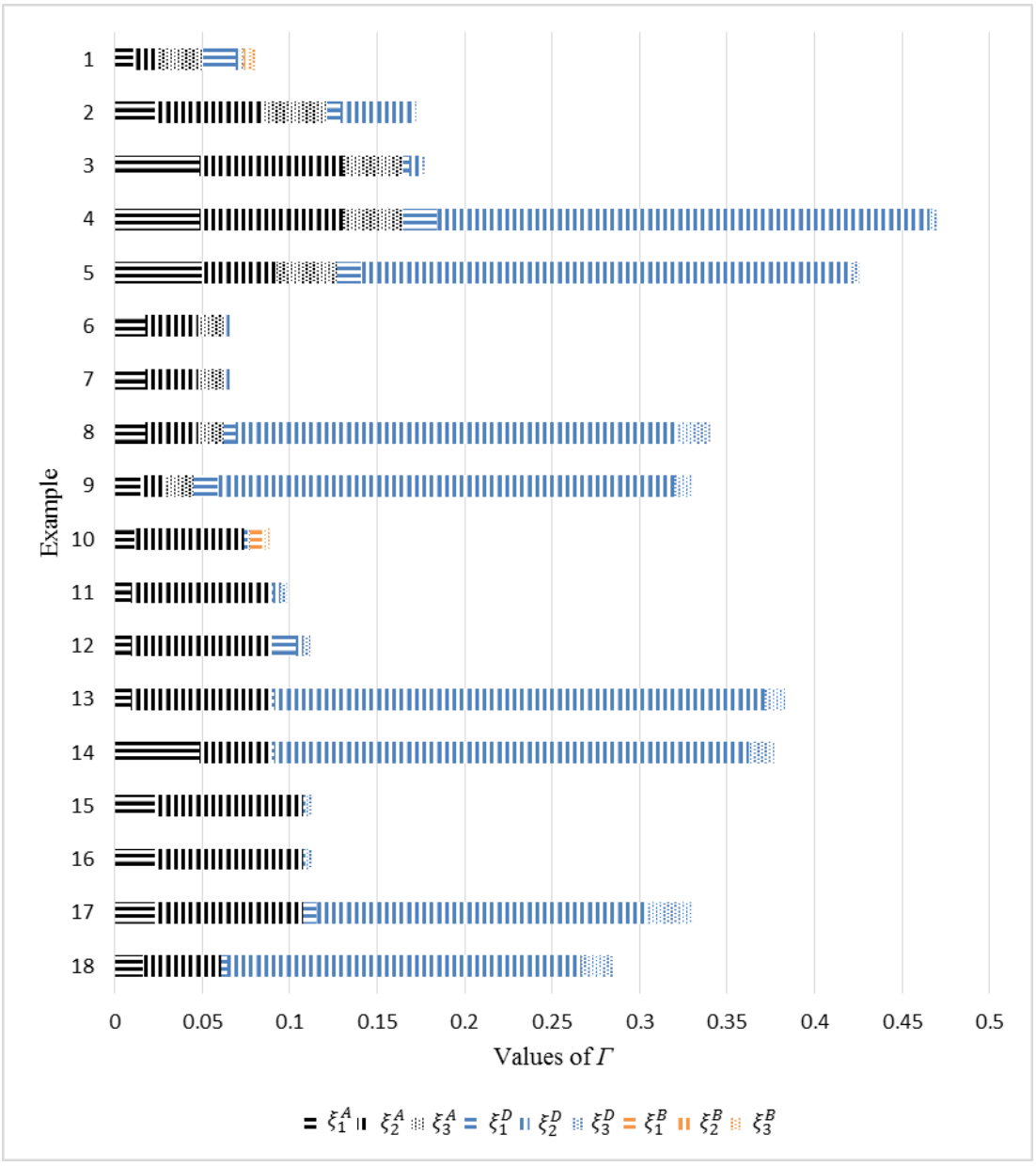

Figure 5.9 The contribution of each lamination parameter to the difference between target and actual lamination parameters for the 18 cases considered.

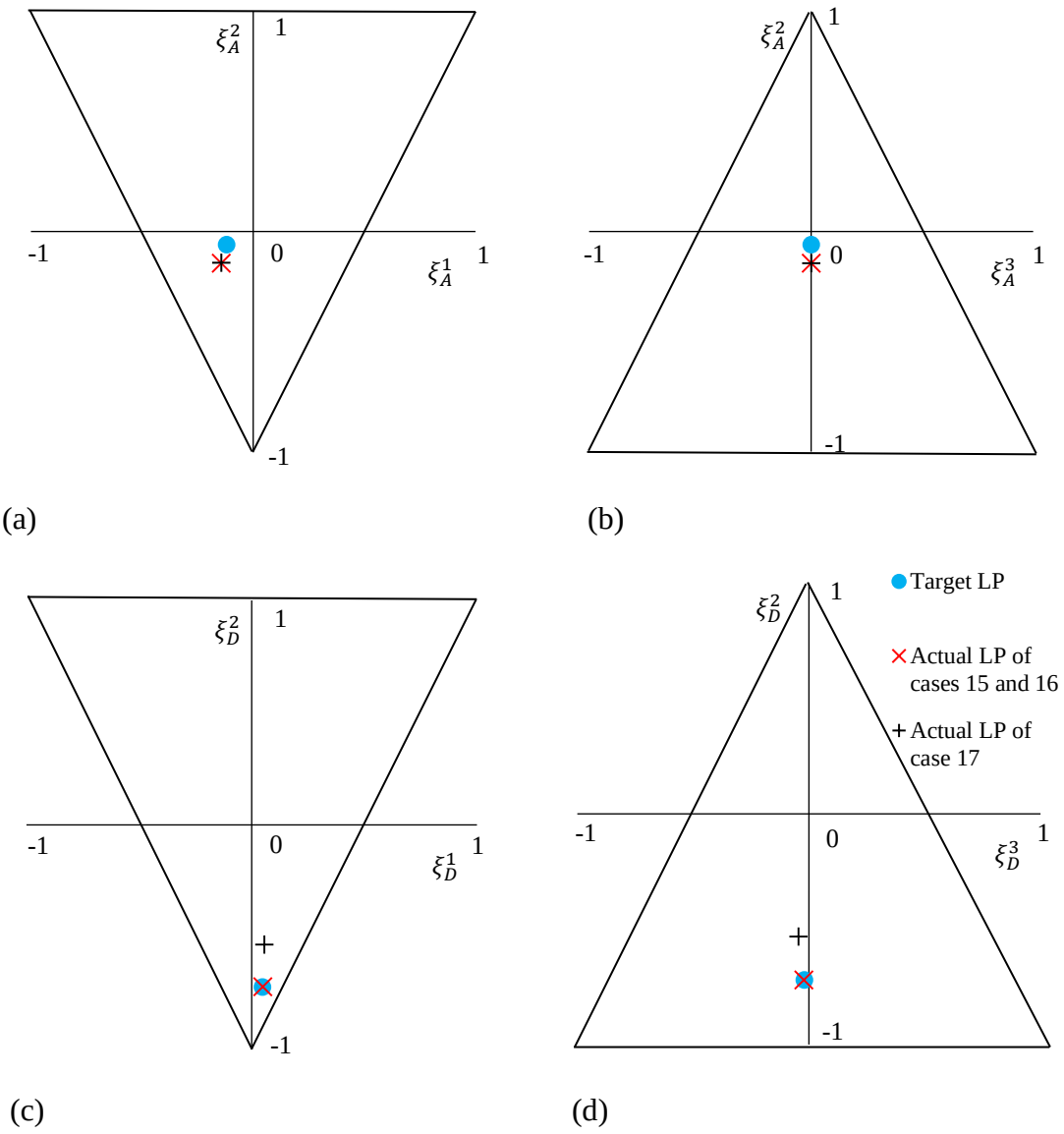

Figure 5.10 Plot of actual lamination parameters against target lamination parameters in lamination parameter space.

Because the disorientation constraint significantly reduces the search space, the total searching time for examples under the disorientation constraint is around 1 second which is much shorter than the other examples as shown in Table 5.4. However the presence of the disorientation constraint makes it quite easy to violate the buckling constraint. The buckling loads p_c for the examples which involve the use of the disorientation constraint are slightly lower than the design load p_d, and so these examples were re-run with the number of plies increased to 29, which increased p_c by

around 10% and thus satisfied the buckling constraint. Note that some examples in Table 5.4 have identical optimal layups but different values of Γ due to their different target values of lamination parameters.

As shown in Table 5.5, four of the symmetric examples listed in Table 5.4 were re-run using GAs in order to make a direct comparison with the improved LBB method in optimising the stacking sequences. Since GAs search randomly for each run, each GA was run 10 times for each example to guarantee the reliability of these comparisons. The times for obtaining the optimal result for each run are listed from the best to the worst in Table 5.5. It is observed that the GA almost always takes longer to find the global optimal result and is only faster than the improved LBB method in one case. In the last column of Table 5.5, as discussed above, the disorientation constraint makes the total searching time shorter for the improved LBB method as more branches can be discarded logically. However, it causes longer solution times for GAs, because the disorientation constraint can easily be violated by the crossover and mutation operators of the GAs during their stochastic search. A comparison between the solution times for the improved LBB method and the best 5 GAs for the symmetric case is shown in Figure 5.11 (a), where the blue circle represents the global optimal result obtained from the improved LBB method and the triangles in other colours represent the global optimal results given by the GAs. It can be seen that the best GA run (shown in red) obtains the optimal result at 0.37 seconds which is faster than the improved LBB method, but before this time point, the improved LBB method finds intermediate solutions quicker than all the GAs. Note that the end of the blue line indicates the end of the logic-based search during which all the possible layups have been implicitly searched, confirming that the global optimal result has been obtained. However, although all the GAs eventually found the same result, they could not confirm its optimality. Table 5.5 shows that the remaining 5 GAs (not shown in Figure 5.11 (a)) took a very long time to find the global optimal result. This is because these runs obtained a layup of $[45/–45/(–45/45)_2/0/–45/45/90_2/0/90_2]_S$ with $\Gamma = 0.17684$ or a layup of $[(–45/45)_3/45/0/90/–45/0/90_3]_S$ with $\Gamma = 0.1784$ at an early stage. Although these Γ are close to the optimal value, the corresponding layups are far away from the optimum layup, and it subsequently took a long time for the GAs to move away from these local optimum results.

Table 5.5 Comparison between GAs and the improved LBB method for four symmetric examples from Table 5.4.

	Example 2 (Γ= 0.1729)	Example 11 (Γ= 0.0984)	Example 16 (Γ= 0.112)	Example 18 (Γ= 0.2853)
GAs				
Time for obtaining the optimal result (s)	0.37	0.29	0.47	0.91
	0.71	0.62	0.88	0.95
	2.28	1.29	1.46	1.38
	9.17	1.32	1.89	5.57
	14.69	1.39	2.73	6.15
	39.02	1.40	2.75	11.43
	47.28	3.14	4.57	13.39
	56.86	5.79	6.03	16.03
	89.59	8.02	9.77	17.40
	136.73	9.79	17.80	42.74
Improved LBB method				
Time for obtaining the optimal result (s)	0.52	0.23	0.3	0.69
Total solution time (s)	7.1	5.95	6.55	1.37

Table 5.6 Comparison between GAs and the improved LBB method for two non-symmetric examples from Table 5.4.

	Example 1	Time for obtaining this result (s)	Example 10	Time for obtaining this result (s)
GAs				
Values of Γ after 300 seconds	0.0851	33.76	0.0911	133.20
	0.0938	219.98	0.0926	55.11
	0.0956	88.10	0.0926	119.39
	0.1000	16.97	0.0932	42.20
	0.1087	12.56	0.0945	191.41
	0.1101	108.57	0.0965	4.25
	0.1113	3.70	0.0965	277.41
	0.1113	9.62	0.0967	8.39
	0.1135	99.67	0.0967	50.09
	0.1235	246.16	0.0977	7.11
Improved LBB method				
Values of Γ after 300 seconds	0.0806	4.77	0.0892	3.76

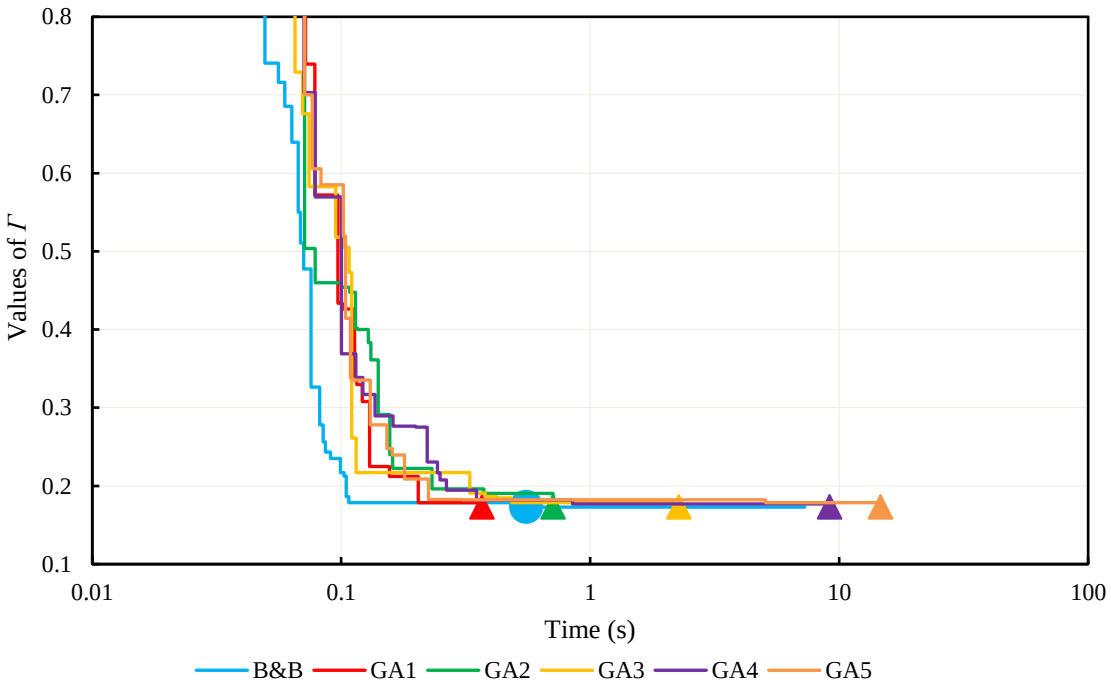

(a)

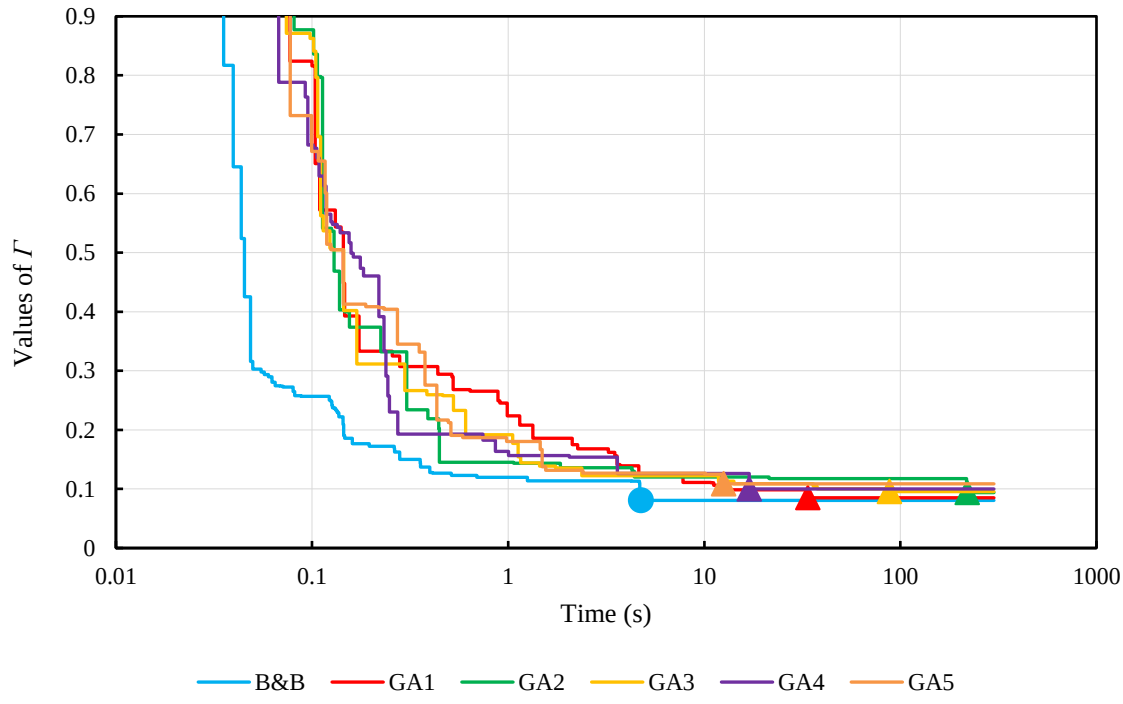

(b)

Figure 5.11 Comparison between GAs and the improved LBB method. (a) Example 2: Symmetric. (b) Example 1: Basic.

To investigate the efficiency of the improved LBB method with larger numbers of plies in comparison with GAs, the basic and balanced cases for which the number of plies in the decision trees are double those for the symmetric cases were re-run 10 times using GAs. Since GAs require a long time to find the same results as the improved LBB method, both methods were run for 300 seconds and comparisons were then made between the final values of Γ for each which are listed from the best to the worst in Table 5.6. For both cases, the improved LBB method found very good results efficiently, whilst the GAs could not achieve the same values of Γ as the improved LBB method even after 300 seconds. It is observed that the advantage of the improved LBB method is more obvious with larger numbers of plies, because it is easier to match the target lamination parameters. However, a larger number of plies also leads to more local optimum results in the second stage optimisation, and more plies need to be changed to move away from these local optimum results, which is to the disadvantage of the stochastic search of GAs. A comparison between the solution times for the improved LBB method and the best 5 GAs for the basic case is shown in Figure 5.11 (b), where the blue circle represents the final result obtained by the improved LBB method in 300 seconds and the triangles in other colours represent the final results given by the GAs. It can be seen that the improved LBB method always takes the lead in the comparison over 300 seconds. These comparisons confirm the advantages of the proposed logic-based search over stochastic-based search in quickly obtaining reliable results, making it more appropriate for layup optimisation. Note that due to manufacturing requirements, the ply angles are usually restricted to 0°, 90°, +45° and −45°, and only these four angles have been considered in this thesis.

5.3.2 Layup optimisation of stiffened panels

To further demonstrate the capability of the improved LBB method for searching layups, target lamination parameters for a range of stiffened panels are taken directly from Herencia *et al.* (2007) with the same number of plies being assumed for comparison purposes. Herencia *et al.* (2007) employed GAs in which the fitness function was formed by calculating the squared differences between the optimum and actual lamination parameters. Here the comparison is focused on which method can find stacking sequences which are closer to the target lamination parameters and also satisfy the required constraints.

The optimised lamination parameters are shown in Table 5.7, while the optimised stacking sequences for each example are listed in Table 5.8. The constraints used for each laminate for the improved LBB method are the same as those in the second stage in Herencia *et al.* (2007) (i.e. contiguity constraint, minimum percentage constraint and a special case of damage tolerance constraint requiring at least one set of ±45° plies at the skin and stiffener surfaces). Global optimality was not always confirmed because a maximum time criterion was imposed for the thicker laminates.

The stacking sequence in Herencia *et al.* (2007) for the skin of example C slightly violates the 10% constraint (6 plies out of 61) while the results given by the improved LBB method satisfy this constraint because it is enforced during the logic-based search. For this example the $\xi^{A}_{1,2,3}$ were constrained to take the same values as in (Herencia *et al.* 2008) and it was not possible to improve on the value of Γ found by Herencia *et al.* (2007). Therefore, direct comparison is not possible for example C in this chapter.

It can be seen from Table 5.7 that for examples A, B and D, the $\xi^{A}_{1,2,3}$ of the laminates resulting from applying the improved LBB method are same as those in Herencia *et al.* (2007), meaning that they have the same strength, percentage of each ply orientation and Poisson's ratio mismatch. However the results from the improved LBB method better match the target values for $\xi^{D}_{1,2,3}$ which determine the buckling performance of each laminate, and hence lower values of Γ are obtained using this method. The buckling load factors for the three optimised configurations obtained in Herencia *et al.* (2007) are 1.117, 1.09 and 0.989, while those given by the improved LBB method have higher values of 1.124, 1.097 and 1.029, respectively, improving the buckling performance between 0.6% and 4.0%. Note that, to make a fair comparison, the buckling load factors presented in this thesis have all been calculated by VICONOPT. For the optimised configurations obtained in Herencia *et al.* (2007), this gives slightly different values from those listed in the paper. These results suggest that the improved LBB method has better capability in searching the stacking sequences. This is because GAs sometimes miss the global optimum or can take too long to find it for problems with many plies, whereas useful results can be obtained quite quickly using the improved LBB method.

Table 5.7 Optimum lamination parameters and Γ for the two methods.

Example	Method	ξ_1^A	ξ_2^A	ξ_3^A	ξ_1^D	ξ_2^D	ξ_3^D	Γ
A	first stage	0.4603	0.3206	0.1208	−0.0028	−0.2908	0.3911	
Skin	second stage (Herencia *et al.* 2007)	0.4237	0.2542	0.1695	0.1346	−0.2123	0.2672	0.4915
(59 plies)	second stage (this thesis)	0.4237	0.2542	0.1695	0.1315	−0.2719	0.3998	0.3136
A	first stage	0.5862	0.5724	0.0002	0.1603	−0.0281	0.0016	
Stiffener	second stage (Herencia *et al.* 2007)	0.4839	0.4839	0	0.2261	0.0102	−0.0532	0.3499
(31 plies)	second stage (this thesis)	0.4839	0.4839	0	0.2261	0.0102	−0.0532	0.3499
B	first stage	0.4551	0.3102	0.1449	0.0434	−0.1356	0.2124	
Skin	second stage (Herencia *et al.* 2007)	0.4483	0.3103	0.1379	0.1098	−0.0872	0.2314	0.1477
(58 plies)	second stage (this thesis)	0.4483	0.3103	0.1379	0.0950	−0.1364	0.2078	0.0710
B	first stage	0.5934	0.5868	0.0009	0.1674	−0.0011	0.0036	
Stiffener	second stage (Herencia *et al.* 2007)	0.4894	0.4894	0	0.2744	0.0862	−0.0079	0.4081
(47 plies)	second stage (this thesis)	0.4894	0.4894	0	0.2698	−0.0035	−0.0055	0.3162
C	first stage	0.4850	0.3700	0.0866	−0.0185	−0.1623	0.2797	
Skin	second stage (Herencia *et al.* 2007)	0.4426	0.2787	0.0984	0.1303	−0.1244	0.1853	0.4266
(61 plies)	second stage (this thesis)	0.4426	0.3443	0.0656	0.2572	−0.1643	0.2829	0.3703
C	first stage	0.3941	0.1881	0	0.3239	−0.2744	0.1030	
Flange	second stage (Herencia *et al.* 2007)	0.3333	0.1111	0	0.3416	−0.2785	0.1235	0.1799
(18 plies)	second stage (this thesis)	0.3333	0.1111	0	0.3416	−0.2785	0.1235	0.1799
C	first stage	0.7541	0.9083	−0.0198	0.6044	0.7372	−0.0542	
Web	second stage (Herencia *et al.* 2007)	0.625	0.75	0	0.6016	0.7559	−0.0396	0.3433
(32 plies)	second stage (this thesis)	0.5625	0.875	0.0625	0.6013	0.9966	0.0017	0.6256
D	first stage	0.4887	0.3775	0.0796	0.0217	−0.2271	0.2897	
Skin	second stage (Herencia *et al.* 2007)	0.4444	0.3968	0.0794	0.2312	−0.0932	0.1409	0.5560
(63 plies)	second stage (this thesis)	0.4444	0.3968	0.0794	0.1792	−0.1888	0.2824	0.2669
D	first stage	−0.0277	−0.3359	0	0.2961	−0.0299	0.0473	
Flange	second stage (Herencia *et al.* 2007)	0	0	0	−0.0937	−0.7500	0.2813	1.7075
(8 plies)	second stage (this thesis)	0	0	0	−0.0937	−0.7500	0.2813	1.7075
D	first stage	0.6947	0.7412	0	0.6671	0.3370	0.0321	
Web	second stage (Herencia *et al.* 2007)	0.6226	0.6981	0	0.7464	0.5427	−0.0181	0.4504
(53 plies)	second stage (this thesis)	0.6226	0.6981	0	0.6268	0.3557	0.0380	0.1801

Table 5.8 Optimum stacking sequences for the two methods.

Example	Method	Layup	Percentage for each angle (%)			
			0°	90°	+45°	−45°
A Skin	(Herencia *et al.* 2007)	$[\pm45/45_3/90_2/(\pm45/0_4)_2/45/0_4/45/0_2/90/0/0]_{MS}$	52.54	10.17	27.12	10.17
	this thesis	$[\pm45/45_4/(90/45)_2/0_4/-45/0_4/45/0_4/90/0_3/-45/0]_{MS}$	52.54	10.17	27.12	10.17
A Stiffener	(Herencia *et al.* 2007)	$[\pm45/90/-45/0_4/45/0_4/90/0/0]_{MS}$	61.29	12.9	12.9	12.9
	this thesis	$[\pm45/90/-45/0_4/45/0_4/90/0/0]_{MS}$	61.29	12.9	12.9	12.9
B Skin	(Herencia *et al.* 2007)	$[\pm45/90_2/45/\pm45/0_2/45_2/(45/0_4)_2/90/0_4/-45/0_2]_S$	55.17	10.34	24.14	10.34
	this thesis	$[\pm45/-45/45/90/45_2/90/45/0_2/90/(0_4/45)_2/0_4/-45/0_2]_S$	55.17	10.34	24.14	10.34
B Stiffener	(Herencia *et al.* 2007)	$[(\pm45)_2/0_2/90_2/0_4/-45/0_4/90/0_4/45/0]_{MS}$	61.7	12.77	12.77	12.77
	this thesis	$[\pm45/90/45/0/-45_2/0_4/45/0_4/90/0_4/90/0_2]_{MS}$	61.7	12.77	12.77	12.77
C Skin	(Herencia *et al.* 2007)	$[\pm45/45/90_2/45/(\pm45/0_2)_2/0_2/45/0_3/45/0_2/90/0_4/45/0/0]_{MS}$	54.1	9.84	26.23	9.84
	this thesis	$[\pm45/45/90/45_4/0_4/-45/0_4(-45/0_3)_2/90/0_2/90/0/90]_{MS}$	55.74	11.48	19.67	13.11
C Flange	(Herencia *et al.* 2007)	$[\pm45/0_2/45/0/-45/90/0]_S$	44.44	11.11	22.22	22.22
	this thesis	$[\pm45/0_2/45/0/-45/90/0]_S$	44.44	11.11	22.22	22.22
C Web	(Herencia *et al.* 2007)	$[0_2/90/0_2/-45/0_2/45/0_4/90/0_2]_S$	75	12.5	6.25	6.25
	this thesis	$[(0_3/90)_2/0/90/0_4/45/0]_S$	75	18.75	6.25	0
D Skin	(Herencia *et al.* 2007)	$[\pm45/45/\pm45/0_2/90/\pm45/45/0_4/90/(90/0_4)_2/45/0_4/-45]_{MS}$	57.14	12.7	19.05	12.7
	this thesis	$[\pm45/45_4/-45/45/90/0_2/(90/0_4)_2/-45/0_4/90/0_4/-45]_{MS}$	57.14	12.7	19.05	12.7
D Flange	(Herencia *et al.* 2007)	$[\pm45/90/0]_S$	25	25	25	25
	this thesis	$[\pm45/90/0]_S$	25	25	25	25
D Web	(Herencia *et al.* 2007)	$[0_4/\pm45/0_2/-45/0_4/45/(0_4/90)_2/90/0/0]_{MS}$	73.58	11.32	7.55	7.55
	this thesis	$[45/-45/0_3/45/0_4/-45/(0_4/90)_3/0]_{MS}$	73.58	11.32	7.55	7.55

Note that the C skin in Herencia *et al.* (2007) slightly violates the 10% constraint. The reason why the C and D webs shown in this table appear to violate the 10% constraint is because they are actually laminates which are sandwiched by flanges on both sides to constitute the actual web, as described in Herencia *et al.* (2007).

5.4 Conclusions

An efficient two-stage method for performing layup optimisation of single composite laminates subject to buckling, manufacturing and lamination parameter constraints, has been presented in this chapter. VICONOPT is employed in the first stage to conduct a gradient-based optimisation process using lamination parameters. The optimised lamination parameters are treated as target values when searching corresponding layups in the second stage where an improved LBB method is employed. This improved LBB method is a combination of the branch and bound method and a global layerwise technique, which can find optimum results for different combinations of constraints (e.g. symmetry, balance and layup design constraints). Restrictions on feasible regions for lamination parameters when using a 10% minimum percentage constraint are studied, showing that the feasible regions for $\xi^{A}_{1,2,3}$ are reduced by 64%, while the feasible regions for $\xi^{D}_{1,2,3}$ are only reduced by around 3%. In the first set of results, 12.5% mass savings are achieved efficiently for a laminate subjected to compressive load under different constraints using this two-stage optimisation, and the efficiency of the improved LBB method is illustrated by comparison with a GA, showing that it is almost always faster in layup optimisation. Benefitting from the checking strategy used, the advantages of the improved LBB method are more obvious when considering layup design constraints. In the second set of results, the improved LBB method is compared with previously published results for stiffened panels based on their target lamination parameters and numbers of plies. The results confirm that the improved LBB method can find results closer to the target values, and hence give a slightly better buckling performance (with an improvement of 0.6% to 4.0%).

Chapter 6
Two-stage Layup Optimisation of Blended Composite Laminates

6.1 Introduction

In this chapter, the two-stage layup optimisation method developed in Chapter 5 is extended to more complex blended composite laminate structures incorporating buckling, blending, manufacturing and lamination parameter constraints. The first stage involves multilevel optimisation based on finite element analysis of a whole structure and exact strip analysis of its component panels. The lamination parameters and the laminate thicknesses of each panel are used as design variables to minimise the weight of the whole structure subject to buckling and lamination parameters constraints. This is achieved by extending VICONOPT MLO, which was introduced in Section 4.4.3, to use lamination parameters and laminate thicknesses as design variables and using this software rather than VICONOPT in the first stage of the optimisation.

For the second stage, a novel dummy layerwise branch and bound (DLBB) method is proposed to search the practical stacking sequences to find those needed to achieve a blended structure based on the use of $-45°$, $0°$, $+45°$ and $90°$ plies and having lamination parameters equivalent to those determined in the first stage. To obtain a blended composite laminate, the layup of a thinner panel should be a subset of that of all its adjacent thicker panels, in terms of both the number of plies of each orientation and also the order of plies in the layup. Unlike the stochastic search methods commonly used to solve such problems, the DLBB method carries out a logical search with similarities between this and the improved LBB method introduced in Chapter 5. The effectiveness of the presented method is demonstrated through the optimisation of a benchmark wing box. This work corresponds to the second journal paper in the publication list in Section 1.4.

6.2 Methodology

6.2.1 First stage optimisation

As discussed in Chapter 4, the disadvantages of using VICONOPT MLO are that because the stacking sequence of each panel is fixed in the optimisation and the thickness of each layer is optimised continuously, no allowance has been made for practical laminate design rules.

In this chapter, VICONOPT MLO is extended to perform layup optimisation of blended composite structures to obtain more practical designs based on the use of lamination parameters as design variables. This extended version of the software is used in the first stage of the optimisation process to determine lamination parameters which are then used to create appropriate designs for individual panels in the second stage.

The modified process can be seen in the flow chart in Figure 6.1. First, the finite element software ABAQUS (Dassault Systèmes 2013) is employed to perform a static analysis on the overall structure with the stiffness matrices calculated from lamination parameters, avoiding using specific layups in the FEA. After obtaining the loading for each component panel from the resulting ABAQUS output file (.dat), VICONOPT input files (.dat) are created (in the first cycle) or modified (in the following cycles), and the component panels are then optimised separately again using lamination parameters.

The optimised lamination parameters and laminate thicknesses from the VICONOPT output files (.res) are then treated as the starting points for the next VICONOPT optimisation cycle as well as being used to recalculate the stiffness matrices for the ABAQUS input file (.inp) for the next static analysis. This iterative multilevel optimisation process repeats until the convergence criteria (i.e. total mass, individual mass and stress distribution of each panel) are reached and thus the optimised lamination parameters and laminate thicknesses are derived.

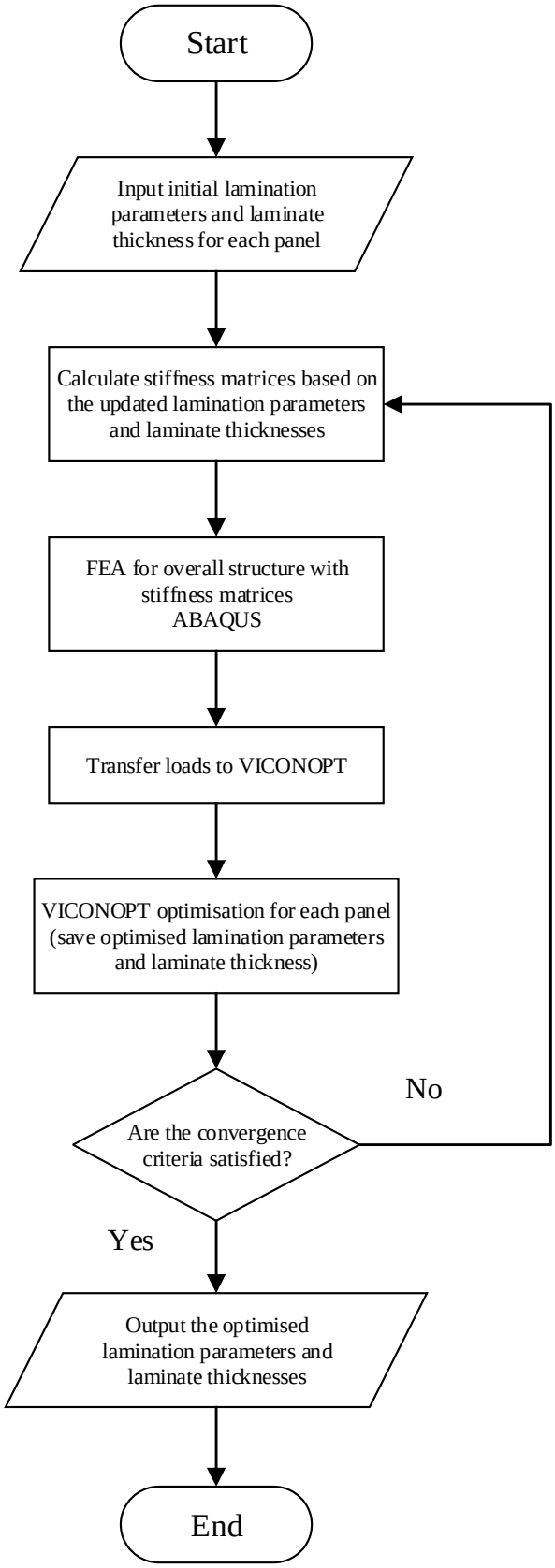

Figure 6.1 Flow chart of the proposed first stage multilevel optimisation using lamination parameters.

VICONOPT assumes the loading on the component panels to be longitudinally invariant in the buckling analysis, so that some approximations need to be made for the transfer of loads from the system level (whole structure) to the panel level (component panels). The load transfer process developed in Fischer *et al.* (2012) is used herein. At the system level, for the analysis of composite laminates the four-node quadrilateral shell element S4R is used, and ABAQUS is required to output the section forces (longitudinal force f_{xi}, transverse force f_{yi} and shear force f_{xyi}) and moments (i.e. longitudinal moment m_{xi}) per unit length for each element i. Since the optimisation process in VICONOPT requires the overall longitudinal axial load and bending moment to be input, these are obtained using the following equations

$$F_{xpanel} = \frac{\sum_{i=1}^{N_e} f_{xi} \cdot w_{ei}}{N_l} \tag{6.1}$$

$$M_{xpanel} = \frac{\sum_{i=1}^{N_e} m_{xi} \cdot w_{ei}}{N_l} \tag{6.2}$$

The transverse and shear forces per unit length for each of the component plates of the panel models are then calculated as

$$f_{yplate} = \frac{\sum_{i=1}^{N_{pl}} f_{yi}}{N_{pl}} \tag{6.3}$$

$$f_{xyplate} = \frac{\sum_{i=1}^{N_{pl}} f_{xyi}}{N_{pl}} \tag{6.4}$$

Here N_e is the number of elements in the panel, N_l is the number of elements along the length of the panel, N_{pl} is the number of elements in the component plate and w_{ei} is the width of element i.

Note that in the previous version of VICONOPT MLO (Fischer *et al.* 2012), the QUAD4 shell element in MSC/NASTRAN is employed for static analysis, for which only the stresses at the top and bottom surfaces of the element can be output. Hence,

further work needs to be done to extract the required section forces from the stresses which are then used to obtain the loads required for the VICONOPT models. Thus the use of ABAQUS which is able to directly output the section forces and moments reduces the complexity of the load transfer in this multilevel optimisation.

6.2.2 Second stage optimisation

In the second stage of the optimisation process, the dummy layerwise branch and bound (DLBB) method illustrated in Figure 6.2 is proposed to obtain the stacking sequences for the whole structure. Instead of searching the stacking sequence stochastically as for the heuristic algorithms, the dummy layerwise technique and the nature of the branch and bound method make DLBB a logical-search based method. The optimised lamination parameters obtained in the first stage are used as the target values for the DLBB which optimises the stacking sequences to match these target values as closely as possible. Blending and the introduction of the four layup design constraints are also implemented through the DLBB.

Once the first stage of the optimisation is completed, the number of plies in each panel is optimised and fixed. Before optimising the stacking sequences in the second stage, all panels are ranked in terms of their number of plies. Then for each panel except the thickest one, dummy plies are added on top to give all the panels the same number of plies as the thickest one, forming a dummy layerwise table as shown in Figure 6.3. The aim of the DLBB is to minimise the objective function Γ obtained by calculating the total difference between the target lamination parameters and the actual lamination parameters related to the chosen ply orientations for all of the panels as follows:

$$\Gamma = \sum_{k=1}^{N_{panel}} \Gamma_{panel\,k} \tag{6.5}$$

$$\Gamma_{panel\,k} = \sum_{i=1}^{3} \sum_{j=A,D} w_j \left| \xi^{j}_{i(k)(actual)} - \xi^{j}_{i(k)(target)} \right| \tag{6.6}$$

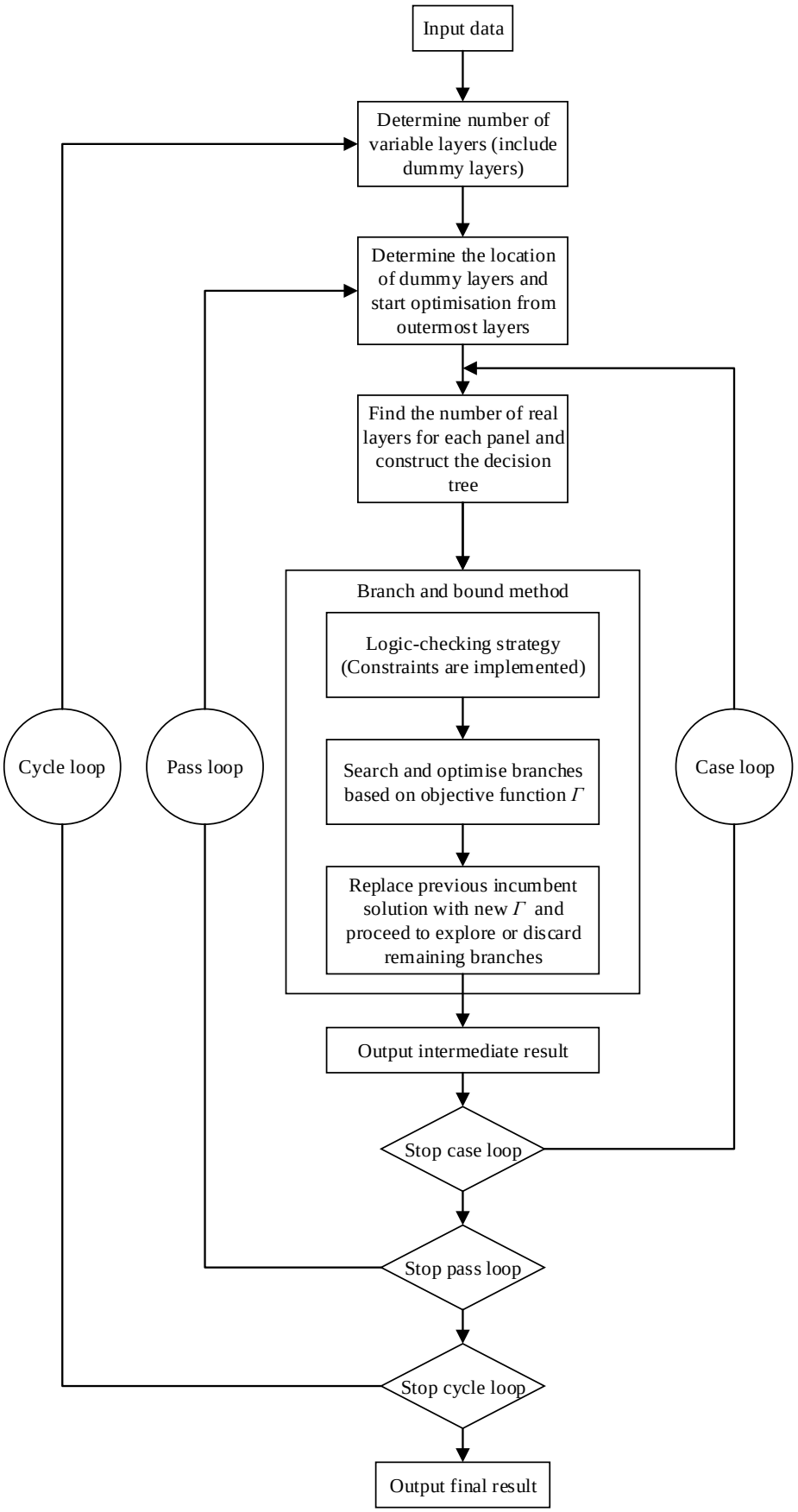

Figure 6.2 Flow chart of the dummy layerwise branch and bound (DLBB) method.

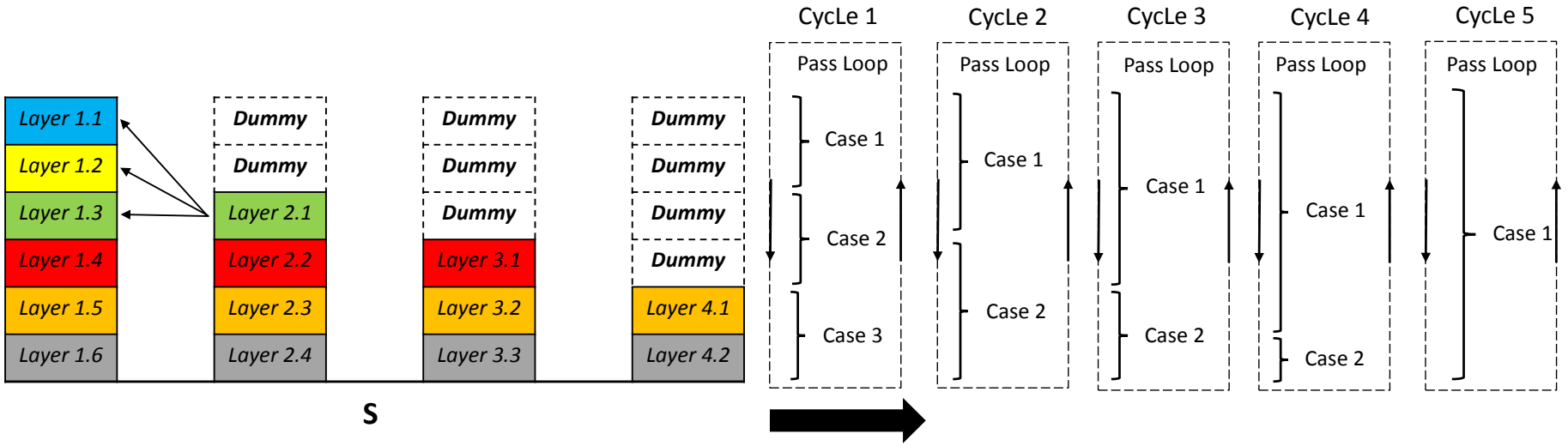

Figure 6.3 The dummy layerwise technique: starting layout of the dummy layerwise table.

where N_{panel} is the number of panels, $w_{A,D}$ are weighting factors, $\xi^{A,D}_{1,2,3(k)(target)}$ are the target lamination parameters for panel k, and $\xi^{A,D}_{1,2,3(k)(actual)}$ are the actual lamination parameters of the chosen layup of panel k.

As for the improved LBB method developed in Chapter 5, the current best result is used as the upper bound in the branch and bound method, and the lower bound is obtained by subtracting the maximum achievable contribution of the remaining levels in the decision tree from the exact value of Γ obtained by considering only the contributions of the chosen levels. Based on these bounds, the branching process choose the branch for the next level with the aim of minimising the value of Γ. However, whilst the dummy plies used to impose the blending constraint are now added into the layerwise process, they are not included in the branch and bound search, since they do not contribute to the stiffness of the laminate.

As illustrated in Figures 6.2 and 6.3, the dummy layerwise technique consists of three loops: the cycle, pass and case, and the ply orientations are optimised successively, working inwards from the outer plies which make the most important contributions to the $\xi^{D}_{1,2,3}$. As shown in Figure 6.3, initially only two plies from each panel are optimised, then three, and so on until in the final cycle all the plies are optimised together. The layup search method embedded in the dummy layerwise technique, the branch and bound process, thus starts with a small problem which only considers a few plies, meaning good results can be obtained quickly. In subsequent cycles, previous incumbent solutions give an upper bound on the objective function when searching the increasingly larger number of plies, and hence many branches can be discarded without being explored, reducing the searching time. Furthermore, the constraints required to be applied for each single panel including the balance, symmetry, and four layup design constraints can be implemented within this optimisation process.

The DLBB method is illustrated in Figures 6.3-6.6 for the example of a blended structure comprising four panels whose symmetric layups contain 12, 8, 6 and 4 layers (i.e. plies), respectively. In the first case of the first cycle, only the two outer real layers in the thickest panel are optimised and the related decision tree used in the branch and

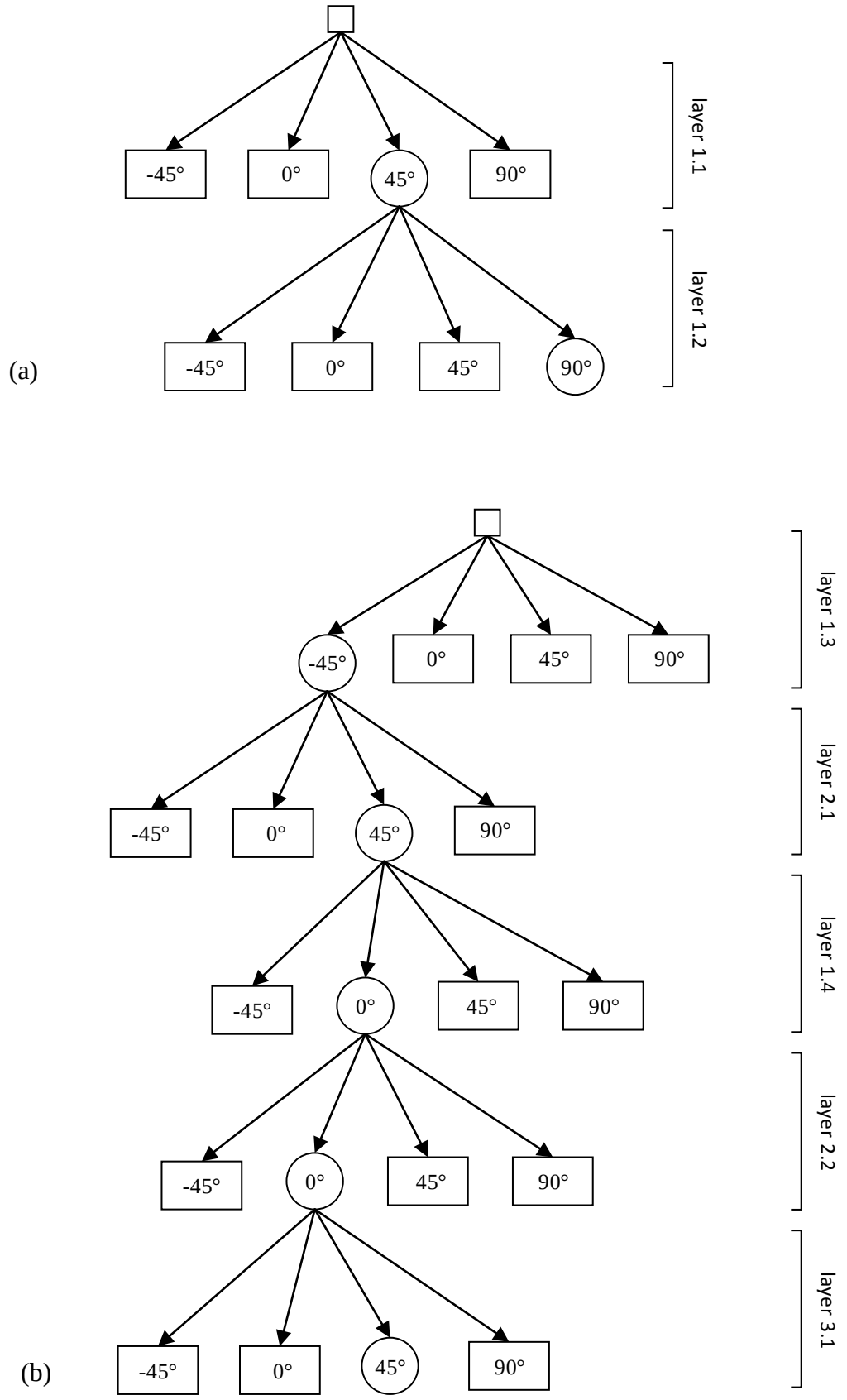

Figure 6.4 Decision trees with a possible determined layup: (a) in the first case of the first pass of the first cycle; (b) in the second case of the first pass of the first cycle.

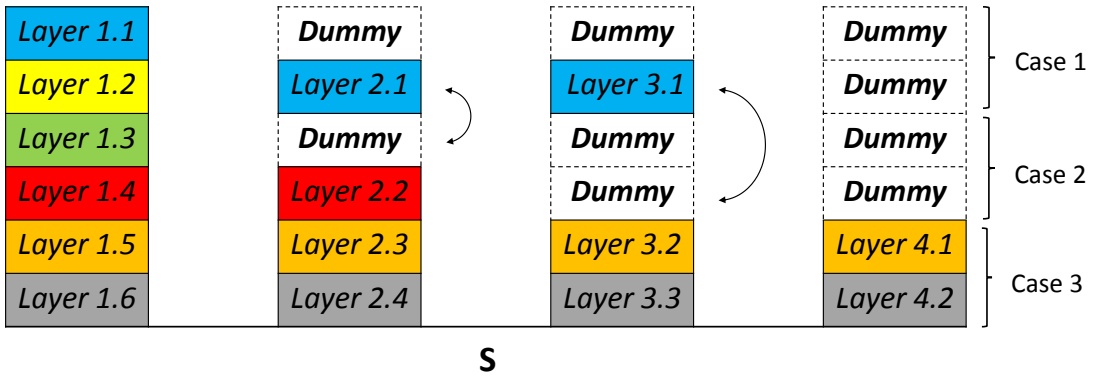

Figure 6.5 Layout changes after the first pass of the first cycle.

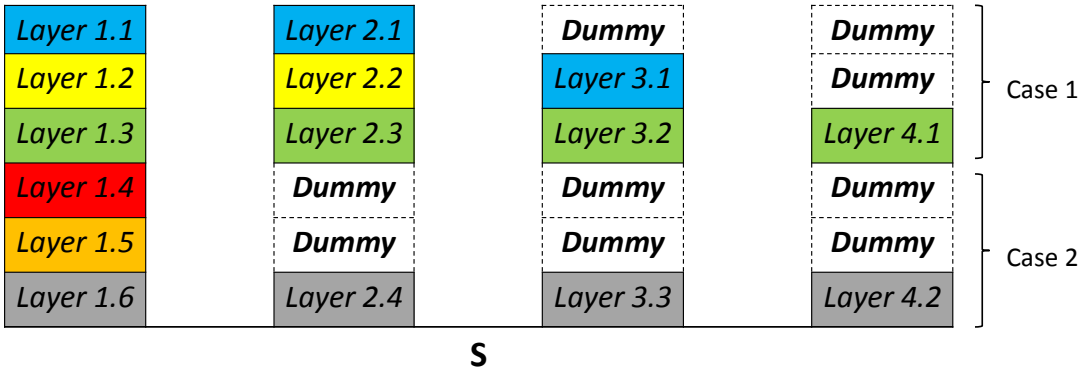

Figure 6.6 A possible starting layup for the second cycle.

bound method with a possible determined layup is shown in Figure 6.4 (a). The order of the layers for optimisation can be described by:

$P_{i.j}$

$i = 1, j = n_{cy} \times n_{ca} - n_{cy} + n_{ca}$ for the first layer

$i = i + 1$ if the layer to the right is not a dummy layer

$i = 1, j = j + 1$ if the layer to the right is a dummy layer or $i > N_{panel}$

where P_{ij} is the position of the layer in the dummy layerwise table, i and j represent the column and row numbers in the dummy layerwise table respectively and n_{cy} and n_{ca} are the cycle number and case number respectively.

Then, in the second case of the first cycle, the newly optimised layup is used as the starting layup and the optimisation starts from layer 1.3, then goes to layer 2.1. Since layers 1.1, 1.2 and 1.3 have already been chosen, layer 2.1 can be chosen to match any of these. After that, layers 1.4, 2.2 and 3.1 are selected. For layer 2.2, the choices available are the angles of the layers which are below the layer in the panel to its left that layer 2.1 has just been chosen to match. The rest of the choices for layer 2.2 are pruned by the branch and bound method. Based on the chosen layup of the panel at the current level, the checking strategy developed in Chapter 5 is implemented to determine which ply should be further pruned to satisfy the layup design constraints. In the same way, for layer 3.1 there are two choices, namely to match layer 2.1 or layer 2.2. Figure 6.4 (b) shows the decision tree with a possible determined layup for the second case, with the branches at different levels from the different panels. Moreover, after layer 3.1 has been chosen, the branch and bound method will go back to check the rest of the possibilities to avoid missing the best layup for the layers in the current case. During this backtracking procedure, it is not necessary to search all the further branches because the result just obtained in the current case further reduces the value of the objective function Γ, and so branches predicted as having a larger value of Γ are discarded. A benefit of the backtracking procedure and optimisation order described above is that decisions regarding the intermediate solutions from each case are made based on a balance between all the panels.

The positions of the dummy layers in the dummy layerwise table are changed according to the layer choices after each case, enabling flexibility in determining the layer drop-off location. Once a layer has been chosen to match the layer which is located in the panel to the left in a former case, the layer in the current case will be dropped and moved up to the corresponding former case, and a dummy layer in the former case will be swapped to the current case. Furthermore, the dummy layers will be located from the top to the bottom in each case to provide more choices for the real layers. For example, if layers 2.1, 2.2 and 3.1 are chosen to match layers 1.1, 1.4 and 2.1, respectively, the dummy layers in the first case swap with the real layers in the second case as shown in Figure 6.5. Hence, the layout of the dummy layerwise table and the optimisation order of the layers are changed for the next pass. In the next pass loop, the layer moved up will be optimised in the same case as the layer it is chosen to match to ensure the blending constraint.

After the last case in a pass loop is completed, a new pass loop starts and repeats the process based on the newly obtained layup from the last loop until convergence to a constant Γ is achieved. After the first cycle, a possible layout of the dummy layerwise table is shown in Figure 6.6, which then becomes the starting layup for the second cycle where three rows of layers can be optimised in a case. As the new case contains the layers from two cases in the previous cycle, the dummy layers in each new case are relocated from the top to the bottom at the beginning of the new cycle. As can be seen in Figure 6.6, the positions of the real layers are more flexible in these cases because more layers are allowed to be optimised together. Based on the process described above, the blended layup can be obtained logically by the branch and bound method embedded within the dummy layerwise technique.

6.3 Results and discussion

The optimisation of the benchmark wing box structure used in the previous work on VICONOPT MLO (Fischer *et al.* 2012) is presented in this chapter to validate the proposed two-stage method. As shown in Figure 6.7, the wing comprises six panels on the top, six panels on the bottom, four ribs and three spars. The details of the skin panels are shown in Figure 6.8. Each panel has three L-shaped stringers reinforcing longitudinal stiffness and increasing local buckling capability. The wing is made of high strength carbon-epoxy and the material properties are given in Table 6.1. Three concentrated loads of magnitudes 50000 N, 30000 N and 15000 N are applied at the rib at the free end, inducing upward bending and twisting of the wing. To model realistic boundary conditions, the wing is attached to a steel adapter clamped at its end instead of directly clamping the root of the wing.

In this chapter, only the panels on the top of the wing are considered in the layup optimisation. The previously optimised configurations in Fischer *et al.* (2012) are taken as starting points for the optimisation presented here. In the previous optimisation the stacking sequences of the skin panels, ribs and spars were fixed as $[-45/45/90/0]_S$ and only the layer thicknesses were optimised. Table 6.2 shows the starting layup for this optimisation.

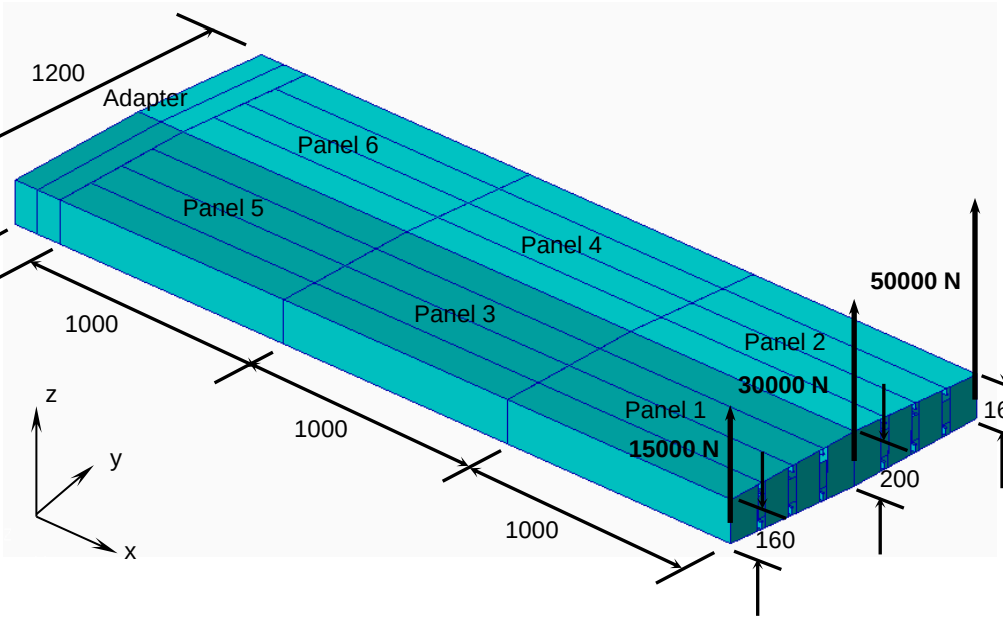

(a)

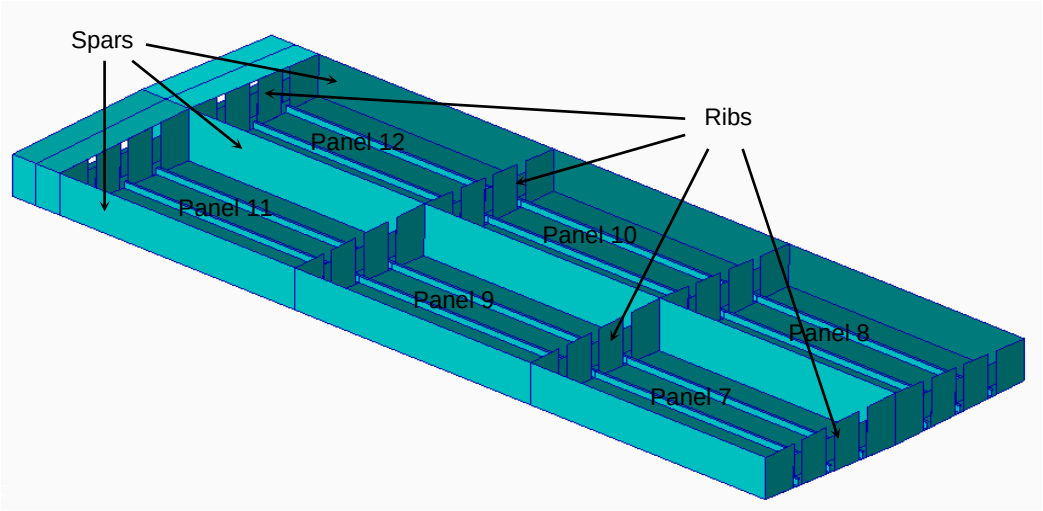

(b)

Figure 6.7 (a) Geometry of the wing box and the load case. (b) Bottom panels, ribs and spars.

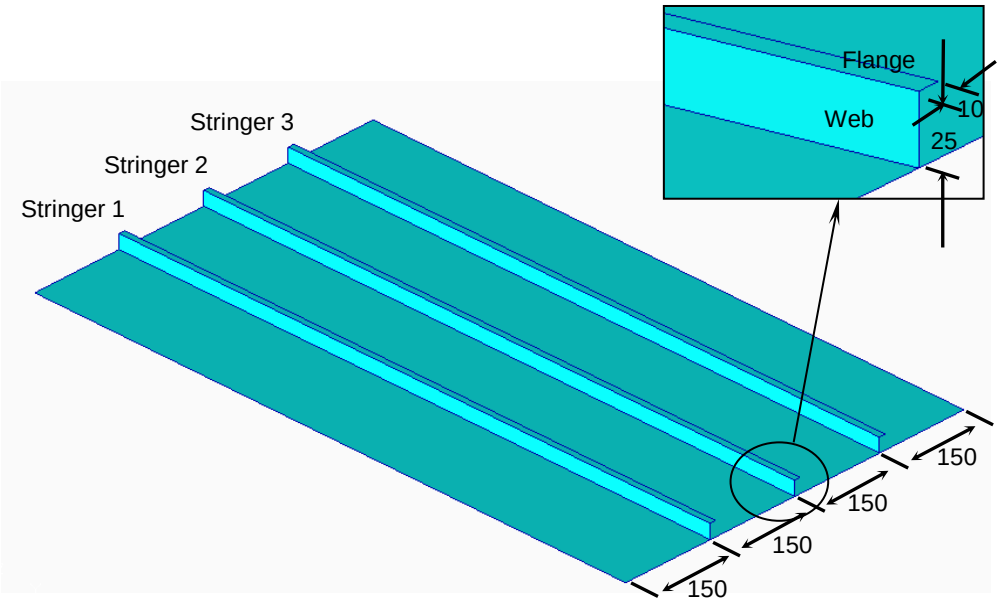

Figure 6.8 Geometry of the component panels (in mm).

Table 6.1 Material properties.

Material properties	Values
Young's modulus in the fibre direction 1, E_{11}	140000 MPa
Young's modulus in the transverse direction 2, E_{22}	10000 MPa
Shear modulus G_{12}	5000 MPa
Poisson's ratio υ_{12}	0.3
Material density ρ	0.0016 g/mm^3
Ultimate longitudinal tensile strength	1500 MPa
Ultimate longitudinal compressive strength	1200 MPa
Ultimate transverse tensile strength	50 MPa
Ultimate transverse compressive strength	250 MPa
Ultimate in-plane shear strength	70 MPa

Table 6.2 Starting layup and ply thicknesses (mm) (optimised results from Fischer *et al.* (2012)).

Top Panels		Panel 1	Panel 2	Panel 3	Panel 4	Panel 5	Panel 6
Skin	t(−45)	0.181	0.736	0.358	1.072	1.304	1.174
	t(45)	0.181	0.125	0.839	0.631	1.500	1.372
	t(90)	0.433	0.215	1.500	1.500	1.500	1.494
	t(0)	0.537	1.500	1.500	1.500	1.500	1.500
Web	t(−45)	0.159	0.282	0.364	0.265	0.308	1.208
	t(45)	0.188	0.282	0.503	0.221	0.308	1.395
	t(90)	0.354	0.125	0.963	0.964	0.125	2.242
	t(0)	0.817	1.500	2.000	2.000	0.125	2.499
Flange	t(−45)	0.280	0.593	1.500	1.500	1.467	1.173
	t(45)	0.280	0.641	1.500	1.500	1.467	1.173
	t(90)	0.559	0.236	1.500	1.500	1.545	1.448
	t(0)	1.500	1.500	2.000	2.000	2.500	2.500
Bottom Panels		Panel 7	Panel 8	Panel 9	Panel 10	Panel 11	Panel 12
Skin	t(−45)	0.13	0.13	0.13	0.13	0.13	0.13
	t(45)	0.13	0.13	0.13	0.13	0.13	0.13
	t(90)	0.54	0.88	0.13	0.13	0.13	0.13
	t(0)	0.13	0.14	0.25	0.32	0.55	0.7
Web	t(−45)	0.13	0.13	0.13	0.13	0.13	0.13
	t(45)	0.13	0.13	0.13	0.13	0.13	0.13
	t(90)	0.13	0.13	0.13	0.13	0.13	0.13
	t(0)	0.13	0.13	0.19	0.15	0.13	0.13
Flange	t(−45)	0.13	0.13	0.13	0.13	0.13	0.13
	t(45)	0.13	0.13	0.13	0.13	0.13	0.13
	t(90)	0.13	0.13	0.13	0.13	0.13	0.13
	t(0)	0.27	0.13	0.19	0.15	0.13	0.13

6.3.1 First stage optimisation results

In the first stage of the optimisation of the wing box, in order to be able to replicate the results from the previous study, 8952 S4R shell elements were used in the static analysis of the whole structure. Elements were uniformly assigned on each panel, and the number of elements used to mesh the geometry for the skin, webs and flanges of each panel were 450, 75 and 75, respectively. The top panels were mainly subjected to compressive loading because they are on the top surface of the wing box. For the tip panels, the force calculation equations (6.1)-(6.4) are all multiplied by an empirical factor α_e which is chosen to be 1.1. This factor takes into account the fact that in the static analysis of the whole structure, the ribs and spars provide a level of support which is between simply supported and free for the panel at the tip, but in the optimisation VICONOPT treats it as simply supported which is an overestimate.

As the layups are required to be symmetric, there are 21 design variables for each panel with the skin, web and flange having 7 variables each (i.e. $\xi_1^A, \xi_2^A, \xi_3^A, \xi_1^D, \xi_2^D, \xi_3^D, h$), hence a total of 126 design variables are specified in this optimisation. Figure 6.9 (a) shows the total mass comparison for the top panels. As can be seen, the final mass at the end of the first stage converges on a value of 49.1 kg. Compared with the optimised configuration in Fischer *et al.* (2012), a 4.9 kg reduction is achieved which represents a 9.1% saving over the previously optimised weight. It is observed that the design space is expanded by using lamination parameters as design variables. The mass change of each individual panel is shown in Figure 6.9 (b) where it can be seen that the majority of the mass saving for the whole structure is achieved in panels 2, 3 and 4 whose stacking sequences change significantly in this optimisation. The mass reductions of panel 5 and 6 are relatively small, while the mass of panel 1 remains almost constant. As expected, the panel mass increases from the tip to the root due to the increase in bending moment along the wing. The panels on the right are heavier than the adjacent panels on the left due to the twisting effect resulting from the unequal magnitudes of the applied loads.

Table 6.3 shows the re-distribution of axial load and bending moment which occurs in each panel, obtained at the end of the multilevel optimisation process based on the optimised structural configurations. Compared with the loading re-distributions of the optimised configurations in (Fischer *et al.* 2012), it is observed that the newly optimised panels are able to carry approximately the same loads with reduced laminate thicknesses. The optimised lamination parameters and laminate thicknesses for each panel are listed in Table 6.4.

Table 6.3 Re-distributions of axial load and bending moment after the multilevel optimisation.

Panel no.		1	2	3	4	5	6
Axial load (kN)	(Fischer *et al.* 2012)	113.03	122.97	423.57	470.88	719.53	799.38
	This thesis	110.79	121.80	422.22	462.88	710.24	804.46
Bending moment (kNm)	(Fischer *et al.* 2012)	1.1963	5.4909	76.048	86.356	219.09	249.36
	This thesis	1.1492	2.6543	68.508	57.671	180.41	251.92

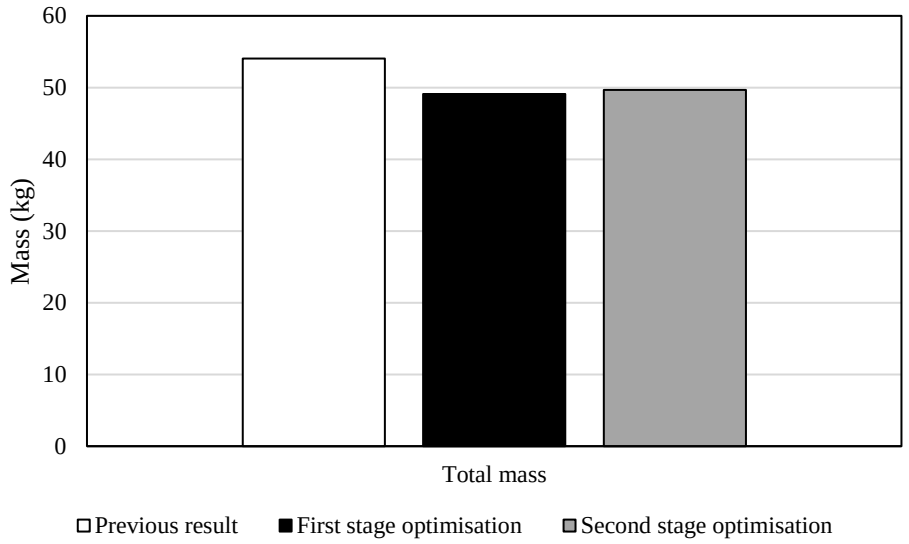

(a)

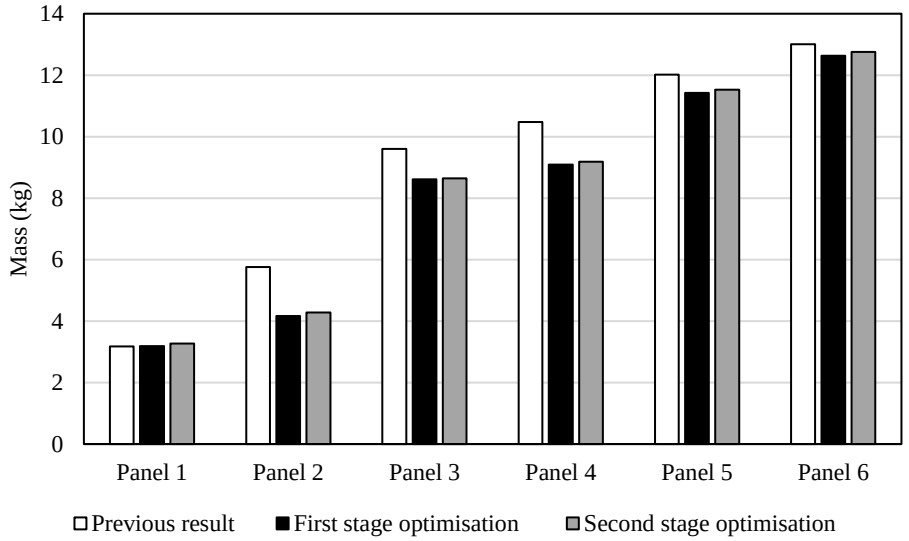

(b)

Figure 6.9 (a) Total mass comparison of the top panels. (b) Mass comparisons of each individual panel.

Table 6.4 Optimisation results of the first stage.

Panel no.		ξ_1^A	ξ_2^A	ξ_3^A	ξ_1^D	ξ_2^D	ξ_3^D	h(mm)	n
1	Skin	0.0791	0.4552	−0.0006	−0.2559	−0.2245	−0.0959	2.674	22
	Web	0.3032	0.5392	0.0173	−0.1470	−0.0817	−0.0240	3.047	25
	Flange	0.3552	0.5678	−0.0035	−0.1069	−0.0247	−0.0612	5.257	43
2	Skin	0.2660	0.1988	−0.0758	−0.0890	−0.1208	−0.4364	3.646	30
	Web	0.4225	0.4028	−0.0274	0.0512	−0.1266	−0.0589	3.598	29
	Flange	0.3024	0.0878	−0.0197	−0.0823	−0.5315	−0.1410	4.918	40
3	Skin	−0.0729	0.1781	−0.0208	−0.4108	−0.1073	0.0478	7.469	60
	Web	0.2158	0.4651	0.0019	−0.2970	0.0238	0.0132	7.101	57
	Flange	0.0527	0.0527	0	−0.1779	−0.5253	−0.0548	12.203	98
4	Skin	−0.0444	0.1639	−0.0359	−0.2338	−0.4526	−0.0274	8.156	66
	Web	0.2265	0.5485	−0.0131	−0.2851	0.2945	−0.0608	5.971	48
	Flange	0.0708	0.0709	0	−0.1286	−0.6492	−0.1735	11.273	91
5	Skin	0.0004	0.0338	0.0338	−0.1028	−0.7205	0.0384	11.027	89
	Web	0	−0.4225	0	−0.0180	−0.9529	−0.4905	1.645	14
	Flange	0.1368	0.1592	0	−0.1023	−0.6183	−0.2087	13.260	107
6	Skin	−0.0200	0.1013	0.0183	−0.1750	−0.4797	0.0114	10.761	87
	Web	0.0131	0.2141	−0.0011	−0.2058	−0.4636	−0.0792	14.261	115
	Flange	0.1537	0.2174	−0.0221	−0.1471	−0.4700	−0.1508	12.342	99

6.3.2 Second stage optimisation results

In the second stage of the optimisation, the lamination parameters obtained in the first stage are used as target values in the DLBB method. Due to manufacturing requirements, ply thickness is chosen to be 0.125 mm in each case. For each panel, the number of plies after rounding up to the nearest larger integer number n is shown in the last column of Table 6.4. After the rounding process, the buckling load factor for the first buckling mode, which is local to panel 1 as shown in Figure 6.10 (a), is 1.15. Note that the small buckling modes are the plate buckling between the stringers. Figure 6.10 (b) shows the second buckling mode involves global buckling of the whole top surface for which the buckling load factor is 1.17.

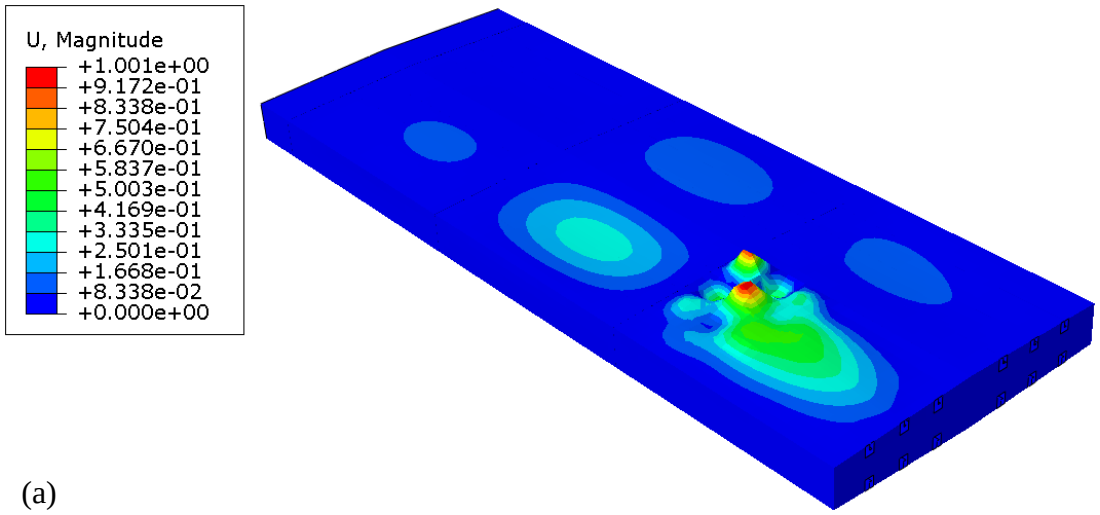

(a)

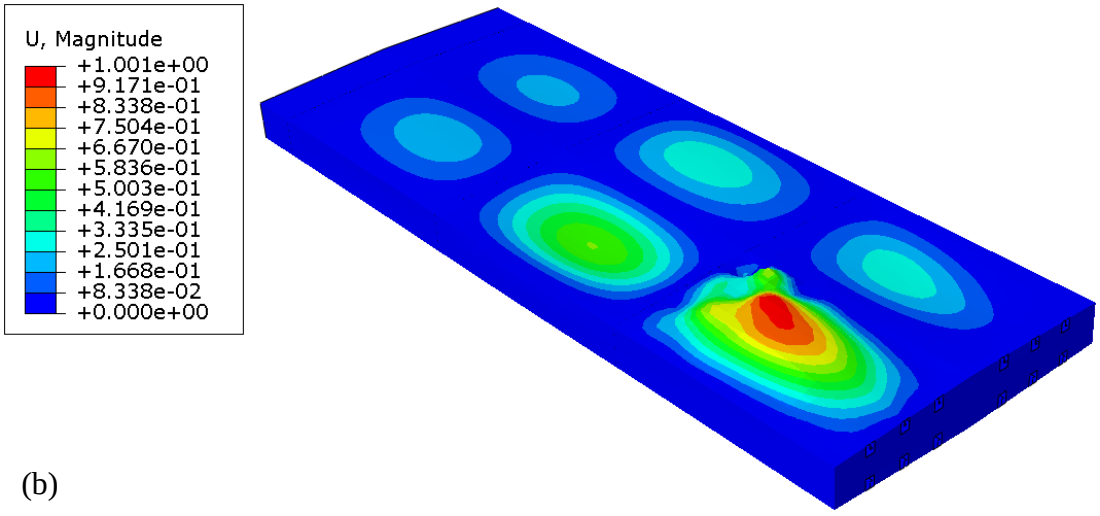

(b)

Figure 6.10 Buckling modes obtained using the optimised lamination parameters and rounded thicknesses. (a) First buckling mode with buckling load factor = 1.15. (b) Second buckling mode with buckling load factor = 1.17.

6.3.2.1 Layup design without blending constraint

In order to validate the DLBB method, the stacking sequences are now optimised separately without imposing the blending constraint. Table 6.5 shows the stacking sequences obtained when optimisation is based only on using the four layup design constraints. Compared with the previous results, the stacking sequences obtained here

Table 6.5 Stacking sequences of top panels without blending constraint.

Panel no.		Stacking sequences
1	Skin	$[45/-45/90_2/-45/0_4/45/90]_S$
	Web	$[45/-45/90_2/-45/0_2/45/0_4/45]_{MS}$
	Flange	$[45/-45_2/90_4/45/0_3/-45/0_4/45/0_4/-45]_{MS}$
2	Skin	$[45/-45/90_2/-45_2/0_2/-45/0_4/45/90]_S$
	Web	$[45/-45/90_2/-45/0_4/45/0_4/-45]_{MS}$
	Flange	$[45/-45_4/90/45_2/90/45/0_3/-45/0_3/45/0_2]_S$
3	Skin	$[45/-45/90/45_2/90/-45/90_2/45/90/-45/90/(-45/90_2)_2/-45/0_2/45/0_4/45/0_2]_S$
	Web	$[45/-45_2/90_3/(45/90)_2/-45/90_2/45/0_4/-45/0_4/45/0_4/-45]_{MS}$
	Flange	$[45/-45_4/90/45_4/90/-45_3/90/45_2/90/-45_3/90/45/90_3/45/0_2/45/90_2/45/0_4/(-45/0_4)_2/45/90]_S$
4	Skin	$[45/-45_4/90/45_4/90/-45/90/45/90_2/-45/90_4/45/0_4/-45/0_4/-45/90]_S$
	Web	$[45/-45/90_4/-45/90_2/-45/(0_4/45)_2/0_3/-45]_S$
	Flange	$[45/-45_4/90/-45_4/90/45_4/90/45_3/90/-45/90_4/(-45/0_4)_2/45/0_4/45/90_2/45/0/0]_{MS}$
5	Skin	$[45/-45_4/90/45_4/90/-45/90/45_4/0/-45_3/0/-45/0_2/(45/90_4)_2/45/0_3/-45/0_4/-45]_{MS}$
	Web	$[45/-45_3/90/45/0]_S$
	Flange	$[45/-45_4/90/-45_4/90/-45_2/90/45_4/90/45_2/90_3/-45/0/45(0_4/45)_2/90_4/-45/(0_4/45)_2/0/0]_{MS}$
6	Skin	$[45/-45_4/90/45_4/90/45_3/90/-45_3/90/-45/90_4/-45/0_3/45/0_4/45/90_4/-45/0_4/45]_{MS}$
	Web	$[45/-45_4/90/45_4/90/-45_4/90/45_3/90/-45_3/90_2/45/90_4/-45/90_4/45/0_4/-45/(0_4/45)_3/90/90]_{MS}$
	Flange	$[45/-45_4/90/-45_3/90/45_4/90/45/90/-45_3/90/45_2/0/-45/90_4/(45/0_4)_3/-45/0_4/-45]_{MS}$

are more practical but have more anisotropy. The lamination parameters related to the optimised stacking sequences together with their Γ are listed in Table 6.6.

As can be seen, the lamination parameters of the obtained stacking sequence are good matches for the target lamination parameters. The thicker laminates have lower values of Γ, because they have larger numbers of plies making their stacking sequences easier to match with the targets. After the stacking sequences are obtained, the optimised configuration is checked for buckling in ABAQUS as shown in Figure 6.11. Results show that the local and global buckling load factors (i.e. the first and second buckling modes) are 1.09 and 1.15, respectively. Comparison of these buckling load factors obtained using the stacking sequences with those obtained using the target lamination parameters directly, shows that there is only a small decrease in buckling performance caused by the mismatch between the target lamination parameters and the actual stacking sequences. Therefore, the stacking sequences obtained based on the four

layup design constraints in the second stage of the optimisation have lamination parameters close to the optimised values obtained in the first stage.

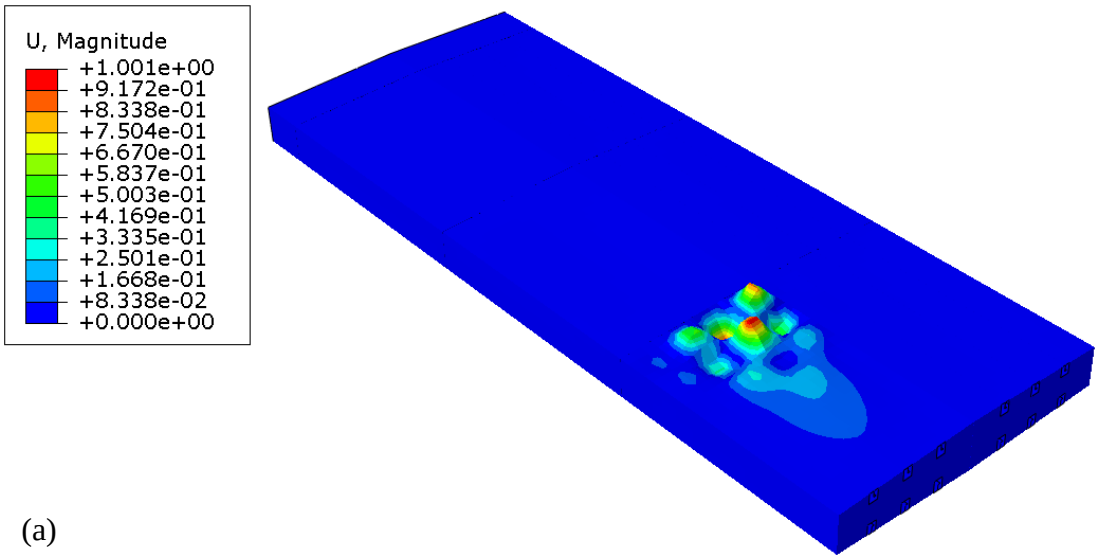

(a)

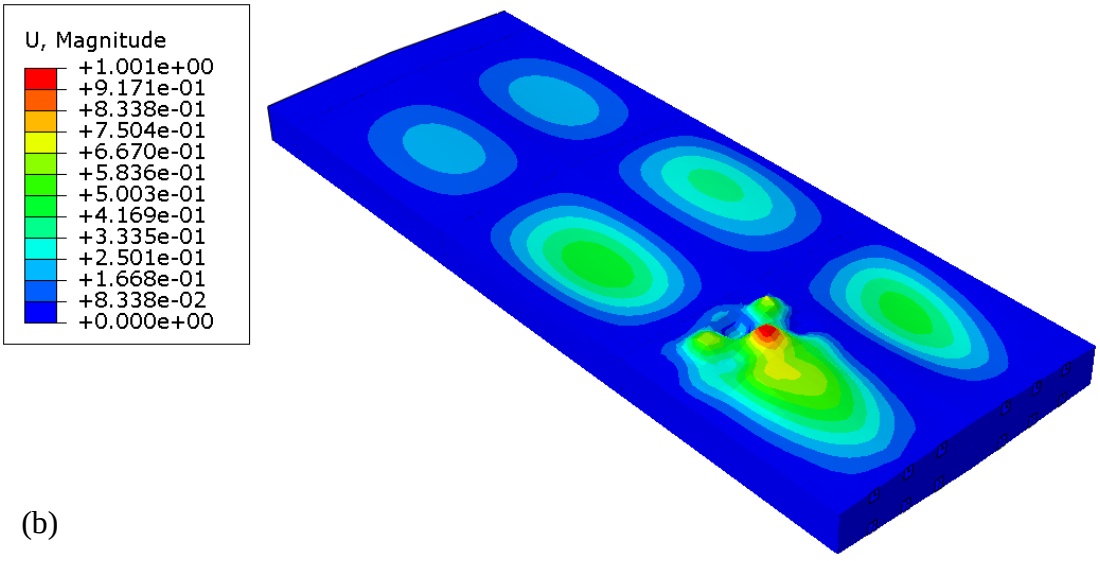

(b)

Figure 6.11 Buckling modes obtained using the stacking sequences without considering blending constraint. (a) First buckling mode with buckling load factor = 1.09. (b) Second buckling mode with buckling load factor = 1.15.

Table 6.6 Lamination parameters of the optimised stacking sequences without blending constraint.

Panel no.		ξ_1^A	ξ_2^A	ξ_3^A	ξ_1^D	ξ_2^D	ξ_3^D	Γ
1	Skin	0.0909	0.2727	0	−0.1345	−0.1059	−0.0451	0.4857
	Web	0.3200	0.2800	0.0400	−0.1009	−0.0886	−0.0245	0.3523
	Flange	0.3256	0.3953	−0.0233	−0.1206	0.0802	−0.0601	0.3415
2	Skin	0.2000	0.2000	−0.1333	−0.0809	−0.1342	−0.1890	0.3936
	Web	0.4138	0.3793	−0.0345	−0.0044	0.0349	−0.0473	0.2680
	Flange	0.3000	0	0	−0.0217	−0.5295	−0.1380	0.1755
3	Skin	−0.0667	0.2000	0	−0.3867	−0.1062	0.0482	0.0745
	Web	0.1754	0.3333	0.0175	−0.2834	0.0286	0.0115	0.2079
	Flange	0.0612	0.0204	0	−0.1707	−0.4474	−0.0544	0.1264
4	Skin	−0.0606	0.0909	−0.0303	−0.2273	−0.4123	−0.0259	0.1431
	Web	0.2083	0.4167	−0.0417	−0.2852	0.2681	−0.0782	0.2225
	Flange	0.0769	0.0330	0	−0.1390	−0.4555	−0.1711	0.2506
5	Skin	0	−0.0112	0.0337	−0.1039	−0.4819	0.0349	0.2887
	Web	0	−0.4286	−0.1429	−0.0525	−0.8834	−0.1603	0.5831
	Flange	0.1402	0.1028	0	−0.1085	−0.3778	−0.2093	0.3071
6	Skin	−0.0230	0.0575	0.0115	−0.1660	−0.4450	0.0141	0.1001
	Web	0.0087	0.0957	0	−0.2120	−0.3976	−0.0814	0.1983
	Flange	0.1616	0.0505	−0.0303	−0.1465	−0.4302	−0.1498	0.2244

6.3.2.2 Layup design with blending constraint

Tables 6.7-6.9 show the optimised stacking sequences which satisfy the four layup design constraints and also the blending constraint. Since the panels are stiffened and the stiffeners run all the way along the wing, there are five separate blending problems including the skins of all of the top panels, the webs of the left hand side panels (i.e. panels 1, 3 and 5) and the right hand side panels (i.e. panels 2, 4 and 6) respectively, and the flanges of the left and right hand side panels respectively. No constraints are applied between the skin, webs and flanges, which are treated as independent laminates in the second stage. The related lamination parameters and the values of Γ are summarised in Tables 6.10-6.12.

Table 6.7 Stacking sequences of skins with blending constraint.

Panel no.	Stacking sequences
5	$[45/-45_4/90/45_4/90/-45_2/90/45_4/90/-45/90/45/90/-45/0_3/-45/90_4/45/0_4/-45/0_4/45/90_2]_{MS}$
6	$[45/-45_4/90/45_4/90/-45_2/90/45_3/90/-45/90/45/90/-45/0_3/-45/90_4/45/0_4/-45/0_4/45/90_2]_{MS}$
4	$[45/-45_3/90/45_3/90/-45/90/45/90/-45/90_2/-45/0_2/-45/90_3/45/0_2/-45/0_4/45/90]_S$
3	$[45/-45/90/45_2/90/-45/90/45/90/-45/90_2/-45/0_2/-45/90_3/45/0_2/-45/0_4/45/90]_S$
2	$[45/-45_2/90_3/-45/0_4/-45/0_2/45]_S$
1	$[45/-45/90_3/-45/0_4/45]_S$

Table 6.8 Stacking sequences of left and right hand side flanges with blending constraint.

Panel no.	Stacking sequences
	left hand side flanges
5	$[45/-45_4/90/-45_4/90/45_3/90/-45_2/90/45_3/90_2/45/90/-45/0_4/45/0_3/45/0_2/45/0_4/45/90_4/-45/0_3/45/0_2]_{MS}$
3	$[45/-45_4/90/-45_3/90/45_3/90/-45_2/90/45_3/90_2/45/90/-45/0_4/45/0_2/-45/0_2/45/0_2/45/90_4/-45/0_3/45/0]_S$
1	$[45/-45/90/-45/90/45/90/-45/0_4/45/0_4/-45/0_3/45]_{MS}$
	right hand side flanges
6	$[45/-45_4/90/-45_4/90/45_4/90/45_2/90/-45/90_2/-45/0/45/0_4/-45/0_4/45/90_4/-45/(0_4/45)_2]_{MS}$
4	$[45/-45_4/90/-45_4/90/45_4/90/45_2/90_3/-45/0/45/0/-45/0_4/45/90_4/-45/(0_4/45)_2]_{MS}$
2	$[45/-45_4/90/45_2/90/45/0_2/-45/0_4/45/0_2]_S$

Table 6.9 Stacking sequences of left and right hand side webs with blending constraint.

Panel no.	Stacking sequences
	left hand side webs
3	$[45/-45_2/90/45/90_2/45/90_3/-45/0_4/45/0_2/-45/90/-45/0_4/45/0_2]_{MS}$
1	$[45/-45/90_2/-45/0_3/-45/90/45/0_2]_{MS}$
5	$[45/-45_3/90/45/0]_S$
	right hand side webs
6	$[45/-45_4/90/-45/90/45_3/90/45/90/-45/90_2/-45/90_3/-45/0_4/45/90/45/0/45/90_3/-45/0_4/45/90_2/-45/0_3/-45/90_2/(45/0_2)_2/0_2/-45]_{MS}$
4	$[45/-45/90_4/-45/90/-45/0_4/45/0_4/45/0_3/-45/90]_S$
2	$[45/-45/90_2/-45/0_4/45/0_4/-45]_{MS}$

Table 6.10 Lamination parameters of the stacking sequences of skins.

Panel no.	ξ_1^A	ξ_2^A	ξ_3^A	ξ_1^D	ξ_2^D	ξ_3^D	Γ
5	−0.0112	0.0112	0.0449	−0.1595	−0.4716	0.0269	0.3624
6	−0.0115	0.0345	0.0230	−0.1632	−0.4493	−0.0011	0.1346
4	−0.0606	0.0909	−0.0303	−0.2286	−0.3262	−0.0419	0.2410
3	−0.0667	0.2000	0	−0.2981	−0.1156	0.0596	0.1817
2	0.2000	0.2000	−0.1333	−0.1556	−0.1271	−0.1890	0.4450
1	0.0909	0.2727	0	−0.2923	−0.0428	−0.0225	0.4863

Table 6.11 Lamination parameters of the stacking sequences of left and right hand side flanges.

Panel no.	ξ_1^A	ξ_2^A	ξ_3^A	ξ_1^D	ξ_2^D	ξ_3^D	Γ
left hand side flanges							
5	0.1215	0.0654	−0.0187	−0.0933	−0.3958	−0.1832	0.3848
3	0.0612	0.0204	0	−0.1245	−0.4075	−0.1558	0.3131
1	0.3721	0.3023	−0.0233	−0.0460	−0.0352	−0.0477	0.3870
right hand side flanges							
6	0.1414	0.0909	−0.0303	−0.0898	−0.4050	−0.1720	0.2904
4	0.0879	0.0549	−0.0110	−0.1250	−0.4365	−0.1695	0.2644
2	0.3000	0	0	−0.0270	−0.5400	−0.1432	0.1760

Table 6.12 Lamination parameters of the stacking sequences of left and right hand side webs.

Panel no.	ξ_1^A	ξ_2^A	ξ_3^A	ξ_1^D	ξ_2^D	ξ_3^D	Γ
left hand side webs							
3	0.1579	0.2982	0	−0.2116	0.0219	0.0162	0.3170
1	0.1200	0.2000	−0.0800	−0.1212	−0.0734	−0.0815	0.7114
5	0	−0.4286	−0.1429	−0.0525	−0.8834	−0.1603	0.5831
right hand side webs							
6	0.0174	0.2174	−0.0087	−0.2044	−0.1122	−0.0785	0.3687
4	0.2083	0.4167	−0.0417	−0.1945	0.2412	−0.0786	0.3403
2	0.4138	0.3793	−0.0345	−0.0044	0.0349	−0.0473	0.2680

As can be seen, the values of Γ in Tables 6.10-6.12 are higher than those in Table 6.6 because the blending constraint narrows the design space and hence reduces the level of match between the target and obtained lamination parameters. For the five blending problems with the exception of the webs on the left hand side, the increase in the value of Γ for each laminate is acceptable. However, as the numbers of plies in the webs on the left hand side are small, which would not be the case in a real aircraft wing design, the blending constraint causes a mismatch between the target and obtained lamination parameters for the web in panel 1 equal to 0.3591, and the majority of the mismatch is in $\xi_{1,2}^{A}$. Since the stiffness of each panel is mainly provided by the skin and flanges, this mismatch only has a small effect on the load-carrying capability of the wing. The obtained stacking sequences are then checked by FEA using ABAQUS and as shown in Figure 6.12, the local and global buckling load factors (i.e. the first and second buckling modes) decrease to 1.08 and 1.14, respectively. It is observed that there is only a slight decrease in the buckling performance when adding the blending constraint, and that the optimised configuration still satisfies the buckling constraint. The DLBB method is therefore seen to perform well in optimising blended stacking sequences to match target lamination parameters from the first stage of the optimisation process. Note that, due to the rounding process at the start of the second stage, the weight of the final optimised wing box is increased slightly to 49.7 kg as shown in Figure 6.9. Compared with the results in Fischer *et al.* (2012), the stacking sequences of the optimised wing box presented herein are more practical, and the weight of the structure is reduced by 8.0%, which will lead to significant reductions in the material cost and fuel consumption of the aircraft.

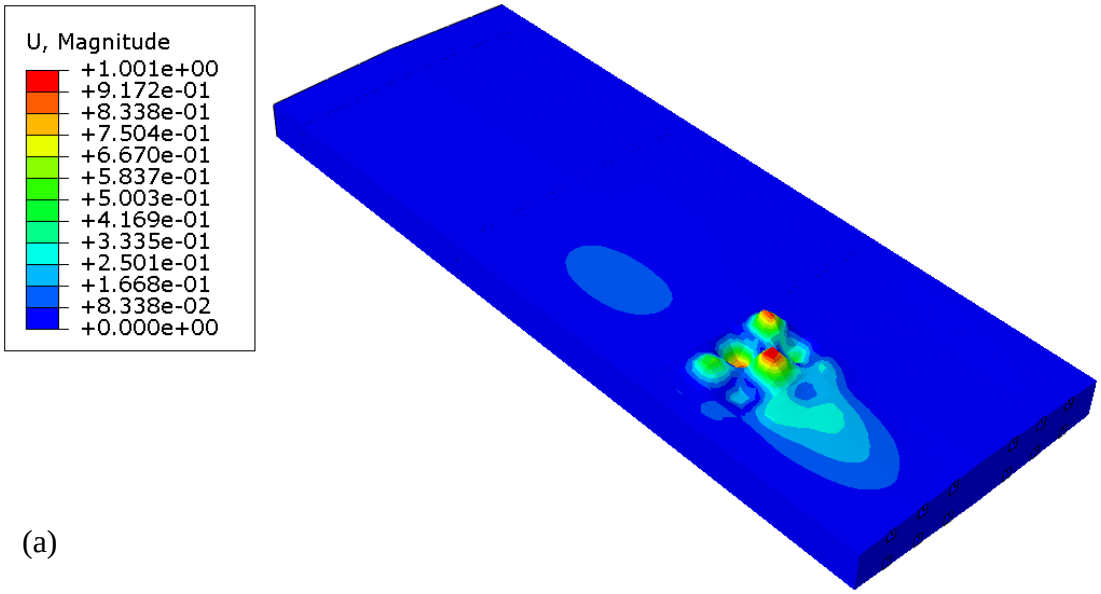

(a)

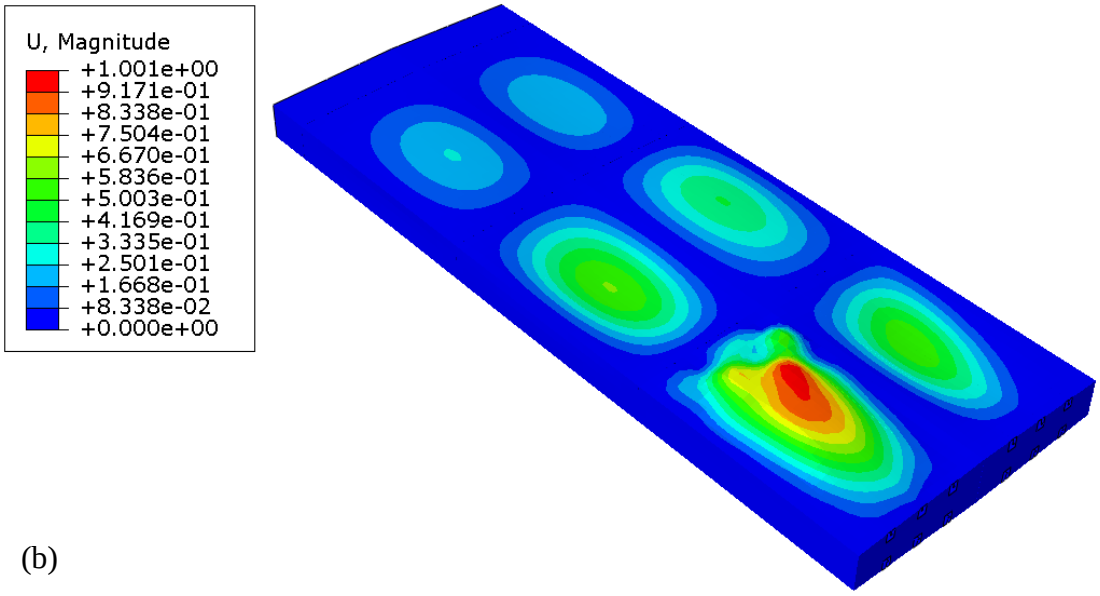

(b)

Figure 6.12 Buckling modes obtained using the blended stacking sequences. (a) First buckling mode with buckling load factor = 1.08. (b) Second buckling mode with buckling load factor = 1.14.

6.4 Conclusions

This chapter presents a two-stage layup optimisation methodology using lamination parameters for the weight minimisation of blended composite structures under buckling, lamination parameter, manufacturing and blending constraints. In the first stage, stacking sequences are replaced by lamination parameters and laminate thicknesses to permit the use of a linear optimiser. This stage uses an extended multilevel optimisation process in which at the start of each design cycle a static analysis of the whole structure is conducted using FEA to determine load distributions between constituent parts, while efficient exact strip software is used to optimise each of these component panels based on these static analysis results. The optimised lamination parameters derived are used as targets in the second stage, and, instead of using the most commonly used heuristic methods to perform a stochastic search, a new DLBB method combining a dummy layerwise technique with the branch and bound method are proposed to search the stacking sequences for those which satisfy blending and layup design constraints to match the targets. The effectiveness of the proposed first stage multilevel optimisation for a three-dimensional composite structure as well as the ability of the DLBB method to optimise the stacking sequences with ply drop-offs is demonstrated by a benchmark problem. Comparison of the results obtained by the presented method with the results in Fischer *et al.* (2012) shows a further weight reduction of 8.0% over the previously determined wing weight even when more constraints are added, making the optimised structure more practical and improving its performance.

Chapter 7
Parallel Computation Method for Optimisation of Composite Laminates

7.1 Introduction

In this chapter, the DLBB method is again proposed for optimising the stacking sequences of blended composite laminates to match target lamination parameters. However, in order to improve the efficiency of the second stage of the optimisation, a parallel optimisation method DLBB-GAGA is developed.

In the first part of the chapter, a guide-based adaptive genetic algorithm (GAGA) is proposed for the blending optimisation problem. According to the performance of each individual in the population, variable probabilities are applied not only to the GA operators but also to different layers in the laminate to improve the searching capability during layup design. The novel parallel DLBB-GAGA method is then developed by combining the stochastic-based search method GAGA with the logic-based search method DLBB in a parallel computation. Messages are passed between the two methods to exchange optimisation information during the parallel process. The combination of these two different methods gives the parallel DLBB-GAGA method the advantages of both, enhancing searching ability for the blended layup optimisation problem. Finally, the superiority of the parallel DLBB-GAGA method is demonstrated through comparisons against the two component methods. The results show the advantages of the parallel DLBB-GAGA method particularly in practical design where more layup design constraints need to be considered.

7.2 Methodology

7.2.1 Guide-based adaptive genetic algorithm

In this section, a guide-based adaptive genetic algorithm (GAGA) is proposed for the second stage optimisation. Several guided-based blending procedures have been developed as discussed in Chapter 2, and the blending procedure in this method is developed based on the concept of PDS (Yang *et al.* 2016). Each individual in the GAGA has two chromosomes, the first chromosome stores the guide layup with a string of genes, the ply angles $-45°$, $0°$, $+45°$ and $90°$ being represented by numbers 1, 2, 3, and 4 respectively. As the layup is symmetric, only half of the layers in the laminate are represented in the chromosome. The second chromosome stores the positions for the layers in the guide with a random order. The layups of the thinner panels are obtained by deleting plies from the guide layup according to the position values from top to bottom in the second chromosome.

A balance repair procedure is proposed for this optimisation process. Firstly, the first chromosome is repaired using the technique described in Section 5.2.2.3. Secondly, the repair procedure is implemented to the second chromosome to ensure that the position value of each $-45°$ ply puts it just behind a $+45°$ ply in order that the position values of the $+45°$ and $-45°$ plies appear as a set in the second chromosome. Then, it is ensured that during the blending process, if a position value selected for deleting a ply is related to a $45°$ ply, the next position value related to a $0°$ or $90°$ ply which is below this set is moved to above it, avoiding deleting different numbers of $\pm 45°$ plies. In addition to this, if a thicker panel with an odd number of layers is adjacent to a thinner panel with an even number of layers, requiring the middle layer in the thicker panel to be deleted to satisfy the blending constraint, the position value corresponding to the middle layer in the second chromosome is moved to the top, leading to the middle layer being deleted first.

The process of the GAGA method is illustrated with an example in Figure 7.1. S denotes a symmetric layup (with a single middle ply if there is an odd number of plies). For each panel, the left hand side is the guide layup and the deleted plies are crossed out, the right hand side gives a random sequence of which plies are to be deleted, and

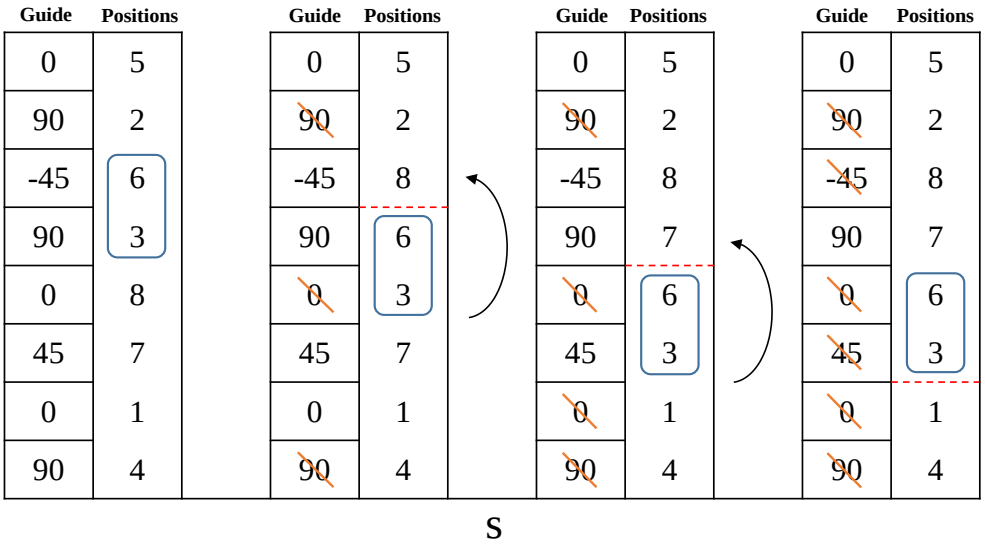

Figure 7.1 An example illustrating the blending process in GAGA.

the plies above the red line have been deleted. The blue box shows +45° and −45° plies which must be retained or deleted together to ensure balance. Here, the number of layers for each panel are 16, 9, 8 and 4 respectively, the guide is 0/90/−45/90/0/45/0/90, and the order of the position values is (5 2 6 3 8 7 1 4). The thickest panel takes the guide layup. For the second thickest panel, according to the position values in the second chromosome, the fifth, second and sixth plies in the guide layup should be deleted. If the balance constraint is imposed, the position value 8 will be inserted above the set of 6 and 3, so the eighth ply will be deleted instead of the sixth ply, making the second panel balanced. Besides, as the second thickest panel has an odd number of plies, there is just one 0 ply in the middle. To obtain the layup for the third panel, as discussed above, the position value 7 will be moved to the top of the second chromosome. Correspondingly, the middle layer of the second panel will be dropped off. Finally, the layup of the fourth panel is obtained by deleting a set of a +45° ply and a −45° ply.

The optimisation process implemented in GAGA is shown in the flow chart of Figure 7.2. As can be seen, the guide chromosomes are optimised using a two-point crossover and a mutation, and the position chromosomes are implemented with a permutation. The biased roulette wheel method is employed in the selection procedure and the elitism operator which keeps the best individuals directly for the next generation is

also implemented in the generation cycle. The objective function in GAGA is represented as:

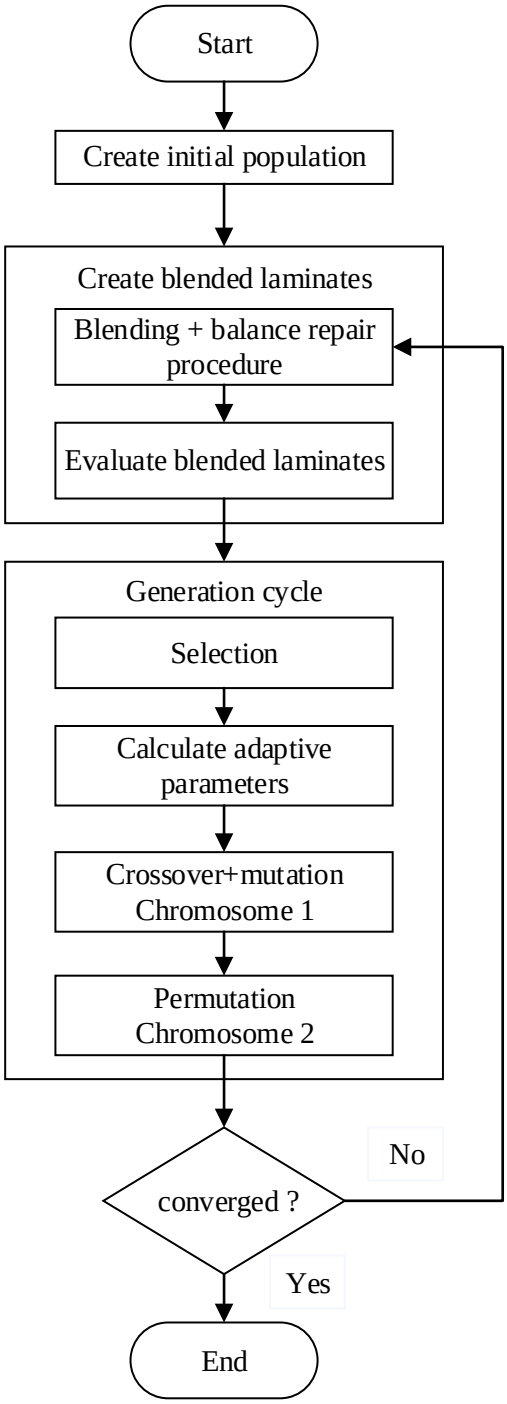

Figure 7.2 Flow chart illustrating the guide-based adaptive genetic algorithm (GAGA).

$$\Gamma = \sum_{k=1}^{N_{panel}} \Gamma_{panel\,k} \tag{7.1}$$

$$\Gamma_{panel\,k} = \sum_{i=1}^{3} \sum_{j=A,D} w_j \left| \xi^{j}_{i(k)(actual)} - \xi^{j}_{i(k)(target)} \right| \tag{7.2}$$

where N_{panel} is the number of panels, $w_{A,D}$ are the weighting factors, $\xi^{A,D}_{1,2,3(k)(target)}$ are the target lamination parameters for panel *k*, and $\xi^{A,D}_{1,2,3(k)(actual)}$ are the actual lamination parameters of the chosen layup of panel *k*.

For standard GAs, performance mainly depends on the predefined crossover and mutation parameters. Normally, a high probability of crossover P_c with a small probability of mutation P_m is used in layup optimisation, because frequent crossovers guarantee a random search toward a local or global optimum and some mutation is needed to prevent the results converging and getting stuck in local optima. However, the values of P_c and P_m in standard GAs are left for the user to determine based on some empirical experience. In this chapter, the values of P_c, P_m and P_p are varied adaptively for each individual during the optimisation according to the fitness values. The equations for the adaptive process are expressed as:

$$P_c = \begin{cases} P_{cmax} \cdot \left(\dfrac{f_{max} - f'}{f_{max} - f_{ave}} \right) + P_{cmin} \cdot \left(\dfrac{f' - f_{ave}}{f_{max} - f_{ave}} \right) & f' \geq f_{ave} \\ P_{cmax} & f' < f_{ave} \end{cases} \tag{7.3}$$

$$P_{cp(i)} = \begin{cases} \dfrac{1}{n_e} & f' \geq f_{ave} \\ \dfrac{1}{n_e} + \left(\dfrac{n_e + 1}{2} - i \right) \cdot d & f' < f_{ave} \end{cases} \tag{7.4}$$

$$P_m = \begin{cases} P_{mmax} \cdot \left(\dfrac{f_{max} - f}{f_{max} - f_{ave}} \right) + P_{mmin} \cdot \left(\dfrac{f - f_{ave}}{f_{max} - f_{ave}} \right) & f \geq f_{ave} \\ P_{mmax} \cdot f_{m(j)} & f < f_{ave} \end{cases} \tag{7.5}$$

$$f_{m(j)} = Z_u - \left(\frac{j-1}{n_e - 1}\right)(Z_u - Z_l) \tag{7.6}$$

$$P_p = \begin{cases} P_{pmax} \cdot \left(\dfrac{f_{max} - f}{f_{max} - f_{ave}}\right) + P_{pmin} \cdot \left(\dfrac{f - f_{ave}}{f_{max} - f_{ave}}\right) & f \geq f_{ave} \\ P_{pmax} & f < f_{ave} \end{cases} \tag{7.7}$$

where f_{max} and f_{ave} are the maximum and average fitness values in the population, respectively; f is the fitness value of each individual, f' is the larger fitness value of the two individuals to be crossed; P_{cmax}, P_{mmax} and P_{pmax} are the maximum values of P_c, P_m and P_p, respectively; P_{cmin}, P_{mmin} and P_{pmin} are the minimum values of P_c, P_m and P_p, respectively; n_e is the number of genes in the chromosome; d is the difference between values of $P_{cp(i)}$ for adjacent genes; $f_{m(j)}$ is the mutation factor giving different genes different P_m; Z_u and Z_l are the upper and lower limits of $f_{m(j)}$; i and j take values from 1 to n_e to calculate $P_{cp(i)}$ and $f_{m(j)}$ from the outermost genes which represent the outermost layers to the innermost ones. In this chapter, the parameters discussed above are set with $P_{cmax} = 0.8$, $P_{cmin} = 0.3$, $P_{mmax} = 0.2$, $P_{mmin} = 0.05$, $P_{pmax} = 0.8$, $P_{pmin} = 0.5$, $d = 0.0002, Z_u = 1.1$, $Z_l = 0.9$, and the population size is 200.

By using equations (7.3), (7.5) and (7.7), P_c, P_m and P_p increase when all the individuals converge to one layup to prevent premature convergence, and the individuals who have fitness values lower than the average value of the population are implemented with the highest P_c, P_m and P_p to provide sufficient ability to get rid of poor results, with P_c, P_m and P_p decreasing as individuals' fitness values increase to avoid disrupting the convergence of good results.

In standard two-point crossover, two genes in each chromosome are randomly selected as cross points in the parents, and the parents swap the genes between these two cross points to generate a new generation. The genes in the chromosome have the same probability P_{cp} of being selected as cross points. In the method used here, for the

individuals whose fitness values are lower than average, higher values of P_{cp} are given to the outer layers which make a greater contribution to $\xi_{1,2,3}^{D}$ using equation (7.4). Based on equation (7.6), values of P_m are also increased for all layers from the innermost to the outermost in these poor individuals. Therefore, for layups which have a poor match with the target lamination parameters, the outer layers are given a larger probability of being selected as cross points and mutating, providing more potential for the improvement of the objective function.

7.2.2 Parallel DLBB-GAGA method

As described in Chapter 6, the DLBB method is a logic-based search method which progressively optimises blended stacking sequences from the outer plies to the inner ones. Good results can be obtained quickly by solving small problems in the first few cycles. However, when the case loop consists of large numbers of plies in later cycles, it takes a long time to complete the optimisation during which only a small number of plies are optimised, limiting the rate of decrease in the value of Γ. As for the GAGA method, which is a stochastic search method based on the natural evolution of Darwin's theory, blended layups at each generation are obtained by randomly deleting plies from the guide. Instead of logically applying the layup design constraints in the searching process as in DLBB, layup design constraints for each panel are imposed using the penalty functions in GAGA, making blended structures with large numbers of component panels easily penalized. In order to combine the advantages of both methods and overcome the disadvantages of each, a parallel DLBB-GAGA method, which computes the two different methods in parallel to improve the searching efficiency, is developed in this section.

MATLAB is used to conduct this parallel optimisation. The SPMD (Single Program Multiple Data) structure in MATLAB provides an option for executing different codes on different cores simultaneously, and information exchange between parallel codes is allowed. MPI (Message Passing Interface) based functions such as LabSend and LabReceive can be used to communicate between parallel works by sending and receiving messages between the cores.

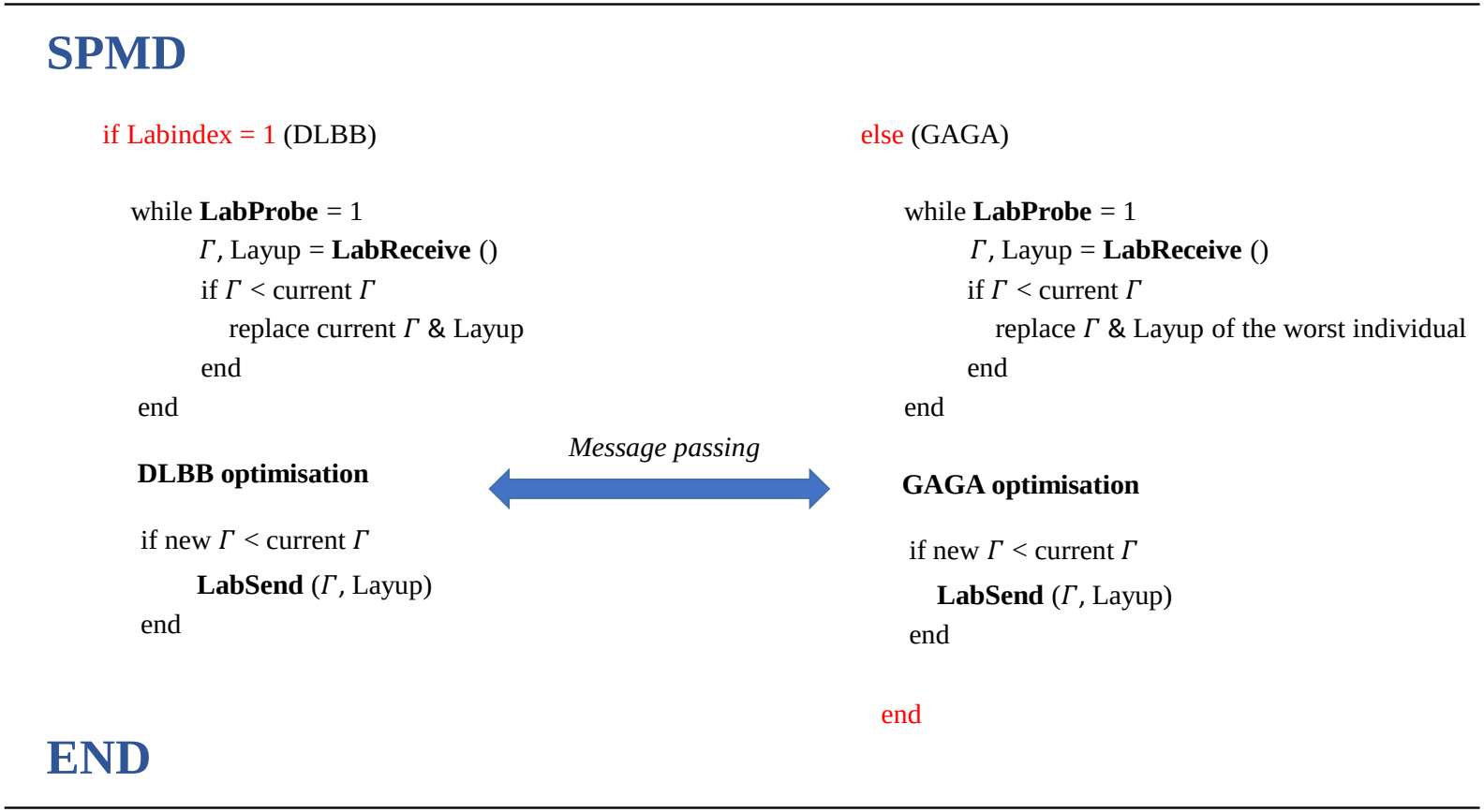

Figure 7.3 Optimisation process for the parallel DLBB-GAGA method in MATLAB. (The left column represents the simplified DLBB process and the right GAGA, and the message passing functions described in text are shown in bold.)

As can be seen from Figure 7.3, the parallel DLBB-GAGA method simultaneously executes the logic-based search method DLBB and the heuristic-based search method GAGA on two cores to solve the same blending optimisation problem.

Once a new result is obtained by DLBB, it is sent to GAGA with the LabSend function. The LabProbe function in GAGA is used to check if any new information has been sent from the other core (with Labindex equal to 1), this result is then received by GAGA using the LabReceive function. If the value of Γ of the received blended stacking sequence is smaller than that of the current best result in GAGA, the received result is accepted. After that, Guide and PDS chromosomes are created based on the received blended layup, and the worst individual in the population is replaced with the received result. GAGA then continues optimising the blended layup with the newly updated population.

Alternatively when GAGA obtains a new result, the Γ and the layup are sent to DLBB. Once the received result is accepted by DLBB, a new dummy layerwise table is created corresponding to the received blended layup. If the result from GAGA is received before a case loop, the current Γ, blended layup and dummy layerwise table are replaced with the new result, based on which the optimisation is carried on. However, if the result is received during a case loop, the Γ is updated and used as a new upper bound during the branch and bound optimisation of the current case loop, meaning more branches can be pruned without being explored. The blended layup and dummy layerwise table are replaced with the received result at the end of the case loop, if DLBB has not obtained a better result by itself during the loop.

The benefits of this parallel process are that, at any time both methods are optimising the blended stacking sequences based on the current best result, improving the efficiency of this time-consuming optimisation problem. The results received from DLBB bring more diversity to the population of GAGA, speeding up the process of moving away from a local optimum result especially when layup design constraints are imposed. The shortcoming of the DLBB method in requiring a long time to complete large case loops in later cycles during which only some of the plies in the

laminate are allowed to be optimised is also overcome by the parallel optimisation method, as any ply in the laminate can be optimised by GAGA during that time.

7.3 Results and discussion

The aim of the second stage optimisation is to obtain a blended stacking sequence which matches the target lamination parameters obtained in the first stage optimisation as closely as possible. The DLBB method, GAGA and the parallel DLBB-GAGA method are used herein to optimise the stacking sequences to minimise the value of Γ based on the target lamination parameters obtained in Chapter 6, and the performance of these three methods is compared. There are two sets of results. In the first set, the blended laminates are only required to be symmetric. In the second, comparisons are made for laminates subjected to the balance constraint and four layup design constraints applied to ensure the design of more practical stacking sequences. Since GAGA is a stochastic search method, GAGA and the parallel DLBB-GAGA method are run 10 times for each example to guarantee the reliability of these comparisons. Besides, the same starting layups are used in the DLBB method and GAGA to make a fair comparison.

7.3.1 Symmetric case

In this section, the five blending problems defined in Chapter 6 are restricted to symmetric designs. A comparison between the DLBB method, GAGA and the parallel DLBB-GAGA method for the blended skins is shown in Figure 7.4 (a). As can be seen, in the early stages GAGA finds better results earlier than the other two methods. However after roughly 10 seconds the differences among the three methods become relatively small and then the parallel method takes the lead until the end. GAGA is more efficient than the DLBB method most of the time, however the final result obtained by the DLBB method is better than that of GAGA. The parallel method achieves the same result as the final result from GAGA after approximately 100 seconds, and the final result of the parallel method is slightly better than that of the DLBB method, demonstrating its good performance in searching blended layups. Note that the parallel method takes longer to obtain its first result because of the overhead of the parallel process. Figure 7.4 (b) compares examples of a GAGA run and a parallel

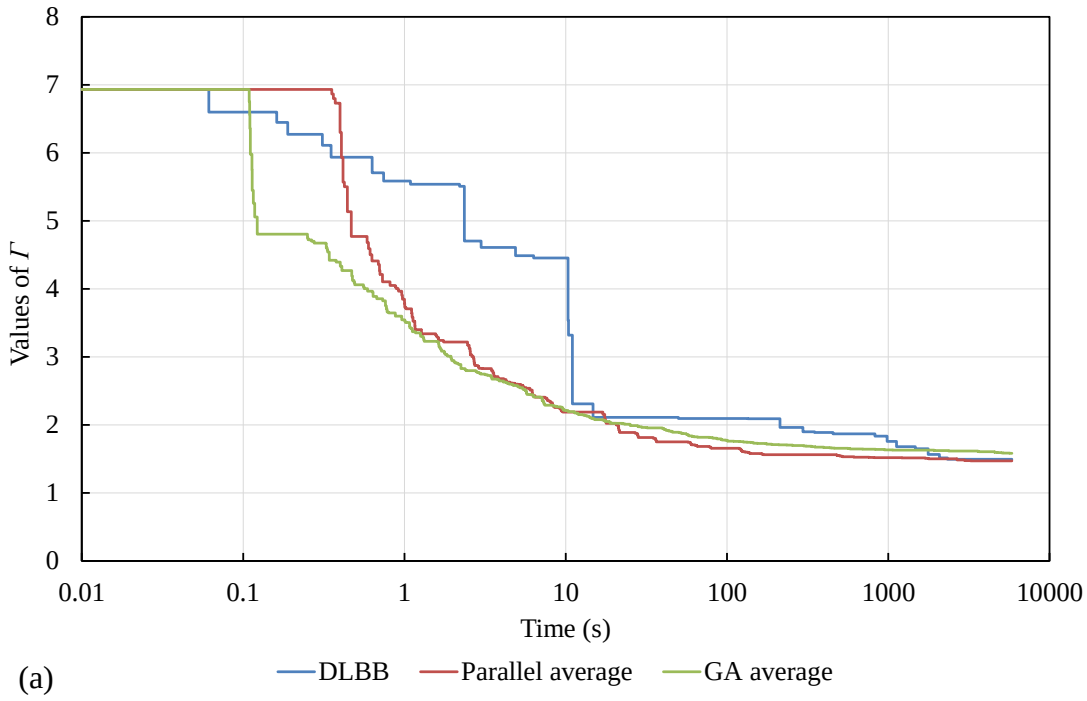

(a)

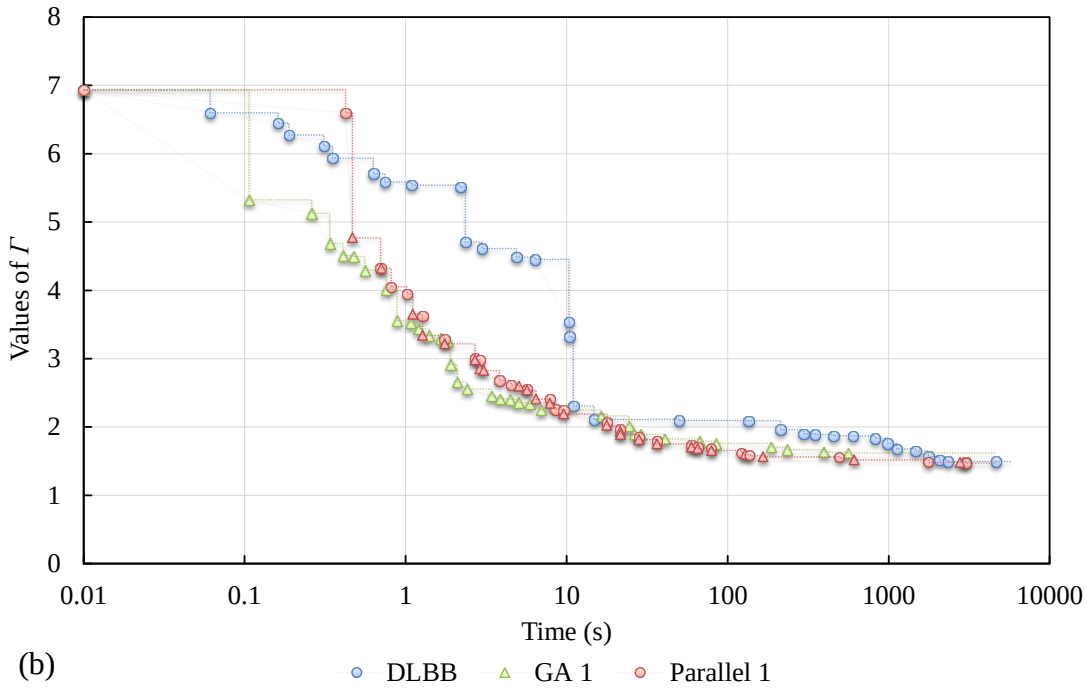

(b)

Figure 7.4 Comparisons between the DLBB method, GAGA and the parallel method for blended skins. (a) The results of GAGA and the parallel method are averaged values of 10 runs. (b) Examples of a GAGA run and a parallel method run are shown in comparison.

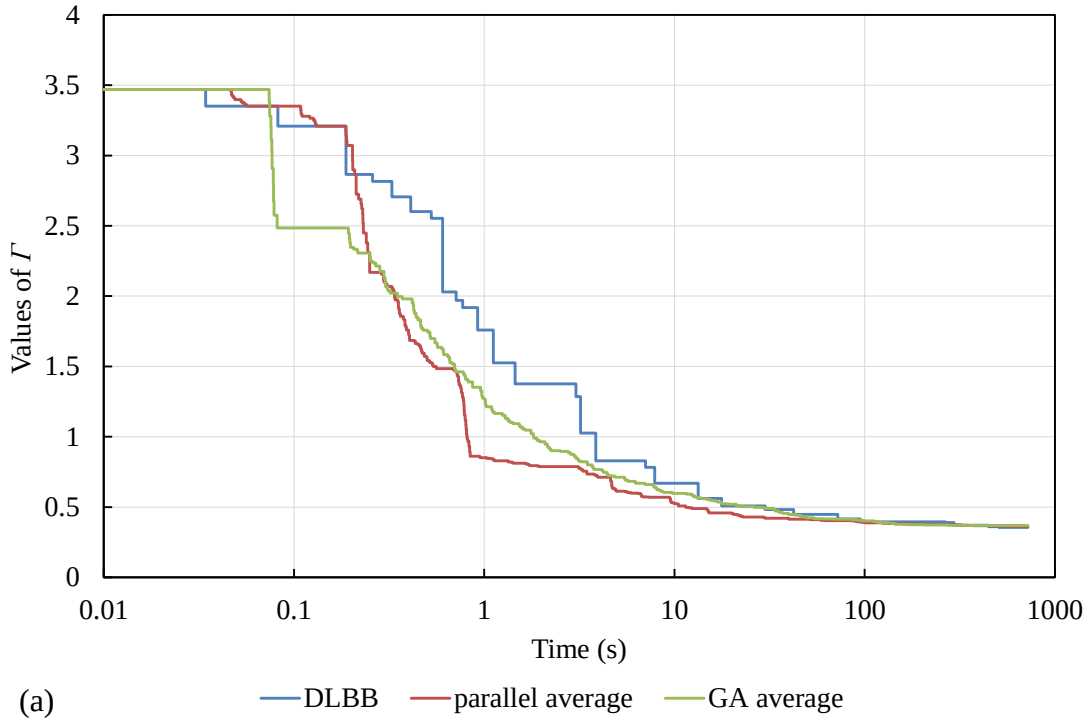

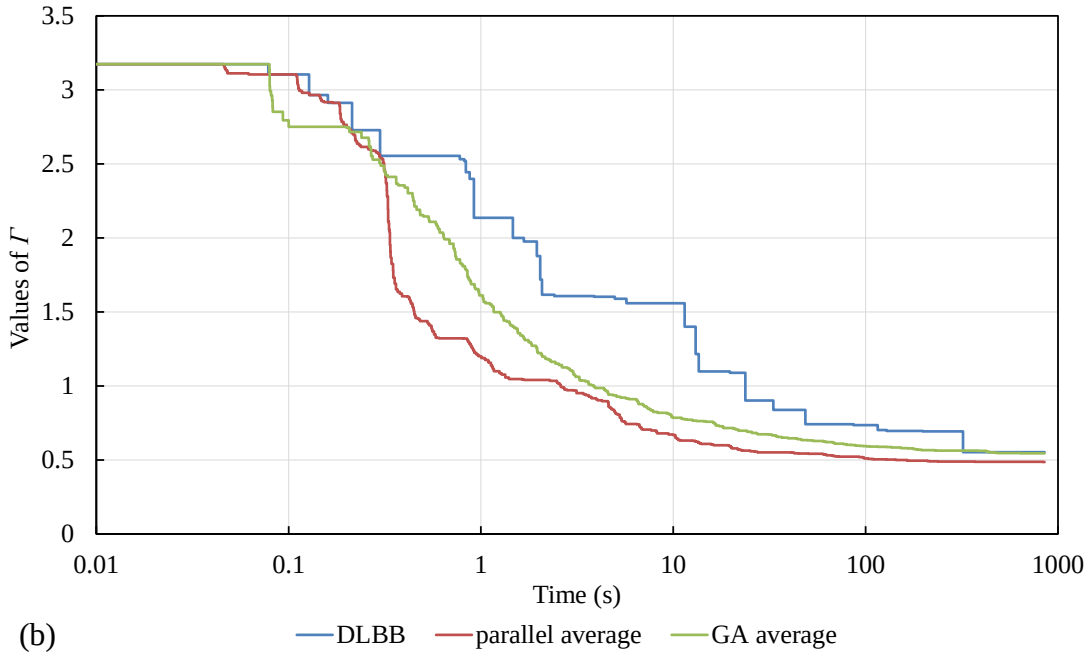

Figure 7.5 Comparisons between the DLBB method, GAGA and the parallel method for (a) blended right hand side flanges and (b) blended left hand side flanges.

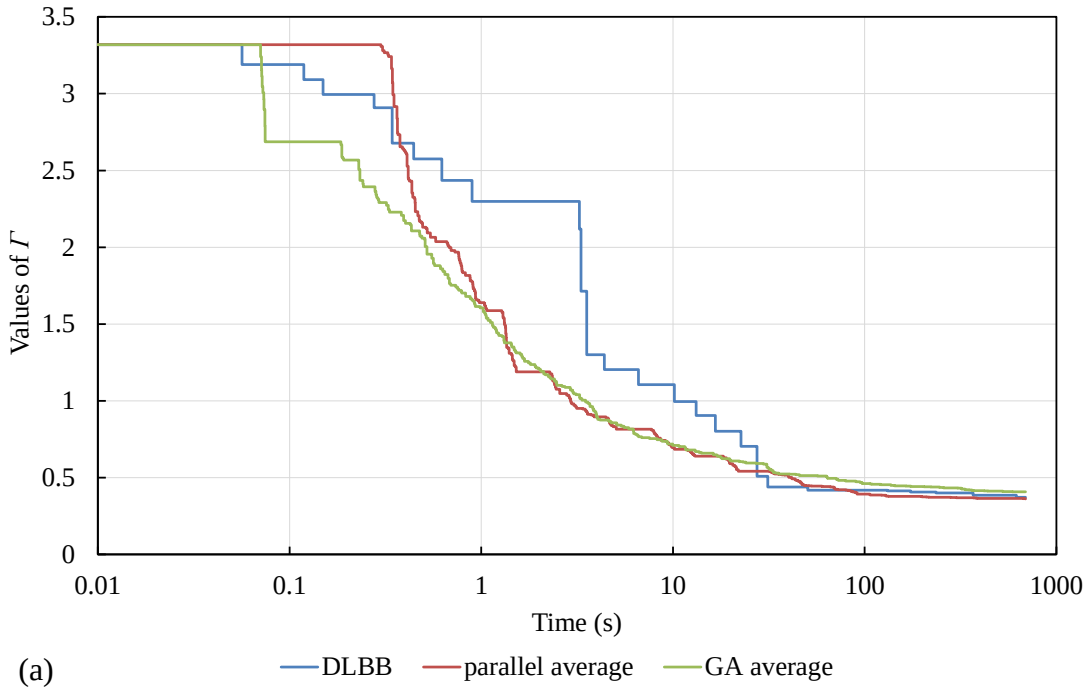

(a)

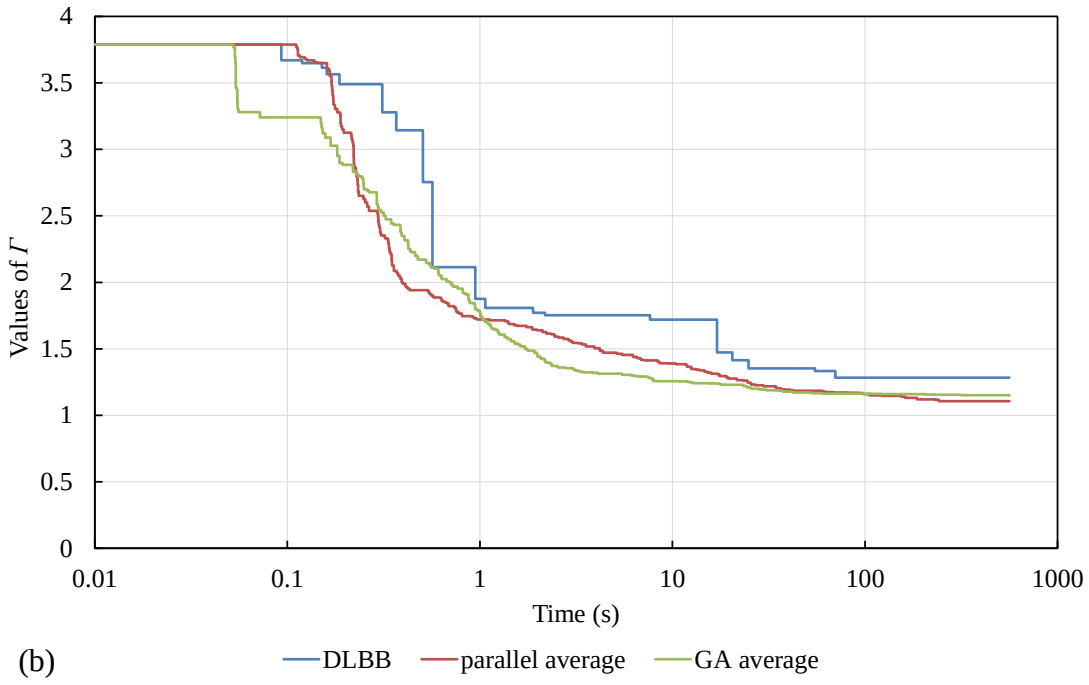

(b)

Figure 7.6 Comparison between the DLBB method, GAGA and the parallel method for (a) blended right hand side webs and (b) blended left hand side webs.

method run, with the blue circles and green triangles representing the results obtained by the DLBB method and GAGA, respectively. The results obtained by running the DLBB method and GAGA in a parallel optimisation are represented by red circles and red triangles, respectively. It can be seen that both of these methods make great contributions to the reduction of Γ in the parallel optimisation and the message passing between the two methods results in obvious mutual promotion throughout the whole period of the parallel process, the combination of the two methods improving the searching capability of each on their own.

For the blended webs and flanges which are relatively small blending problems, the performances of the three methods are again compared. Comparisons for the right hand side blended flanges are shown in Figure 7.5 (a), where it is observed that GAGA performs better than the DLBB method in the first 20 seconds, after which the two methods results are closely aligned until the end. The parallel method obtains better results more quickly than the other two methods from a very early stage in this optimisation. Figure 7.5 (b) compares the methods for the blended left flanges, where it can be seen that the parallel method not only achieves higher efficiency but also performs better in finding lower values of Γ than each of the two component methods. It only takes the parallel method 10 seconds to reach the same value of Γ that is achieved by the other two methods at almost 1000 seconds. As can be seen from Figure 7.6 (a), GAGA finds better results earlier than the DLBB method until 50 seconds into the process after which the DLBB method obtains better results earlier than GAGA. The parallel method performs well during the whole optimisation period taking the lead after around 90 seconds. Figure 7.6 (b) shows the comparisons for the blended left hand webs. It is observed that GAGA performs better than the DLBB method in this optimisation, and the parallel method surpasses GAGA from approximately 200 seconds. As expected, the parallel method performs better than the two methods for the blended layup optimisation in this section.

7.3.2 Constrained case

For more practical designs, the balance and four layup design constraints need to be imposed in the second stage optimisation. Figure 7.7 shows a comparison between the three different techniques for blended skins when these are added. It can be seen that the values of Γ are larger than those obtained without considering the extra layup design constraints which narrow the design space. GAGA does not achieve the same final value of Γ as the DLBB method and the parallel method, and the differences between the solutions obtained by the different techniques are greater than those found without considering the layup design constraints. The reason for this is that the layup design constraints are easily violated in the stochastic search of the GA process, especially for a blended structure with several component panels, and because results violating these constraints are penalized in the optimisation process, the search capability of GAGA is diminished. However, this is not the case for the parallel method; on the contrary, the superiority of the parallel method is more obvious as it leads from the beginning of the optimisation with a more distinct advantage. It takes

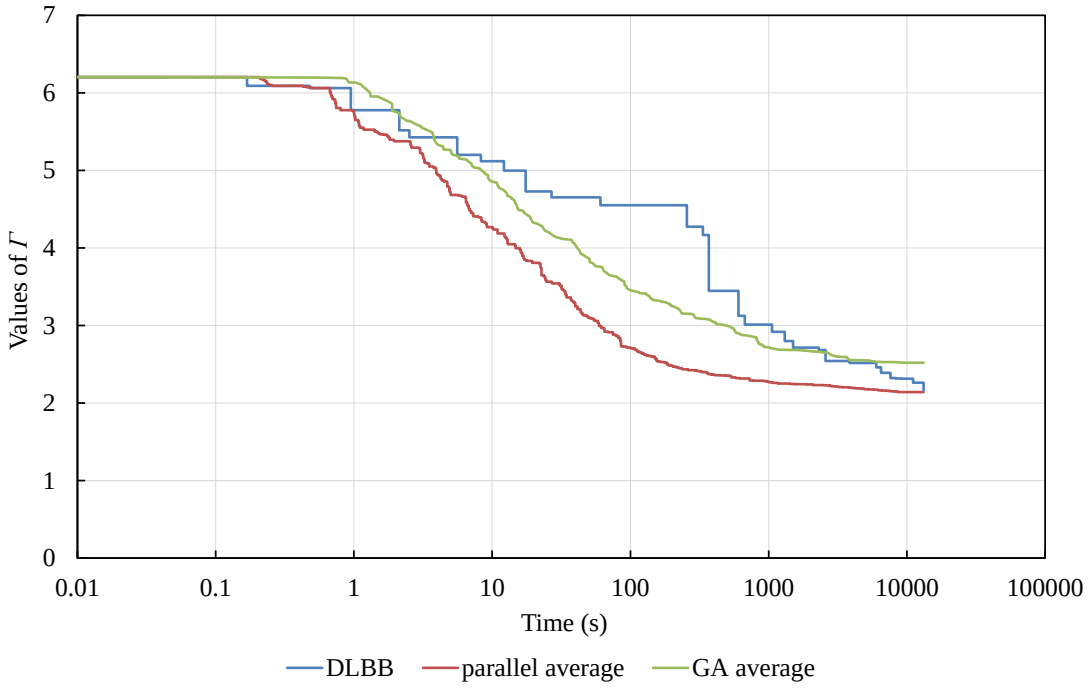

Figure 7.7 Comparison between the DLBB method, GAGA and the parallel method for blended skins under symmetry, balance, and four layup design constraints.

the parallel method around 200 seconds to achieve the final value of Γ achieved by GAGA in this example. The results suggest that the combination of these two methods overcomes the disadvantages of each and even provides further improvements, making it more appropriate for blended layup design.

The comparisons for the right and left hand side flanges are shown in Figure 7.8 (a) and (b), respectively. In contrast to the results obtained without considering the layup design constraints, the DLBB method performs better than GAGA most of the time during the optimisations, and it obtains lower final values of Γ than GAGA. With the extra layup design constraints being added, the lead of the parallel method is more apparent from the start of the optimisation. Better still, the parallel method achieves lower final values of Γ than the other two methods. For the right hand side flanges, it takes the DLBB method and GAGA roughly 1000 and 10000 seconds, respectively, to reach the same value of Γ achieved by the parallel method in 100 seconds. Figure 7.9 (a) shows comparisons for the right hand side webs, where it is observed that after roughly 1 second the parallel method starts to find better results more quickly than the other two methods, and achieves a lower value of Γ at the end. The competition between the DLBB method and GAGA is intense, and in the final stage the DLBB method obtains lower values of Γ than GAGA. The comparisons for the left hand side webs are shown in Figure 7.9 (b). In this case the DLBB method performs better than GAGA in the first 10 seconds, after which GAGA gradually surpasses the DLBB method, but the DLBB method achieves the same value of Γ as the other two methods at a later stage. The parallel method, again, takes a good lead during the optimisation, and almost achieves its final value of Γ after just 10 seconds.

The stacking sequences obtained at 350s using the three methods, for which the buckling performances are compared, are shown in Tables 7.1-7.9. The stacking sequences obtained by the DLBB method are listed in Tables 7.1-7.3. Results of a typical GAGA run and a parallel method run are used for comparison. The stacking sequences of GAGA are listed in Tables 7.4-7.6, and those of the parallel method are listed in Tables 7.7-7.9. The lamination parameters of these stacking sequences and the related values of Γ are shown in Appendix A. The buckling performance of the obtained stacking sequences are checked using ABAQUS. For the results obtained by

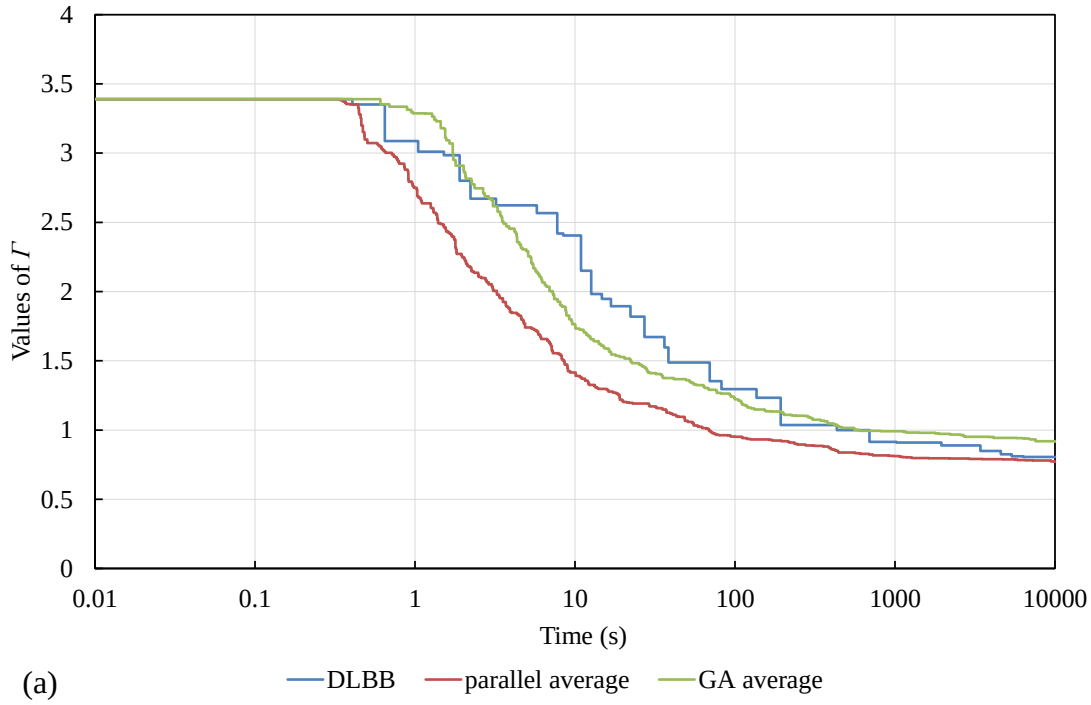

(a)

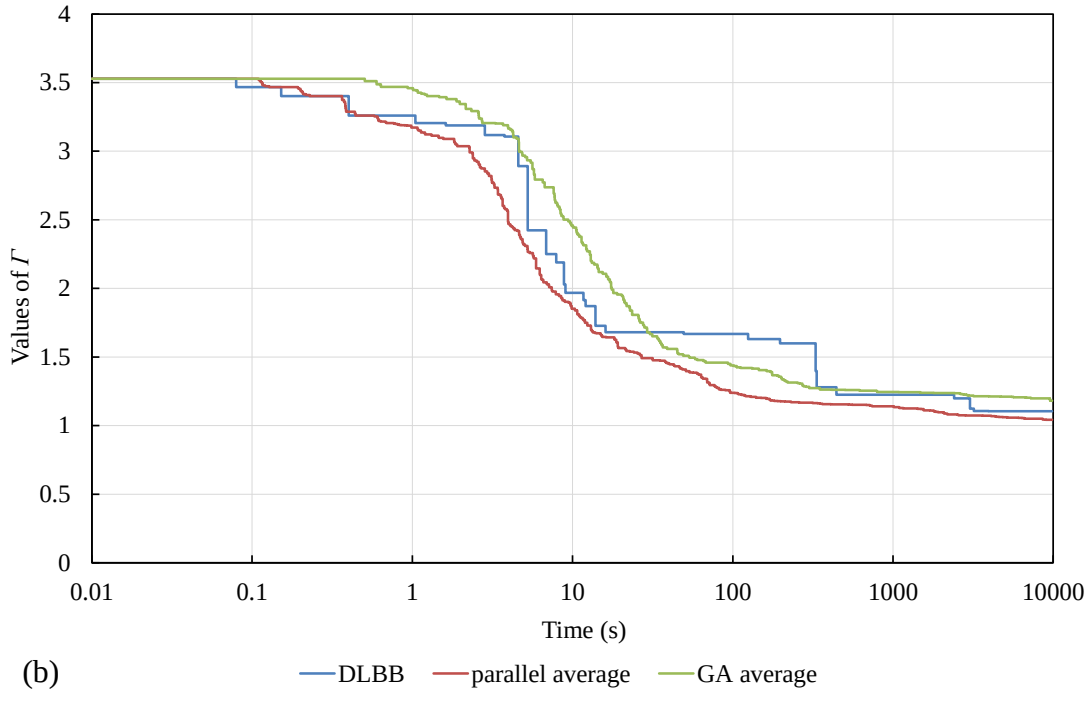

(b)

Figure 7.8 Comparison between the DLBB method, GAGA and the parallel method for (a) blended right hand side flanges and (b) blended left hand side flanges, under symmetry, balance, and four layup design constraints.

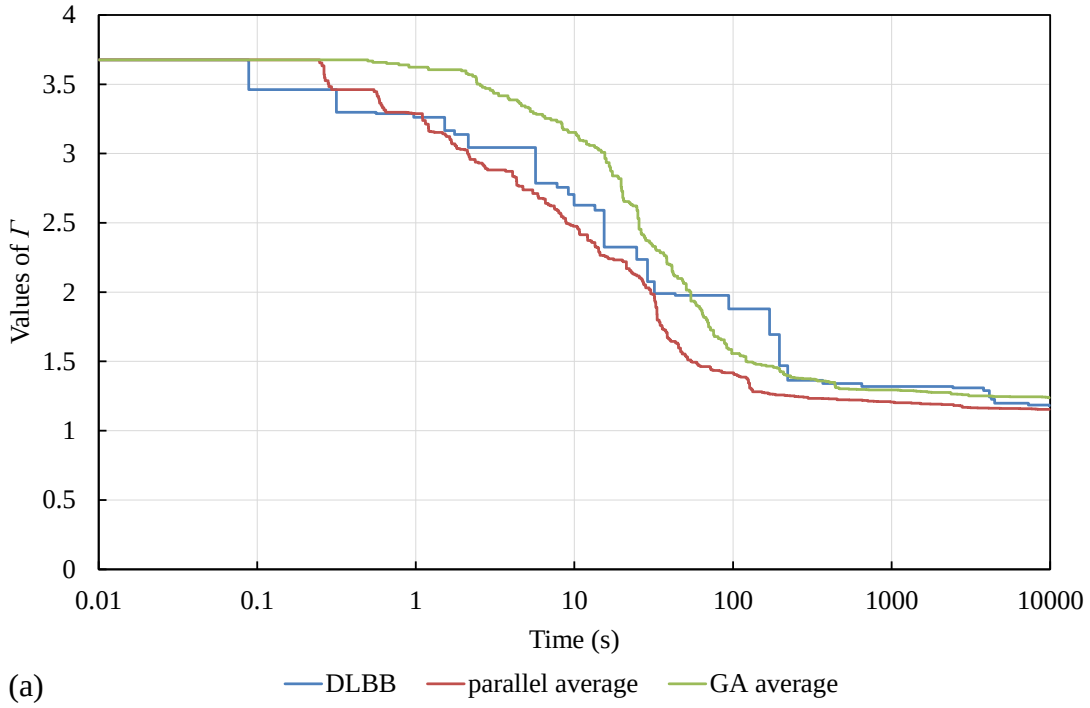

(a)

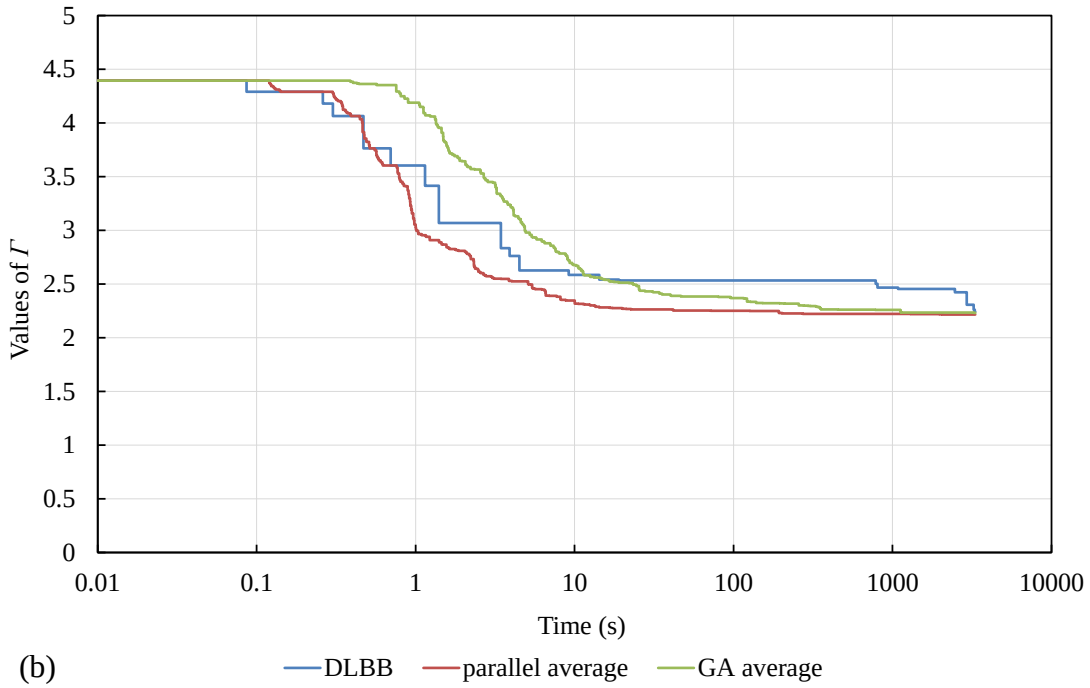

(b)

Figure 7.9 Comparisons between the DLBB method, GAGA and the parallel method for (a) blended right hand side webs and (b) blended left hand side webs, under symmetry, balance, and four layup design constraints.

the DLBB method, the first and second buckling modes are local buckling occurring in panel 1 with buckling load factors equal to 1.06 and 1.11, respectively, and the third buckling mode is a global buckling mode with a buckling load factor equal to 1.15. The same buckling modes occur for the results obtained using GAGA, with buckling load factors of 1.03, 1.13, and 1.15, respectively. The buckling load factors for the results obtained by the parallel method are slightly higher at 1.08, 1.14, and 1.15, respectively. The corresponding buckling modes for the three methods are shown in Appendix B.

These comparisons confirm the advantages of the parallel method in optimising blended layups, which are more obvious when imposing the extra layup design constraints. The combination of the logic-based search and stochastic-based searches significantly enhances the searching capability for the whole optimisation period, resulting in the value of Γ decreasing until the end. Note that for practical design, the optimisation can be terminated as soon as an acceptable result is found (e.g. when the value of Γ of each component panel is less than 0.3).

Table 7.1 Stacking sequences of skins obtained using DLBB method.

Panel no.	Stacking sequences
5	$[45/-45/0/-45/(90/45_2)_2/90/-45_2/90/45/0_2/-45_3/90/-45/90_2/45/0_2/45/90/-45_2/(0/45)_2/0_3/45/90_3/-45/0/0]_{MS}$
6	$[45/-45/0/-45/(90/45_2)_2/90/-45_2/90/45/0/-45_3/90/-45/90_2/45/0_2/45/90/-45_2/(0/45)_2/0_3/45/90_3/-45/0/0]_{MS}$
4	$[45/-45/0/-45/90/45/90_3/45/0/(-45/90)_2/90/45/0/45/90/-45_2/0/45/0_4/45/90_2/-45/0]_S$
3	$[45/-45_2/90/45/90_2/45/0/(-45/90)_2/45/0/45/90/-45_2/0/45/0_4/45/90_2/-45/0]_S$
2	$[45/-45/90_2/(-45/0)_2/45/0_3/45/90_2]_S$
1	$[45/-45/90_2/-45/0_3/45/90_2]_S$

Table 7.2 Stacking sequences of left and right hand side flanges obtained using DLBB method.

Panel no.	Stacking sequences
	left hand side flanges
5	$[45/-45_4/90/45_3/90_2/-45_4/90/45_4/0/45/(90/-45_2)_2/0/45_2/0_3/-45/90_4/45/0_3/45/0_2/-45/0_4/45/0/0]_{MS}$
3	$[45/-45_4/90/45_3/90_2/-45_4/90/45_4/0/45/(90/-45)_2/-45/0/45_2/0_2/-45/90_4/45/0_4/-45/0_4/45/0]_S$
1	$[45/-45/90_3/-45/0/45_2/0_2/-45/0_3/-45/0_4/45/0]_{MS}$
	right hand side flanges
6	$[45/-45_2(-45_2/90)_2/-45/90/45_3/90/-45_2/0_2/45/90/45_3/0_2/45/(90/-45)_2/0_3/45/90_3/-45/0_3/45/0_4/45/0/0]_{MS}$
4	$[45/-45(-45_3/90)_2/45_3/90/-45/0_2/45/90/45_2/0/45/(90/-45)_2/0_3/45/90_3/-45/0_3/45/0_4/45/0/0]_{MS}$
2	$[45/-45_2/(-45/90)_2/45_3/0_3/-45/0_3/45/0/0]_S$

Table 7.3 Stacking sequences of left and right hand side webs obtained using DLBB method.

Panel no.	Stacking sequences
	left hand side webs
3	$[45/(-45/90)_2/(45/90)_2/90_2/-45/0_3/-45/0/45/0_3/45/0_4/-45/0/0]_{MS}$
1	$[45/(-45/90)_2/45/0_3/-45/0/45/0]_{MS}$
5	$[45/-45/90/-45/0_2/45]_S$
	right hand side webs
6	$[45/-45_4/90_3/45_4/90/-45_3/0_2/-45/90/45/90_3/-45/0/(0/45)_2/0_3/(-45/90_2)_2/90/45/90_3/45/0/(45/0_4)_2/-45/90]_{MS}$
4	$[45/-45/90_4/-45/0_4/45/0_4/-45/90_4/45/0/0]_S$
2	$[45/-45/90/-45/0_2/45/0_3/-45/90/45/0/0]_{MS}$

Table 7.4 Stacking sequences of skins obtained using GAGA.

Panel no.	Stacking sequences
5	$[45/-45_3/0/-45/(90/45_2)_2/45/90_3/-45/0_2/45/90_2/45/0/-45/90_3/-45/0/45/(0/-45)_2/0_2/-45/90/-45/0/45_2/0/0]_{MS}$
6	$[45/-45_4/(90/45_2)_2/45/90_3/-45/0_2/45/90_2/45/0/-45/90_3/-45/0/45/(0/-45)_2/0_2/-45/90/-45/0/45_2/0/0]_{MS}$
4	$[45/-45_3/90/45_3/90_3/-45/0/45/(90_2/-45)_2/0/45/0_4/-45/90/-45/0/45_2/0]_S$
3	$[45/-45_2/90/45_2/90_3/-45/0/45/(90_2/-45)_2/0/45/0_3/-45/90/-45/0/45_2/0]_S$
2	$[45/-45/90_2/(-45/0)_2/45/0/-45/0/45_2/0]_S$
1	$[45/-45/90_2/(-45/0)_2/45_2/0]_S$

Table 7.5 Stacking sequences of left and right hand side flanges obtained using GAGA.

Panel no.	Stacking sequences
	left hand side flanges
5	$[45/-45_4/90/-45_3/90/45_4/90/-45_2/90/45/90_3/-45/0_3/(-45/0)_3/0/45/90_3/45/0_4/45_2/90/45/0_3/(45/0)_2/0]_{MS}$
3	$[45/-45_4/90/-45_2/90/45_4/90/-45_2/90/45/90_3/-45/0_3/(-45/0)_3/45/90_3/45/0_3/45/90/45/0_2/(0/45)_2/0]_S$
1	$[45/-45_2/90/45/90_3/(-45/0_4)_2/45/0/45/0]_{MS}$
	right hand side flanges
6	$[45/-45_3/90/-45_2/90/-45/0/(45/90)_2/-45_3/(90/45)_2/0/-45/90/45_2/0_2/45/0/-45/90/45/90_3/45/0_3/-45/0_2/45/0_3/45/0/0]_{MS}$
4	$[45/-45_4/90/-45/0/(45/90)_2/-45_3/90/45/90/-45/90/45_2/0_2/45/0/-45/90/45/90_3/45/0_3/-45/0_2/45/0_3/45/0/0]_{MS}$
2	$[45/-45_4/90/45_2/90/45/0_3/-45/0_4/45/0]_S$

Table 7.6 Stacking sequences of left and right hand side webs obtained using GAGA.

Panel no.	Stacking sequences
	left hand side webs
3	$[45/-45/90/45/90_2/-45/90_4/45/0/-45_2/0_4/45/0/-45/0_4/45/0/0]_{MS}$
1	$[45/-45/90_3/-45/0_4/45/0/0]_{MS}$
5	$[45/-45/90/-45/0/45/0]_S$
	right hand side webs
6	$[45/-45_4/(90/45/90/-45)_2/0/45/90_2/45_2/0/-45/90/-45/90_2/-45/(0/45)_2/90_4/45/0_3/-45/90_3/45/0_2/-45/0_3/45/90/-45/0_3/45/0/0]_{MS}$
4	$[45/(-45/90_2)_2/90/45/0_3/-45/0_3/45/90/-45/0_3/45/0]_S$
2	$[45/-45/90/-45/0_3/45/90/-45/0_3/45/0]_{MS}$

Table 7.7 Stacking sequences of skins obtained using parallel method.

Panel no.	Stacking sequences
5	$[45/-45_3/90/45_4/90/-45/0/45_2/0/45/90/-45_3/90_3/-45/90_2/-45/0_2/45/0/-45/0_3/45/90_3/45/0_2/-45/0/0]_{MS}$
6	$[45/-45_3/90/45_4/90/-45/0/45_3/90/-45_3/90_3/-45/90_2/-45/0_2/45/0/-45/0_3/45/90_3/45/0_2/45/0/0]_{MS}$
4	$[45/-45_2/90/45_3/(90/-45)_2/-45/90_4/-45/0_2/45/0_4/45/90_3/45/0_2/-45/0]_S$
3	$[45/-45/90/45_2/(90/-45)_2/-45/90_4/-45/0_2/45/0_3/45/90_3/45/0_2/-45/0]_S$
2	$[45/-45/90_2/-45_2/0_4/45/90/45/0_2]_S$
1	$[45/-45/90_2/-45/0_4/45/90]_S$

Table 7.8 Stacking sequences of left and right hand side flanges obtained using parallel method.

Panel no.	Stacking sequences
	left hand side flanges
5	$[45/-45_4/90/45_4/90/-45_4/90/45_3/90/-45_2/90_3/45/0/-45/0_4/45/90_3/(45/0_3)_2/-45/90/-45/0_4/45/0/0]_{MS}$
3	$[45/-45_4/90/45_4/90/-45_3/90/45_2/90/-45_2/90_3/45/0/-45/0_2/45/90_3/(45/0_3)_2/-45/90/-45/0_4/45/0]_S$
1	$[45/-45_2/90_3/45/0/-45/0_3/45/0_3/-45/0_3/45/0]_{MS}$
	right hand side flanges
6	$[45/-45_4/90/45/90/-45_4/90/45_4/0/-45/90/45/90_2/-45/90_3/45/0_4/-45/0_4/(45/0_4)_2/45/90/90]_{MS}$
4	$[45/-45_4/90/45/90/-45_4/90/45_4/0/-45/90/45/90/-45/90_3/45/0/-45/0_4/(45/0_4)_2/45/90/90]_{MS}$
2	$[45/-45_3/90/-45/90/45_3/0_2/-45/0_4/45/0/0]_S$

Table 7.9 Stacking sequences of left and right hand side webs obtained using parallel method.

Panel no.	Stacking sequences
	left hand side webs
3	$[45/-45/90/-45/90/45/90_2/-45/90/45/90_2/45/0_4/-45/0_2/45/0_4/-45/0/0]_{MS}$
1	$[45/-45/90/-45/90/45/0_3/-45/0/45/0]_{MS}$
5	$[45/-45_2/90/45/0/0]_S$
	right hand side webs
6	$[45/-45_2/90/45/90/(90/-45_2)_2/90/45_4/90/-45_2/90/45/0/-45/0_3/45/90_3/-45/0_4/-45/90_4/-45/90/45/0_4/45/90/45/0_4/45/0/0]_{MS}$
4	$[45/-45/90_4/-45_2/90/45/0_4/45/90/-45/0_4/45/0/0]_S$
2	$[45/-45/90/-45/0_2/45/90/-45/0_4/45/0]_{MS}$

7.4 Conclusions

In this chapter, a parallel optimisation method which implements two different methods in a parallel process is developed for the problem of finding a blended layup with lamination parameters that are as close as possible to the target lamination parameters calculated for optimum design. In order to develop the parallel method, a guide-based blending optimisation method incorporated within an improved adaptive genetic algorithm (GAGA) is developed. The resulting stochastic search method GAGA is run in parallel with the logic-based search method DLBB in the parallel DLBB-GAGA method, combining the advantages of both. The performances of the three methods in searching for a blended stacking sequence to match the target lamination parameters are compared. Results suggest that GAGA performs better than the DLBB method most of the time when the stacking sequence is required only to be symmetric, but the DLBB method is more appropriate than GAGA for optimisation problems in which extra layup design constraints are considered. As expected, the parallel DLBB-GAGA method is shown to have the best performance in terms of searching capability and efficiency, and the advantage of the parallel DLBB-GAGA method is more obvious when imposing extra layup design constraints in practical design.

Chapter 8
Conclusions and Suggestions for Future Work

8.1 Conclusions

The main objective of this thesis is to develop effective and efficient methods for the layup optimisation of laminated composite structures, and also extend the applicability of VICONOPT and VICONOPT MLO by providing functionality to enable the design of lighter and more practical structures. Two-stage optimisation methods based on the use of lamination parameters are proposed for single laminates as well as large scale blended laminates. These novel techniques are introduced in Chapters 5, 6, and 7.

Contributions related to the optimisation of single composite laminates are presented in Chapter 5, with manufacturing requirements (i.e. symmetry, balance and four layup design constraints) considered in the two-stage layup optimisation method developed based on lamination parameters. In the first stage, VICONOPT is used to optimise the laminate's thickness and lamination parameters subject to buckling and lamination parameter constraints. The 10% minimum percentage constraint is studied and imposed in the VICONOPT optimisation by restricting the feasible regions of the lamination parameters for the four predefined ply angles $-45°$, $0°$, $+45°$ and $90°$. In the second stage, the layerwise branch and bound method is employed to match the lamination parameters obtained in the first stage optimisation, and extended with a checking strategy to logically search for stacking sequences satisfying the manufacturing requirements. Benefits of the checking strategy are that the branches which lead to the violation of the layup design constraints can be logically discarded, so narrowing the search space. Comparisons between the improved global layerwise branch and bound method and GAs suggest that the global layerwise branch and bound method is more efficient and effective than the GAs, particularly when layup design constraints are imposed or the laminate has a large number of plies. The performance of the improved LBB method in searching stacking sequences is further illustrated by comparisons with the results in Herencia *et al.* (2007). Using the same target

lamination parameters and number of plies the improved LBB method finds stacking sequences closer to the target lamination parameters, achieving better buckling performance.

In Chapter 6, achievements in the development of a two-stage optimisation method for more complex blended laminates are presented, which are extensions of the method presented in Chapter 5. The multilevel optimisation software VICONOPT MLO is first improved to include lamination parameters as design variables, and then employed in the first stage of the optimisation to obtain optimised lamination parameters and laminate thicknesses subject to buckling and lamination parameter constraints. During the iterative multilevel optimisation, ABAQUS is used to conduct the static FE analysis of the whole structure to obtain load distributions, based on which VICONOPT optimises each of the component panels. Following this, in the second stage of the optimisation, a novel dummy layerwise branch and bound method (DLBB) which incorporates the dummy layerwise technique into the branch and bound method is developed to logically search the blended stacking sequences for large scale structures subject to layup design constraints to match the optimised lamination parameters. This two-stage method is applied to a benchmark problem which Fischer *et al.* (2012) optimised using the previous version of VICONOPT MLO. A comparison of the results demonstrates that the proposed two-stage method obtains a lighter and more practical structure, with a further 8.0% reduction in weight over the previous optimisation results even with blending and layup design constraints imposed.

Chapter 7 introduces parallel computing in the second stage optimisation to solve blending problems more efficiently. First of all, a guide-based adaptive genetic algorithm (GAGA) which is a stochastic-based optimisation method, is developed. Different probabilities of crossover, mutation and permutation are implemented to different individuals according to their fitness. For individuals whose fitness values are lower than average, higher probabilities of being selected as cross points and mutating are given to the outer plies of the laminate. Next, a parallel DLBB-GAGA method which simultaneously executes the logic-based search of the DLBB method and the stochastic-based search of GAGA is developed. In order to improve the efficiency of the optimisation, the current best result from each method is shared with the other method to combine the advantages of these two different types of search.

Comparisons between the DLBB, GAGA and the parallel DLBB-GAGA methods shows that benefit is gained from combining the advantages of different methods, and the parallel DLBB-GAGA method performs with significant superiority in terms of both efficiency and ability to find closer matches to the target lamination parameters, especially when the extra layup design constraints are considered.

As discussed in the last three paragraphs, the objectives of the author's research work are achieved in this thesis. Several novel optimisation methods for the design of laminated composite structures are developed and validated by numerical results which demonstrate their high levels of performance.

8.2 Suggestions for future work

Based on the study carried out in this thesis, several extensions to the presented two-stage layup optimisations can be explored to develop the code further. A number of suggestions for future work are discussed in the following paragraphs.

The Matlab codes developed could be converted into Fortran or C++ languages so the optimisation methods presented in this thesis could be more easily compiled into VICONOPT and VICONOPT MLO, providing enhanced functionality and making the codes more competitive in the design of composite structures.

The parallel DLBB-GAGA method could be extended by adding more parallel cores, implementing more GAGA runs in the parallel process or adding new optimisation methods into the parallel method to further improve the efficiency of the optimisation, and conducting the parallel DLBB-GAGA method in a more stable and efficient parallel computing environment.

The adaptive genetic algorithm could be improved by applying adaptive parameters for the population size and number of elite in each generation.

Adding strength constraints, more layup design constraints (e.g. the maximum number of consecutive dropped plies is limited to three) and some other structural behaviours

(e.g. postbuckling behaviour) into the two-stage layup optimisations could make the methods more appropriate for practical design.

The thickness rounding process after the first stage optimisation should be further explored to obtain more accurate optimisation results.

The feasible regions and optimisations of lamination parameters could be explored in terms of more layup design constraints and structural behaviours.

The feasible regions should be defined using proper VICONOPT constraints (with derivative calculations) instead of by penalty functions.

More permissible ply angles could be included (e.g. ply angles with an increment of 5° or 10°) in the second stage optimisations, and comparisons made between the different methods for the increased set of permissible ply angles.

References

Abdalla, M.M., Kassapoglou, C. and Gürdal, Z. (2009). formulation of composite laminate robustness constraint in lamination parameters space. *50th AIAA/ASME/ASCE/ AHS/ASC Structures, Structural Dynamics and Materials Conference*. pp. 1–15.

Abouhamze, M. and Shakeri, M. (2007). Multi-objective stacking sequence optimization of laminated cylindrical panels using a genetic algorithm and neural networks. *Composite Structures* **81**(2):253–263. doi: https://doi.org/10.1016/j.compstruct.2006.08.015.

Adams, D.B., Watson, L.T. and Gürdal, Z. (2003). Optimization and Blending of Composite Laminates Using Genetic Algorithms with Migration Optimization and Blending of Composite Laminates. *Mechanics of Advanced Materials and Structures* **10**(June 2012):37–41. doi: https://doi.org/10.1080/15376490306741.

Adams, D.B., Watson, L.T., Gürdal, Z. and Anderson-Cook, C.M. (2004). Genetic algorithm optimization and blending of composite laminates by locally reducing laminate thickness. *Advances in Engineering Software* **35**(1):35–43. doi: https://doi.org/10.1016/j.advengsoft.2003.09.001.

Adams, D.B., Watson, L.T., Seresta, O. and Gürdal, Z. (2007). Global/local iteration for blended composite laminate panel structure optimization subproblems. *Mechanics of Advanced Materials and Structures* **14**(2):139–150. doi: https://doi.org/10.1080/15376490600719212.

Akbulut, M. and Sonmez, F.O. (2011). Design optimization of laminated composites using a new variant of simulated annealing. *Computers and Structures* **89**(17–18):1712–1724. doi: https://doi.org/10.1016/j.compstruc.2011.04.007.

Akoussan, K., Hamdaoui, M. and Daya, E.M. (2017). Improved layer-wise optimization algorithm for the design of viscoelastic composite structures. *Composite Structures* **176**:342–358. doi: https://doi.org/10.1016/j.compstruct.2017.05.047.

Albanesi, A., Bre, F., Fachinotti, V. and Gebhardt, C. (2018). Simultaneous ply-order, ply-number and ply-drop optimization of laminate wind turbine blades using the inverse finite element method. *Composite Structures* **184**:894–903. doi: https://doi.org/10.1016/j.compstruct.2017.10.051.

Albazzan, M.A., Harik, R., Tatting, B.F. and Gürdal, Z. (2019). Efficient design optimization of nonconventional laminated composites using lamination parameters: A state of the art. *Composite Structures* **209**:362–374. doi: https://doi.org/10.1016/j.compstruct.2018.10.095.

Almeida, F.S. (2016). Stacking sequence optimization for maximum buckling load of composite plates using harmony search algorithm. *Composite Structures* **143**:287–299. doi: https://doi.org/10.1016/j.compstruct.2016.02.034.

Almeida, F.S. and Awruch, A.M. (2009). Design optimization of composite laminated structures using genetic algorithms and finite element analysis. *Composite Structures* **88**(3):443–454. doi: https://doi.org/10.1016/j.compstruct.2008.05.004.

An, H., Chen, S. and Huang, H. (2015). Laminate stacking sequence optimization with strength constraints using two-level approximations and adaptive genetic algorithm. *Structural and Multidisciplinary Optimization* **51**(4):903–918. doi: https://doi.org/10.1007/s00158-014-1181-0.

Anderson, M.S. and Kennedy, D. (1993). Inclusion of Transverse Shear Deformation in the Exact Buckling and Vibration Analysis of Composite Plate Assemblies. *AIAA Journal* **31**(10):1963–1965. doi: https://doi.org/10.2514/6.1992-2287.

Anderson, M.S., Williams, F.W. and Wright, C.J. (1983). Buckling and vibration of any prismatic assembly of shear and compression loaded anisotropic plates with an arbitrary supporting structure. *International Journal of Mechanical Sciences* **25**(8):585–596. doi: https://doi.org/10.1016/0020-7403(83)90050-4.

Antonio, C.A.C., Marques, A.T. and Soeiro, A.V. (1995). optimization of laminated composite structures using a bilevel strategy. *Composite Structures* **33**(4):193–200. doi: https://doi.org/10.1016/0263-8223(95)00102-6.

Autio, M. (2000). Determining the real lay-up of a laminate corresponding to optimal lamination parameters by genetic search. *Structural and Multidisciplinary Optimization* **20**(4):301–310. doi: https://doi.org/10.1007/s001580050160.

Aymerich, F. and Serra, M. (2008). Optimization of laminate stacking sequence for maximum buckling load using the ant colony optimization (ACO) metaheuristic. *Composites Part A: Applied Science and Manufacturing* **39**(2):262–272. doi: https://doi.org/10.1016/j.compositesa.2007.10.011.

Bach, C., Jebari, R., Viti, A. and Hewson, R. (2017). Composite stacking sequence optimization for aeroelastically tailored forward-swept wings. *Structural and Multidisciplinary Optimization* **55**(1):105–119. doi: https://doi.org/10.1007/s00158-016-1477-3.

Balabanov, V., Kaufman, M., Knill, D., Haim, D., Golovidov, O., Giunta, A.A., Haftka, R.T., Grossman, B., Mason, W.H. and Watson, L.T. (1996). Dependence of optimal structural weight on aerodynamic shape for a High Speed Civil Transport. *6th Symposium on Multidisciplinary Analysis and Optimization*. American Institute of Aeronautics and Astronautics.doi: https://doi.org/10.2514/6.1996-4046.

Bargh, H.G. and Sadr, M.H. (2012). Stacking sequence optimization of composite plates for maximum fundamental frequency using particle swarm optimization algorithm. *Meccanica* **47**(3):719–730. doi: https://doi.org/10.1007/s11012-011-9482-5.

Barroso, E.S., Parente Jr, E. and Cartaxo de Melo, A. (2017). A hybrid PSO-GA algorithm for optimization of laminated composites. *Structural and Multidisciplinary Optimization* **55**(6). doi: https://doi.org/10.1007/s00158-016-1631-y.

Blasques, J.P. and Stolpe, M. (2011). Maximum stiffness and minimum weight optimization of laminated composite beams using continuous fiber angles. *Structural and Multidisciplinary Optimization* **43**(4):573–588. doi: https://doi.org/10.1007/s00158-010-0592-9.

Bloomfield, M.W., Diaconu, C.G. and Weaver, P.M. (2009). On feasible regions of lamination parameters for lay-up optimization of laminated composites. *Proceedings of the Royal Society A: Mathematical, Physical and Engineering Sciences* **465**(2104):1123–1143. doi: https://doi.org/10.1098/rspa.2008.0380.

Bloomfield, M.W., Herencia, J.E. and Weaver, P.M. (2009). Enhanced two-level optimization of anisotropic laminated composite plates with strength and buckling constraints. *Thin-Walled Structures* **47**(11):1161–1167. doi: https://doi.org/10.1016/j.tws.2009.04.008.

Bloomfield, M.W., Herencia, J.E. and Weaver, P.M. (2010). Analysis and benchmarking of meta-heuristic techniques for lay-up optimization. *Computers and Structures* **88**(5–6):272–282. doi: https://doi.org/10.1016/j.compstruc.2009.10.007.

Bruyneel, M., Beghin, C., Craveur, G., Grihon, S. and Sosonkina, M. (2012). Stacking sequence optimization for constant stiffness laminates based on a continuous optimization approach. *Structural and Multidisciplinary Optimization* **46**(6):783–794. doi: https://doi.org/10.1007/s00158-012-0806-4.

Bruyneel, M. and Fleury, C. (2002). Composite structures optimization using sequential convex programming. *Advances in Engineering Software* **33**(7–10):697–711. doi: https://doi.org/10.1016/S0965-9978(02)00053-4.

Butler, R. and Williams, F. (1990). Optimum design features of VICONOPT, an exact buckling program for prismatic assemblies of anisotropic plates. *31st Structures, Structural Dynamics and Materials Conference*. long beach, CA: American Institute of Aeronautics and Astronautics, pp. 1289–1299.

Butler, R. and Williams, F.W. (1992). Optimum design using VICONOPT, a buckling and strength constraint program for prismatic assemblies of anisotropic plates. *Computers and Structures* **43**(4):699–708. doi: https://doi.org/10.1016/0045-7949(92)90511-W.

Callahan, K.J. and Weeks, G.E. (1992). Optimum design of composite laminates using genetic algorithms. *Composites Engineering* **2**(3):149–160. doi: https://doi.org/10.1016/0961-9526(92)90001-M.

Chang, N., Wang, W., Yang, W. and Wang, J. (2010). Ply stacking sequence optimization of composite laminate by permutation discrete particle swarm optimization. *Structural and Multidisciplinary Optimization* **41**(2):179–187. doi: https://doi.org/10.1007/s00158-009-0417-x.

Cheung, Y.K. (1976). *Finite Strip Method in Structural Analysis*. New York: Pergamon Press Ltd.

Dassault Systèmes (2014). ABAQUS, version 6.14.

Dawe, D.J. (1977). Finite strip buckling analysis of curved plate assemblies under biaxial loading. *International Journal of Solids and Structures* **13**(11):1141–1155. doi: https://doi.org/10.1016/0020-7683(77)90083-X.

Deka, D.J., Sandeep, G., Chakraborty, D. and Dutta, A. (2005). Multiobjective optimization of laminated composites using finite element method and genetic algorithm. *Journal of Reinforced Plastics and Composites* **24**(3):273–285. doi: https://doi.org/10.1177/0731684405043555.

Diaconu, C.G., Sato, M. and Sekine, H. (2002). Feasible Region in General Design Space of Lamination Parameters for Laminated Composites. *AIAA Journal* **40**(3):559–565. doi: https://doi.org/10.2514/2.1683.

Diaconu, C.G. and Sekine, H. (2004). Layup Optimization for Buckling of Laminated Composite Shells with Restricted Layer Angles. *AIAA Journal* **42**(10):2153–2163. doi: https://doi.org/10.2514/1.931.

Dillinger, J.K.S., Klimmek, T., Abdalla, M.M. and Gürdal, Z. (2013). Stiffness Optimization of Composite Wings with Aeroelastic Constraints. *Journal of Aircraft* **50**(4):1159–1168. doi: https://doi.org/10.2514/1.c032084.

Dutra, T.A. and Almeida, S.F.M. (2015). Composite plate stiffness multicriteria optimization using lamination parameters. *Composite Structures* **133**:166–177. doi: https://doi.org/10.1016/j.compstruct.2015.07.029.

Erdal, O. and Sonmez, F.O. (2005). Optimum design of composite laminates for maximum buckling load capacity using simulated annealing. *Composite Structures* **71**(1):45–52. doi: https://doi.org/10.1016/j.compstruct.2004.09.008.

Fakhrabadi, M.M.S., Rastgoo, A. and Samadzadeh, M. (2013). Multi-objective design optimization of composite laminates using discrete shuffled frog leaping algorithm. *Journal of Mechanical Science and Technology* **27**(6):1791–1800. doi:

https://doi.org/10.1007/s12206-013-0430-2.

Fan, H.T., Wang, H. and Chen, X.H. (2016). An optimization method for composite structures with ply-drops. *Composite Structures* **136**:650–661. doi: https://doi.org/10.1016/j.compstruct.2015.11.003.

Fischer, M. (2002). *Multilevel Optimisation of Aerospace and Lightweight Structures*. PhD thesis, Cardiff University.

Fischer, M., Kennedy, D. and Featherston, C. a. (2012). Multilevel framework for optimization of lightweight structures. *Proceedings of the Institution of Mechanical Engineers, Part G: Journal of Aerospace Engineering* **226**(4):380–394. doi: https://doi.org/10.1177/0954410011411637.

Fletcher, R. and Powell, M.J.D. (1963). A Rapidly Convergent Descent Method for Minimization. *The Computer Journal* **6**(2):163–168. doi: https://doi.org/10.1093/comjnl/6.2.163.

Foldager, J., Hansen, J.S. and Olhoff, N. (1998). A general approach forcing convexity of ply angle optimization in composite laminates. *Structural Optimization* **16**(2):201. doi: https://doi.org/10.1007/s001580050021.

Fukunaga, H. and Sekine, H. (1992). Stiffness design method of symmetric laminates using lamination parameters. *AIAA Journal* **30**(11):2791–2793. doi: https://doi.org/10.2514/3.11304.

Fukunaga, H. and Sekine, H. (1994). A Laminate Design for Elastic Properties of Symmetric Laminates with Extension-Shear or Bending-Twisting Coupling. *Journal of Composite Materials* **28**(8):708–731. doi: https://doi.org/10.1177/002199839402800802.

Fukunaga, H., Sekine, H., Sato, M. and Iino, A. (1995). Buckling design of symmetrically laminated plates using lamination parameters. *Computers and Structures* **57**(4):643–649. doi: https://doi.org/10.1016/0045-7949(95)00050-Q.

Fukunaga, H. and Vanderplaats, G.N. (1991). Strength optimization of laminated composites with respect to layer thickness and/or layer orientation angle. *Computers*

and Structures **40**(6):1429–1439. doi: https://doi.org/10.1016/0045-7949(91)90413-G.

Fukunaga, Hisao and Vanderplaats, G.N. (1991). Stiffness Optimization of Orthotropic Laminated Composites Using Lamination Parameters. *AIAA Journal* **29**(4):641–646. doi: https://doi.org/10.2514/3.59931.

GARTEUR (1997a). *Assessment of Benchmark Problems on Stiffened Panel Design and Multilevel Optimisation. Final Report of the GARTEUR Action Group on Structural Optimisation SM(AG13) [Limited Literature]*. Farnborough, UK.

GARTEUR (1997b). *A Compendium of European Software Facilities for Stiffened Plate Design and Multilevel Optimisation. Final Report of the GARTEUR Action Group on Structural Optimisation SM(AG13) [Open Literature]*. Farnborough, UK.

GARTEUR (1997c). *System Level Structural Optimisation: A Compendium of European Aerospace Programs. Final Report of the GARTEUR Action Group on Structural Optimisation SM(AG13) [Open Literature]*. Farnborough, UK.

Gasbarri, P., Chiwiacowsky, L.D. and De Campos Velho, H.F. (2009). A hybrid multilevel approach for aeroelastic optimization of composite wing-box. *Structural and Multidisciplinary Optimization* **39**(6):607–624. doi: https://doi.org/10.1007/s00158-009-0429-6.

Giles, G.L. (1971). Procedure for automating aircraft wing structural design. *Journal of the Structural Division* **97**(1):99–113.

Graesser, D.L., Zabinsky, Z.B., Tuttle, M.E. and Kim, G.I. (1991). Designing laminated composites using random search techniques. *Composite Structures* **18**(4):311–325. doi: https://doi.org/10.1016/0263-8223(91)90002-G.

Grenestedt, J.L. and Gudmundson, P. (1993). Layup Optimization of Composite Material Structures. In: Pedersen, P. (ed.). *Optimal Design with Advanced Materials*. Lyngby: Elsevier, pp. 311–336.

Gürdal, Z., Haftka, R.T. and Hajela, P. (1999). *Design and Optimization of Laminated Composite Materials*. New York: Wiley.

Haftka, R.T. and Walsh, J.L. (1992). Stacking-sequence optimization for buckling of laminated plates by integer programming. *AIAA Journal* **30**(3):814–819. doi: https://doi.org/10.2514/3.10989.

Hawk, J. (2005). The Boeing 787 Dreamliner More Than an Airplane. AIAA/AAAF Aircraft Noise and Emissions Reduction Symposium. American Institute of Aeronautics and Astronautics and Association Aéronautique et Astronautique de France., pp. 1–29.

Hellard, G. (2008). A Long Story of Innovations and Experiences Composites in Airbus Table of Content. *Global Investor Forum*. Airbus, pp. 1–26.

Hemmatian, H., Fereidoon, A. and Assareh, E. (2014). Optimization of hybrid laminated composites using the multi-objective gravitational search algorithm (MOGSA). *Engineering Optimization* **46**(9):1169–1182. doi: https://doi.org/10.1080/0305215X.2013.832234.

Henderson, J.L. (1994). Laminated plate design using genetic algorithms and parallel processing. *Computing Systems in Engineering* **5**(4–6):441–453. doi: https://doi.org/10.1016/0956-0521(94)90025-6.

Herencia, J. E., Haftka, R.T., Weaver, P.M. and Friswell, M.I. (2008). Lay-Up Optimization of Composite Stiffened Panels Using Linear Approximations in Lamination Space. *AIAA Journal* **46**(9):2387–2391. doi: https://doi.org/10.2514/1.36189.

Herencia, J. Enrique, Haftka, R.T., Weaver, P.M. and Friswell, M.I. (2008). Optimization of anisotropic composite panels with T-shaped stiffeners using linear approximations of the design constraints to identify their stacking sequences. *Proceedings of 7th ASMO UK/ISSMO Conference*. Bath, UK, pp. 175–199.

Herencia, J.E., Weaver, P.M. and Friswell, M.I. (2007). Optimization of Long Anisotropic Laminated Fiber Composite Panels with T-Shaped Stiffeners. *AIAA Journal* **45**(10):2497–2509. doi: https://doi.org/10.2514/1.26321.

Herencia, J. Enrique, Weaver, P.M. and Friswell, M.I. (2008). Initial sizing optimisation of anisotropic composite panels with T-shaped stiffeners. *Thin-Walled*

Structures **46**(4):399–412. doi: https://doi.org/10.1016/j.tws.2007.09.003.

Hirano, Y. (1979). Optimum design of laminated plates under axial compression. *AIAA Journal* **17**(9):1017–1019. doi: https://doi.org/10.2514/3.61269.

Holland, J.H. (1975). *Adaptation of Natural and Artificial Systems*. Ann Arbor: MI: University of Michigan Press.

Honda, S., Kumagai, T., Tomihashi, K. and Narita, Y. (2013). Frequency maximization of laminated sandwich plates under general boundary conditions using layerwise optimization method with refined zigzag theory. *Journal of Sound and Vibration* **332**(24):6451–6462. doi: https://doi.org/10.1016/j.jsv.2013.07.010.

Honda, S., Narita, Y. and Sasaki, K. (2009). Discrete optimization for vibration design of composite plates by using lamination parameters. *Advanced Composite Materials* **18**(4):297–314. doi: https://doi.org/10.1163/156855109X434739.

Hu, H. (1991). Influence of Shell Geometry on Buckling Optimization of Fiber-Composite Laminate Shells. *Journal of Pressure Vessel Technology* **113**:465–470. doi: https://doi.org/10.1115/1.2928782.

Hwang, S.F., Hsu, Y.C. and Chen, Y. (2014). A genetic algorithm for the optimization of fiber angles in composite laminates. *Journal of Mechanical Science and Technology* **28**(8):3163–3169. doi: https://doi.org/10.1007/s12206-014-0725-y.

ICAO (2013). Present and Future Trends in Aircraft Noise and Emissions.

ICAO (2016). 39th Session Report of the Executive Committee on Agenda Item 22.

IJsselmuiden, S.T., Abdalla, M.M. and Gürdal, Z. (2008). Implementation of Strength-Based Failure Criteria in the Lamination Parameter Design Space. *AIAA Journal* **46**(7):1826–1834. doi: https://doi.org/10.2514/1.35565.

IJsselmuiden, S.T., Abdalla, M.M., Seresta, O. and Gürdal, Z. (2009). Multi-step blended stacking sequence design of panel assemblies with buckling constraints. *Composites Part B: Engineering* **40**(4):329–336. doi:

https://doi.org/10.1016/j.compositesb.2008.12.002.

Irisarri, F.-X., Abdalla, M.M. and Gürdal, Z. (2012). Improved Shepard's Method for the Optimization of Composite Structures. *AIAA Journal* **49**(12):2726–2736. doi: https://doi.org/10.2514/1.j051109.

Irisarri, F.X., Lasseigne, A., Leroy, F.H. and Le Riche, R. (2014). Optimal design of laminated composite structures with ply drops using stacking sequence tables. *Composite Structures* **107**:559–569. doi: https://doi.org/10.1016/j.compstruct.2013.08.030.

Irisarri, F.X., Laurin, F., Leroy, F.H. and Maire, J.F. (2011). Computational strategy for multiobjective optimization of composite stiffened panels. *Composite Structures* **93**(3):1158–1167. doi: https://doi.org/10.1016/j.compstruct.2010.10.005.

Jenny, C. (2014). Reducing the weight of aircraft interiors. *Reinforced Plastics* **58**(4):36–37. doi: https://doi.org/10.1016/S0034-3617(14)70180-8.

Jin, P., Song, B. and Zhong, X. (2011). Structure Optimization of Large Composite Wing Box with Parallel Genetic Algorithm. *Journal of Aircraft* **48**(6):2–5. doi: https://doi.org/10.2514/1.C031493.

Jin, P., Zhong, X., Yang, J. and Sun, Z. (2016). Blending design of composite panels with lamination parameters. *Aeronautical Journal* **120**(1233):1710–1725. doi: https://doi.org/10.1017/aer.2016.88.

Jing, Z., Fan, X. and Sun, Q. (2015a). Stacking sequence optimization of composite laminates for maximum buckling load using permutation search algorithm. *Composite Structures* **121**:225–236. doi: https://doi.org/10.1016/j.compstruct.2014.10.031.

Jing, Z., Fan, X. and Sun, Q. (2015b). Global shared-layer blending method for stacking sequence optimization design and blending of composite structures. *Composites Part B: Engineering* **69**:181–190. doi: https://doi.org/10.1016/j.compositesb.2014.09.039.

Jing, Z., Sun, Q. and Silberschmidt, V. V. (2016). A framework for design and optimization of tapered composite structures. Part I: From individual panel to global

blending structure. *Composite Structures* **154**:106–128. doi: https://doi.org/10.1016/j.compstruct.2016.05.095.

Jones, R.M. (1999). *Mechanics Of Composite Materials*. second edi. New York: Taylor and Francis.

Joubert, G.R., Nagel, W.E., Peters, F.J. and Walter, W. V (2004). *Parallel Computing : Software Technology, Algorithms, Architectures and Applications*. 1st ed. Amsterdam: Elsevier.

Kam, T.Y. and Lai, M.D. (1989). Multilevel optimal design of laminated composite plate structures. *Computers and Structures* **31**(2):197–202. doi: https://doi.org/10.1016/0045-7949(89)90225-3.

Kameyama, M. and Fukunaga, H. (2007). Optimum design of composite plate wings for aeroelastic characteristics using lamination parameters. *Computers and Structures* **85**(3–4):213–224. doi: https://doi.org/10.1016/j.compstruc.2006.08.051.

Kathiravan, R. and Ganguli, R. (2007). Strength design of composite beam using gradient and particle swarm optimization. *Composite Structures* **81**(4):471–479. doi: https://doi.org/10.1016/j.compstruct.2006.09.007.

Kennedy, D. and Featherston, C.A. (2010). Exact strip analysis and optimum design of aerospace structures. *Aeronautical Journal* **114**(1158):505–512. doi: https://doi.org/10.1017/S0001924000003997.

Kennedy, D., Ong, T.J., O'Leary, O.J. and Williams, F.W. (1999). Practical optimisation of aerospace panels. *Proceedings of the 1st ASMO UK/ISSMO Conference.* Ilkley, pp. 217–224.

Kennedy, D., Park, B. and Unsworth, M.D. (2010). Towards Global Layup Optimization of Composite Panels with Initial Buckling Constraints. *Proceeding of 8th ASMO UK/ISSMO Conference.* London, pp. 221–231.

Kennedy, D. and Williams, F.W. (1991). More efficient use of determinants to solve transcendental structural eigenvalue problems reliably. *Computers and Structures* **41**(5):973–979. doi: https://doi.org/10.1016/0045-7949(91)90290-3.

Kicher, T.P. and Chao, T.-L. (1971). Minimum weight design of stiffened fiber composite cylinders. *Journal of Aircraft* **8**(7):562–569. doi: https://doi.org/doi:10.2514/6.1974-101.

Kim, T.U. and Hwang, I.H. (2005). Optimal design of composite wing subjected to gust loads. *Computers and Structures* **83**(19–20):1546–1554. doi: https://doi.org/10.1016/j.compstruc.2005.02.002.

Kogiso, N., Watson, L.T., Gürdal, Z. and Haftka, R.T. (1994). Genetic algorithms with local improvement for composite laminate design. *Structural Optimization* **7**(4):207–218.

Kristinsdottir, B.P., Zabinsky, Z.B., Tuttle, M.E. and Neogi, S. (2001). Optimal design of large composite panels with varying loads. *Composite Structures* **51**(1):93–102. doi: https://doi.org/10.1016/S0263-8223(00)00128-8.

Kumar, N. and Tauchert, T.R. (1991). Design of Composite Cylindrical Panels for Maximum Axial and Shear Buckling Capacity. *journal of energy resources technology* **113**(3):204–209. doi: https://doi.org/10.1115/1.2905806.

Le-Manh, T. and Lee, J. (2014). Stacking sequence optimization for maximum strengths of laminated composite plates using genetic algorithm and isogeometric analysis. *Composite Structures* **116**(1):357–363. doi: https://doi.org/10.1016/j.compstruct.2014.05.011.

Little, J.D., Murty, K., Sweeney, D. and Karel, C. (1963). An algorithm for the traveling salesman problem. *Operations research* **11**(6):972–989. doi: https://doi.org/10.1287/opre.11.6.972.

Liu, B. (2001). *Two-Level Optimization of Composite Wing Structures Based on Panel Genetic Optimization*. PhD thesis, University of Florida.

Liu, B. and Haftka, R.T. (2001). Composite wing structural design optimization with continuity constraints. *19th AIAA Applied Aerodynamics Conference*. Anaheim,CA: American Institute of Aeronautics and Astronautics.

Liu, B., Haftka, R.T. and Akgün, M.A. (2000). Two-level composite wing structural optimization using response surfaces. *Structural and Multidisciplinary Optimization* **20**(2):87–96. doi: https://doi.org/10.1007/s001580050140.

Liu, B., Haftka, R.T. and Trompette, P. (2004). Maximization of buckling loads of composite panels using flexural lamination parameters. *Structural and Multidisciplinary Optimization* **26**(1–2):28–36. doi: https://doi.org/10.1007/s00158-003-0314-7.

Liu, D., Toropov, V. V., Querin, O.M. and Barton, D.C. (2011). Bilevel Optimization of Blended Composite Wing Panels. *Journal of Aircraft* **48**(1):107–118. doi: https://doi.org/10.2514/1.C000261.

Liu, D. and Toropov, V. V. (2013). A lamination parameter-based strategy for solving an integer-continuous problem arising in composite optimization. *Computers and Structures* **128**:170–174. doi: https://doi.org/10.1016/j.compstruc.2013.06.003.

Liu, D., Toropov, V. V., Barton, D.C. and Querin, O.M. (2015). Weight and mechanical performance optimization of blended composite wing panels using lamination parameters. *Structural and Multidisciplinary Optimization* **52**(3):549–562. doi: https://doi.org/10.1007/s00158-015-1244-x.

Liu, W. and Butler, R. (2007). Optimum Buckling Design of Composite Wing Cover Panels. *48th AIAA/ASME/ASCE/AHS/ASC Structure, Structural Dynamics, and Material Conference*. Honolulu, Hawaii, pp. 1–11.

Liu, W., Butler, R. and Kim, H.A. (2008). Optimization of composite stiffened panels subject to compression and lateral pressure using a bi-level approach. *Structural and Multidisciplinary Optimization* **36**(3):235–245. doi: https://doi.org/10.1007/s00158-007-0156-9.

Liu, W. and Krog, L. (2008). A Method for Composite Ply Layout Design and Stacking Sequence Optimisation. *Proceeding of the 7th ASMO UK Conference on Engineering Design Optimization*. Bath, UK, pp. 306–317.

Macquart, T., Bordogna, M.T., Lancelot, P. and De Breuker, R. (2016). Derivation and application of blending constraints in lamination parameter space for composite

optimisation. *Composite Structures* **135**. doi: https://doi.org/10.1016/j.compstruct.2015.09.016.

Macquart, T., Werter, N. and De Breuker, R. (2017). Aeroelastic Design of Blended Composite Structures Using Lamination Parameters. *Journal of Aircraft* **54**(2):561–571. doi: https://doi.org/10.2514/1.C033859.

Mahadevan, S. and Liu, X. (1998). Probabilistic optimum design of composite laminates. *Journal of Composite Materials* **32**(1):68–82. doi: https://doi.org/10.1177/002199839803200104.

MathWorks (2017). MATLAB, version 9.2.

Meddaikar, Y.M., Irisarri, F.X. and Abdalla, M.M. (2017). Laminate optimization of blended composite structures using a modified Shepard's method and stacking sequence tables. *Structural and Multidisciplinary Optimization* **55**(2):535–546. doi: https://doi.org/10.1007/s00158-016-1508-0.

Miki, M. (1982). Material design of composite laminates with required in-plane elastic properties. *Progress in Science and Engineering of Composites, Proceedings of the 4th International Conference on Composite Materials*:1725–1731.

Miki, M. (1985). Design of Laminated Fibrous Composite Plates with Required Flexural Stiffness. In: Vinson, J. and Taya, M. (eds.). *Recent Advances in Composites in the United States and Japan*. ASTM STP 8. Philadelphia, PA: American Society for Testing and Materials, pp. 387–400.

Miki, M. and Sugiyama, Y. (1993). Optimum design of laminated composites plates using lamination parameters. *AIAA Journal* **31**(5):921–922. doi: https://doi.org/10.2514/3.49033.

Morimoto, T., Kobayashi, S., Nagao, Y. and Iwahori, Y. (2017). A new cost/weight trade-off method for airframe material decisions based on variable fuel price. *Cogent Engineering* **4**(1). doi: https://doi.org/10.1080/23311916.2017.1285483.

MSC SOFTWARE CORPORATION (1999a). MSC/NASTRAN, VERSION 70.7.

MSC SOFTWARE CORPORATION (1999b). MSC/PATRAN, VERSION 9.0.

Nagendra, S., Haftka, R.T. and Gürdal, Z. (1992). Stacking sequence optimization of simply supported laminates with stability and strain constraints. *AIAA Journal* **30**(8):2132–2137. doi: https://doi.org/10.2514/3.11191.

Nagendra, S., Jestin, D., Giirdal, Z., Haftka, R.T. and Watson, L.T. (1996). Improved Genetic Algorithm for the Design of Stiffened Composite Panels. *Com/nmrs & Sfrucrures* **58**(3):543–555. doi: https://doi.org/10.1016/0045-7949(95)00160-I.

Narita, Y. (2003). Layerwise optimization for the maximum fundamental frequency of laminated composite plates. *Journal of Sound and Vibration* **263**(5):1005–1016. doi: https://doi.org/10.1016/S0022-460X(03)00270-0.

Narita, Y. and Hodgkinson, J.M. (2005). Layerwise optimisation for maximising the fundamental frequencies of point-supported rectangular laminated composite plates. *Composite Structures* **69**(2):127–135. doi: https://doi.org/10.1016/j.compstruct.2004.05.021.

Narita, Y. and Turvey, G.J. (2004). Maximizing the buckling loads of symmetrically laminated composite rectangular plates using a layerwise optimization approach. *Proceedings of the Institution of Mechanical Engineers, Part C: Journal of Mechanical Engineering Science* **218**(7):681–691. doi: https://doi.org/10.1243/0954406041319554.

Nikbakt, S., Kamarian, S. and Shakeri, M. (2018). A review on optimization of composite structures Part I: Laminated composites. *Composite Structures* **195**:158–185. doi: https://doi.org/10.1016/j.compstruct.2018.03.063.

Niu, M.C.-Y. (1992). *Composite Airframe Structures: Practical Design Information and Data*. Hong Kong: Conmilit.

Omkar, S.N., Venkatesh, A. and Mudigere, M. (2012). MPI-based parallel synchronous vector evaluated particle swarm optimization for multi-objective design optimization of composite structures. *Engineering Applications of Artificial Intelligence* **25**(8):1611–1627. doi: https://doi.org/10.1016/j.engappai.2012.05.019.

Othman, M., Silva, G.H.C., Cabral, P.H., Prado, A.P., Pirrera, A. and Cooper, J.E. (2018). A robust and reliability-based aeroelastic tailoring framework for composite aircraft wings. *Composite Structures* **208**:101–113. doi: https://doi.org/10.1016/j.compstruct.2018.09.086.

Pai, N., Kaw, A. and Weng, M. (2003). Optimization of laminate stacking sequence for failure load maximization using Tabu search. *Composites Part B: Engineering* **34**(4):405–413. doi: https://doi.org/10.1016/S1359-8368(02)00135-X.

Park, C.H., Lee, W. Il, Han, W.S. and Vautrin, A. (2008). Improved genetic algorithm for multidisciplinary optimization of composite laminates. *Computers and Structures* **86**(19–20):1894–1903. doi: https://doi.org/10.1016/j.compstruc.2008.03.001.

Park, W.J. (1982). An Optimal Design of Simple Symmetric Laminates Under the First Ply Failure Criterion. *Journal of Composite Materials* **16**(4):341–352. doi: https://doi.org/10.1177/002199838201600407.

Plank, R.J. and Wittrick, W.H. (1974). Buckling under combined loading of thin, flat-walled structures by a complex finite strip method. *International Journal for Numerical Methods in Engineering* **8**(2):323–339. doi: https://doi.org/10.1002/nme.1620080211.

Poulton, G. (2018). *Aviation's Material Evolution From Heavy Metal to Lightweight High-Tech.Airbus*. Available at: http://company.airbus.com/company/heritage/now-and-then/Material-evolution.html#.

Powell, M.J.D. (1964). An efficient method for finding the minimum of a function of several variables without calculating derivatives. *The Computer Journal* **7**(2):155–162. doi: https://doi.org/10.1093/comjnl/7.2.155.

Punch, W.F., Averill, R.C., Goodman, E.D., Lin, S.C., Ding, Y. and Yip, Y.C. (1994). Optimal design of laminated composite structures using coarse-grain parallel genetic algorithms. *Computing Systems in Engineering* **5**(4–6):415–423. doi: https://doi.org/10.1016/0956-0521(94)90023-X.

Qu, S., Kennedy, D. and Featherston, C.A. (2011). A multilevel framework for optimization of an aircraft wing incorporating postbuckling effects. *Proceedings of the*

Institution of Mechanical Engineers, Part G: Journal of Aerospace Engineering **226**(7):830–845. doi: https://doi.org/10.1177/0954410011415158.

Ragon, S.A., Gürdal, Z., Haftka, R.T., Tzong, T.J. (1997). Global/local structural wing design using response surface techniques. *38th Structures, Structural Dynamics, and Materials Conference*. American Institute of Aeronautics and Astronautics.

Raju, G., Wu, Z. and Weaver, P. (2014). On Further Developments of Feasible Region of Lamination Parameters for Symmetric Composite Laminates. *55th AIAA/ASME/ASCE/AHS/ASC Structures, Structural Dynamics, and Materials Conference*. American Institute of Aeronautics and Astronautics.

Rao, A.R.M. and Arvind, N. (2005). A scatter search algorithm for stacking sequence optimisation of laminate composites. *Composite Structures* **70**(4):383–402. doi: https://doi.org/10.1016/j.compstruct.2004.09.031.

Rao, A.R.M. and Arvind, N. (2007). Optimal stacking sequence design of laminate composite structures using tabu embedded simulated annealing. *Structural Engineering and Mechanics* **25**(2):239–268. doi: https://doi.org/10.12989/sem.2007.25.2.239.

Le Riche, R. and Haftka, R.T. (1993). Optimization of laminated stacking sequence for buckling load maximization by genetic algorithm. *AIAA Journal* **31**(5):951–956. doi: https://doi.org/10.2514/3.11710.

Rocha, I.B.C.M., Parente, E. and Melo, A.M.C. (2014). A hybrid shared/distributed memory parallel genetic algorithm for optimization of laminate composites. *Composite Structures* **107**(1):288–297. doi: https://doi.org/10.1016/j.compstruct.2013.07.049.

Sadr, M.H. and Bargh, G.H. (2012). Optimization of laminated composite plates for maximum fundamental frequency using Elitist-Genetic algorithm and finite strip method. *Journal of Global Optimization* **54**(4):707–728. doi: https://doi.org/10.1007/s10898-011-9787-x.

Schmit, L.A. and Farshi, B. (1977). Optimum design of laminated fibre composite plates. *International Journal for Numerical Methods in Engineering* **11**(4):623–640.

doi: https://doi.org/10.1002/nme.1620110403.

Schmit, L.A. and Mehrinfarf, M. (1982). Multilevel Optimum Design of Structures with Fiber-Composite Stiffened-Panel Components. *AIAA Journal* **20**(1):138–147. doi: https://doi.org/10.2514/3.51060.

Sebaey, T.A., Lopes, C.S., Blanco, N. and Costa, J. (2011). Ant Colony Optimization for dispersed laminated composite panels under biaxial loading. *Composite Structures* **94**(1):31–36. doi: https://doi.org/10.1016/j.compstruct.2011.07.021.

Seresta, O., Gürdal, Z., Adams, D.B. and Watson, L.T. (2007). Optimal design of composite wing structures with blended laminates. *Composites Part B: Engineering* **38**(4):469–480. doi: https://doi.org/10.1016/j.compositesb.2006.08.005.

Setoodeh, S., Abdalla, M. and Gürdal, Z. (2006). Approximate Feasible Regions for Lamination Parameters. *11th AIAA/ISSMO Multidisciplinary Analysis and Optimization Conference*. American Institute of Aeronautics and Astronautics.

Shrivastava, S., Mohite, P.M. and Limaye, M.D. (2019). Optimal design of fighter aircraft wing panels laminates under multi-load case environment by ply-drop and ply-migrations. *Composite Structures* **207**:909–922. doi: https://doi.org/10.1016/j.compstruct.2018.09.004.

Sjølund, J.H., Peeters, D. and Lund, E. (2018). A new thickness parameterization for Discrete Material and Thickness Optimization. *Structural and Multidisciplinary Optimization* **58**(5):1885–1897. doi: https://doi.org/10.1007/s00158-018-2093-1.

Sobieszczanski, J. and Leondorf, D. (1972). A Mixed Optimization Method for Automated Design of Fuselage Structures. *Journal of Aircraft* **9**(12):805–811. doi: https://doi.org/10.2514/3.59080.

Soremekun, G., Gürdal, Z., Haftka, R.T. and Watson, L.T. (2001). Composite laminate design optimization by genetic algorithm with generalized elitist selection. *Computers and Structures* **79**(2):131–143. doi: https://doi.org/10.1016/S0045-7949(00)00125-5.

Soremekun, G., Gürdal, Z., Kassapoglou, C. and Toni, D. (2002). Stacking sequence blending of multiple composite laminates using genetic algorithms. *Composite*

Structures **56**(1):53–62. doi: https://doi.org/10.1016/S0263-8223(01)00185-4.

Sørensen, S.N., Sørensen, R. and Lund, E. (2014). DMTO - A method for Discrete Material and Thickness Optimization of laminated composite structures. *Structural and Multidisciplinary Optimization* **50**(1):25–47. doi: https://doi.org/10.1007/s00158-014-1047-5.

Spallino, R., Giambanco, G. and Rizzo, S. (1999). A design algorithm for the optimization of laminated composite structures. *Engineering Computations* **16**(3):302–315. doi: https://doi.org/10.1108/02644409910266421.

Srinivas, M. and Patnaik, L.M. (1994). Adaptive Probabilities of Crossover and Mutation in Genetic Algorithms. *IEEE Transactions on Systems, Man and Cybernetics* **24**(4):656–667. doi: https://doi.org/10.1109/21.286385.

Sun, G. (1989). A practical approach to optimal design of laminated cylindrical shells for buckling. *Composites Science and Technology* **36**(3):243–253. doi: https://doi.org/10.1016/0266-3538(89)90023-7.

Sun, G. and Hansen, J.S. (1988). Optimal Design of Laminated-Composite Circular-Cylindrical Shells Subjected to Combined Loads. *Journal of Applied Mechanics* **55**(1):136–142. doi: https://doi.org/10.1115/1.3173619.

Suresh, S., Sujit, P.B. and Rao, A.K. (2007). Particle swarm optimization approach for multi-objective composite box-beam design. *Composite Structures* **81**(4):598–605. doi: https://doi.org/10.1016/j.compstruct.2006.10.008.

Todoroki, A. and Haftka, R.T. (1998). Stacking sequence optimization by a genetic algorithm with a new recessive gene like repair strategy. *Composites Part B: Engineering* **29**(3):277–285. doi: https://doi.org/10.1016/S1359-8368(97)00030-9.

Todoroki, A. and Ishikawa, T. (2004). Design of experiments for stacking sequence optimizations with genetic algorithm using response surface approximation. *Composite Structures* **64**(3–4):349–357. doi: https://doi.org/10.1016/j.compstruct.2003.09.004.

Todoroki, A. and Sasai, M. (1999). improvement of design reliability for buckling load

maximization of composite cylinder using genetic algorithm with recessive-gene-like repair. *JSME International Journal Series A* **42**(4):530–536. doi: https://doi.org/10.1299/jsmea.42.530.

Todoroki, A. and Sasai, M. (2002). Stacking Sequence Optimizations Using GA with Zoomed Response Surface on Lamination Parameters. *Advanced composite matetrials* **11**(3):299–318. doi: https://doi.org/10.6089/jscm.26.187.

Todoroki, A. and Sekishiro, M. (2008). Stacking sequence optimization to maximize the buckling load of blade-stiffened panels with strength constraints using the iterative fractal branch and bound method. *Composites Part B: Engineering* **39**(5):842–850. doi: https://doi.org/10.1016/j.compositesb.2007.10.003.

Todoroki, A. and Terada, Y. (2004). Improved Fractal Branch and Bound Method for Stacking-Sequence Optimizations of Laminates. *AIAA Journal* **42**(1):141–148. doi: https://doi.org/10.2514/1.9038.

Topal, U. and Uzman, Ü. (2007). Optimum design of laminated composite plates to maximize buckling load using MFD method. *Thin-Walled Structures* **45**(7–8):660–669. doi: https://doi.org/10.1016/j.tws.2007.06.002.

Topal, U. and Uzman, Ü. (2009). Effects of nonuniform boundary conditions on the buckling load optimization of laminated composite plates. *Materials and Design* **30**(3):710–717. doi: https://doi.org/10.1016/j.matdes.2008.05.012.

Tsai, S.W., Halpin, J.C. and Pagano, N.J. (1968). *Composite Materials Workshop*. Stamford: Stamford, Conn. : Technomic Pub. Co.

Vanderplaats, G.N. (1983). *CONMIN: A FORTRAN Program for Constrained Function Minimization: User's Manual*. NASA Technical Memorandum TM-X-62282.

Vanderplaats, G.N. and Moses, F. (1973). Structural optimization by methods of feasible directions. *Computers and Structures* **3**(4):739–755. doi: https://doi.org/10.1016/0045-7949(73)90055-2.

Vanderplaats, G.N. and Weisshaar, T.A. (1989). Optimum design of composite

structures. *International Journal for Numerical Methods in Engineering* **27**(2):437–448. doi: https://doi.org/10.1002/nme.1620270214.

Vosoughi, A.R., Darabi, A. and Dehghani Forkhorji, H. (2017). Optimum stacking sequences of thick laminated composite plates for maximizing buckling load using FE-GAs-PSO. *Composite Structures* **159**:361–367. doi: https://doi.org/10.1016/j.compstruct.2016.09.085.

Walker, M. and Smith, R.E. (2003). A technique for the multiobjective optimisation of laminated composite structures using genetic algorithms and finite element analysis. *Composite Structures* **62**(1):123–128. doi: https://doi.org/10.1016/S0263-8223(03)00098-9.

Wang, W., Guo, S., Chang, N., Zhao, F. and Yang, W. (2010). A modified ant colony algorithm for the stacking sequence optimisation of a rectangular laminate. *Structural and Multidisciplinary Optimization* **41**(5):711–720. doi: https://doi.org/10.1007/s00158-009-0447-4.

Watkins, R.I. and Morris, A.J. (1987). A multicriteria objective function optimization scheme for laminated composites for use in multilevel structural optimization schemes. *Computer Methods in Applied Mechanics and Engineering* **60**(2):233–251. doi: https://doi.org/10.1016/0045-7825(87)90111-3.

Williams, F.W. and Kennedy, D. (1988). Reliable use of determinants to solve non-linear structural eigenvalue problems efficiently. *International Journal for Numerical Methods in Engineering* **26**(8):1825–1841. doi: https://doi.org/10.1002/nme.1620260810.

Williams, F.W., Kennedy, D., Anderson, M.S. and Butler, R. (1991). VICONOPT - Program for exact vibration and buckling analysis or design of prismatic plate assemblies. *AIAA Journal* **29**(11):1927–1928. doi: https://doi.org/10.2514/3.10820.

Wittrick, W.H. and Williams, F.W. (1971). A general algorithm for computing natural frequencies of elastic structures. *The Quarterly Journal of Mechanics and Applied Mathematics* **24**(3):263–284. doi: https://doi.org/10.1093/qjmam/24.3.263.

Wittrick, W.H. and Williams, F.W. (1973). An algorithm for computing critical buckling loads of elastic structures. *Journal of Structural Mechanics* **1**(4):497–518. doi: https://doi.org/10.1080/03601217308905354.

Wittrick, W.H. and Williams, F.W. (1974). Buckling and vibration of anisotropic or isotropic plate assemblies under combined loadings. *International Journal of Mechanical Sciences* **16**(4):209–239. doi: https://doi.org/10.1016/0020-7403(74)90069-1.

Wu, Z., Raju, G. and Weaver, P.M. (2013). Feasible Region of Lamination Parameters for optimization of Variable Angle Tow (VAT) Composite Plates. *54th AIAA/ASME/ASCE/AHS/ASC Structures, Structural Dynamics, and Materials Conference*:1–10. doi: https://doi.org/10.2514/6.2013-1481.

Wu, Z., Raju, G., White, S. and Weaver, P. (2014). Optimal Design of Postbuckling Behaviour of Laminated Composite Plates using Lamination Parameters. *55th AIAA/ASME/ASCE/AHS/ASC Structures, Structural Dynamics, and Materials Conference*. Maryland: American Institute of Aeronautics and Astronautics, pp. 1–15.

Yamazaki, K. (1996). Two-level optimization technique of composite laminate panels by genetic algorithms. *Collection of Technical Papers - AIAA/ASME/ASCE/AHS/ASC Structures, Structural Dynamics and Materials Conference* **3**:1882–1887. doi: https://doi.org/doi:10.2514/6.1996-1539.

Yang, J., Song, B., Zhong, X. and Jin, P. (2016). Optimal design of blended composite laminate structures using ply drop sequence. *Composite Structures* **135**:30–37. doi: https://doi.org/10.1016/j.compstruct.2015.08.101.

Zein, S., Basso, P. and Grihon, S. (2014). A constraint satisfaction programming approach for computing manufacturable stacking sequences. *Computers and Structures* **136**:56–63. doi: https://doi.org/10.1016/j.compstruc.2014.01.016.

Zein, S., Madhavan, V., Dumas, D., Ravier, L. and Yague, I. (2016). From stacking sequences to ply layouts: An algorithm to design manufacturable composite structures. *Composite Structures* **141**:32–38. doi: https://doi.org/10.1016/j.compstruct.2016.01.027.

Zeng, J., Huang, Z., Chen, Y., Liu, W. and Chu, S. (2019). A simulated annealing approach for optimizing composite structures blended with multiple stacking sequence tables. *Structural and Multidisciplinary Optimization* **60**(2):537–563. doi: https://doi.org/10.1007/s00158-019-02223-9.

Appendix A
Lamination Parameters of the Layups Obtained in Chapter 7

Table A.1 Lamination parameters of the layups of skins obtained using DLBB.

Panel no.	ξ_1^A	ξ_2^A	ξ_3^A	ξ_1^D	ξ_2^D	ξ_3^D	Γ
5	0.0112	0.0112	0	−0.0795	−0.2201	0.0226	0.6067
6	−0.0115	−0.0115	0	−0.1085	−0.2529	0.0190	0.4405
4	−0.0303	0.1515	0	−0.1708	0.0058	−0.0032	0.6080
3	0	0.0667	0	−0.1920	−0.1650	−0.0002	0.5297
2	0.0667	0.2000	0	−0.0726	−0.1093	−0.0942	0.6464
1	−0.0909	0.2727	0	−0.1540	−0.1240	−0.0361	0.6153

Table A.2 Lamination parameters of the layups of left and right hand side flanges obtained using DLBB.

Panel no.	ξ_1^A	ξ_2^A	ξ_3^A	ξ_1^D	ξ_2^D	ξ_3^D	Γ
left hand side flanges							
5	0.1028	−0.0467	0	−0.1306	−0.4483	−0.0724	0.5745
3	0.0612	−0.0612	0	−0.1486	−0.4660	−0.0668	0.2231
1	0.3488	0.2558	0	−0.0711	0.0342	0.0045	0.4824
right hand side flanges							
6	0.1111	0.0303	0	−0.1041	−0.3576	−0.1640	0.4203
4	0.1209	0.0330	0	−0.0804	−0.3909	−0.1612	0.4068
2	0.3000	0	0	−0.0517	−0.4695	−0.1455	0.2070

Table A.3 Lamination parameters of the layups of left and right hand side webs obtained using DLBB.

Panel no.	ξ_1^A	ξ_2^A	ξ_3^A	ξ_1^D	ξ_2^D	ξ_3^D	Γ
left hand side webs							
3	0.2281	0.2982	0	−0.2161	0.0304	0.0140	0.2693
1	0.2000	0.0400	0	−0.1272	−0.2457	−0.0261	0.8056
5	0.1429	−0.1429	0	−0.1020	−0.4927	0	1.4572
right hand side webs							
6	0.0087	0.1652	0	−0.1436	−0.1681	−0.0807	0.4136
4	0.0833	0.5000	0	−0.0862	0.3125	−0.0334	0.4490
2	0.3103	0.1724	0	0.1372	−0.1228	−0.0413	0.4773

Table A.4 Lamination parameters of the layups of skins obtained using GAGA.

Panel no.	ξ_1^A	ξ_2^A	ξ_3^A	ξ_1^D	ξ_2^D	ξ_3^D	Γ
5	0.0112	0.0112	0	−0.1145	−0.2094	0.0209	0.6074
6	−0.0115	−0.0115	0	−0.1809	−0.2703	0.0283	0.3718
4	−0.0303	0.0303	0	−0.2239	−0.2454	−0.0072	0.4209
3	−0.0667	0.0667	0	−0.2756	−0.1179	0.0149	0.3172
2	0.2000	−0.0667	0	−0.0880	−0.1496	−0.1102	0.7633
1	−0.0909	−0.0909	0	−0.1931	−0.2261	−0.0766	0.6422

Table A.5 Lamination parameters of the layups of left and right hand side flanges obtained using GAGA.

Panel no.	ξ_1^A	ξ_2^A	ξ_3^A	ξ_1^D	ξ_2^D	ξ_3^D	Γ
left hand side flanges							
5	0.1028	0.0280	0	−0.1141	−0.3363	−0.2023	0.4654
3	0.0612	0.0204	0	−0.1412	−0.3381	−0.1705	0.3804
1	0.2558	0.2558	0	−0.1282	−0.0473	−0.0767	0.4742
right hand side flanges							
6	0.0707	0.0303	0	−0.1436	−0.2848	−0.1856	0.5158
4	0.0769	0.0330	0	−0.1282	−0.3120	−0.1719	0.3833
2	0.3000	0	0	−0.0202	−0.5265	−0.1395	0.1785

Table A.6 Lamination parameters of the layups of left and right hand side webs obtained using GAGA.

Panel no.	ξ_1^A	ξ_2^A	ξ_3^A	ξ_1^D	ξ_2^D	ξ_3^D	Γ
left hand side webs							
3	0.1579	0.2982	0	−0.3066	0.1014	0.0130	0.3141
1	0.2000	0.3600	0	−0.2424	0.0221	−0.0338	0.5086
5	0.1429	−0.1429	0	−0.1195	−0.5277	0.0175	1.4572
right hand side webs							
6	−0.0087	0.1652	0	−0.2037	−0.1364	−0.0779	0.4023
4	0.1667	0.3333	0	−0.2137	0.1751	−0.0430	0.4968
2	0.3103	0.1724	0	0.0929	−0.1051	−0.0679	0.4421

Table A.7 Lamination parameters of the layups of skins obtained using parallel method.

Panel no.	ξ_1^A	ξ_2^A	ξ_3^A	ξ_1^D	ξ_2^D	ξ_3^D	Γ
5	0.0112	0.0112	0	−0.1017	−0.3715	0.0444	0.4234
6	−0.0115	−0.0115	0	−0.1386	−0.4083	0.0406	0.2766
4	−0.0303	0.1515	0	−0.2248	−0.2303	−0.0137	0.3075
3	−0.0667	0.2000	0	−0.2832	−0.1027	−0.0020	0.2310
2	0.2000	0.2000	0	−0.0862	−0.1022	−0.1298	0.4710
1	0.0909	0.2727	0	−0.1345	−0.1059	−0.0451	0.4857

Table A.8 Lamination parameters of the layups of left and right hand side flanges obtained using parallel method.

Panel no.	ξ_1^A	ξ_2^A	ξ_3^A	ξ_1^D	ξ_2^D	ξ_3^D	Γ
left hand side flanges							
5	0.1028	0.0280	0	−0.1280	−0.4249	−0.0591	0.5338
3	0.0612	0.0204	0	−0.1609	−0.4126	−0.0554	0.1712
1	0.3488	0.2558	0	−0.0391	−0.0285	−0.0625	0.3948
right hand side flanges							
6	0.1313	0.1111	0	−0.1327	−0.3538	−0.1555	0.2862
4	0.0989	0.0330	0	−0.1371	−0.4192	−0.1710	0.3071
2	0.3000	0	0	−0.0570	−0.4800	−0.1508	0.1965

Table A.9 Lamination parameters of the layups of left and right hand side webs obtained using parallel method.

Panel no.	ξ_1^A	ξ_2^A	ξ_3^A	ξ_1^D	ξ_2^D	ξ_3^D	Γ
left hand side webs							
3	0.1579	0.2982	0	−0.2878	0.0229	0.0069	0.2431
1	0.2000	0.0400	0	−0.1272	−0.2457	−0.0261	0.8056
5	0.1429	−0.1429	0	−0.0845	−0.7376	−0.0175	1.1773
right hand side webs							
6	0.0261	0.1652	0	−0.1957	−0.1582	−0.0800	0.3792
4	0.1667	0.3333	0	−0.2666	0.1317	−0.0612	0.4698
2	0.3103	0.1724	0	0.0417	−0.1563	−0.0640	0.4142

Appendix B

Buckling Modes of the Wing Box Structures Obtained in Chapter 7

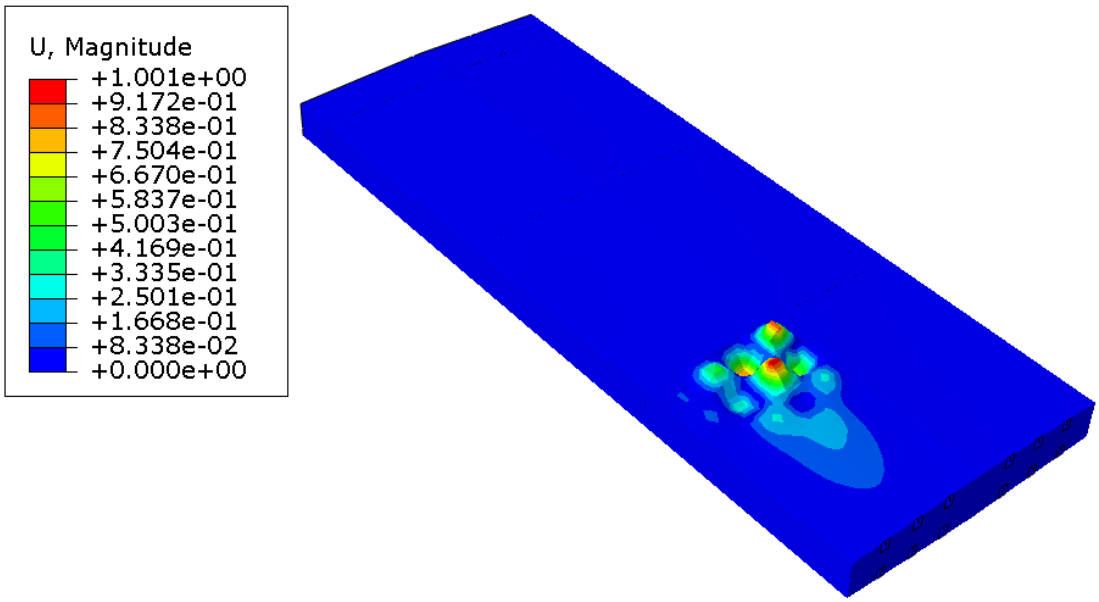

Figure B.1 First buckling mode with buckling load factor = 1.06 (DLBB method).

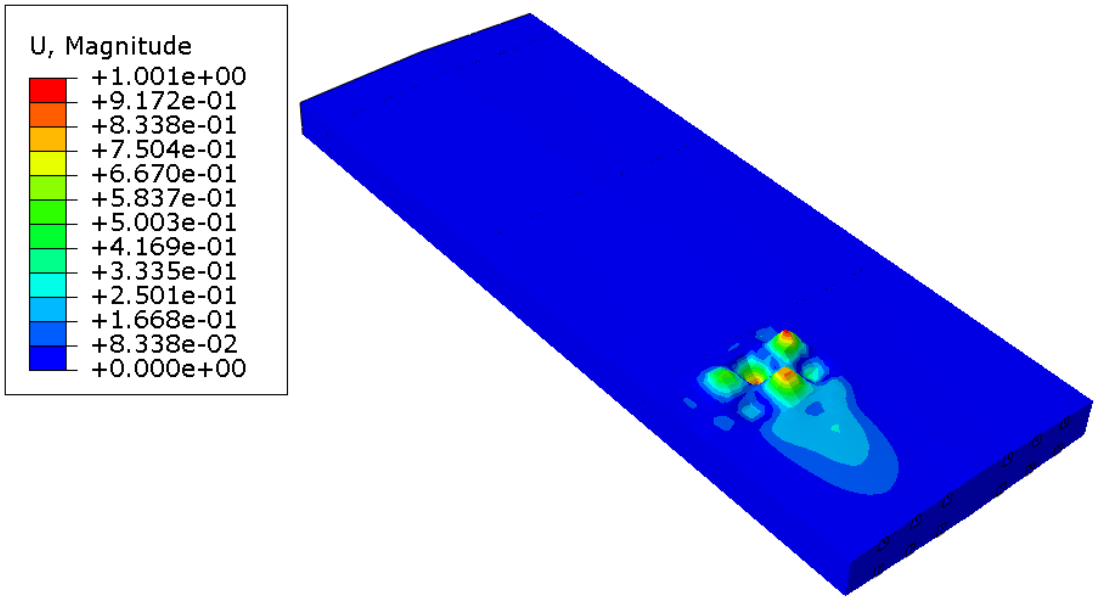

Figure B.2 Second buckling mode with buckling load factor = 1.11 (DLBB method).

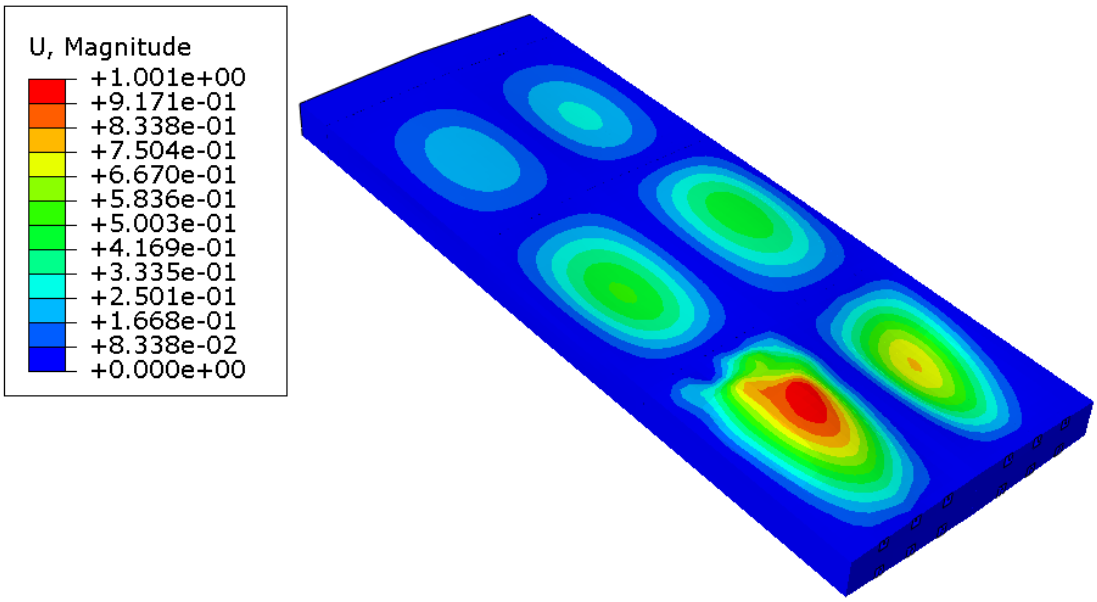

Figure B.3 Third buckling mode with buckling load factor = 1.15 (DLBB method).

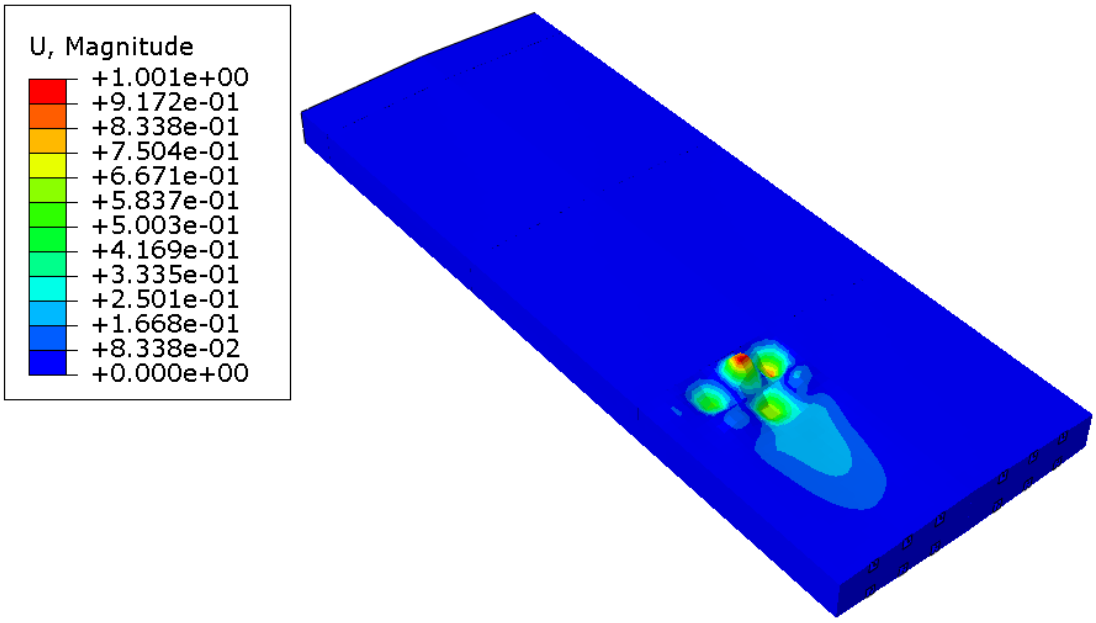

Figure B.4 First buckling mode with buckling load factor = 1.03 (GAGA).

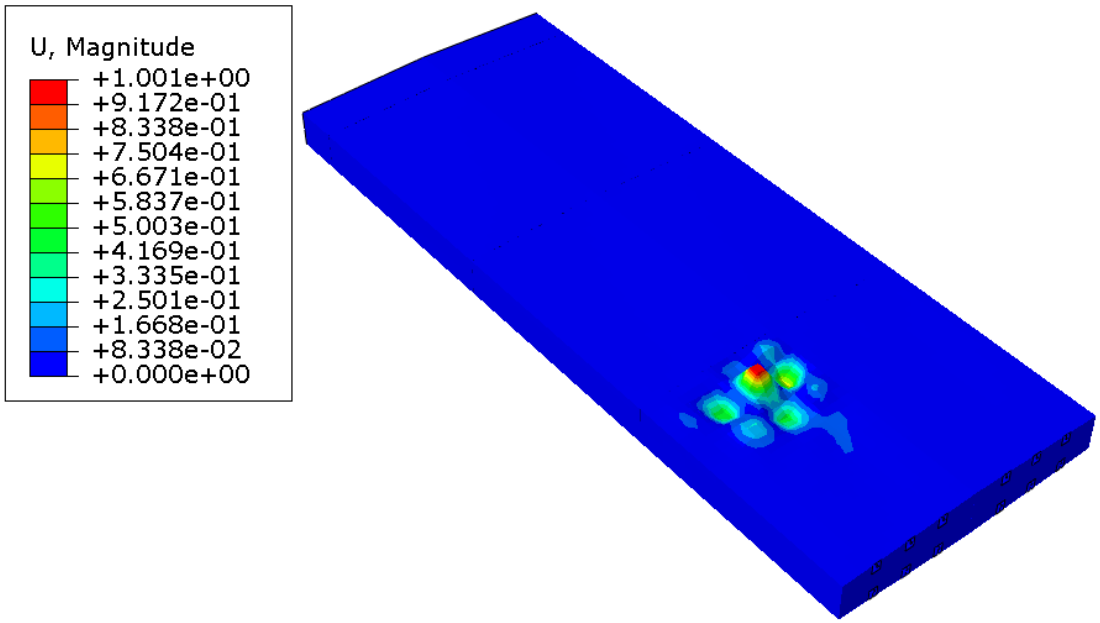

Figure B.5 Second buckling mode with buckling load factor = 1.13 (GAGA).

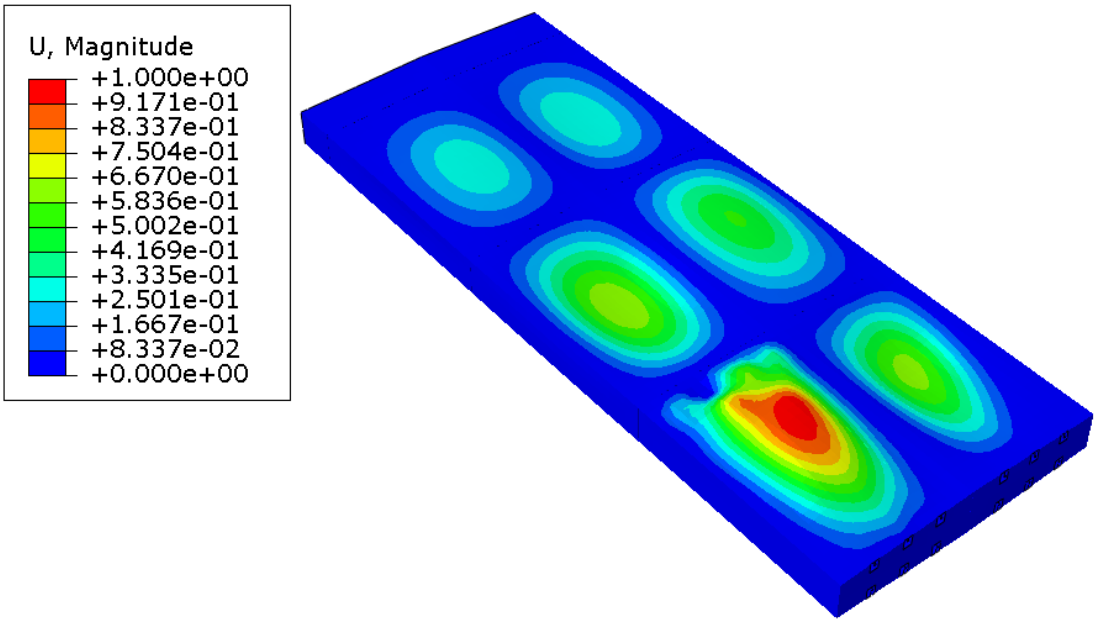

Figure B.6 Third buckling mode with buckling load factor = 1.15 (GAGA).

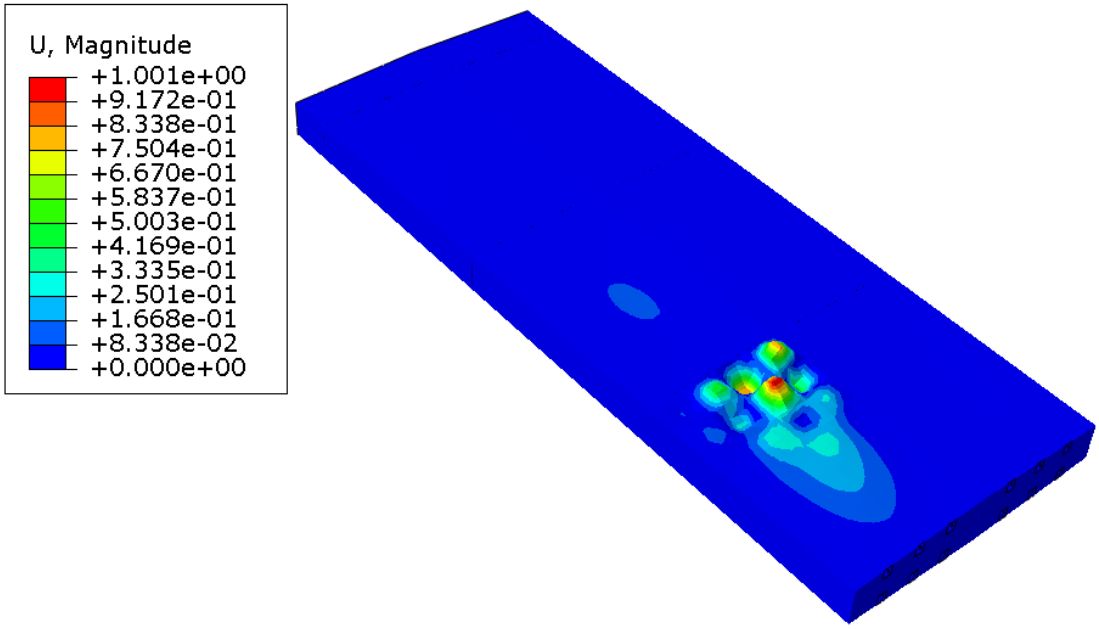

Figure B.7 First buckling mode with buckling load factor = 1.08 (parallel method).

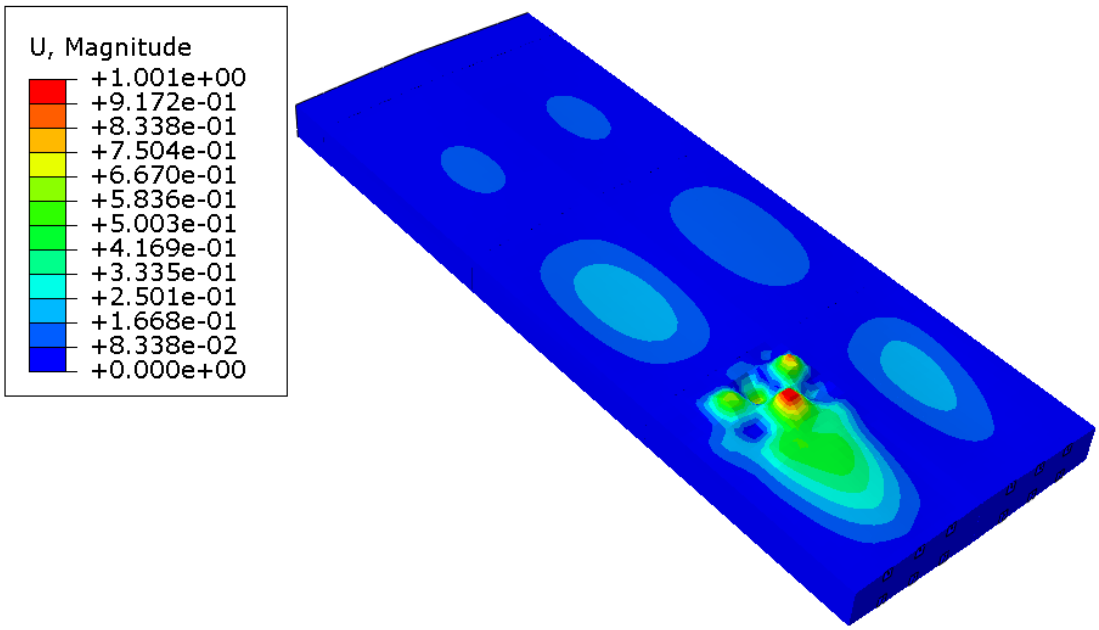

Figure B.8 Second buckling mode with buckling load factor = 1.14 (parallel method).

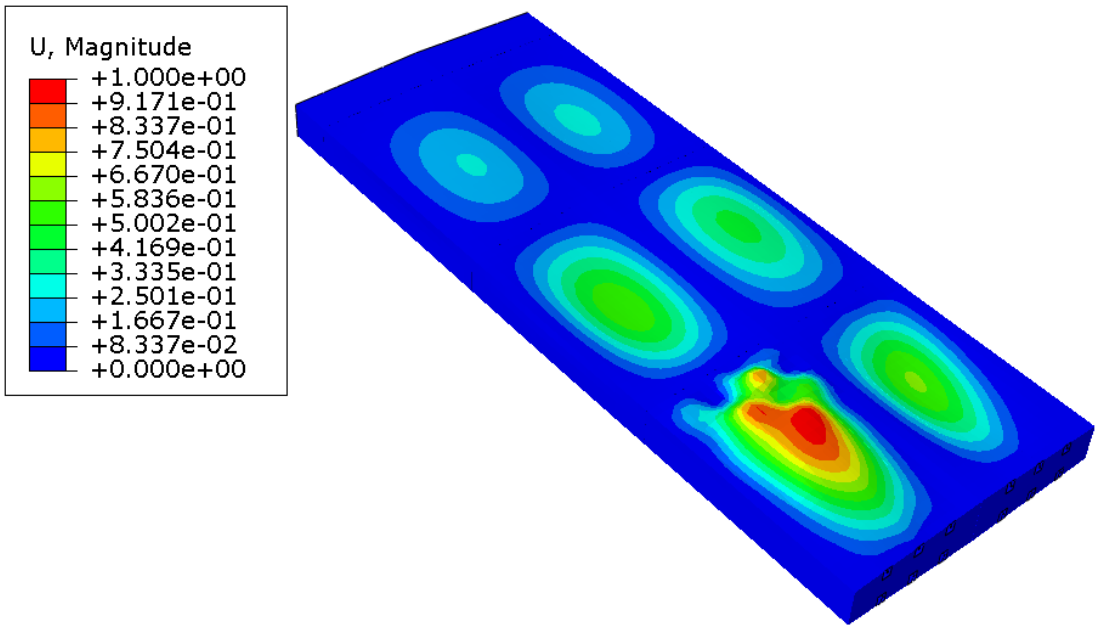

Figure B.9 Third buckling mode with buckling load factor = 1.15 (parallel method).